UNIVERSITEIT VAN PRETORIA
UNIVERSITY OF PRETORIA
YUNIBESITHI YA PRETORIA

Titania Recovery from Low-grade Titaniferrous Minerals

by

Arao J Manhique

A thesis submitted in partial fulfilment of the requirements for the degree

Philosophiae Doctor in Chemistry

in the

Department of Chemistry

Faculty of Natural and Agricultural Sciences

University of Pretoria

Pretoria

November 2012

Promoter: Professor Walter Focke

Declaration

I declare that this dissertation is my own unaided work. It is being submitted for the Degree of Philosophiae Doctor at the University of Pretoria, Pretoria. It has not been submitted before for any degree or examination to any other University

……

(Signature of Candidate)

On this ……. day of …… year……

Abstract

Titanium dioxide or titania is applied in paints, in the paper industry, fibbers, cosmetics, sunscreen products, toothpaste, foodstuffs, optical coatings, beam splitters and anti-reflection coatings. It is also used as support catalyst and its use as humidity and high-temperature oxygen sensor is under consideration. These applications are related to its high refractive index, oil absorption, tinting strength and inert chemical properties.

Commonly, titania is recovered either by leaching ilmenite with sulphuric acid and subsequently hydrolysing the resulting sulfate solution by boiling. In another process, titanium feedstock is converted into titanium tetrachloride and further oxidised to titanium dioxide. These methods are reportedly time-consuming and environmentally unfriendly. They are also unable to use all existing types of titanium minerals.

In this study, a novel process for the extraction of titanium valuables from its minerals is presented. The process entails the roasting of titanium ore with alkaline metal salt. The roasted product is hydrolysed with water and acid, and subsequently reacted with sulphuric acid. Alternatively, the hydrolysed product can be used as feedstock in the chloride process.

Roasting at 900 ^{o}C and using a 2:1 (NaOH:ilmenite) mole ratio proved to be the most efficient in releasing titanium units from its ore. Ternary phases dominate under these conditions. $Na_{0.75}Fe_{0.75}Ti_{0.25}O_2$ was the dominant titanium-bearing phase. $NaFeTiO_4$ and$Na_2Fe_2Ti_3O_{10}$ were also present. Whenever the Ti:Fe atom ratio was different from one, the surplus titanium was accommodated in single titanates, mainly Na_2TiO_3, while iron was accommodated in $NaFeO_2$. In many cases $Na_8Ti_5O_{14}$ was also present as a result of Na_2TiO_3 polymerisation. This is consistent with a fusion period of one hour or more. Shorter fusion periods tended to produce binary

phases. Similar results were obtained when lower fusion temperatures were employed, i.e. below 550 ^{o}C.

When anatase reactant was used to resemble an anatase ore, $Na_2Ti_6O_3$,Na_2TiO_3, $Na_8Ti_5O_{14}$ and $Na_{16}Ti_{10}O_{28}$ were identified in the products. Optimum recoveries were obtained using a 1:1 NaOH:TiO_2 mole ratio, and fusing at 800 ^{o}C for 2 h. Close to 100% of the titanium was recovered.

A one-step leaching process was found to be effective compared with multi-step leaching. The leaching step was found to be dependent on time, solid:liquid ratio and temperature. The optimum conditions for solid:liquid ratio, time and temperature were found to be 0.20, and 15 min at 75 ^{o}C, respectively.

Acidic hydrolysis was controlled by the relative amount of iron and titanium in solution. It was found that less than 1% was dissolved between 3 and 7 in pH units. Higher pH values are recommended, since less acid will be used.

Any excess of sulphuric acid in the sulfation step proved to be unnecessary. No significant changes were observed in the amount of dissolved iron and titanium. Therefore the stoichiometric amount can be used in the sulfation process.

Dedication

To my late father

Joao Manhique

And my late mother

Marta Zandamela

To the Almighty

Acknowledgements

I wish to express my deep and sincere gratitude to Professor WW Focke for his guidance, counselling and encouragement when the uncertaintiesof the success of the work drove me to a sentiment of failure. In those moments his encouraging words were there to push me forward.

My special thanks to Professor Carvalho Madivate for giving me the opportunity to join his research group at UniversityEduardoMondlane and for the friendship and guidance.

Financial support for this research from the University Eduardo Mondlane, Mozambique and the THRIP program of the Department of Trade and Industry and the National Research Foundation of South Africa as well as Xyris Technology CC is gratefully acknowledged.

I would like also express my appreciation to the help and useful discussions during the work with

- Doctor Sabine Verryn
- Doctor Maggi Lobster
- Doctor Linda Prinsloo
- Mrs Pravina Maharaj, Mrs Priscilla Appana, Mrs Suzette Seymore and Mrs Annetjie de Kok
- Mrs Isbe van der Westhuizen
- MrOllie del Fabbro

My gratitude is extended to my colleagues at the IAM whom devoted their time and attention to me when their help was needed, especially to Jeff, Zola, Robert, Nontete, Lumbi, Herminio and Pedro. To all of you my sincere thanks. To all friends I made here and made my stay and my study in South Africa a pleasure my sincere recognition.

My gratitude also goes to my brothers, sister and cousins for the encouragement during this long journey.

I would like also to express my gratitude to my family who were deprived of my attention and support for six long years. For Maria and Martinha my great thanks – "*muito obrigado pelo esforço e compreensão*"

To all of you who got involved directly or indirectly in this journey

my special thanks

Contents

List of Figures

List of Tables

List of Symbols

AFDI	Alkali Fusion Decomposed Ilmenite
Fe^{2+}	Iron (II), ferrous ion
Fe^{3+}	iron (III), ferric ion
$FeTiO_3$	Ilmenite, iron titanate
Fe_2O_3	iron oxide, iron (III) oxide, iron trioxide, hematite
FeOOH	goethite
FeO	iron oxide, iron (II) oxide, iron dioxide
$FeSO_4$	iron sulfate, iron (II) sulfate, ferrous sulfate
$FeSO_4.7H_2O$	iron sulfate heptahydrate, copperas
$Fe_2(SO_4)_3$	iron sulfate, iron (III) sulfate, ferric sulfate
FT-IR	Fourier transform infra-red spectrometry
g	grams
H_2SO_4	sulphuric acid
HCl	hydrochloric acid, hydrogen chloride
ICP-MS	Inductively coupled plasma mass spectroscopy
K	Kelvin
L	liquid
l	litre
M	concentration, mol/l
mL	millilitres
$NaTiO_2$	sodium metatitanate
Na_2TiO_3	sodium titanate
$Na_8Ti_5O_{14}$	sodium orthotitanate
$NaFeO_2$	sodium ferrate
$NaFeTiO_4$	sodium and iron titanate
Na_2CO_3	sodium carbonate
NaOH	sodium hydroxide
REE	rare earth elements
S	solid
SEM	scanning electron microscopy
TiO_2	titania, titanium dioxide, rutile, anatase
$Ti(SO_4)_2$	titanium sulfate
TiO_2^{2+}	titanyl ion
$TiOSO_4$	titanyl sulfate
XRD	X-ray diffraction

1 Introduction

Titanium dioxide (TiO_2) is a white powder with high opacity, brilliant whiteness, excellent covering power and resistance to colour change. These properties have made it a valuable pigment and opacifier for a broad range of applications in paints, in the paper industry, in fibbers, cosmetics, sunscreen products, toothpaste, foodstuffs, optical coatings, beam splitters and anti-reflection coatings. It is also used as support catalyst. Its use as a humidity sensor and high-temperature oxygen sensor is under consideration. Titanium dioxide is also a starting material for titanium metal production. Titanium metal is applied in construction projects, aircraft, spacecraft, turbine engines and missiles. The metal is also used in the chemical industry (Alemany *et al.*, 2000; Barksdale, 1966; Mellor, 1960; Nielsen and Chang, 1996; Samuel *et al.*, 2005; Stamper, 1970; Stanaway, 1994).

Titanium dioxide is manufactured from naturally occurring *rutile* (TiO_2), *ilmenite* ($FeTiO_3$)and *leucoxene* minerals, as well as from titanium slag, upgraded slag and synthetic rutile. Rutile is an impure form of titanium dioxide, whereas ilmenite contains titanium combined with iron as a compound oxide. Leucoxene is an altered form of ilmenite. Although common throughout the world, these minerals are most readily exploited in Australia, the US, India, South Africa and Mozambique. Other titanium minerals with no commercial importance at present are *perovskite* ($CaTiO_3$), *sphene* [$CaTi(SiO_4)O$] and *anatase* (TiO_2) (Afonso and Marques, 1993; Barksdale, 1966; Habashi, 1997; Nielsen and Chang, 1996).

Two routes are currently exploited industrially to retrieve titanium dioxide from its ores. The sulfate route applies sulphuric acid to convert titanium into a soluble sulfate form. Titania is crystallized the sulfate solution obtained. Titania is then calcined and further processed. In the chloride process, titania ore is converted into titanium tetrachloride using chlorine. Titanium tetrachloride is then burned to produce titania (Barksdale, 1966; Doan, 2003; Lahiri *et al.*, 2006; Nielsen and Chang, 1996; Toromanoff and Habashi, 1985).

The sulfate process produces high quantities of iron sulfate by-product which is not readily saleable. The chloride process can be viewed as a solution for the iron sulfate problem. However it needs high quality feedstock. High titanium slag and synthetic rutile are the preferred feedstocks. The production of slag and synthetic rutile entails high energy consumptions which can be associated with greenhouse gases production. Both processes are unable to deal with radioactive impurities in the ore. They are also unable to use a large variety of titanium minerals (Doan, 2003; Jha *et al.,* 2005; Hollit *et al.*, 2003; de Matos *et al.*, 2002).

There is a need to convert the existing methods to ecologically and environmentally friendly and cost-effective methods. Aspects of concern are the corrosion and toxicity problems caused by the acids that have to be disposed of (Berksdale, 1966; Doan, 2003; Nielsen and Chang, 1996). Other limitations are related to the cost of titania pigments; for instance, they amount to 30% of the total mineral costs in the paper industry although they make up only 3% of all the minerals used. According to Cole (2001), because of global demand, the price of titanium dioxide will continue to increase and it is likely that consumption will soon reach production capacity. This situation will consequently trigger further increases in the price of titanium dioxide. There is, therefore, a need to develop new extract titanium dioxide from the most abundant raw material, ilmenite.

We propose here a new rote that will enable the sulfate process to deal with a vast range of titanium minerals that are, until now, not used as ores for titania production. Minerals such as anatase, titanomagnetites, titanohematites and pseudobrookite can be included in this class. The new rote has the potentiality of dealing with radioactive impurities as well.

Modification of the de Wet process, zircon processing, combined with the sulfate process could make it possible to use a wide variety of titania ores (de Wet, 1999). The process uses the known alkaline fusion reaction of ilmenite to produce alkaline titanates (Richter and Elizabeth, 1933). The alkaline titanates are then hydrolysed with water and diluted mineral acids to

produce hydrous titanium. The hydrous titania produced in this way is reacted with sulphuric acid to titanyl sulfate.

1.1 Aim of the Study

The aim is to establish and optimise an alternative route to the traditional sulfate route. The new method will enable the sulfate process to treat ores previously considered economically untreatable, such as anatase (90–95% TiO_2), titanomagnetites [$Fe(Ti)Fe_2O_4$] and other low-grade ilmenites with high contents of calcium and magnesium (Yuan *et al.*, 2005).

It is also important to note that the traditional sulfate route is inappropriate for ores with high levels of chromium, vanadium and niobium because they impart colour to the pigment. High levels of calcium and phosphate are also stated to hinder proper crystal development in the sulfate route (Stanaway, 1994).

1.2 Methodology

The proposed route consists in fusing ore with an alkali compound. The identity of the fused products was verified by X-ray diffraction (XRD). After fusion, the fused product was subjected to a leaching process. The leachate was subjected to an acid hydrolysis and the hydrolysate was reacted with sulphuric acid. The product was dissolved in water and unreacted solids were filtered out. The aqueous solution was subjected to elemental analysis by inductively coupled plasmamass spectrometry (ICP-MS) for iron and titanium determination. Accessory characterisation techniques such as scanning electron microscopy (SEM) and Fourier transform infra-red spectrometry (FT-IR) were used.

Three steps in the process were optimised: fusion, leaching and sulfation. Temperature, time, mole ratio and particle size were the parameters tested for fusion optimisation by evaluating the yield in function of these parameters. For leaching time, the temperature and solid:liquid ratio were the parameters considered, while for sulfation the amount of acid was the sole parameter analysed.

1.3 Rationale

According to Pong *et al.* (1995), for a process to be commercially acceptable, it should be environmentally benign, result in minimal chemical loss through recycling, be able to use all grades of ores, produce manageable intermediate products and be economically favourable.

Existing commercial processes are either environmentally unfriendly or are costly, generate high levels of waste or products that need to be recycled, or are unable to process low-grade ores, as well as ores such as anatase, perovskite and sphene (Bulatovic and Wislouzyl, 1999; Cole, 2001; Hsu *et al.*, 1993; Nielsen and Chang, 1996; Yuan *et al.*, 2005). There are unexploited important reserves of *anatase* (Brazil) and *perovskite* (Colorado, US) due to the lack of, for instance, economical methods of extraction (Nielsen and Chang, 1996).

Generally, low-grade titaniferrous ores are submitted to a slagging process. However, this process faces an uncertain future due to its higher energy consumption and greenhouse gas emissions. In addition, slagging is unable to treat radioactive ores, since the radionuclides remain in the solid solution during the slagging process. With increasingly stringent environmental policies on radionuclides content, further treatment has to be conducted to reduce this content. This will result in additional production costs (Aminesh *et al.*, 2005; Habashi, 1997; Lahiri *et al.*, 2006; Nielsen and Chang, 1996).

Alkaline earths and rare earth impurities are not eliminated during the slagging process. Both the alkaline hearths and silica clog the fluidising bed in the chlorination process. Rare earths such as Cr_2O_3, V_2O_5 and Nb_2O_5 degrade pigment properties (Aminesh *et al.*, 2005; Habashi, 1997; Hollitt *et al.*, 2002; Lahiri *et al.*, 2006; Nielsen and Chang, 1996).

The route presented in this work has the following advantages:

- reduces the time consumed in the traditional digestion process
- addresses the concerning problem of acid disposal, reducing the amount of acid required for digestion
- has the ability to process all types of titaniferrous ores (Mellor, 1960; Nielsen and Chang, 1996).

1.4 References

Afonso, R. S., and Marques, J. M., **1993**. Recursos Minerais da República de Moçambique. Instituto de Investigação Científica Tropical – Centro de Geologia, Lisboa; Direcção Nacional de Geologia, Maputo.

Alemany, L. J., Banãres, M. A., Pardo, E., Martín-Jiménez, F., and Blasco, J. M., **2000**. Morphological and structural characterization of titanium dioxide system. *Materials Characterization*, 44: 271–275.

Aminesh, J., Antony, M. P., and Dattatray, T. V., **2007**. US Application Patent 20070110647.

Barksdale, J., **1966**. *Titanium: Its Occurrence, Chemistry, and Technology*, 2nd edition. New York: The Roland Press Co.

Bulatovic, S., and Wislouzyl, D. M., **1999**. Process development for treatment of complex perovskite, ilmenite and rutile ores. *Minerals Engineering*, 12(12): 1407–1417.

Cole, A., **2001**. All right on the white? TiO_2 versus alternative white minerals.*Industrial Minerals*, May 27: 31.

De Wet, W. J., **1999**. Beneficiation of zircon. Provisional SA Patent No. 99/3815.

Doan, P., **2003**. Sustainable development in the TiO_2 industry: Challenges and opportunities. Paper presented at the TiO_2 Intertech Conference, Miami, Florida, US.

Habashi, F. (Ed.), **1997.** Titanium. In: *Handbook of Extractive Metallurgy, Vol. II*. Weinheim, Germany: Wiley-VCH, pp 1129–1180.

Hollitt, M. J., McClelland, R. A., and Tuffley, J. R., **2002**. Upgrading titanoferous materials. US Patent Application 20020104406.

Hsu, W. P., Yu, R., and Matijevic, E., **1993**. Paper whiteners. I. Titania-coated silica. *Journal of Colloid and Interface Science*, 156: 56–65.

Lahiri, A., Kumari, E. J., and Jha, A., **2006**. Kinetic studies on the soda-ash roasting of titanoferous ores for the extraction of TiO_2. *Proceedings of theSohn International Symposium. Advanced Processing of Metals and Materials. Vol. 1: Thermo and Physicochemical Principles: Non-Ferrous High-Temperature Processing*, pp 115–123.

Mellor, J. W., **1960**. *A Comprehensive Treatise on Inorganic and Theoretical Chemistry,* Vol. VII. London: Longmans, pp 1–97.

Nielsen, R., and Chang, T.W. **1996**. In: Elvers, B., Hawkins, S. and Schultz, G. (Eds), *Ullman's Encyclopaedia of Industrial Chemistry,* 5th edition, Vol. A28, Weinheim, Germany, Wiley VCH, pp 543–567 and 95–122.

Pong, T. K., Besida, J., O´Donnell, T. A., and Wood, D., **1995**. A novel fluoride process for producing TiO_2 from titaniferous ore. *Industrial Engineering and Chemical Research*, 34: 308–313.

Richter, H.W. and Elizabeth, N. J., **1933**. Making titanium dioxide. US Patent No. 1 932 087.

Samuel, V., Pasricha, R., and Ravi, V., **2005**. Synthesis of nanocrystalline rutile. *Ceramics International*, 31: 555–557.

Stamper, J. W., **1970**. Titanium. In: *Mineral Facts and Problems*. Bureau of Mines, Department of Interior, USA, pp 773–794.

Stanaway, K. J., **1994**. Overview of titanium dioxide feedstocks. *Mining Engineering*, 12: 1367–1370.

Toromanoff, I. and Habashi, F., **1985**. The dissolution of activated titanium slag in dilute sulfuric acid. *The Canadian Journal of Chemical Engineering*, 63: 288–293.

Yuan, Z., Wang, X., Xu, C., Li, W., and Kwauk, M., **2005**. A new process for comprehensive utilization of complex titania ore. *Minerals Engineering*, 19(9): 975–978.

2 Literature Review

2.1 Titanium Minerals and Ores

Titanium occurs chiefly in two forms, ilmenite and rutile. Those are the two commercial minerals. Other natural occurring titanium minerals are listed in Table 8 (Grey and Reid, 1975; Murphy and Frick, 2006; Pownceby*et al*., 2008; Teufer and Temple, 1966).

Table 1: Non-commercial natural occurring titanium minerals

Mineral	**Formula**	**TiO_2, %**	**Characteristics**
Anatase	TiO_2	95 – 100	Rutile polymorph. It forms blue or black tetragonal crystals. Is formed by alteration of titanium minerals
Brookite	TiO_2	95 – 100	It is a rare orthorhombic polymorph of rutile, originated by ilmenite minerals alteration
Pseudorutile	$Fe_2Ti_3O_9$ ($Fe_2O_3.3TiO_2$)	60 – 65	Also known as arizonite is an altered ilmenite with properties resembling rutile. It crystalizes in hexagonal form.
Altered ilmenite	$FeTiO_3$-$FeTiO_9$	53 – 70	This term is used for alteration with composition between ilmenite and pseudorutile. Is optically homogeneous and amorphous
Leucoxene		70 – 100	It is an altered form of all titanium containing minerals with high content of TiO_2. They are optically distinguished from rutile and anatase by their internal reflection.
Titanite (sphene)	$CaTiSiO_5$	40	Is a reddish brown, gray, yellow, green or red gem. Occurs as accessory mineral in various rocks and minerals
Perovskite	$CaTiO_3$	58	Is a relatively rare accessory mineral. It occurs as accessory mineral in metamorphic and igneous rocks.
Ulvospinel	$FeTiO_4$	36	Is a black, brown to reddish brown accessory mineral in igneous rocks. Occurs commonly in titaniferous magnetite iron ores, in kimberlites, in strongly reduced iron-bearing basalts, among others.
Pseudobrookite	Fe_2TiO_5	33	It is a rare mineral with thin needle acicular prismatic crystals. Is associated with pyroxenes, hornblende, tridymite, topaz, hematite and bixbyite. Is dark black mineral.
Titanomagnetite	$(Fe, Ti)_3O_4$	0 – 34	Is a homogeneous cubic mineral with Fe_2O_3 as dominant phase. It contains above 5% TiO_2. It is a solid solution of ulvospinel and magnetite.
Titanohematite	$(Fe, Ti)_2O_3$	0 – 30	Is a solid solution of hematite-ilmenite. It has a light-gray to white appearance. Has lower reflectance.

There is also a set of minor titanium naturally occurring minerals listed in Table 2 (Mackey, 1994). These minerals are not of economic importance.

Table 2: Minor titanium bearing naturally occurring minerals

Mineral	**Formula**	**Mineral**	**Formula**
Anosovite	Ti_3O_5	Hydrorutile	$TiO_2.xH_2O$
Chrictonite	$(Ca,Ln,Ac)_{2-x}(Ti,Mg,Al,Fe,Tr)_{21}O_{38}$	Kalkowskyn	$Fe_2Ti_3O_9$
Knopite	$(Ca,Ti, Ce_2)O_3$	Doetlerite	TiO_2
Pyrophanite	$MnTiO_3$	Fulvite	TiO
Mananilmenite	$(Fe,Mn)TiO_5$	Geikielite	$MgTiO_3$
Picroilmenite	$(Mg,Ge)TiO_5$	Tielite	$AlTiO_3$
Yttrocrasite	$YTh_2Ti_4O_{11}$		

2.1.1 Rutile

Rutile is a titania (TiO_2) polymorph. It is the most common naturally occurring titania mineral. The other two are anatase and brookite. Large reserves of anatase exist in Brazil and these are in the process of being developed for commercial use (de Matos *et al.*, 2002; Nielsen and Chang, 1996; Paixão and de Mendonça, 1979).

Brookite possesses an orthorhombic structure and transforms spontaneously to rutile at around 750 °C. Anatase presents as a tetragonal structure and it changes to rutile at 915 °C. Rutile is the more stable form and presents as a densely packed anatase structure (tetragonal); see Figure 1. Anatase has a density of 3.899 g/cm^3, while rutile has a density of 4.250 g/cm^3 (Farrell, 2001).

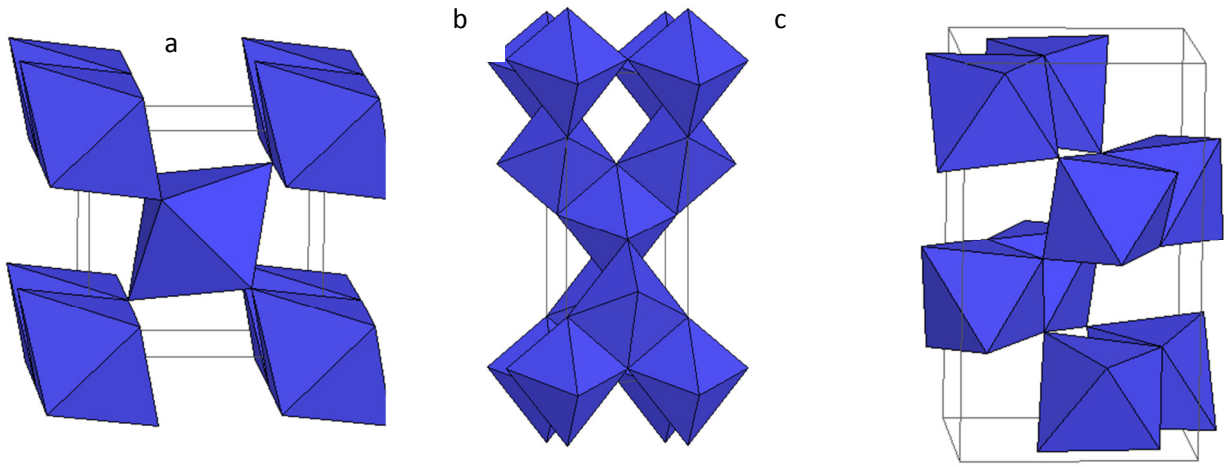

Figure 1: Crystal structure of rutile (a), anatase (b) and brookite (c)

Rutile is the end product of ilmenite and other titanium bearing minerals alteration. The alteration path involves the oxidation of iron to ferric state and progressively leaching out the iron in the ilmenite (Grey and Reid, 1975). It is found in mineral sands, occurs as an accessory mineral of high pressure and high temperature igneous rocks in placers. Is diamagnetic and it can be easily separated from the paramagnetic and ferromagnetic fraction of the heavy mineral, although rutile samples with high iron content can exhibit paramagnetic behaviour owing to losses in magnetic separation (Meinhold, 2010).

2.2 Ilmenite

Ilmenite is an iron-black or steel-grey mineral commonly found as accessory to igneous and metamorphic rocks. It is composed by 36.8% iron, 31.6% titanium and 31.6% oxygen. This corresponds to 52.6% TiO_2, ideally. In practice the percentage of iron is higher than the presented due, either by partial substitution of titanium by iron or other elements or by the presence of Fe_2O_3 as impurity. Moreover the ferrous iron in ilmenite structure is partially oxidized to ferric state (Grey and Reid, 1975; Murphy and Frick, 2006).

Ilmenite has a hexagonal structure similar to corundum, Al_2O_3. In ilmenite structure iron octahedral layers alternate with titanium octahedron layers. The two octahedrons share the edge oxygen atoms, Figure 2. Titanium oxygen bonds are strong and are difficult to break. Due to that ilmenite alteration occurs in the iron layers, affecting ilmenite magnetic properties. Ilmenite has a density of 4.7 to 4.8, hardness of 5.5 to 6.0 Moh. Pure crystals melt at 1392 °C (Agui*et al*., 2001; Murphy and Frick, 2006; Wechsler and Prewitt, 1984).

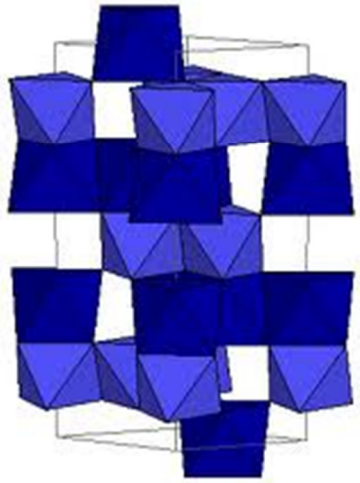

Figure 2: Crystal structure of ilmenite.

Ilmenite occurs in heavy mineral sands (HMS). HMS's possess specific gravity above 4.0. Heavy minerals concentrate in placers as a result of intense wind and waves. The most important minerals economically in HMS are ilmenite and its alteration products, indicated in Table 1, rutile, zircon, and monazite. A list of other minerals commonly associated with HMS is presented in Table 3 (Pownceby*et al*., 2008).

Generally ilmenite is the main component in HMS deposits. However its chemistry is altered by the presence of impurities in its composition. Titanium and iron, in ilmenite lattice (Figure 2), can be substituted by elements such as magnesium, manganese, chromium and cobalt (Agui*et al*., 2001; Pownceby*et al*., 2008). Other elements can be incorporated in ilmenite crystals. These

elements include aluminium, silicon, thorium, phosphorus and chromium, typically. These alterations in ilmenite composition bring difficulties in processing of such ores and reduce its market value (Powncebyet *al*., 2008).

Table 3: Minerals associated with HMS and their typical impurities

Mineral	**Ideal formula**	**Typical impurities**	**Specific gravity**
Ilmenite	$FeTiO_3$	Mg, Mn, V, Nb, Fe^{3+}	4.7-4.8
Rutile	TiO_2	Nb, Ta, Sn, Fe	4.2-5.5
Pseudorutile	$Fe_2Ti_3O_9$	Mg, Mn, Fe^{3+}, Cr, OH^-, (H_2O, Al_2O_3, SiO_2)[1]	3.3-3.8
Zircon	$ZrSiO_4$	Hf, Fe, Al, U, Th	4.6-4.7
Monazite	$CePO_4$	La, Y, Ca, Th, U, Al, Fe^{3+}	5.0-5.3
Spinel[2]	$Fe^{2+}Cr_2O_4$ - chromite	Mn, Zn, Fe^{3+}	5.1
	$Fe^{2+}Al_2O_4$ - hercynite		4.4
	$MgCr_2O_4$ - magnesiochromite		4.4
	$MgAl_2O_4$ - spinel		3.5
	$Fe^{2+}{}_2TiO_4$ - ulvospinel		4.8
	$Fe^{2+}Fe^{3+}{}_2O_4$ - magnetite		5.2
Garnet[3]	$Fe^{2+}{}_2Al_2Si_3O_{12}$ - almandine	Ca, Mn, Mg, Ti, Cr, Fe^{3+}, OH^-	3.5-4.3
Staurolite	$Fe^{2+}{}_2Al_9Si_4O_{23}(OH)$	Fe^{3+}, Mg, OH^-	3.7-3.8
Tourmaline	$NaFe^{2+}{}_3Al_6Si_6B_3O_{27}(OH)_4$ - schorl	Mg, Mn, Li, F^-	3.0-3.2
Sillimanite (kyanite – high P polymorph)	Al_2SiO_5	Fe^{3+}	3.2-3.3 (3.5-3.6)
Goethite	FeO.OH	Si, Mn^{3+}, Al	~ 4.3
Quartz	SiO_2	Al, Fe^{3+}, Ti	2.6-2.7

P – pressure

[1] commonly co-precipitated with, or adsorbed during weathering

[2] general name for a group of minerals with formula AB_2O_3

[3]garnets are group of silicates that has been as gems, with general formula $X_3Y_2(SiO_4)_3$, where *X* can be Ca^{2+}, Fe^{2+} or Mg^{2+}, and *Y* Al^{3+}, Fe^{3+} or Cr^{3+}. The most common in the group are with aluminium in Y site (pyralspite) and with calcium in *X* site (ugrandite)

Ilmenite can occur in two types of igneous rocks. In rocks related to massif anorthisites and in layered mafic intrusions. The former are of less commercial interest due to extensive intergrowth of ilmenite with magnetite. Anorthosite deposits are characteristically hosted in alkaline rocks rendering ilmenite with high contents of alkaline oxides such as CaO and MgO. Ores from such deposits are suitable for sulfate processing only. They can be also used in the chloride process after alkaline oxides removal (Murphy and Frick, 2006).

Sedimentary deposits are a result of weathering and erosion of titanium minerals from igneous and metamorphic rocks, followed by fluvial transportation and deposition in river beds and coastal shorelines. This process also results in ilmenite alteration and formation of high-grade titanium minerals (Murphy and Frick, 2006).

2.2.1 Titanium Minerals Occurrence

According to US Geological Survey (2010) 95% of the titanium minerals consumption was used in TiO_2 production. The remaining was used in titanium metal production. Australia is the world leader in titanium minerals supplier. Other countries include China, Norway, Canada, South Africa, India, United States and Ukraine. Mozambique is reported to hold half of the total African reserves. In 2010 the world production totalled seven million metric tons for ilmenite and leucoxene, while rutile totalled 710 thousands of metric tons (Gambogi, 2010; Murphy and Frick, 2006).

2.2.2 Mining

Large titanium reserves are in the form of anatase and titanomagnetite. These reserves correspond to 50% of the total world reserves. Currently, these are not economically workable under current technologies (Habashi, 1997; Murphy and Frick, 2006).

Ilmenite and rutile are the two mineral sources of titanium with commercial importance. The preferred ilmenite concentrate must contain 50 to 60% of titania. Lower grades are also used. For pigment production, the ore content of chromium oxide and vanadium pentoxide must be 0.2 and 0.5% or less respectively. The mining method depends on the type of ore and on its size. For sand deposits, a concentration of 5 to 7% in TiO_2 is required for economic exploitation. Dredging is used in large scale operation while dry mining is used in small scale operations or where there is no sufficient water available, in hard rock operations or if the clay content is high (Habashi, 1997; Murphy and Frick, 2006; Stamper, 1970).

Sand with 1 to 10% of heavy minerals is usually wet dredged and sieved. The slurriedsandis pumped to a wet concentrator. The concentrator and dredge are both in pool of water and are moved as the operations proceed. The concentrator removes silica, by gravity concentration. The obtained product has a concentration of 90 to 98% in heavy minerals. The separated silica and rocks separated are returned to the mined area while part of the water is recovered and reused (Habashi, 1997; Murphy and Frick, 2006; Stamper, 1970).

Dry mining operations are conducted in the conventional way, involving scrapers, excavators and trucks. For rock mining a primary blasting and the rock is transported for crushing and subsequent separation operations (Murphy and Frick, 2006).

Ilmenite is magnetically and conductively separated from the enriched sand. Leucoxene and other weathered ilmenite fractions are recovered in high-intensity magnetic separators. Rutile

is separated from zircon electrostatically. A small portion of ilmenite comes from hard-rock deposits (Habashi, 1997; Murphy and Frick, 2006).

2.3 Synthetic Feedstock

Environmental pressure on waste disposal has led to an increasing demand for materials with higher titania contents. The synthetic materials are a result of the removal of iron from ilmenite or titanomagnetite (Habashi, 1997; Stanaway, 1994). Feed stocks are classified according to their suitability to either sulfate or chloride process (Murphy and Frick, 2006):

Chloride-grade feed stocks:

Chloride-grade ilmenite, typically 60% TiO_2

Leucoxene, typically 75% to 91 % TiO_2

Rutile, typically 95% TiO_2

Chloride-grade slag, typically 86% TiO_2

Upgraded slag (UGS), typically 95% TiO_2

Synthetic rutile (SR), typically 90% to 93% TiO_2

Sulfate-grade feed stocks:

Sulfate-grade ilmenite, typically 44% to 57% TiO_2

Sulfate-grade slag, typically 75% to 80% TiO_2

2.3.1 Titanium slag

The process is conducted at 1 650 to 1 700 °C. The extent of rutile formation in slagging has to be limited, especially in the slag to be used in the sulfate process. It is also important to maximize the formation of phases with composition M_3O_5. These phases are soluble in sulphuric acid. The main reactions occurring in the process are

$$FeO + C = Fe + CO$$

$$TiO_2 + C = Ti_2O_3 + CO$$

Anthracite or coke is used as reducing agent. As the process proceeds and FeO concentration diminishes the operating temperature has to be raised. FeO acts as a fluxing agent. Due to that FeO removal is limited to up to 90%. Impurity oxides are also partially reduced to metal (Habashi, 1997; Murphy and Frick, 2006). The so produced slag is mainly composed by pseudobrookite and a glassy silicate. The pseudobrookite is a solid solution of iron and titanium oxides with the general formula (van Dyk, 1999).

A relatively new process that enables production of chloride grade slag (UGS) was developed by Canadian QIT[4]. The process was developed to improve Canadian ilmenite, with relatively high concentrations of alkaline oxides. These oxides are less amenable to acid leach. In this process the slag is initially oxidized in order to convert al Ti(III) in Ti(IV) and Fe(II) to Fe(III)as shown in the following equation (Borowiec *et al*., 1998; van Dyk, 1999).

$$(FeTi_2O_5)_{0.32}(MgTi_2O_5)_{0.33}(Ti_3O_5)_{0.35} + 0.255O_2 \rightarrow (Fe_2TiO_5)_{0.16}(MgTi_2O_5)_{0.33} + 1.53TiO_2$$

The aim of the oxidation process is to reduce the content of pseudobrookite phase (M_3O_5) and increase rutile proportion. Apart from the major rutile phase with minor M_3O_5 phase there is a glassy silicate phase. This phase decomposes into wollastonite ($CaSiO_3$) and tridymite (SiO_2) due to Fe(II) to Fe(III) oxidation according to the reaction (Borowiec *et al*., 1998; van Dyk, 1999; van Dyk *et al.*, 2004).

$$(Ca, Al, MgFeTi)SiO_3 + O_2 \rightarrow Fe_2O_3 + CaSiO_3 + SiO_2 + Al_2SiO_5 + TiO_2$$

During the oxidation process iron migrates to the surface of titania slag particles and into the pores perimeter. This makes it easier to leach it out (van Dyk, 1999; van Dyk *et al.*, 2004). The oxidized slag is then reduced. The aim here is to convert all the iron into the ferrous state. In the reduction stage besides FeO, rutile, pseudobrookite with reduced concentration of MgO and a solid solution of ilmenite-geikielite ($MgTiO_3$).

[4] Quebec Iron and Titanium

Finally the reduced slag is leached with dilute HCl solution under pressure, washed and calcined. The resulting slag has a 95% content of TiO_2, while MgO, CaO, Cr_2O_3, and V_2O_5 amount typically to 0.67%, 0.08%, 0.06%, and 0.35% respectively (Borowiec *et al*., 1998; van Dyk, 1999).

2.3.2 Synthetic rutile

Economic reserves of natural rutile (95% TiO_2) are rare compared with ilmenite reserves. Natural rutile is the favourite feedstock for the chloride process. Its advantage includes its bulk density, low trace element content and low iron content (Habashi, 1997; Murphy and Frick, 2006; Stanaway, 1994).

Several processes for converting ilmenite into synthetic rutile (85–96% TiO_2) have been developed to overcome its high price and scarcity. All the processes entail the reduction of Fe^{3+} using carbon or hydrogen. In some cases ilmenite is activated by oxidation prior to reduction. Reduced ilmenite containing Fe^{2+} is preferably treated with hydrochloric acid or diluted sulphuric acid under pressure (Habashi, 1997; Murphy and Frick, 2006). The two most important technologies are: the Becher process (A) and the Benelite process (B) (Murphy and Frick, 2006).

A. The Becher Process

It was developed to upgrade ilmenite with TiO_2 content around 55% to levels as high as 90%. The process is conducted in a rotary kiln using subbituminous coal as reducing agent at 1 050 °C to 1 150 °C. Iron, coal, and sulphur are introduced into the kiln. The Fe(III) is reduced partial or completely to Fe(II), while part of Ti(IV) is also reduced to Ti(III). Sulphur reacts with manganese and iron forming a complex sulphide phase. This complex phase is removed by sulphuric acid (Murphy and Frick, 2006).

Reduced ilmenite from the kiln is mixed with aerated ammonium chloride solution to dissolve iron. Ammonium ions act as buffer preventing localized high pH values consequently avoiding $Fe(OH)_2$ precipitation in the rutile matrix. Ammonia ions also complex Fe(II) ions allowing them to diffuse away from high pH zones. The chloride ions from NH_4Cl help in breaking any passive film that eventually might during aeration (Farrow *et al*., 1987; Murphy and Frick, 2006).

The product obtained after ammonium chloride treatment is leached with diluted sulphuric acid to remove manganese and residual iron. The product, synthetic rutile (SR), is washed and dried. The so obtained SR is 90% to 93% in TiO2 (Farrow *et al*., 1987; Murphy and Frick, 2006).

The Becher process is unable to deal with impurities such as manganese, magnesium aluminium, uranium and thorium. These elements are retained in the kiln in the minor pseudobrookite (M_2O_5). This phase is insoluble therefore the impurities remain in the SR. Only manganese is partially removed (de Matos *et al*., 2002; Doan, 2003; Hollit *et al*., 2003; Murphy and Frick, 2006; Smith and Castro, 2007).

Other constraining aspect in the Becher process is the higher reduction temperature and the time retention in the rotary kiln. The retention is function of the level of weathered of ilmenite. Extensively weathered ilmenite presents cracks that increase the surface available for CO interaction (Murphy and Frick, 2006).

An alternative to overcome this is to operate above 1 200 °C. At this temperature a phase composed by impurities is formed on ilmenite crystals. This phase can be leached in a series of acid leaching steps, taking away manganese, magnesium, thorium, and uranium. A borate salt is used as flux agent to reduce the reaction temperature and form a glassy phase. This process, although successful is costly and there is a threat of acid disposal (Murphy and Frick, 2006).

B. The Benilite Process

In the Benelite process ilmenite containing typically 54 to 65% in TiO_2 is heated up to 870 °C in a rotary kiln mixed with fuel oil. Fuel oil is used as reducing agent to convert Fe(III) to Fe(II). Reduced ilmenite is digested with 18 – 20% at 140 °C. Fe(II) is dissolved as $FeCl_2$, while TiO_2 is left in solid state. TiO_2 are water washed and calcined. The final product has 94% of TiO_2. The $FeCl_2$ is recovered in later stage and HCl concentrated for reuse (Gambogi, 2010; Murphy and Frick, 2006).

Synthetic feed stocks such as synthetic rutile and titanium slag are available for titania production. The production of slag or synthetic rutile is aimed at ameliorating the environmental burden of waste disposal in the direct use of ilmenite, which is the most abundant and viable source of titania. Although these synthetic feed stocks partially solve the immediate problem of iron waste, such procedures are unable to deal with radioactive and other impurities that are of environmental concern, such as lead and chromium. Such impurities are at present simply discharged. In future, additional costs for waste treatment will exert pressure on the price of the product (de Matos *et al*., 2002; Doan, 2003; Hollit *et al*., 2003; Murphy and Frick, 2006; Smith and Castro, 2007).

On the other hand, slagging involves high energy consumption and greenhouse gas emissions (Jha and Dattatray, 2005; Mahmoud *et al*., 2004; Murphy and Frick, 2006). There is a need to develop new processes that will be able to use a number of raw materials with less and/or recyclable waste. Moreover, the waste generated must not constitute any environmental threat.

2.4 Titanium Processing Technology Overview

There are currently two industrial processes for titania production: the sulfate process and the chloride process. The sulfate process uses low-grade raw materials (ilmenite or titania slag), while the chloride process requires comparatively higher grade and more expensive raw material (natural or synthetic rutile, leucoxene and titania slag) (Gambogi, 2010; Murphy and Frick, 2006).

2.4.1 The Sulfate Process

Dried ilmenite or slag (labelled "titanium ore" in Figure 3) is pulverised and mixed with concentrated sulphuric acid. Water or steam is injected to initiate the reaction (Figure 3). The main reaction can be described by the following equation.

$$FeTiO_3 + H_2SO_4 \rightarrow TiOSO_4 + FeSO_4 + 2H_2O$$

The cake is allowed to mature (1–12 h) and dissolved in water or recycled dilute sulphuric acid. The temperature must be maintained at 85 °C to avoid premature hydrolysis. Ferric ions in solution are reduced to the ferrous state but a small proportion of titanic ions must also be reduced to the titanous state (Ti^{3+}), preferentially, to ensure the reduction of ferric species.

The solution is filtered to remove solids. The filtrate is cooled under vacuum, precipitating $FeSO_4$ as copperas (ferrous sulfate – $FeSO_4.7H_2O$). Copperas is used in sewage water treatment and as raw material for iron oxide pigment. Alternatively, the filtrate can be roasted to Fe_2O_3 and SO_2, thereby recovering sulphuric acid (Habashi, 1997; Lynd and Lefond, 1975).

The final solution is thermally hydrolysed to TiO_2, according to the reaction below. For higher yields, TiO_2 nuclei are added. Hydrous titania is collected and washed with weak acid. The

product is bleached with acid and mixed with zinc or aluminium powder. The titania is finally dried, calcined and processed (Habashi, 1997).

$$TiOSO_4 + 2H_2O \rightarrow TiO_2.xH_2O + H_2SO_4$$

Spent acid (20–28% H_2SO_4) is concentrated to 70–80% and reused. In another approach, the spent acid is neutralised with lime. Alternatively, the spent acid can be used in the fertiliser industry. The process is summarised in Figure 3 (Habashi, 1997).

Some concerning aspects in this process are listed below for each of the processing steps:

a. **Preliminary drying**. Preliminary drying of the ore is required to avoid premature reaction due to the heat of hydration of H_2SO_4. Drying increases energy consumption.

b. **High acid consumption**. From 2.4 to 3.5 tons of concentrated H_2SO_4 are required to produce a ton of TiO_2. The acid is discharged as spent acid (6–9 tons). This high volume of spent acid in some cases is simply neutralised and discharged to the environment (Lynd and Lefond, 1975).

c. **Time consumption**. The whole process can take more than 32 hours (German Federal Environmental Agency, 2001).

d. **Productivity**. The sulfate process is a batch one and, as indicated before, is a time-consuming process, which implies poor productivity.

e. **Environment.** The sulfate process impacts negatively on the environment, due mainly to the huge amounts of pollutants that are discharged into the environment. This includes not only the sulphuric acid already mentioned, but also the disposal of iron by-products and the emission of TiO_2, SO_2 and volatile organic compounds.

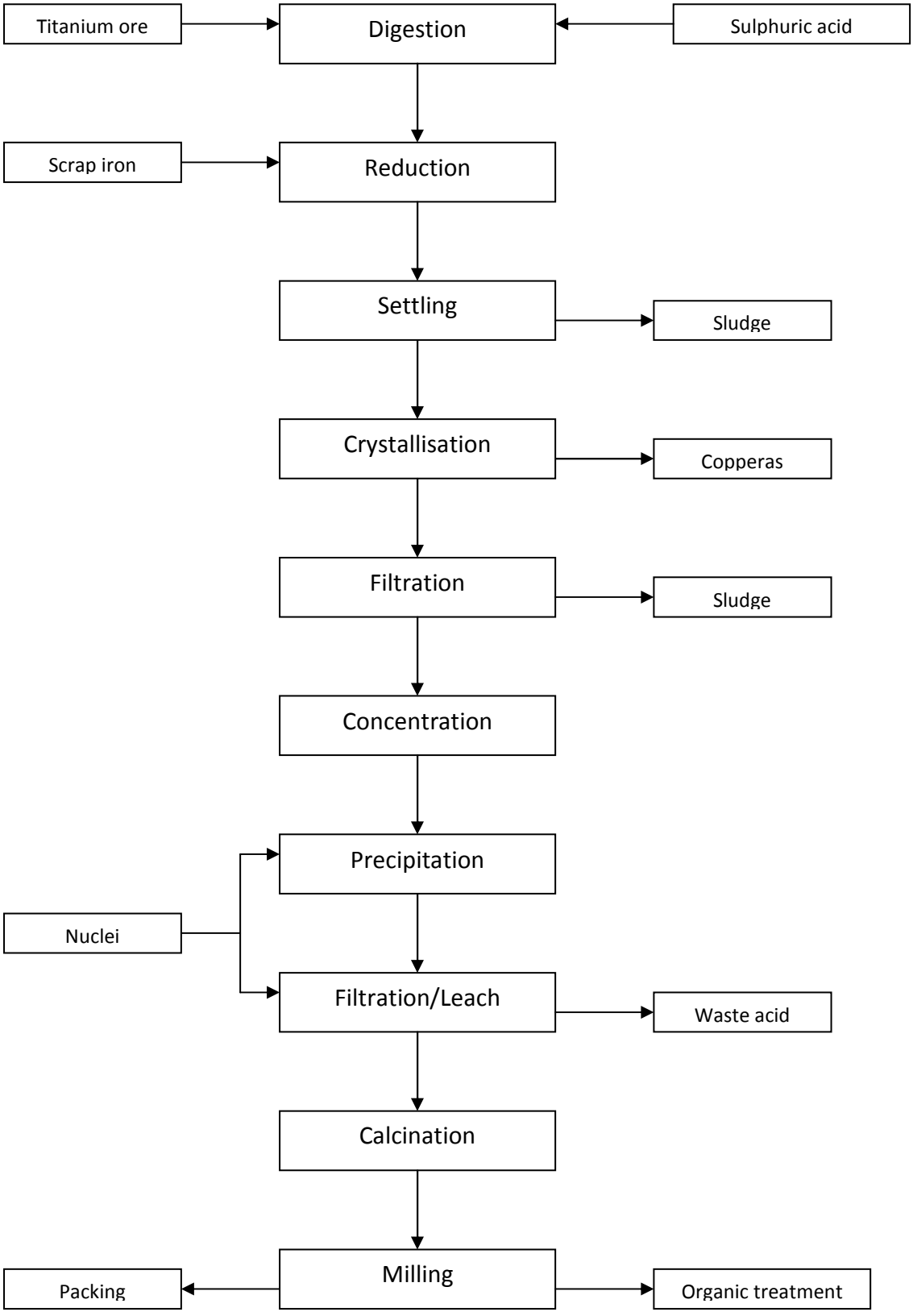

Figure 3: The sulfate process

Part of the titanium sulfate by-product crystallised as copperas is used in water treatment plants and sewerage, as well as in the production of iron oxide pigments. The remainder is disposed of. Attempts to recover sulphur and iron have proved to be technologically, economically or ecologically impracticable. The quantities of iron by-products generated also raise questions concerning their marketability and selling prices (German Federal Environmental Agency, 2001; Lynd and Lefond, 1975).

2.4.2 The Chloride Process

The chloride process (Figure 4) uses mostly slag, rutile, synthetic rutile and, rarely, ilmenite or leucoxene as raw materials. Calcined petroleum coke is used as reducing agent. This coke has low ash content and low volatiles content. This is a continuous process and the main reactions are as given below (Habashi, 1997):

$$TiO_2 + 2Cl_2 + C \rightarrow TiCl_4 + CO_2 + CO \qquad \text{(chlorination)}$$

$$TiCl_4 + O_2 \rightarrow TiO_2 + 2Cl_2 \qquad \text{(combustion)}$$

The chlorination process is conducted at 1 000 °C. Under these conditions, most of the metal chlorides are gaseous. However, the magnesium and calcium chlorides are liquid and clog the chlorination surface bed. Their content in the raw material must not exceed 1% and 0.2% respectively as oxides. SiO_2 must also be kept within certain limits (1.5%) as it coats mineral grains and reduces their reactivity. All the raw materials must be dry to avoid losses of chlorine as HCl. The conversion rate in this process is high, 98–100% for chlorine and 90–100% for TiO_2 (Habashi, 1997; Lynd and Lefond, 1975; Stanaway, 1994).

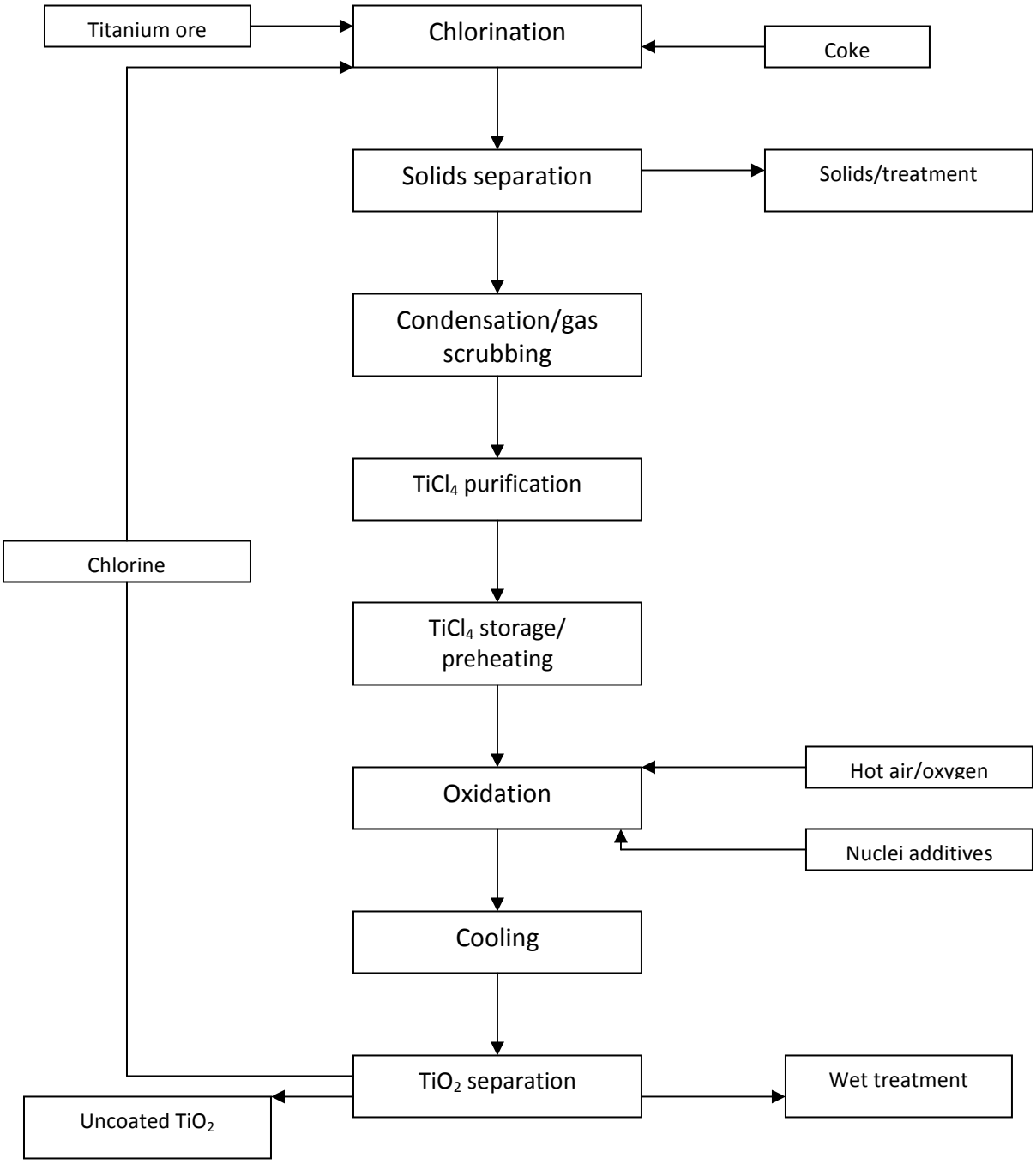

Figure 4: The chloride process

$TiCl_4$, together with other gaseous metal chlorides, combustion gases and residual TiO_2, SiO_2 and petroleum coke, are discharged from the reactor and cooled, by adding cold $TiCl_4$, to a

temperature just above the boiling point of $TiCl_4$. Most of the chlorides condense, are separated from the residual solids and are then dissolved in water. This solution is used in wastewater treatment as precipitation agent, provided it contains mainly $FeCl_2$. If the solution has a different composition, it is neutralised with lime and discharged (Habashi, 1997; Lynd and Lefond, 1975).

$TiCl_4$ is cooled and separated from the gases. The liquid $TiCl_4$ is refined by the addition of a reducing agent and distillation in order to eliminate vanadium. Vanadium, even in trace amounts, gives a yellow colour to the pigment. Small amounts of $AlCl_3$ are added to the purified $TiCl_4$, prior to oxidation, todisrupt the TiO_2 lattice.This prevents paints from chalking. $TiCl_4$ is then burned to TiO_2 in oxygen. Thereafter, the TiO_2 is finally processed to obtain the desired qualities (Habashi, 1997; Lynd and Lefond, 1975).

The chloride process is less harmful to the environment compared with the sulfate process. Like the previous process, the chloride process emits volatile organic compounds that can cause cancer or vomiting and are also responsible for ozone production. Excess ozone causes permanent lung damage.

Chlorine itself is highly corrosive and poisonous. Special reaction vessels are therefore required. The reaction conditions are said to be less flexible and reaction occurs at high temperature (Barton, 1916).

One of the most hampering aspects in the chloride process is the need for raw material with a high titania content. $FeCl_3$ does not have a commercial value and would result in a waste of chlorine. So, for the chloride process there is a need to pre-treat the most abundant source, ilmenite, resulting in additional production costs (Clark, 1968).

Another aspect of concern is related to the inability of the process to produce anatase-type pigment. The chloride process produces only titania of rutile modification (Loughbrough, 1992).

Both the chloride and sulfate processes release particulate pollution as titania dust to the atmosphere. According to the US Environmental Protection Agency (EPA, 2010), one-third of the titania dust inhaled remains in the lungs and can cause lung damage.

Both processes also result in waste sludge that can contaminate local groundwater, resulting in acute toxicological effects or chronic effects such as kidney and liver disease (EPA, 2010).

2.4.3 Surface Crystal Treatment

This procedure is common to the sulfate and chloride processes and is aimed at producing specific properties in the titania crystals required in some applications.

The base pigment is dispersed in water, milled and classified. The desired particle size for pigment applications is approximately 0.2 μm[5]. In order to improve characteristics such as better dispersion, gloss and durability, the titania crystals are coated with aluminium oxide and silica. Zirconia (ZrO_2) is also used as coating material (Qiu and Starr, 2007). This treatment minimises the photocatalytic activity of titania. The coating process is carried out by selective precipitation via time/temperature pH cycles. Coated particles are dried and micronized in organic solvents (Figure 5) (Habashi, 1997; Lynd and Lefond, 1975).

[5]DuPont brochure on coatings (Titanium dioxide for coatings). Available at http://www2.dupont.com/home/en-us/index.html

2.5 Other Processes

Several other processes for titanium recovery have been described in the literature without, however, much attention being paid to commercial use. They are regarded as cumbersome, low yield and involving high energy consumption in general (George and Mohan Das, 1985).

2.5.1 Direct leaching

In direct leaching, titaniferous material is leached in order to selectively dissolve iron and other impurities, enriching its titanium content. In some recent modifications, however, titanium is dissolved instead of iron (Liu *et al.*, 2006). The influencing parameters are acid concentration, temperature, particle size, stirring speed, additives, ratio of ore to acid and pre-treatment.

A concentrate with 90% TiO_2 and 0.8% Fe_2O_3, after leaching of ilmenite (41% TiO_2) at 110 °C, using 20% HCl, for 5 h, was reported (Mahmoud *et al.*, 2004). Iron powder was added at the proportion of 0.1 g per gram of feed. Impurity levels were reported to be 0.12% in total for colouring (MnO_2, Cr_2O_3 and V_2O_5) and 0.08% for chlorine-consuming (CaO, MgO, Al_2O_3) impurities. The process, however, was unable to deal with SiO_2 as 5.8% in the product was reported (Mahmoud *et al.*, 2004).

Using 80% KOH solution, Liu *et al.* (2006) reported solubilisation of 80–85% of titanium at 220 °C with a 7:1 alkali:ilmenite mass ratio.

Iron powder promotes the reduction of Fe^{3+} to Fe^{2+}. An extension to Ti^{4+} - Ti^{3+} reduction is desirable. Titanous ions are believed to have a role in the dissolution of ferric ions (Ibrahim *et al.*, 2003). Ibrahim *et al.* (2003) found approximately 10% iron powder to be optimum, while Lasheen (2005) reported 7%.

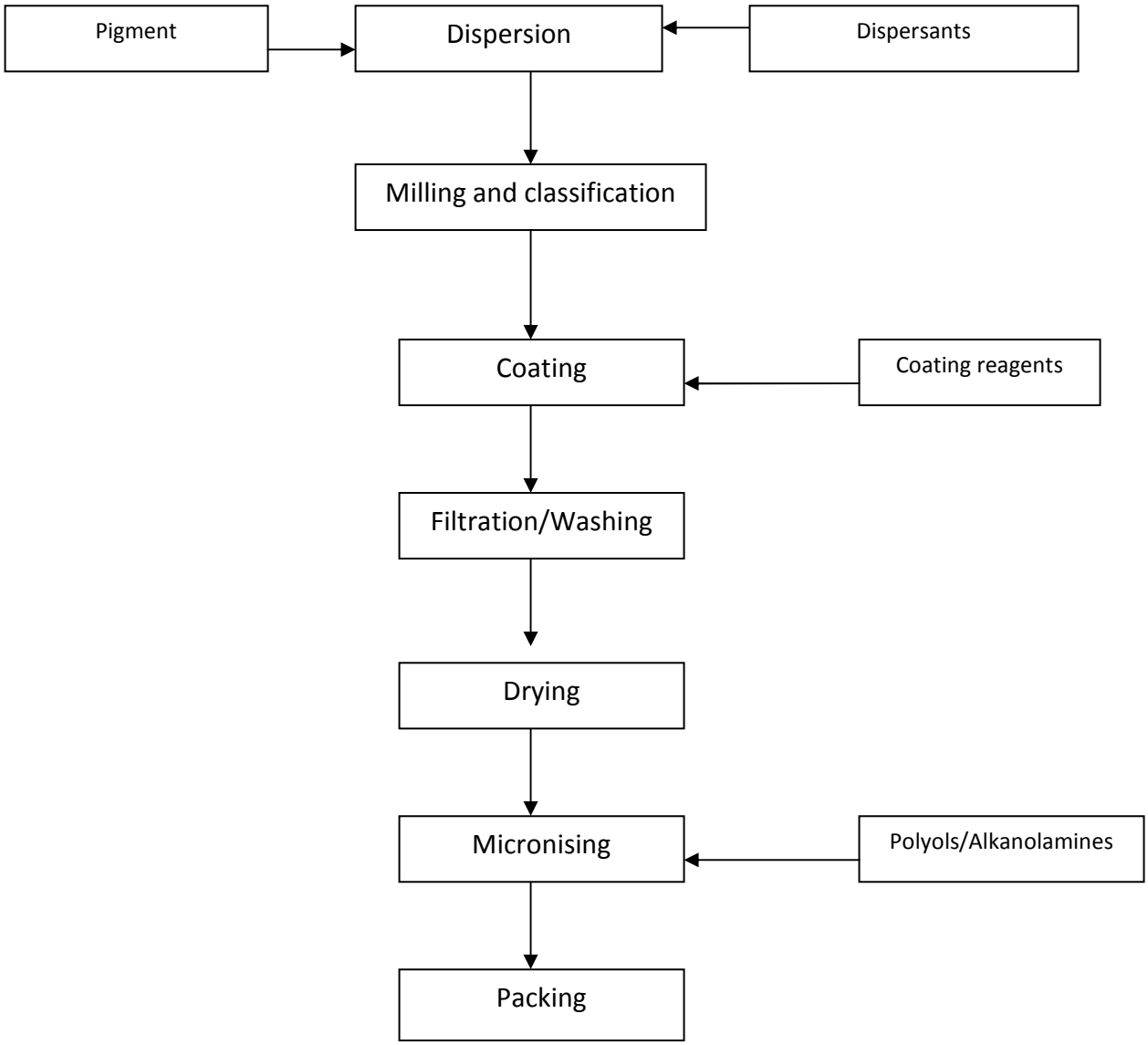

Figure 5: Surface treatment

Oxidation prior to reduction was found to enhance the rate and extent of leaching. Optimum temperatures were reported to be 950 and 850 °C for oxidation and reduction respectively (Sarker *et al.*, 2006; Sinha, 1984).

Ball milling is reported to improve leaching since it reduces particle size and produces particle strain. Combined milling and leaching is said to be very effective (Li *et al.*, 2006b and 2007).

Alcohol solutions were found to lower leaching temperature (Girgin and Turker, 1986). Girgin (1990) found the mixture HCl – CH_3OH to exert a stabilising effect on titanium ions preventing them from hydrolysing (compared to HCl – H_2O and HCl – H_2O – CH_3OH).

Direct leaching can provide concentrates with TiO_2 content as high as 90% (Mahmoud *et al.*, 2004). The main parameters are particle size, acid concentration, temperature, stirring time and speed, acid:ilmenite ratio, presence of additives, as well as pre-treatment.

It was established that ilmenite must be pre-treated, oxidised and reduced (950 and 850 °C respectively) in order to obtain better results. This increases energy consumption. In addition, 10% of iron must be added to the feed. The optimum leaching temperature is about 100–110 °C. Various values for the ilmenite:acid ratio are presented in the literature, although higher ratios seem to be beneficial.

George and Mohan Das (1985) indicated as disadvantageous aspects the need for concentrated solutions of the leachant, extensive leaching times and excessive amounts of leachants, among others. It is important to note that the leaching procedure is intended to produce an intermediate feedstock for pigment processing.

On the other hand, this procedure is unable to tackle the problem of waste in the titanium industry. Iron is leached out as iron chloride or sulfate. In addition, the method is incapable of eliminating or immobilising radioactive impurities and is therefore susceptible to environmental criticism.

2.5.2 Reduction and leaching

In this approach iron in ilmenite is reduced to the elemental state. The elemental iron is then leached out with HCl, leaving TiO_2 as a residue. In some modifications, however, iron reduction is conducted up to the ferrous state. Various reducing agents are used, the most common being hydrogen, coal, coke, carbon monoxide and natural gas. Dilute HCl and H_2SO_4 are the most common leachants, but $FeCl_2$ solution is also used.

Preferentially, ilmenite is oxidised prior to reduction. The oxidation process is intended to make the ore composition uniform. Natural ores contain a mixture of different oxides, giving rise to different rates of reduction and sometimes, to a lesser extent, of iron dissolution. Oxidation reportedly produces lattice strain, which enhances leaching (George and Mohan Das, 1985; Sarker *et al.,* 2006).

El-Tawil *et al.* (1996) roasted ilmenite with carbon in the presence of Na_2CO_3. The addition of Na_2CO_3 was aimed at increasing the reduction rate and coarsening the iron. The optimum amount was found to be 20% to the feed. Roasting was conducted at 1 000–1 200 °C for 0.5–3 h.

Sinha (1984) and George and Mohan Das (1985) reported 850 °C to be the optimum reduction temperature, although Zhang *et al.* (2007) reported 1 300 °C. For oxidation the optimum was reported to be approximately 950 °C (George and Mohan Das, 1985; Sinha, 1984).

Kucukkaragoz and Eric (2006) found the first stage of the reaction to comprise Fe^{3+} reduction to Fe^{2+} and Fe and the formation of Fe_3C, as well as the reduction of Ti^{4+} to Ti^{3+}. The second stage encompasses the reduction of Ti^{3+} to Ti^{2+} and eventually the formation of the TiO_{1-x} oxygen-deficient phase (Kucukkaragoz and Eric, 2006).

This process produces TiO_2 feedstock to both chlorination and sulfation. George and Mohan Das (1985) pointed out the ability of the process to be commercially exploited, the use of coal as reductant and energy source, and the flexibility to operate in a continuous fashion as the main advantages. The fact that two stages are involved is the only disadvantage they pointed out (George and Mohan Das, 1985). The inability to tackle environmental issues is another disadvantage that should be added. The sole purpose in all the work reported on this process was to extract iron and enrich the TiO_2 content. Impurities such as Al, Si and P, as well as radionuclides, are not mentioned. In reducing roasting, chromium forms chromite species, which are not leachable and remain in the residue as pointed out by Tathavadkar and Jha (2004).

2.5.3 Dissolution

Dissolution techniques involve the solubilisation of both iron and titanium, using mineral acids, generally. The solvents mainly used are hydrochloric and sulphuric acid. The reaction in each case can be described by the following equations:

$$FeTiO_3 + 2H_2SO_4 \rightarrow Fe^{2+}(aq) + TiO^{2+}(aq) + SO_4^{2-} + 2H_2O$$

$$FeTiO_3 + 4HCl \rightarrow Fe^{2+}(aq) + TiO^{2+}(aq) + 4Cl^{-} + 2H_2O$$

The most influential parameters are acid concentration, particle size, ratio of ilmenite to acid, temperature, stirring speed and additives. These individual parameters will now be reviewed since the proposed method relies partially on the dissolution reaction.

Extended milling also improves ilmenite dissolution in mineral acids. According to Welham and Llewellyn (1998) milling has the effect of reducing the particle size and in the crystallite size. This is considered to enhance the mass transport phenomenon by increasing the number of grain boundaries.

A. Effect of acid concentration

Ilmenite dissolution, in general, increases with acid concentration. Han *et al.* (1987) observed a maximum at 14 M with H_2SO_4. This was attributed to the peaking of H^+ ion concentration at this acid concentration. In concentrated solutions, $TiOSO_4$ and $FeSO_4$ tend to cover the surface of the crystals, hindering further reaction. In dilute solutions, the products are dissolved, leaving the surface available for further reaction (Han *et al.*, 1987). Li *et al.* (2007), however, observed a steady situation while working with dilute acid solutions. Dissolved Ti did not change with time in weaker solutions and in the case of 20% solution, the Ti in solution even dropped (Li *et al.*, 2007).

El-Hazek *et al.* (2007), using HCl as solvent, reported 12 M as the optimum. Lower concentrations, 7 M HCl, resulted in the dissolution of much of the Fe, while Ti remained in approximately half of the Fe dissolved. Hydrolysis of TiO_2^{2+} was suggested as the reason for this (El-Hazek *et al.*, 2007). Van Dyk *et al.* (2002) reported conflicting results. Quoting an earlier work from Hussein*et al*. (1976) they report dissolution of mainly iron by HCl, while from Jackson and Wadswoth (1976) it was reported dissolution of both titanium and iron (van Dyk *et al*., 2002).

Biswas and Mondal (1987) found hydrofluoric acid (HF) to be the most effective dissolution agent. They determined the optimum concentration as 6.4 M at boiling point, at a 1:20 solid:liquid ratio. They reported that after 5 h, 81% Ti had dissolved and 26% of Fe. Hansen and Traut (1989) and Olanipekun (1998) found the leaching rate to be linearly dependent on HF concentration and that Ti leached much faster than Fe, independent of the stirring speed. The dissolution rates were found to be consistent with the reaction-controlled kinetic model (Hansen and Traut, 1989; Olanipekun, 1998).

B. Effect of particle size

It is commonly accepted that the leaching rate is inversely affected by particle size, i.e. the larger particles will dissolve slowly compared with the fine ones (Han *et al.*, 1987; Hansen and Traut, 1989; El-Hazek *et al.*, 2007; Olanipekun, 1999).

It is important to note, however, that this effect is also related to slurry density. El-Hazek *et al*. (2007) found that leaching rate was inversely related to slurry density. Working with 12 M HCl they were able to dissolve 92% of titanium at 1/20 slurry density (molar acid/ilmenite ratio). Using a slurry solids-to-liquid ratio of 9/1 only 11% of titanium was dissolved. Apparently this is also connected to the acid concentration as well as to titanium concentration in solution. Lower acid concentrations ($[H_3O^+] < 0.5$ M) coupled with high titanium concentration ($[Ti(IV)] > 10^{-3}$ M) lead to titanium polymerization, reducing therefore titanium solubility, due to lower mobility of polymerized titanium species formed in solution (Nabivanets and Kudritskaya, 1976; van Dyk *et al*., 2002).

The particle size can also play a role on slurry density effect. Lower densities (higher liquid:solid ratios) particle size will not affect the dissolution process, whereas at higher densities it does.

C. Effect of ilmenite to acid ratio

Li *et al.* (2006b) reported a positive influence when the ratio of ilmenite to acid (w/w) increased from 1:1.4 to 1:1.6 (0.1 increments). Above that point no increase was observed (Li *et al.*, 2006b). El-Hazek *et al.* (2007) reported similar behaviour. Sasikumar *et al.* (2007), however, did not observe any effect (ratios of 1:10 and 1:100).

The critical factor here is acid (H_3O^+) and titanium (Ti(IV)) concentration in solution as was observed by Nabivanets and Kudritsakaya (1976) and van Dyk (2002). Polymerisation leads to

reduced diffusion of titanium species in solution. The polymerisation can lead eventually to $TiOCl_2$ precipitation, depending on Cl^- and Ti(IV) concentration in solution.

D. Effect of temperature

In all three systems, HCl – $FeTiO_3$, HF – $FeTiO_3$ and H_2SO_4 – $FeTiO_3$, reported results show an increase in the rate and extension of dissolution. Biswas and Mondal (1987) reported this finding in the HF – $FeTiO_3$ system, while Olanipekun (1999) and El-Hazek *et al.* (2007) reported it in the HCl system.

El-Hazek *et al.* (2007) observed a maximum reaction at 80 °C (98% Ti) and suggested that this should be considered the optimum for the reaction. Their results indicate a decreasing reaction with a further increase in temperature due to Ti polymerisation and hydrolysis enhancement without affecting iron (El-Hazek *et al.*, 2007).

Li *et al.* (2006b) reported an increase up to 120 °C. Using 100% H_2SO_4, 80% Ti was dissolved after 2 h. A decline was observed due to hydrolysis afterwards. Li *et al.* (2007), using dilute solutions (5–20% H_2SO_4), found that iron dissolution increased with temperature while the percentage of Ti decreased.

E. Effect of stirring speed

Tushida *et al.* (1984) and Olanipekun (1999) found ilmenite dissolution to be independent of stirring speed, using 11.4 M HCl at 70 °C, a 1:69 ilmenite:acid mole ratio, and 7.2 M HCl at 70 °C, respectively.

Jonglertjuania and Rubcumintara (2012) studied the leaching of ilmenite in sulphuric acid (4 M) at 90 °C, using three different stirring speeds (250, 500 and 750 rpm). They obtained the best results at 750 rpm (14.5% of titanium). They attributed this direct relation between titanium

dissolution and stirring speed to the turbulence created in the leaching area. The higher the intensity of the turbulence, the higher the dissolution rate was.

Nayl *et al*. (2009) leaching ilmenite treated with KOH with 6 M sulphuric acid at 150 °C concluded that above 375 rpm the dissolution rate was independent on the stirring speed. The study was conducted on 105 – 74 µm ilmenite on the range of 50 to 500 rpm.

F. Effect of additives

Duncan and Metson (1982) reported Ti dissolution to be seriously affected by additives, attributing this to the chemistry of Ti ions in solution.

Girgin (1990) found better results using HCl in CH_3OH compared with aqueous solutions with or without CH_3OH added. It was then indicated that HCl – CH_3OH exerted a stabilising effect on Ti ions.

Ibrahim *et al.* (2003) found iron powder addition to be beneficial in ilmenite leaching. This was later confirmed by Mahmoud *et al.* (2004) and Lasheen (2005).

2.5.4 Oxidative roasting/fusion

Ilmenite is fused with an alkaline and/or an alkaline earth metal compound to produce, mainly, oxides of iron and titanium. The metal impurities can be in the oxide form or not. The fused product is subjected to selective leaching or complete dissolution of both iron and titanium, followed by separation methods.

In earlier developments, ilmenite was fused with alkali metal compounds or hydroxides in the presence of reductants. The product was leached with dilute mineral acid or water. The residue was calcined to give titania (Barksdale, 1966; George and Mohan Das, 1985).

Sadykhov *et al.* (1994) investigated the effect of Na_2O on the reduction of low-titanium titanomagnetite ore by hydrogen at 700 – 1 200 °C. They found that Na_2O was used mainly to bind SiO_2 into aluminosilicates, while FeO, MgO and CaO were displaced from the silicate phase. Excessive amounts of Na_2O as well as low temperatures (≤ 900 °C) resulted in the formation of bronzes. Higher temperatures (≥ 1 100 °C) favoured sodium titanates (Sadykhov *et al.*, 1994).

In a subsequent report, Sadykhov *et al.* (1998) studied the effect of aluminosilicates such as nepheline ($NaAlSiO_4$) and albite ($NaAlSi_3O_8$), and other phases such as $MgAl_2O_4$, anosovite ($Me^{3+}TiO_5.MgTi_2O_5$, Me^{3+}= Fe, Al, or Mn), titanium lovingerite isostructural, $Ca(Fe, Mn, Mg)_8Ti_{13}O_{38}$ and titanium bronzes $Na_2(Fe, Mn)_2Ti_nO_{2n+4}$ ($6 \leq n \leq 8$), as well as free rutile on autoclave leaching with sulphuric and hydrochloric acid (25–45% H_2SO_4, 180–200 °C). Vanadium was selectively extracted by roasting with soda. They found albite and titanium bronzes to be inert.Titanium bronzes did decompose at much more severe conditions (65–75%, 220 °C). Bronzes are a series of sodium iron titanates with general formula Na_xTiO_2 or $Na_{4+x}Ti_{5-x}O_{12}$ (Nalbandyan *et al.*, 1998; Reid and Sienko, 1967). An insoluble phase was released, $TiO_2.0,1Fe_2O_3.1,3SO_3$ (Sadykhov *et al.*, 1998).

El-Tawil *et al.* (1996) applied Na_2CO_3 in the reduction of ilmenite ore in carbon. They observed an enhancement in ilmenite reduction efficiency. A maximum metallisation of 85% at 1 200 °C using 30% Na_2CO_3 was reported. The rest of the iron was accommodated in sodium iron titanates (El-Tawil *et al.*, 1996).

Biswas *et al.* (1996) roasted ilmenite ore with salt-water vapour and leached the product with HCl. Yields of 73%, 96% (NaCl), 35%, 56% (Na_2SO_4) and 87%, 71% ($NaNO_3$) were achieved for titanium and iron respectively. The roasting was conducted at 800 °C (885 °C for Na_2SO_4), for 90 min, for $NaNO_3$ and Na_2SO_4 (75 min for NaCl) and a ratio of 0.67 ilmenite to salt for NaCl (Biswas *et al.*, 1996).

De Matos *et al.* (2002) used anatase to produce artificial ilmenite to enable it to be used in current processing methods. They roasted anatase ore with Na_2CO_3 or K_2CO_3. No reducing agents were used to avoid iron solubilisation. The fusion was intended to convert aluminium, silicon and phosphorus into soluble forms. The fused product was leached with alkaline solution (pH ≈ 10) for 60 min at 60–90 °C. The leached cake was calcined at 900–1 300 °C for 20 to 60 min. The calcined product was again leached with HCl or H_2SO_4 (> 50 g/l) for 20–240 min at 60–90 °C. The final product, artificial ilmenite, contained 50% TiO_2 and 41% Fe_2O_3 as reported, which corresponded to 100% and 94% recoveries respectively. Impurity metal valuables (Al_2O_3, P_2O_5 and SiO_2) were reported to be recoverable from the leach liquor (de Matos *et al.*, 2002).

Borowiec *et al.* (2003), in a process claimed to be appropriate for ores with substantial contents of iron, manganese, chromium, vanadium, aluminium, silicon and alkaline earths, oxidised slag at 950 °C to decompose silicate glassy phases. The oxidised slag was afterwards reduced at 700 °C for 30 min, to reduce only iron. The calcined and subsequently reduced slag was leached with mineral acid at 125 °C under pressure. The final product was washed and calcined again at 600–800 °C (Borowiec *et al.*, 2003).

Hollit *et al.* (2003) applied the fusion method to remove radioactive impurities. They fused titaniferous ore with alkali metal compounds and boron, such as borax, caustic soda, soda ash and silica, at temperatures less than 1 300 °C for 4 h. The product was cooled slowly in order to avoid crystallisation. The alkali metal compounds were added in order to ensure the formation of glassy phases, while borax was added to avoid the formation of alkali ferric titanates and sodium titanate bronzes ($NaTiO_3$). Phosphorus compounds can also be used for this purpose. In cases where the titaniferous material proved to contain such components, no additive was used. Alkali ferric titanates and sodium titanate bronzes are reportedly not amenable to leaching. The solidified phase was leached with acid or alkali solution. A product with a 96% TiO_2 content was reported (Hollit *et al.*, 2003).

Jha *et al.* (2010) mixed titaniferrous ore with Na_2CO_3 or K_2CO_3, or the mixture of both, CaO (1–4%) and alumina (20%). The mixture was roasted at 950 °C for 120 min. The roasted mass was leached with hot water at 80 °C for 40 min. The residue was persistently washed until pH 7 was achieved. As impurities (Fe, Al, Nb, U, Th and rare earths) may be precipitated as hydroxides from the leachate, the pH was adjusted by adding ammonium salts. Controlled precipitation was conducted by bubbling CO_2 or by organic acid addition. The solid titania residue was leached with 5% HCl at 70 °C for 10 min. It was then washed with dilute acid solution. The leachate solution was found to contain Nb, U, Zr and REE. The solid residue was dried and mixed with $NaHSO_4$ or $NaHCO_3$ and roasted at 300 °C in air for 1 h. The roasted residue was then water leached at 80°C for 30 min and washed until pH 7 was achieved. The final residue was dried (Jha *et al.,* 2005).

Lahiri *et al.* (2006) fused ilmenite with Na_2CO_3 in stoichiometric proportions at 873–1173 K for 4 h. The fused ilmenite was leached with water for 30 min. The authors reported the formation of Na_2TiO_3 and Na_4TiO_4 in the fused product at 600 and 700 °C respectively. Na_2CO_3 was also reported to be present in the fused product. The conversion achieved was around 50% (Lahiri *et al.*, 2006).

In another modification, Jha and Thatavadkar (2009) alkali roasted a titaniferous ore with alumina and calcium oxide sources. The roasted material was leached in water or alkali solution (to enhance selectivity in leaching). The residue was leached with acid to remove CaO and Al_2O_3. The residual solid was essentially TiO_2. Further purification was effected by fusing it with $NaHSO_4$ or $NaHCO_3$, followed by water leaching. TiO_2 with 95% purity was reported. Metal contaminants (Al_2O_3, CaO, V_2O_3, Fe_2O_3 and Cr_2O_3) were recovered from the leaching aqueous solution by acidification (Jha and Thatavadkar, 2010).

In recent years, the focus of studies on oxidative roasting has been on extracting impurities such as aluminium, chromium, silicon, phosphorus, vanadium, calcium and magnesium, as well as radionuclides (uranium and thorium), among others. These impurities are converted into soluble forms and can therefore be leached out, leaving the material free of their hazardous effect. Some of these impurities have been the deterrents for using some of the ores (Jha *et al.*, 2005; de Matos *et al.*, 2002; Nielsen and Chang, 1996; Smith and de Castro 2007).

The fusion product can be selectively leached with either alkali or acid. In this approach the product is intended to be processed further, to be used as a feedstock for currently used techniques. This implies additional steps which will result in a costly end-product.

The main intention with slagging is to separate iron from ilmenite. Other impurities remain in the slag (Hollit *et al.*, 2003; Jha *et al.,* 2005; de Matos *et al.*, 2002; Smith and de Castro, 2007). There is also uncertainty about slagging due to its high power consumption and greenhouse gas emissions (Jha *et al.,* 2005). In addition, with increasingly stringent environmental regulations regarding radioactive levels in spent liquors, wastes and pigment-containing products, there will be increasing pressure on the pigment producers to use feed stocks with lower radionuclide contents (Doan, 2003).

Another interesting feature of the fusion/roasting process is the possibility of producing phases that can be regarded as radionuclide immobilisers. Zirconolite $[(Ca, Fe, Y, Th)_2(Fe, Ti, Nb)_3Zr_2O_7]$ and hiarnite $[(Ca, Mn, Na)_2(Zn, Mn)_5(Sb, Ti, Fe)_2O_{16}$ are such phases (de Hoog and van Bergen, 1997; Jha *et al.*, 2005).

However, the aforementioned methods are affected mainly by the following disadvantageous aspects:

- Multiple steps are involved in these methods.

- The fusion temperatures are considerably higher, bearing in mind that they are intended to pre-treat the raw material.

In some approaches a pre-treated (slag) feedstock was used. This simply means that the challenging problems related to slag production, as indicated earlier, remain.

George and Mohan Das (1985) indicated energy consumption, the corrosive nature of the melt and low yields as, essentially, the major drawbacks for development of the fusion process on a commercial scale. It is worth pointing out that the average fusion temperature is comparable to that of slagging. The slagging process also involves dealing with the corrosiveness of chlorine gas, as well as of alkali in chlorine gas production. The major challenging aspect is therefore the improvement of recovery levels. However, the fusion procedure does tackle, as established, the challenging aspect of radioactive waste (de Hoog and van Bergen, 1997; Jha *et al.*, 2005).

2.5.5 Remarks on Titania Technology

It seems obvious from the brief review presented in this chapter that the titanium industry is surrounded by environmental and operational challenges. Although on the one hand, the chloride process presents a partial solution to the iron waste problem presented by sulfate process, on the other hand the process itself is faced with high energy consumption and highly corrosive reactants, leading to a short life-time for the equipment. Furthermore, there is the already indicated problem of greenhouse gas emissions and the inability to eliminate or immobilise radioactive impurities (Jha *et al.,* 2005; Hollit *et al.*, 2003; de Matos *et al.*, 2002). The chloride process as it now operates is unable to treat different types of raw material (Habashi, 1997; Murphy and Frick, 2006; Pong *et al.*, 1995).

It was pointed out that in a considerable number of titania applications the anatase form is preferable. The chloride process is incapable of producing pigments with anatase crystal

structure, i.e. incapable of anatase modification (Loughbrough, 1992; Murphy and Frick, 2006). This reality means that the sulfate route will continue coexisting with the chloride one. The task now is to reduce the environmental burden of the sulfate process, as well as to make it more economically viable, producing in a cost-effective way. In addition, it has to be updated in manner that will enable it to deal with most, if not all, types of ore. This is the main goal of the investigation presented here.

2.6 Phase Diagrams

The alkali fusion reaction of ilmenite can produce a mixture of alkali titanates and alkali iron titanates. The relative proportion of different phases is dependent on the mole ratio of ilmenite to alkali, temperature and reaction time. Alkali phases releasing proportionally high quantities of titanium are preferred.

2.6.1 System Na_2O–TiO_2

Sodium titanates have been extensively investigated due to their applicability in photocatalysts, fuel cell electrolytes, ion exchange processes, ceramic capacitors, as dielectric resonators in microwave oscillator band pass filters, reinforcing agents of plastic, oxygen sensors and as adiabatic materials. Some are effective in the separation of radioactive nuclides (Meng *et al.,* 2004; Ramírez-Salgado *et al.,* 2004). Nevertheless, there is controversy regarding the phases occurring in this system (Bamberger and Begun, 1987; Hill *et al.*, 1985; Mitsuhashi and Fujiki, 1985; Nalbandyan, 2000).

Most of the titanates can be grouped into two series, namely $Na_2Ti_nO_{2n+1}$ and $Na_4Ti_nO_{2n+2}$. For the previous series ($Na_2Ti_nO_{2n+1}$) compounds with n = 1–9 are known or merely reported, while

for the latter series only compounds with *n* = 1, 3, 5 and 9 are reported (Clearfield and Lehto, 1988).

The partial phase diagrams published by Bouaziz and Mayer (1971) and Gicquel *et al.* (1972) seem to have been commonly approved (Figure 6) (Bamberger and Begun, 1987; Glasser and Marr, 1979; Roth *et al.*, 1981). These include the Na_2TiO_3 (α and β), $Na_8Ti_5O_{14}$, $Na_2Ti_3O_7$, $Na_2Ti_6O_{13}$, Na_4TiO_4 and $Na_6Ti_2O_7$ phases. Previous literature, however, included Na_2TiO_3 and $Na_2Ti_2O_5$, as reported in the reference literature (*Gmelins Handbuch*, 1951).

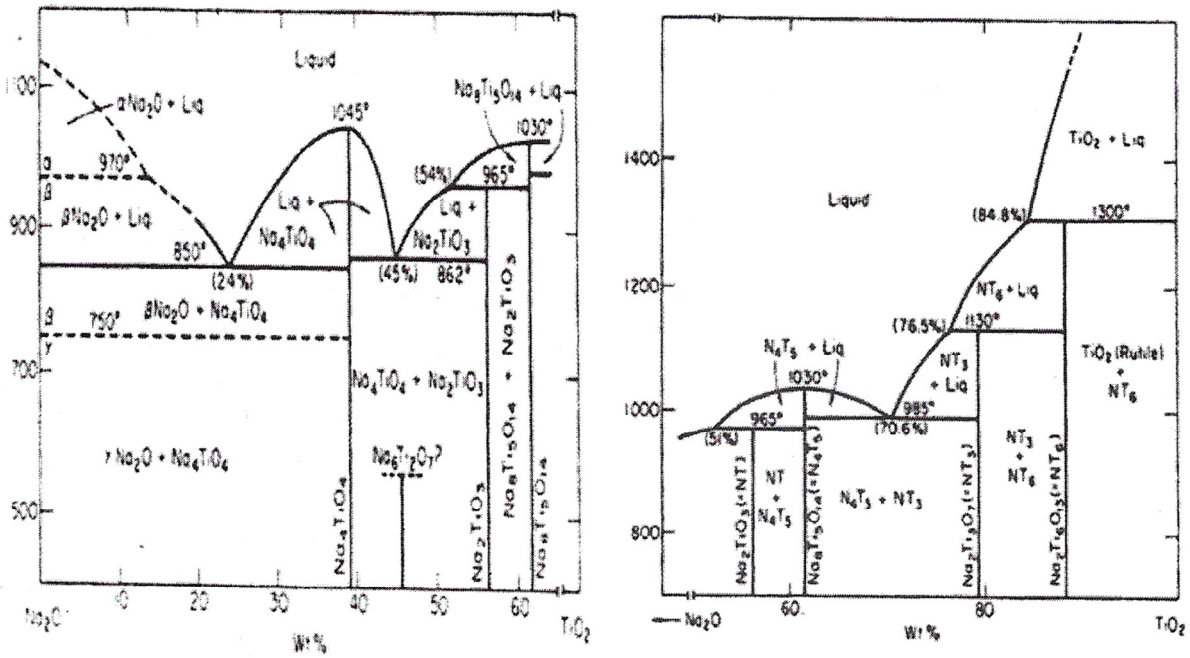

Figure 6: Na_2O – TiO_2 phase diagrams (Bouaziz and Mayer, 1971; Gicquel *et al.*, 1972)

Anderson and Wadsley (1961) identified the phase they obtained by fusing Na_2CO_3 and TiO_2 (1:2 mole ratio) at 1 300 °C as $Na_2Ti_3O_7$. The same phase was reported to have been produced hydrothermally (Watanabe, 1981). Ramírez-Salgado *et al.* (2004) reported the synthesis of

$Na_2Ti_3O_7/Na_2Ti_6O_{13}$ and $Na_2Ti_6O_{13}/TiO_2$ mixtures by the sol-gel method using alkoxide precursors.

Plumley and Orr (1961) claimed to have produced $Na_2Ti_6O_{13}$ by metatheses of $K_2Ti_6O_{13}$ with NaCl. In fusing the mixture of Na_2CO_3 and TiO_2 (1:6 mole ratio) at 1 300 °C, Anderson and Wadsley (1962) reported the production of $Na_2Ti_6O_{13}$. The same result was claimed by Anderson and Wadsley (1962) on heating $Na_2Ti_3O_7$ (950 °C). Sauvet *et al.* (2004) reported the production of $Na_2Ti_3O_7$ and $Na_2Ti_6O_{13}$ by the sol-gel method. $Na_2Ti_3O_7$ was found to decompose into $Na_2Ti_6O_{13}$ upon heating, as previously observed by Anderson and Wadsley (1962) (Sauvet *et al.*, 2004). Watanabe (1981) and latterly Seo *et al.* (2004) reported the hydrothermal synthesis of $Na_2Ti_6O_{13}$ from TiO_2 and NaOH solutions at mild temperatures (between 250 and 350 °C).

Belyaev and Golovanova (1962) studied the system $Na_2O – TiO_2 – V_2O_5$ and identified Na_2TiO_3, $Na_8Ti_5O_{14}$ and $Na_2Ti_3O_7$ in the $Na_2O – TiO_2$ side of the system, by X-ray diffraction. Belyaev and Belyaeva (1965) found $Na_8Ti_5O_{14}$ along with Na_2TiO_3 in the NaCl-Na_2TiO_3-TiO_2 system. They also suggested the existence of $Na_2Ti_3O_7$ in this system.

Batygin (1967), studying the formation of titanates from NaOH+TiO_2 mixtures, concluded that the XRD data attributed to metatitanate (Na_2TiO_3) was, in fact, that of $Na_8Ti_5O_{14}$. This observation was later supported by Glasser and Marr (1979). Batygin (1967), in the same report, heated Na_2TiO_3 and observed the broadening of the lines d = 2.25 and 2.60, giving an indication of the formation of $Na_8Ti_5O_{14}$.

Batygin (1967) identified the product of 1:2 mole ratio (Na_2O:TiO_2) fusion at 700 °C (for prolonged times) as $Na_2Ti_2O_5$, since the XRD pattern did not show similarities to known titanates. He also reported that, on heating, dititanate ($Na_2Ti_2O_5$) transforms into $Na_8Ti_5O_{14}$. It was pointed out that this finding had prevented other researchers from producing $Na_2Ti_2O_5$

(Batygin, 1967). Belyaev *et al.* (1970) described the formation of $Na_2Ti_2O_5$ along with $Na_8Ti_5O_{14}$ and $Na_2Ti_4O_9$ as an intermediate stage in the formation of Na_2TiO_3 in mixtures of Na_2CO_3 with TiO_2 (1:1 mole ratio). Bouaziz and Mayer (1971) expressed some concern about the existence of $Na_2Ti_2O_5$.

According to Batygin (1967), the XRD pattern assigned to sodium pentatitanate ($Na_2Ti_5O_{11}$) in the ASTM[6] index, allegedly taken from Plumley and Orr (1961), belongs to a mixture of pentatitanate and hexatitanate, since it was recorded from a mixture in which $Na_2Ti_6O_{13}$ was the dominant phase. Glasser and Marr (1979) indicated that the pattern under debate belonged to the mixture of $Na_2Ti_3O_7$ and $Na_2Ti_6O_{13}$. This ultimate correction was rejected by Bamberger and Begun (1987). They tried to synthesise $Na_2Ti_5O_{11}$ as reported by D'Ans and Löfler (1930), using mixtures of Na_2CO_3 and TiO_2 (1:2) at 1 100 °C and cooling slowly. A mixture of $Na_2Ti_3O_7$ and $Na_8Ti_5O_{14}$ was obtained. Trials with 1:5 mixtures at 900 °C produced mixtures of $Na_2Ti_3O_7$ and $Na_2Ti_6O_{13}$ (Bamberger and Begun, 1987).

Wadsley and Mumme (1968) reported isolation of $Na_2Ti_7O_{15}$ crystals after heating a mixture of $Na_2C_2O_4$, Al_2O_3 and TiO_2 (1:1:2 mole ratios). They believe that $Na_2Ti_7O_{15}$ and $Na_2Ti_8O_{17}$ cannot be obtained by a single oxides mixing and heating experiment. The sole prediction was $Na_2Ti_8O_{17}$. $Na_2Ti_7O_{15}$ was believed to result from the decomposition of $Na_2Ti_6O_{13}$, according to the following equation (Wadsley and Mumme, 1968):

$$7Na_2Ti_6O_{13} \rightarrow 6Na_2Ti_7O_{15} + Na_2O$$

Belyaev *et al.* (1970) established the nature of an intermediate phase initially denominated by β-titanate as $Na_4Ti_3O_8$. This phase decomposes into $Na_8Ti_5O_{14}$ and $Na_2Ti_3O_7$ (Belyaev *et al.*, 1970). Furthermore, as indicated previously, they found $Na_8Ti_5O_{14}$, $Na_2Ti_2O_5$ and $Na_2Ti_4O_9$ to be intermediates in Na_2TiO_3 formation. Surprisingly, $Na_2Ti_4O_9$ (sodium tetratitanate) is indicated as one of the intermediates without any supporting substantiation in the text. Dion *et al.* (1978),

[6] American Standards and Testing Materials

however, reported the preparation of $Na_2Ti_4O_9$ by metatheses of $Tl_2Ti_4O_9$ with NaCl. Later, Akimoto and Takei (1989b) reported this from mixtures of Ti_2O_3 and Na_2O, and Watanabe (1981) reported the hydrothermal synthesis of $Na_2Ti_4O_9$ from TiO_2 and NaOH at 250–350 °C. Sun *et al.* (2002) observed that $Na_2Ti_4O_9$ hydrothermally produced decomposes into $Na_2Ti_3O_7$ and $Na_2Ti_6O_{13}$ at 900 °C.

Belyaev (1976) analysed sodium metatitanate formation from Na_2CO_3/TiO_2 mixtures. He concluded that the reaction proceeded via successive reactions of Na_2CO_3 and TiO_2 with $Na_2Ti_2O_5$, $Na_4Ti_3O_8$ and $Na_8Ti_5O_{14}$ intermediates. The reaction of Na_2CO_3 with $Na_8Ti_5O_{14}$ was indicated to be the determinant stage. According to Belyaev (1976), $Na_8Ti_5O_{14}$ possesses a compact layer which is resistant to Na^+ and O^{2-} diffusion.

Glasser and Marr (1979) were unable to produce $Na_2Ti_2O_5$, $Na_2Ti_5O_{11}$ and $Na_2Ti_7O_{15}$ as reported earlier (*Gmelins Handbuch*, 1951). These authors claim to have crystallised $Na_6Ti_2O_7$ from melts containing 46–48% mol of TiO_2 as bright green crystals. Hill *et al.* (1985), however, identified these green crystals as γ-Na_2TiO_3 by electron microprobe analysis. $Na_2Ti_2O_5$ and Na_2TiO_3 were reported to have been produced from mixtures of TiO_2 powder and 4 N NaOH solutions for 10 h at 1 020 and 1 080 K respectively (Mitsuhashi and Fujiki, 1985).

Watanabe *et al.* (1979) reported the synthesis of $Na_2Ti_9O_{19}$ by hydrothermal means, using TiO_2 gel with NaOH aqueous solution, at 450–600 °C. Watanabe (1981) also reported hydrothermal synthesis of $Na_2Ti_9O_{19}$ at 250–530 °C. The product was identified by electron microprobe analysis and single-crystal XRD.

Werthmann and Hoppe (1984) claim to have synthesized a new titanate, $Na_4Ti_5O_{12}$, from mixtures of TiO_2 and Na_2O at 1 000 °C in an Au crucible after 6 days of fusion. Nalbandyan *et al.* (1998) determined the existence conditions of $Na_4Ti_5O_{14}$. They found it to decompose at 900–950 °C into $Na_2Ti_3O_{14}$ and $Na_8Ti_5O_{14}$. Nalbandyan (2000) later determined the unit cell

parameters of $Na_4Ti_5O_{14}$. He concluded that the XRD pattern previously attributed to disputed $Na_2Ti_2O_5$ belonged, in fact, to $Na_4Ti_5O_{14}$ (Bamberger and Begun, 1987; Bouaziz and Mayer, 1971; Glasser and Marr, 1979). Avdeev and Kholkin (2000) resolved the crystal structure of $Na_4Ti_5O_{12}$.

Bamberger and Begun (1987) admitted Na_4TiO_4, α, β and γ Na_2TiO_3, $Na_8Ti_5O_{14}$, $Na_2Ti_3O_7$ and $Na_2Ti_6O_{13}$ as the only existing phases in the system $Na_2O - TiO_2$. They considered the existence of phases such as $Na_2Ti_2O_5$, $Na_4Ti_3O_8$ and $Na_6Ti_2O_7$ as an artefact. They failed to produce $Na_2Ti_2O_5$ as previously described by other researchers (Mitsuhashi and Fujiki, 1985). According to Bamberger and Begun (1987), the product previously denominated $Na_2Ti_2O_5$ was, in fact, a mixture of $Na_2Ti_3O_7$ and $Na_8Ti_5O_{14}$, identified by Raman spectroscopy. In their review, Bamberger and Begun (1987) point out some questionable cards on the powder diffraction file, namely the Na_2TiO_3, $Na_4Ti_{0.3}O_{2.6}$ and $Na_2Ti_5O_{11}$. They considered the typing of $Na_4Ti_{0.3}O_{2.6}$ in that card as a typographical error since the original reference indicated $Na_4Ti_3O_8$ (considered by Bamberger and Begun not to exist).

Clearfield and Lehto (1988) reacted NaOH with anatase or titanium isopropoxide via hydrothermal reaction and reported $Na_4Ti_9O_{20}.xH_2O$, based on the neutron activation analysis and XRD pattern of the product.

Yang *et al.* (2003) concluded that the nanotube synthesised hydrothermally from mixtures of TiO_2 and NaOH solutions was $Na_2Ti_2O_4(OH)_2$, based on the XRD pattern from powder diffraction files (JCPDS)[7]. Tsai and Teng (2006) claim to have identified $Na_2Ti_2O_5.H_2O$ after hydrothermally processing mixtures of TiO_2 and NaOH solutions, based on the XRD patterns. These researchers support their claim through the determination of the unit cell parameters.

[7] Joint Committee on Powder Diffraction Standards

2.6.2 System Na_2O-TiO_2-Fe_2O_3

The phase diagram published by Li *et al.* (1971) and included in the reference book *Phase Diagrams for Ceramists* (Roth *et al.*, 1981) presents $NaFeTiO_4$, $NaFeTi_3O_8$ and $Na_xFe_xTi_{2-x}O_4$ ($0.90 \geq x \geq 0.75$) (Figure 7).

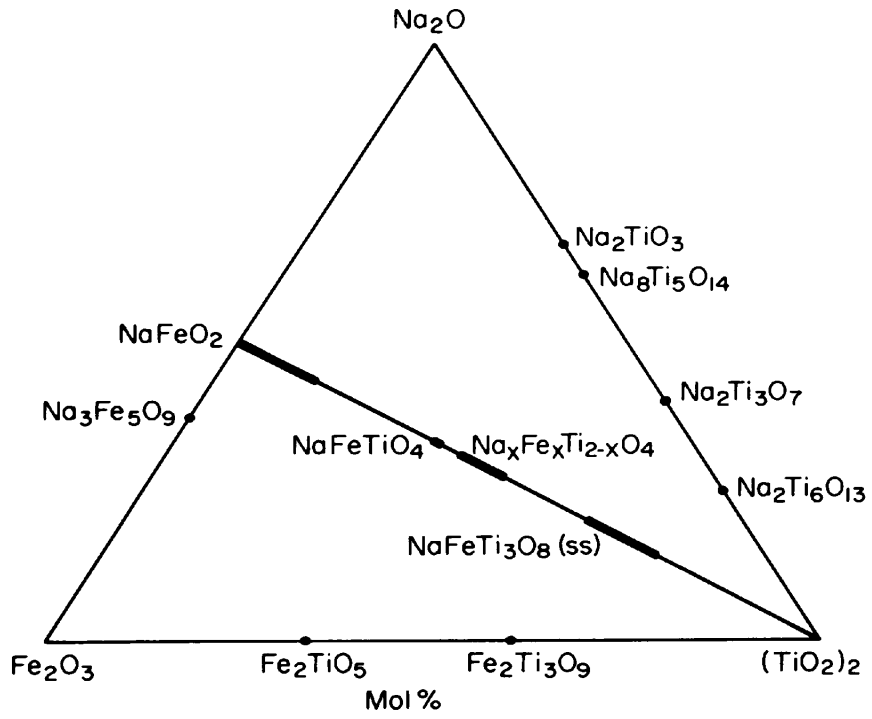

Figure 7: Na_2O – Fe_2O_3 – TiO_2 phase diagram (Li *et al.*, 1971)

Wadsley (1964) found crystallographic similarity between freudenbergite ($Na_2Fe_2Ti_7O_{18}$) and Na_xTiO_2. Freudenbergite is a titaniferrous mineral present in alkali syenite rock.

Bayer and Hoffmann (1965) reported six structures in the series $Na_xFe_xTi_{8-x}O_{16}$. Attempts to replace completely sodium ions with potassium led to the formation of a compound resembling priderite.

Mumme and Reid (1968) reported the preparation of $Na_xFe_xTi_{2-x}O_4$ ($0.75 \leq x \leq 0.90$) by melting $NaFeTiO_4$ at 1 000 °C. They found $Na_xFe_xTi_{2-x}O_4$ to be structurally related to $NaFeTiO_4$. $NaFeTiO_4$ is an isotype of $CaFe_2O_4$.

Foley and MacKinnon (1970) roasted ilmenite ($FeTiO_3$) with soda ash (Na_2CO_3) at 860 °C and observed $Na_xFe_xTi_{8-x}O_{16}$ ($1.20 \leq x \leq 2.00$), $Na_xFe_xTi_{1-x}O_2$ ($0.67 \leq x \leq 1.00$) and $Na_xFe_xTi_{2-x}O_4$ ($0.75 \leq x \leq 0.90$), based on the XRD patterns. $Na_xFe_xTi_{2-x}O_4$ was only obtained at 1 040 °C. They found that the phases obtained were readily interconvertible. The excessive iron was found to be accommodated in α-Fe_2O_3 and titanium in single titanates, mainly Na_2TiO_3. Equilibrium products were found to be dependent only on the Na:Ti ratios.

Akimoto *et al.* (2004) reported the synthesis of a new member of the series $Na_{2+x}Fe_xTi_{4-x}O_9$ (x = 0.65) from a mixture of Na_2CO_3, Fe_2O_3 and TiO_2 at 1 000 °C. The structure was found to consist of large tunnels in the *b*-axis with three types of Na atom.

Biswas *et al.* (1996) roasted ilmenite with salt water vapour (NaCl, $NaNO_3$ and Na_2SO_4). They suggest that roasting with NaCl led to the formation of Na_4FeTiO_5, based on the optimum ratio of $FeTiO_3$:NaCl. This suggestion could not be confirmed by XRD. For $NaNO_3$ and Na_2SO_4, $NaFeTiO_4$ was observed along with an unknown phase, suggested to be $NaO_{0.5}.FeO_{1.5}.TiO_2$ on the basis of XRD analysis. The optimum ratio suggested $NaO_{0.5}.FeO.TiO_2$. According to these authors, the latter is not stable thermodynamically, unlike the former.

Kuhn *et al.* (1996) studied the effect of extracting sodium on the formation of substructures on the composition $Na_xFe_xTi_{2-x}O_4$ ($0.75 \leq x \leq 0.90$). They were able to produce crystals with sodium contents ranging from 0.58 to 0.87. For starting material with a sodium content of x = 0.79, the upper level of extraction was found to be 0.30. In studying the effect of sodium removal, they found that the *a* parameter increased correspondingly, while the *b* parameter increased only slightly. The volume of the cell did not, mostly, change partly because of irregular changes in the *c* parameter (Kuhn *et al.*, 1997).

El-Tawil *et al.* (1996) applied Na_2CO_3 in slag production. They carbon-reduced ilmenite in the presence of Na_2CO_3 at 1 000 to 1 200 °C for periods up to 180 min. $Na_{0.9}Fe_{0.9}Ti_{1.1}O_4$, $NaFeTi_3O_6$, $Na_2Fe_2Ti_3O_{10}$, as well as the single titanates Na_2TiO_3, Na_4TiO_4, $Na_2Ti_3O_7$ and $Na_8Ti_5O_{14}$ were observed. The single titanates were found to be temperature dependent. At lower temperature (1 000 °C) $Na_2Ti_3O_7$ and $Na_8Ti_5O_{14}$ were present, while Na_2TiO_3, Na_4TiO_4 and $Na_8Ti_5O_{14}$ were observed between 1 100 and 1 200 °C. Sodium iron titanates were observed in all experiments. $NaFeTi_3O_6$ was present after extensive roasting periods, equal to or above 2 h (El-Tawil *et al.*, 1996).

2.6.3 Comments on the phase diagrams

The available phase diagrams on the Na_2O-TiO_2system, from Bouaziz and Mayer (1971) and Gicquel *et al.* (1972), indicate the existence of Na_2TiO_3 (α and β), $Na_8Ti_5O_{18}$, $Na_2Ti_3O_7$, $Na_2Ti_6O_{13}$ and Na_4TiO_4. In addition, $Na_2Ti_2O_5$ and $Na_6Ti_2O_7$ are mentioned.

Later literature reported the following phases: $Na_2Ti_4O_9$ (Akimoto and Takei, 1989b; Belyaev *et al.*, 1970; Dion *et al.*, 1978; Watanabe, 1981), $Na_2Ti_7O_{15}$ (Wadsley and Mumme, 1968), $Na_4Ti_3O_8$ (Belyaev *et al.*, 1970), $Na_2Ti_9O_{19}$ (Watanabe *et al.*, 1979; Watanabe 1981), $Na_4Ti_5O_{12}$ (Werthmann and Hoppe, 1984), γ - Na_2TiO_3 (Hill *et al.*, 1985) and $Na_4Ti_9O_{20}$ (Clearfield and Lehto, 1988). $Na_2Ti_8O_{17}$ was predicted (Wadsley and Mumme, 1968).

There seems to be consensus regarding the existence of members n = 1, 3, 4, 6, 7 and 9 in the $Na_2Ti_nO_{2n+1}$ family, while n = 8 has been predicted. With regard to the missing members (n = 2 and 5), although they are reported in literature, their existence is still surrounded by a certain amount of controversy (Bamberger and Begun, 1987; Glasser and Marr 1979; Hill *et al.*, 1985; Nalbandyan, 2000).

Batygin (1967) reported $Na_2Ti_2O_5$ to be stable below 800 °C and to transform to $Na_4Ti_5O_{14}$ above that temperature. He indicated the instability of $Na_2Ti_2O_5$ as the difficulty faced by other researchers in attempting to produce $Na_2Ti_2O_5$. Belyaev *et al.* (1970) found $Na_4Ti_5O_{14}$ to be one of the intermediates in Na_2TiO_3 formation (850–950 °C). Later Glasser and Marr (1979) and Bamberger and Begun (1987) were unable to produce $Na_2Ti_2O_5$, suggesting the improbability of its existence. This was supported by Nalbandyan (2000) who indexed to $Na_4Ti_5O_{12}$ the XRD pattern previously attributed to $Na_2Ti_2O_5$, and by Avdeev and Kholkin (2000) who resolved the crystal structure of $Na_4Ti_5O_{12}$.

Recent publications, however, brought back the discussion around the existence of $Na_2Ti_2O_5$ and the reliability of its XRD pattern (Mitsuhashi and Fujiki, 1985; Nian and Teng, 2006; Tsai and Teng, 2006; Yang *et al.*, 2003; Zhang *et al.*, 2005). These researchers claim to have identified $Na_2Ti_2O_5$ in the form of either $Na_2Ti_2O_5.H_2O$ or $Na_2Ti_2O_4(OH)_2$. This last structure was previously rejected by Nalbandyan (2000) as the $Na_2Ti_2O_5$ structure, since the compound was obtained either with NaOH or with Na_2CO_3.

Other disputed phases are $Na_2Ti_5O_{11}$, $Na_4Ti_3O_8$ and $Na_6Ti_2O_7$ (Bamberger and Begun, 1987; Batygin, 1967; Belaev *et al.*, 1970; Belyaev, 1976; Glasser and Marr, 1979; Hill *et al.*, 1985).

For Batygin (1967) the XRD pattern previously attributed to $Na_2Ti_5O_{11}$ was, in fact, that of a mixture of $Na_2Ti_5O_{11}$ and $Na_2Ti_6O_{13}$. Glasser and Marr (1979) attributed this pattern to a mixture of $Na_2Ti_3O_7$ and $Na_2Ti_6O_{13}$. Nishizawa and Aoki (1985) claim to have observed traces of $Na_2Ti_5O_{11}$ while reacting TiO_2 gel with aqueous NaOH, based on the XRD patterns. For Bamberger and Begun (1987), however, only $Na_2Ti_6O_{13}$ was present, thus indicating that the pattern in question belonged to this phase ($Na_2Ti_6O_{13}$). Despite this controversy, Kokubo and Namakura (2000) reported that, while studying the formation mechanism of apatite on the surface of titanium metal, they observed $Na_2Ti_5O_{11}$. Hedouin and Seguelong (2001) reported $Na_2Ti_5O_{11}$ as one of the phases existing in the pigment they produced. Torres-Martínez *et al.* (2006) in studying the system Na_2O-Li_2O-TiO_2 after fusing the starting material at 950 °C for 24

h, using different proportions, claim to have observed $Na_2Ti_5O_{11}$ formation, based on the XRD patterns.

Belyaev *et al.* (1970) found the intermediate previously reported as β-titanate to be $Na_4Ti_3O_8$. According to these researchers, it decomposes into Na_2TiO_3 and $Na_8Ti_5O_{14}$. Belyaev (1976) found $Na_4Ti_3O_8$ to be an intermediate in the formation of Na_2TiO_3. Bamberger and Begun (1987), although they expressed some doubt about the existence of $Na_4Ti_3O_8$, did not report any attempt at producing this phase. Lizuka *et al.* (2005), however, indicate $Na_4Ti_3O_8$ as one of the phases in the exhaust cleaner of their invention.

A search with regard to the $Na_6Ti_2O_7$ phase initially reported by Glasser and Marr (1979) was not fruitful, suggesting that the correction made by Hill *et al.* (1985) is acceptable.

Apart from the previously mentioned there are bronze-type oxides, such as Na_xTiO_2 and $Na_xTi_4O_8$, (Anderson and Wadsley, 1962; Bayer and Hoffmann, 1965; Wadsley, 1964) and mixed valence oxides, such as $NaTi_2O_4$ and $NaTi_8O_{13}$ (Akimoto and Takei, 1989a; Akimoto and Takei, 1991).

The phase diagram of this system Na_2O-TiO_2-Fe_2O_3 by Li *et al.* (1971) and published elsewhere (Roth *et al.*, 1981) includes $NaFeTiO_4$, $NaFeTi_3O_8$ and $Na_xFe_xTi_{2-x}O_4$ ($0.90 \geq x \geq 0.75$). Other literature, however, points out the existence of additional phases such as $Na_2Fe_2Ti_3O_{10}$, $Na_2Fe_2Ti_7O_{18}$, $Na_xFe_xTi_{8-x}O_{16}$, $Na_{2+x}Fe_xTi_{4-x}O_9$ and $Na_xFe_xTi_{1-x}O_2$ (Akimoto *et al.*, 2004; Bayer and Hoffmann, 1965; Foley and Mackinnon, 1970; Wadsley, 1964).

2.7 The Proposed Process

The proposed process is a combination of the De Wet process of zirconia recovery from zircon sands (de Wet, 1999) and the Richter process of making titanium dioxide (Richter and Elizabeth, 1933). The overall process is summarised in Figure 8.

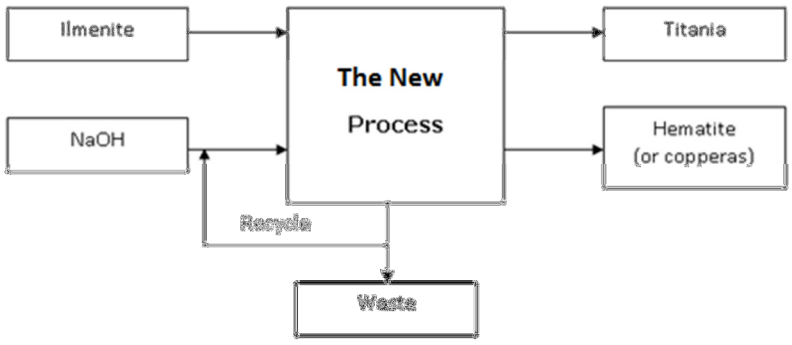

Figure 8: Block diagram of the proposed process of titania recovery using ilmenite ore

In essence, the ore is roasted with an alkali compound, preferably sodium hydroxide or sodium carbonate. The aim is to produce highly soluble species and simultaneously produce radionuclide-immobilising compounds. Zirconolite, $CaZrTi_2O_7$, has the ability to be used as radionuclide immobiliser owing to its ability to exist in a wide range of substitutions (de Hoog and van Bergen, 1997). Zirconolite is a potential product of the alkali roasting reaction (Jha *et al.*, 2005). The procedure also provides a method of removing silicon efficiently.

2.7.1 The Richter Process

Richter and Elizabeth (1933) found that when fine ilmenite or rutile is mixed with sodium hydroxide, in the proportion of 2:1 ($NaOH:TiO_2$) mole ratio, reacts with formation of sodium titanate. The reaction takes place on the temperature range of 280° to 650 °C. Sodium hydroxide can be replaced by potassium hydroxide but, according to authors, the results are

pure. The addition of carbonated alkali, that is, soda ash was viewed as beneficial (Richter and Elizabeth, 1933). Apparently soda ash acts as fondant in the reaction.

In one particular experiment they mixed equal masses of rutile and sodium hydroxide solution (75%). The mixture was heated, up to 300 °C, in kneading equipment and an equivalent of a quarter of the mass of sodium hydroxide in soda ash was added to the vessel. The mass was transferred to a rotary kiln at 600-650 °C, for 30 minutes. The obtained powder was leached with water allowing to the recovery of much of the soda used in the reaction, 80 to 90%. The residue was then leached with dilute sulphuric acid. Much of the iron contained in the ore and other impurities are said to dissolve in this stage of the process. The crude titania can be purified further by acid washing or by dissolving in sulphuric acid 50% and subsequently hydrolysing thermally. In order to enhance the product purity, Fe(III) must be reduced to Fe(II) (Richter and Elizabeth, 1963).

2.7.2 The de Wet Process

The de Wet process was developed by de Wet (1999) to extract zirconia from zircon sands. The process consists in fusing zircon with sodium hydroxide or soda ash. The intension is to break $ZrO_2.SiO_2$ bonds. They are thermally and chemically and require aggressive reaction conditions (Farnworth *et al.*, 1980; Nielsen and Chang, 1996; Zeis and Giesekke, 1997). The net reaction in the de Wet process is as following

$$ZrSiO_4 + 2Na_2O \rightarrow XNa_2ZrO_3 + (2X-1)Na_2SiO_3 + (1-X)Na_2ZrSiO_5 + (1-X)\,Na_4SiO_4$$

operating at temperatures above 700 °C (Manhique *et al.*, 2003). The *X* value has importance on the economy of the process. Higher yields of Na_2ZrSiO_5 in the reaction prevent extensive

recoveries of the alkali used in the reaction. It does not hydrolyze in water. It has to be acid treated in order to release its zirconium content.

The fusion cake obtained at optimum conditions, 2:1 ($NaOH:ZrSiO_4$) mole ratio for 2 h at 850 °C, is leached with water to dissolve soluble silicates and to hydrolyze sodium zirconates owing to the recovery of alkali. Alkali solution obtained after leaching was then treated with ammonium to precipitate silica. The zirconium containing residue was treated with dilute mineral acid (HCl preferably) to hydrolyze sodium zirconium silicates. The residue from the HCl treatment consists essentially of hydrous zirconia and unreacted zircon. This later residue is dissolved in concentrated H_2SO_4 to produce acid zirconium sulfate tetrahydrate (AZST). The AZST is separated from the residue of unreacted zircon by dissolving it in water and recrystallizing. Zirconia or any other zirconium chemical can be produced from the AZST obtained in this process (Manhique *et al.*, 2003).

2.7.3 Description of the New Process

The process proposed in this work is aimed to extract titania from titanoferrous minerals. The process relies on the alkali fusion reaction followed by sulfation of the obtained cake. We describe each step and the idea behind it.

A. Fusion

Ilmenite or other titanoferrous mineral is intimately mixed with a sodium containing chemical, preferably NaOH. The aim of the fusion reaction is to produce sodium iron titanates, since they comprise the least sodium hydroxide consuming phases in their formation. The reaction can also produce sodium titanates and sodium ferrates. According to the literature the main sodium iron titanates are $NaFeTiO_4$, $NaFeTi_3O_8$, $Na_xFe_xTi_{8-x}O_{16}$, $Na_xFe_xTi_{1-x}O_2$ and $Na_xFe_xTi_{2-x}O_4$ (Foley and MacKinnon, 1970; Mumme and Reid, 1968). Economically the phases containing less

sodium per unit titanium are ideal. The hypothetic reactions for the indicated ternary phases are

$$2Na_2O + 4FeTiO_3 + O_2 \rightarrow 4NaFeTiO_4$$

$$6Na_2O + 12FeTiO_3 + 3O_2 \rightarrow 4NaFeTi_3O_8 + 8NaFeO_2$$

$$5Na_2O + 8FeTiO_3 + 2O_2 \rightarrow Na_xFe_xTi_{8-x}O_{16} + (8 - x)NaFeO_2 + xNa_2TiO_3$$

$$6Na_2O + 2FeTiO_3 + O_2 \rightarrow 4Na_xFe_xTi_{1-x}O_2 + 4(1-x)NaFeO_2 + 4xNa_2TiO_3$$

$$4Na_2O + 4FeTiO_3 + O_2 \rightarrow 2Na_xFe_xTi_{2-x}O_4 + 2(2- x)NaFeO_2 + 2xNa_2TiO_3$$

The stoichiometry of the first two reactions is 1:1 mole ratio. The following are 5:4, 6:1 and 2:1 ($NaOH:FeTiO_3$) mole ratio. First reaction does not allow a good alkali recovery. Thus reaction conditions have to be such that $NaFeTiO_4$ be at minimum levels or, if possible, its formation avoided. However reaction products are a mix of the described phases as was observed by Foley and MacKinnon (1970) and by Biswas *et al* (1996), including sodium titanates and sodium ferrates. The challenge then is to determine optimum conditions for the reaction, i.e., conditions were the desired phases are predominant in the product spectrum.

B. Water leaching

The water leaching process is aimed to hydrolyse the titanates and ferrates in order to recover the NaOH used in the fusion reaction. The less stable sodium iron titanates will also hydrolyse (Biswas *et al.*, 1996). Bronze like titanates are not amenable to water leach. Several impurities also leached out in this stage of the process. Leachate is essentially composed by sodium hydroxide as well as soluble impurities. Temperature, time and slurry density are the important parameters for this step.

C. Acid Leach

This step is intended to leach the least soluble impurities. Most of the impurities are converted into oxides in the fusion step. These oxides are of basic nature therefore soluble in acids producing soluble chlorides (Biswas *et al*., 1996). Some of the sodium iron titanates are hydrolysed in this stage. The most important parameter in this step is the acid concentration. The acid solution has to be concentrated enough to dissolve impurities. High concentration acid can lead to titanium loss. The idea here is to selectively dissolve impurities and hydrolyse titanium bearing phases in the residue. The hydrolysis reduces the amount of acid to be consumed in the sulfationstep. This treatment is effective to remove impurities such as Cr, V, Ca, Zr, Nb, Ce, Nd, U and Th, as was reported by Jha *et al*. (2009) and Jha and Tathavadkar (2010).

D. Sulfation

The residue from the previous step is mainly composed by hydrous titania. Some of the impurities are also present in the residue. The idea here is to dissolve titania containing phases in the residue. Insoluble impurities remain in the residue and can be removed by filtration.

2.7.4 Benchmarks of the Proposed Process

This process reduces the environmental pressure exerted by the traditional sulfate process. Compared with the traditional sulfate process, it offers:

(i) reduced operation time

(ii) low sulphuric acid consumption

(iii) ability to treat a wide variety of ores

(iv) reduction of environmental harm

(v) recyclability of a considerable proportion of the reactants

(vi) no acid disposal

George and Mohan Das (1985) have suggested that rutile production through fusion is hindered by the need for high quantities of alkali, high energy inputs and lower recoveries. We dispute these findings since in our experiments considerably high recoveries were achieved using substoichiometric correlations at comparatively mild operating temperatures.

2.8 References

Agui, A., Mizumzki, M., Saitoh, Y., Mitsushita, T., Nakatani, T., Fukaya, A., and Torikai, E., **2001**. Soft X-ray absorption spectra of ilmenite family. *Journal of Synchrotron Radiation*, 8:907-909.

Akimoto, J., and Takei, H., **1989a**. Synthesis and crystal structure of $NaTi_2O_4$: A new mixed-valence sodium titanate. *Journal of Solid State Chemistry*, 79: 212–217.

Akimoto, J., and Takei, H., **1989b**. A large tunnel structure of triclinic $Na_2Ti_4O_9$. *Journal of Solid State Chemistry*, 83: 132–139.

Akimoto, J., and Takei, H., **1991**. Synthesis and crystal structure of $NaTi_2O_4$. *Journal of Solid State Chemistry*, 90: 147–154.

Akimoto, J., Takahashi, Y., Kijima, N., and Gotoh, Y., **2004**. Synthesis and structure analysis of a new sodium iron titanate $Na_{2+X}Fe_xTi_{4-X}O_9$ with x = 0.65. *Solid State Ionics*, 172: 495–497.

Anderson, S., and Wadsley, A.D., **1961**. The crystal structure of $Na_2Ti_3O_7$. *Acta Crystallographica*, 14: 1245–1249.

Anderson, S., and Wadsley, A.D., **1962**. $Na_xTi_4O_8$, an alkali metal dioxide bronze. *Acta Crystallographica*, 15: 201–206.

Anderson, S., and Wadsley, A.D., **1962**. The structures of $Na_2Ti_6O_{13}$ and $Rb_2Ti_6O_{13}$ and the alkali metal titanates. *Acta Crystallographica*, 15: 194–201.

Avdeev, M., and Kholkin, A., **2000**. Low-temperature $Na_4Ti_5O_{12}$ from X-ray and neutron powder diffraction data. *Acta Crystalographica Section C: Crystal Structure Communications*, C56: e539–e540.

Bamberger, C.E., and Begun, G.M., **1987**. Sodium titanates: Stoichiometry and Raman spectra. *Journal of the American Ceramic Society*, 70(3):C-48–C-51.

Batygin, V.G., **1967**. Formation and some properties of sodium titanates. *Russian Journal of Inorganic Chemistry*, 12(6): 762–767.

Barksdale, J., **1966**. *Titanium: Its Occurrence, Chemistry, and Technology*, 2nd edition. New York: The Roland Press Co.

Barton, L.E., **1916**. US Patent No. 1 201 541.

Bayer, V.G., and Hoffman, W., **1965**. Über Verbindungen vom Na_xTiO_2-Typ. *Zeitschrift für Kristallographie*, *Bd.*, 121: S.9–13.

Belyaev, E.K., Panasenko, N.M., and Linnik, E.V., **1970.** Formation of tetrasodium trititanate in mixtures of sodium carbonate and titanium dioxide. *Russian Journal of Inorganic Chemistry*, 15(3):336-338.

Belyaev, E.K., **1976**. The formation of sodium metatinate in sodium carbonate – Titanium dioxide mixtures. *Russian Journal of Inorganic Chemistry*, 21(6): 830–833.

Belyaev, I.N., and Belyaeva, A.G., **1965**. The NaCl-Na_2TiO_3-TiO_2 system. *Russian Journal of Inorganic Chemistry*, 10(2): 252–254.

Belyaev, I.N., and Golovanova, T.G., **1962**. Reaction between titanates and vanadates in melts. *Russian Journal of Inorganic Chemistry*, 7(12): 1440–1442.

Biswas, R.K., Islam, M.F., and Habib, M.A., **1996**. Processing of ilmenite through salt-water vapour roasting and leaching. *Hydrometallurgy*, 42: 367–375.

Biswas, R. K., and Mondal, M. G. K., **1987**. A study on the dissolution of ilmenite sand. *Hydrometallurgy*, 17(3): 385–390.

Biswas, R. K., Islam, M. F., and Habib, M. A., **1996**. Processing ilmenite through salt-water vapour roasting and leaching. *Hydrometallurgy*, 42: 367–375.

Bonhôte, P., Gogniat, E., Campus, F., Walder, L., and Grätzel, M., **1999**. Nanocrystalline electochromic displays. *Displays*, 20: 137–144.

Borowiec, K., Grau, A.E., Gueguin, M., and Cedilla, J.-F., **1998**. Method to upgrade titania slag and resulting product. US Patent No. 5 830 420.

Borowiec, K., Grau, A. E., Gueguin, M., and Turgeon, J-F., **2003**. TiO_2 containing product including rutile, pseudobrookinte and ilmenite. US Patent No. 6 531 110.

Bouaziz, R., and Mayer, M., **1971**. The binary sodium oxide-titanium dioxide. *C. R. Hebd. Sceances Acad. Sc. Ser. C.*, 272C: 1874–1877.

Chen, X., Gu, G., Liu, H., and Cao, Z., **2004a**. Synthesis of nanocrystalline TiO_2 particles by hydrolysis of titanyl organic compounds at low temperature. *Journal of the American Ceramic Society*, 87(6): 1035–1039.

Chen, G., Luo, G., Yang, X., Yang, X., Sun, Y., and Wang, J., **2004b**. Anatase-TiO_2 nano-particle preparation with a micro-mixing technique and its photocatalytic performance. *Materials Science and Engineering A*, 380: 320–325.

Chernet, T., **1999**. Applied mineralogical studies on Australian sand ilmenite concentrate with special reference to its behaviour in the sulfate process. *Minerals Engineering*, 12(5): 485–495.

Christie, T., and Brathwaite, B. **S/D**. Mineral Commodity Report 16 – Titanium. Institute of Geological and Nuclear Sciences Ltd, New Zealand.

Clark, G., **1987**. Zircon: In demand as availability squeezed. *Industrial Minerals*, 35–46.

Clark, R. J. H., **1968**. The chemistry of titanium and vanadium. An introduction to the chemistry of the early transition elements. In: P.L. Robinson (Ed.), *Topics in Inorganic and General Chemistry.* Amsterdam: Elsevier, pp 1–17.

Clearfield, A., and Lehto, J., **1988**. Preparation, structure, and ion-exchange properties of $Na_4Ti_9O_{20}.xH_2O$. *Journal of Solid State Chemistry*, 73: 98–106.

Coaldrake, J. E., **1979**. Coastal sandmining and landscape rehabilitation in Eastern Australia. *Landscape Planning*, 6: 359–374.

Dannenberg, R., and Greene, P., **2000**. Reactive sputter deposition of titanium dioxide. *Thin Solid Films*, 360: 122–127.

D'Ans, J., and Löfler, J., **1930**. Metal oxides and sodium hydroxide (Metalloxyde und atznatron – in german). *Chemische Berichte*, 63: 1446–1455.

De Hoog, J. C. M., and van Bergen, M. J., **1997**. Notes on the chemical composition of zirconolite with thorutite inclusions from Walaweduwa, Sri Lanka. *Mineralogical Magazine*, 61[10]:721-725.

De Matos, J. M. J., de Freitas, L.R., and Horta, R. de M., **2002**. Process for the production of titanium concentrate from anatase ores with high utilization of the iron contents of the ore. US Patent No. 6 346 223.

De Wet, W. J., **1999**. Beneficiation of zircon. Provisional SA Patent No. 99/3815.

Diebold, U., **2003**. The surface science of titanium dioxide. *Surface Science Reports*, 48: 53–229.

Dion, M., Piffard, Y., and Tournoux, M., **1978**. The tetratinates $M_2Ti_4O_9$ (M = Li, Na, K, Rb, Cs, Tl, Ag). *Journal of Inorganic and Nuclear Chemistry*, 40: 917–918.

Doan, P., **2003**. Sustainable development in the TiO_2 industry: Challenges and opportunities. Paper presented at the TiO_2 Intertech Conference, Miami, Florida, US.

Duncan, J. F., and Metson, J.B., **1982**. Acid attack on New Zealand Ilmenite. I. The mechanism of dissolution. *New Zealand Journal of Science*, 25: 103–109.

El-Hazek, N., Lasheen, T. A., El-Sheik, R., and Zaki, S. A., **2007**. Hydrometallurgical criteria for TiO_2 leaching from Rosetta ilmenite by hydrochloric acid. *Hydrometallurgy*, 87(1): 45–50.

El-Tawil, S. Z., Morsi, I. M., Yehia, A., and Francis, A. A., **1996**. Alkali reductive roasting of ilmenite ore.*Canadian Metallurgical Quarterly*, 35(1): 31–37.

Environmental Protection Agency (EPA) of the US, **2010**. State of the science literature review: Nano titanium dioxide environmental matters. Task order n° 94, Washington DC.

Farnworth, E.; Jones, S. L.; McAlpine, I.The Production, Properties and uses of zirconium chemicals. In *Speciality Inorganic Chemicals*; Thompson, R., Ed.; Special Publication No. 40; Royal Society of Chemistry: London, 1980; p 248.

Farrell, K. A., **2001**. Synthesis effects on grain size and phase content in the anatase-rutile TiO_2 system. MSc Thesis, Worcester Polytechnic, UK.

Farrow, J.B., Ritchie, I.M., and Mangano, P., **1987**. The reaction between reduced ilmenite and oxygen in ammonium chloride solutions. *Hydrometallurgy*, 18:21-38.

Foley, E., and Mackinnon, K.P., **1970**. Alkaline roasting of ilmenite. *Journal of Solid State Chemistry*, 1: 566–575.

Gambogi, J., **2010**. Titanium. Minerals Yearbook. U.S. Geological Survey.

George, A., and Mohan Das, P. N. M., **1985**. Relative merits of various processes available for the production of rutile. *Journal of Scientific and Industrial Research*, 44: 443–450.

German Federal Environmental Agency, **2001**. Large volume solid inorganic chemicals. Titanium dioxide. Final Report. June.

Gicquel, C., Mayer, M., and Bouaziz, R., **1972**. The binary sodium oxide-titanium dioxide. *C. R. Hebd. Sceances Acad. Sc. Ser. C.*, 275C: 1427–1430.

Girgin, I, and Turker, L., **1986**. Hydrochloric acid leaching of ilmenite – Effect of alcohol species. *Bulletin and Proceedings. Australasia Institute of Mining and Metallurgy*, 291(5): 61–64.

Girgin, I., **1990**. Leaching ilmenite in HCl – H_2O, HCl – CH_3OH – H_2O and HCl – CH_3OH solutions. *Hydrometallurgy*, 24(1): 127–134.

Glasser, F.P. and Marr, J., **1979**. Phase relations in the system Na_2O-TiO_2-SiO_2. *Journal of the American Ceramic Society*, 62(1–2): 42–47.

Gmelins Handbuch Der Anorganischen Chemie, 8th edition. **1951**. Titan, System-Nummer 41. Weinheim, Germany: Verlag Chemie GMBH, pp 381–389.

Greenwood, N. N. and Earnshaw, A., **1984**. *Chemistry of the Elements*, Oxford: Pergamon Press, pp 1111–1137.

Grey, I.E., and Reid, A.F., **1975**. The structure of pseudorutile and its role in the natural alteration of ilmenite. *The American Mineralogist*, 60:898-906.

Habashi, F. (Ed.), **1997.** Titanium. In: *Handbook of Extractive Metallurgy, Vol. II*. Weinheim, Germany: Wiley-VCH, pp 1129–1180.

Han, K. N., Rubcumintara, T., and Fuerstenau, M. C., **1987**. Leaching behavior of ilmenite with sulfuric acid. *Metallurgical Transactions B. Process Metallurgy*, 18B(2): 325–330.

Hansen, D. A., and Traut, D. E**., 1989.** Kinetics of leaching rock ilmenite with hydrofluoric acid. *Journal of Metals*, 41(5): 34–36.

Hedouin, C., and Seguelong, T., **2001**. Titanium, cerium and alkaline or earth-alkaline based compound. Preparation methods and use as colouring pigment. US Patent No. 6 294 011.

Hill, W.A., Moon, A.R., and Higginbotham, G., **1985**. Alkali oxide-rich sodium titanates. *Journal of the American Ceramic Society*, 68(10): C-266–C267.

Hollit, M. J., McClelland, R. A., and Tuffley, J. R., **2003**. Upgrading titaniferous materials. US Patent Application No. 20030129113.

Ibrahim, I.A., Mahmoud, M.H.H., Afifi, A.A.I., and El-Sayed, B.A., **2003.** Direct hydrochloric acid leaching of an Egyptian ilmenite ore for production of synthetic rutile. *Proceedings of the TMS Fall Extraction and Processing Conference*, Vol.I, pp.555-564.

Jha, A. R. A., and Dattatray, T. V., **2005**. Process for the recovery of titanium dioxide from titanium-containing compositions. US Application Patent 20070110647 (W2005028369).

Jha, A., Kumari, E.J., and Lahiri, A., **2009**. Titanoferous ore beneficiation. US Patent No. 7 494 631.

Jha, A., and Tathavadkar, V.D., **2010**. Process for the recovery of titanium dioxide from titanium-containing compositions. US Patent No. 7 771 679.

Jonglertjuania, W., and Rubcumintara, T., **2012**. Titanium and iron dissolutions from ilmenite by acid leaching and microbiological oxidation techniques. *Asia-Pacific Journal of Chemical Engineering*, in press.

Kim, S-J., Park, S-D.and Jeong, Y. H., **1999**. Homogeneous precipitation of ultrafine TiO_2 powders from aqueous $TiOCl_2$ solution. *Journal of the American Ceramic Society*, 82(4): 927–932.

Kobuko, T., and Namakura, T., **2000**. Mechanism of apatite formation on bioactive titanium metal. *Proceedings of the Materials Research Society Symposium,* 599: 129–134.

Kucukkaragoz, C. S., and Eric, R. H., **2006**. Solid state reduction of a natural Ilmenite.*Minerals Engineering*, 19: 334–337.

Kuhn, A., Garciá-Alvarado, F., Morán, E., Alario-Franco, M.A., and Amador, U., **1996**. Structural effects of sodium extraction on $Na_xFe_xTi_{2-X}O_4$, single crystals. *Solid State Ionics*, 86–88: 811–818.

Kuhn, A., Menéndez, N., Garciá-Alvarado, F., Morán, E., and Alario-Franco, M.A., **1997**. Topotactic oxidation of the quadruple-rutile-type chain structure $Na_{0.875}Fe_{0.875}Ti_{1.125}O_4$. *Journal of Solid State Chemistry*, 130: 184–191.

Lahiri, A., Kumari, E. J., and Jha, A., **2006**. Kinetic studies on the soda-ash roasting of titanoferous ores for the extraction of TiO_2. *Proceedings of the Sohn International Symposium on Advanced Processing of Metals and Materials. Vol. 1: Thermo and Physicochemical Principles: Non-Ferrous High-Temperature Processing*, pp 115–123.

Lasheen, T. A. I., **2005**. Chemical beneficiation of Rosetta ilmenite by direct reduction leaching. *Hydrometallurgy*, 76: 123–129.

Lee, C. T., and Sohn, H. Y., **1989**. Recovery of synthetic rutile and iron oxide from ilmenite ore by sulfation with ammonium sulfate. *Industrial Engineering and Chemistry Research*, 28: 1802–1808.

Li, C., Liang, B., and Cheng, S-P., **2006**a. Enhancement effects of mechanical milling facilities on dissolution of Panzhihua ilmenite. *Journal of the Chemical Industry and Engineering* (China), 57(4): 832–837.

Li, C., Liang, B., and Cheng, S-P., **2006b**. Combining milling-dissolution of Panzhihua ilmenite in sulphuric acid. *Hydrometallurgy*, 82: 93–99.

Li, C., Liang, B., and Guo, L-H., **2007**. Dissolution of mechanically activated Panzhihua ilmenite in dilute solutions of sulphuric acid.*Hydrometallurgy*, 89(1–4): 1–10.

Li, C., Reid, A.F., and Saunders, S., **1971**. Nonstoichiometric alkali ferrites and aluminates in the systems $NaFeO_2$–TiO_2, $KFeO_2$–TiO_2, $KAlO_2$–TiO_2, and $KAlO_2$–TiO_2. *Journal of Solid State Chemistry*, 3: 614–620.

Liu, Y., Qi, T., Chu, J., Tong, Q., and Zhang, Y., **2006**. Decomposition of ilmenite by concentrated KOH solution under atmospheric pressure. *International Journal of Mineral Processing*, 81: 79–84.

Lizuka, H., Okude, K., Kaneeda, M., Nagayama, K., Yamashita, H., Kuroda, O., and Kitahara, Y., **2005**. Method for cleaning exhaust gas from an internal combustion engine. US Patent No. 6 883 305.

Loughbrough, R., **1992**. TiO_2 pigment – Overcapacity hits again. *Industrial Minerals*, June 37: 53.

Lynd, L. E. and Lefond, S. J., **1975**. Titanium minerals. In: *Industrial Minerals and Rocks,* 4th edition, Society of Mining Engineers of AIME, pp 1149–1208.

Mackey, T.S., **1994**. Upgrading ilmenite into high-grade synthetic rutile. *Journal of Metals*, April:59-64.

Maeda, H., Kasuga, T., and Nogami, M., **2004**. Apatite formation on titania-vaterite powders in simulated body fluid. *Journal of the European Ceramic Society*, 24: 2125–2130.

Mahmoud, M.H.H., Afifi, A.A.I., and Ibrahim, I.A., **2004**. Reductive leaching of ilmenite ore in hydrochloric acid for preparation of synthetic rutile. *Hydrometallurgy*, 73:99-109.

Manhique, A., Kwela, Z., and Focke, W.W., **2003**. De Wet process for the beneficiation of zircon: Optimization of the alkali fusion step. *Industrial and Engineering Chemistry Research*, 42:777-783.

Meinhold, G., **2010**. Rutile and its applications in earth sciences. *Earth-Science Reviews*, 102:1-28.

Meng, X.-D., Whang, D.-Z., Liu, J.-H., and Zhang, S.-Y., **2004**. Preparation and characterization of sodium titanate nanowires from Brookite nanocrystallites. *Materials Research Bulletin*, 39: 2163–2170.

Mitsuhashi, T., and Fujiki, Y., **1985**. Thermochemistry of alkali-metal titanates. *Thermochimica Acta*, 88: 177–184.

Mumme, W.G., and Reid, A.F., **1968**. Non-stoichiometric sodium iron titanate, $Na_xFe_xTi_{2-x}O_4$, $0.90>x>0.75$.*Acta Crystallographica*, B24: 625–631.

Murphy, P., and Frick, L., **2006**. Titanium. In: Kogel, J.E., Trivedi, N.C., Barker, J.M., and Krukowski, S.T. (Eds.), *"Industrial Minerals and Rocks – Commodities, Markets and Uses"*, 7th edition, Society for Mining Metallurgy, and Exploration, Inc., Colorado – USA, pp. 987-1003.

Nabivanets, B.I., Kudritskaya, L.N., **1967**. A study of the polymerisation of titanium(IV) in hydrochloric acid solutions. *Russian Journal of Inorganic Chemistry*, 12[5]:616-620

Nalbandyan, V. B., **2000**. The low-temperature hexagonal phase $Na_4Ti_5O_{12}$. *Russian Journal of Inorganic Chemistry*, 45: 675–678.

Nalbandyan, V.B., Avdeev, V.B., and Lukov, V.V., **1998**. New sodium titanium bronze and other nonstoichiometric phases of $Na_4Ti_5O_{12}$ Structure: Synthesis and characterization. *Russian Journal of Inorganic Chemistry*, 43(2): 148–153.

Nayl, A.A., Awwad, N.S., and Aly, H.F., **2009**. Kinetics of acid leaching of ilmenite decomposed by KOH. Part 2: Leaching by H_2SO_4 and $C_2H_2O_4$. *Journal of Hazardous Materials*, 168:793-799.

Nian, J., and Teng, H., **2006**. Hydrothermal synthesis of single-crystal anatase TiO_2nanorods with nanotubes as the precursor. *Journal of Physical Chemistry*, 110 (9): 4193–4198.

Nielsen, R., and Chang, T.W. **1996**. In: Elvers, B., Hawkins, S. and Schultz, G. (Eds), *Ullman's Encyclopaedia of Industrial Chemistry,* 5th edition, Weinheim, Germany, Wiley VCH, pp 95–122 (Vol. A27), pp 543–567 (Vol. A28).

Nishizawa, H., and Aoki, Y., **1985**. The crystallization of anatase and the conversion to bronze-type TiO_2 under hydrothermal conditions. *Journal of Solid State Chemistry*, 56: 158–165.

Ogasawara, T., and de Araújo, R. V. V., **2000**. Hydrochloric acid leaching of pre-reduced Brazilian ilmenite concentrate in autoclave. *Hydrometallurgy*, 56: 203–216.

Olanipekun, E. O., **1998**. Kinetics of ilmenite dissolution by hydrofluoric acid. *Pakistan Journal of Scientific and Industrial Research*, 41(4): 175–179.

Olanipekun, E.O., **1999**. A kinetic study of the leaching of a Nigerian ilmenite ore by hydrochloric acid. *Hydrometallurgy*, 53(1): 1–10.

Paixão, J. M. J., and de Mendonça, P. A. F., **1979**. Process for concentration of titanium containing anatase ore. US Patent 4 176 159.

Phani, G., Tuloch, G., Vittorio, D., and Skryabin, I., **2001**. Titania solar cells: New photovoltaic technology. *Renewable Energy*, 22: 303–309.

Plumley, A.L., and Orr, W.C., **1961**. Replacement of potassium ions in solid potassium hexatitanate by sodium ions from a chloride flux. *Journal of the American Chemical Society*, 83: 1289–1291.

Pong, T. K., Besida, J., O´Donnell, T. A., and Wood, D., **1995**. A novel fluoride process for producing TiO_2 from titaniferous ore. *Industrial and Engineering Chemistry Research*, 34: 308–313.

Pownceby, M.I., Sparrow, G.J., Fisher-White, M.J., **2008**. Mineralogical characterisation of Eucla Basin ilmenite concentrates – first results from a new global resource. *Minerals Engineering*, 21:587-597.

Qiu, S., and Starr, T.L., **2007**. Zirconium doping in titanium oxide photocatalytic films prepared by atomic layer deposition. *Journal of Electrochemical Society*, 154[6]:H472-H475.

Ramírez-Salgado, J., Djurado, E., and Fabry, P., **2004**. Synthesis of Sodium Titanate Composites by Sol-Gel Method for use in Gas Potentiometric Sensors. *Journal of the European Ceramic Society*, 24:2477-2483.

Reid, A.F., and Sienko, M.J., **1967**. Some characteristics of sodium titanium bronze and related compounds. *Journal of Inorganic Chemistry*, 6[2]:321-324.

Richter, H.W. and Elizabeth, N. J., **1933**. Making titanium dioxide. US Patent No. 1 932 087.

Roth, R.S., Negas, T., and Cook, L.P. (Eds), **1981**. *Phase Diagrams for Ceramists*, Columbus, US: American Ceramic Society, Figs 5123, 5124 and 5338.

Sadykhov, G. B., Reznichenko, V. A., Karyazin, I. A., and Naumova, L. O., **1994**. Effect of soda on phase transformations when reducing titanomagnetite concentrate by hydrogen. *Izvetia Akademii Nauk SSSR* (*Metally)*, 1: 9–16.

Sadykhov, G. B., Reznichenko, V. A., Karyazin, I. A., and Naumova, L. O., **1998**. Behavior of oxide phases in the autoclave acidic decomposition of titanate products. *Izvetia Akademii Nauk SSSR* (*Metally)*, 4: 21–28.

Sarker, M. K., Rashid, A. K. M. B., and Kurny, A. S. W., **2006**. Kinetics of leaching of oxidized and reduced ilmenite in dilute hydrochloric acid solutions. *International Journal of Mineral Processing*, 80: 223–228.

Sasikumar, C., Rao, D. S., Srikanth, S., Mukhopadhyay, N. K., and Mehrotra, S. P., **2007**. Dissolution studies of mechanically activated Manavalakurichi ilmenite HCl and H_2SO_4. *Hydrometallurgy*, 88: 154–169.

Sauvet, A.-L., Baliteau, S., Lopez, C., and Fabri, P., **2004**. Synthesis and characterization of sodium titanates $Na_2Ti_3O_7$ and $Na_2Ti_6O_{13}$. *Journal of Solid State Chemistry*, 177:4508-4515.

Seo, D.-K., Kim, H., and Lee, J.-K., **2004**. Hydrothermal synthesis of $Na_2Ti_6O_{13}$ and TiO_2 whiskers. *Journal of Crystal Growth*, 275:e2371-e2376.

Sinha, H. N., **1984**. Hydrochloric acid leaching of ilmenite. *Symposia Series. Australasia Institute of Mining and Metallurgy*, 36: 163–168.

Smith Jr., E. M. and de Castro, S. A., **2007**. Titaniferous ore beneficiation. US Patent Application 200709241.

Stamper, J.W., Titanium. In: *Mineral Facts and Problems*, **1970** edition. Bureau of Mines, Department of Interior, US, pp 773–794.

Stanaway, K. J., **1994**. Overview of titanium dioxide feedstocks. *Mining Engineering*, 12: 1367–1370.

Sun, X., Chen, X., and Li, Y., **2002**. Large-scale synthesis of sodium and potassium titanate nanobelts. *Inorganic Chemistry*, 41: 4996–4998.

Tang, H., Prasad, K., Sanjinés, R., and Lévy, F., **1995**. TiO_2 anatase thin film as gas sensors. *Sensors and Actuators B*, 26[1-3]:71-75.

Tathavadkar, V., and Jha, A., **2004**. The effect of molten sodium titanate and carbonate salt mixture on the alkali roasting of ilmenite and rutile minerals. *Proceedings of the VIIth International Conference on Molten Slags Fluxes and Salts*, South African Institute of Mining and Metallurgy, pp 255–261.

Teufer, G., and Temple, A.K., **1966**. Pseudorutile –a new mineral intermediate between ilmenite and rutile in the N alteration of ilmenite. *Nature*, 211:179-181.

Torres-Martínez, L.M., Ibarra, J., Laredo, J. R., and Lorena, L., **2006**. Phase formation and crystal structure of the ternary compound $Na_2Li_2Ti_6O_{14}$. *Solid State Sciences*, 8: 1281–1289.

Tsai, C.-C., and Teng, H., **2006**. Structural features of nanotubes synthesized from NaOH treatment on TiO_2 with different post-treatments. *Chemistry of Materials*, 18: 363–373.

Tushida, H., Narita, E., Takeuchi, H., Adachi, M., and Okabe, T., **1984**. Manufacture of high pure titanium (IV) oxide by the chloride process. I. Kinetic study on leaching of ilmenite ore

in concentrated hydrochloric acid solution. *Bulletin of the Chemical Society of Japan*, 55(6): 1934–1938.

Van Dyk, J.P., **1999**. Process development for the production of beneficiated titania slag. Ph.D. thesis. University of Pretoria, Pretoria – South Africa.

Van Dyk, J. P., Vegter, N. M., and Pistorius, P. C., **2002**. Kinetics of ilmenite dissolution in hydrochloric acid. *Hydrometallurgy*, 65: 31–36.

Vad Dyk, J.P., Vegter, N.M., Visser, C.P., de Lange, T., Winter, J.D., Walpole, E.A., and Nell, J., **2004**. Beneficiation of titania slag by oxidation and reduction treatment. US Patent n° 6 803 024 B1.

Wadsley, A.D., **1964**. The possible identity of freudenbergite and Na_xTiO_2. *Zeitschrift für Kristallographie*, *Bd.*, 120: S.396–398.

Wadsley, A.D., and Mumme, W.G., **1968**. The crystal structure of $Na_2Ti_7O_{15}$, an ordered intergrowth of $Na_2Ti_6O_{13}$ and '$Na_2Ti_8O_{17}$'. *Acta Crystallographica*, B24: 392–396.

Watanabe, M., **1981**. The investigation of sodium titanates by the hydrothermal reactions of TiO_2 with NaOH. *Journal of Solid State Chemistry*, 36: 91–96.

Watanabe, M., Bando, Y., and Tsutsumi, M., **1979**. A new member of sodium titanates, $Na_2Ti_9O_{19}$. *Journal of Solid State Chemistry*, 28: 397–399.

Wechsler, B.A., and Prewitt, C.T., **1984**. Crystal structure of ilmenite ($FeTiO_3$) at high temperature and at high pressure. *American Mineralogist*, 69:176-185.

Welham, N.J., and Llewellyn, D.J., **1998**. Mechanical enhancement of the dissolution of ilmenite. *Minerals Engineering*, 11[9]:827-841.

Werthmann, R., and Hoppe, R., **1984**. Über Oxotitanate der Alkalimetalle Zur Kenntnis von $Na_4Ti_5O_{12}$. *Zeitschrift für Anorgsnische und Allgemeine Chemie*, 519: 117–119.

Yang, J., Jin, Z., Wang, X., Li, W., Zhang, J., Zhang, S., Guo, X., and Zhang, Z., **2003**. Study on composition, structure and formation process of nanotube $Na_2Ti_2O_4(OH)_2$. *Journal of the Chemical Society, Dalton Transactions*, 3898–3901.

Zhang, C., Zhang, C., Jiang, X., Tian, B., Wang, X., Zhang, X., and Du, Z., **2005**. Modification and assembly of titanate sodium nanotubes. *Colloids and Surfaces A: Physicochemical Aspects*, 257–258: 521–524.

Zhangfu, Y., Znag, J., Li, B. and Li, J., **2007**. Comprehensive utilization of complex titania ore. *Journal of Steel and Iron Research, International*, 14(1): 1–6.

Zeis, L. A.; Giesekke, E. W., **1997**. Potential for Industrial Applications of Locally Produced Zirconium Chemicals. *South African Journal of Chemistry*, 50:136-.

3 Experimental

Raw ilmenite grit was obtained from Kumba Iron Ore Limited- South Africa, and used as is. It, as well as fused samples, were characterised using different methods as described in this Chapter.

3.1 Characterisation Techniques and Materials

3.1.1 X-ray powder diffraction (XRD)

The samples were prepared for XRD analysis using a back loading preparation method. They were analysed with a PANalytical X'Pert Pro powder diffractometer with X'Celerator detector and variable divergence- and receiving slits with Fe filtered Co-Kα radiation. The phases were identified using X'Pert Highscore plus software.The receiving slit was placed at 0.040°. The counting area was from 5 to 70° on a 2θ scale. The step time (counting time) was 1.5 s. The temperature-scanned XRD data were obtained using an Anton Paar HTK 16 heating chamber with Pt heating strip.

The semi quantitative phase amounts (weight percent) were estimated using the Reference Intensity Method in the X'Pert Highscore plus software. The Reference Intensity Ratio method (RIR) was used as not all crystal structures needed for the Rietveld method were available. Amorphous phases, if present, were not taken into account in the quantification.

3.1.2 X-ray fluorescence (XRF)

Elemental analyses were done in an ARL9400+ wavelength-dispersive instrument. The samples were ground to a particle size of less than 75 µm in a tungsten carbide milling vessel. The

ground samples were then roasted at 1 000 °C to determine the loss on ignition (LOI) value. To 1 g of the sample, 9 g of lithium tetraborate ($Li_2Bi_4O_7$) were added and the mixture was fused into a glass bead. All elements present in the sample were then analysed.

3.1.3 FT-IR absorption

Fourier transform infrared spectra (FT-IR) were recorded in a Perkins Elmer Spectrum RX I system using the KBr pellets method. The pressed pellets contained approximately 2 mg of sample and 100 mg of KBr. Data were taken in a frequency range of 400 to 4000 cm^{-1}. A spectral resolution of 2 cm^{-1} was used. The spectra were recorded at an average of 32 scans for each sample. They were corrected using a pure KBr pellets in similar conditions.

3.1.4 Thermogravimetric analysis

Thermogravimetric analysis (TGA) experiments were performed on a Mettler Toledo STAR^e TGA/SDTA 851e simultaneous TGA-DTA thermal analyser. The runs were conducted in air as a purging gas, at a heating rate of 10 °C/min. For kinetic analysis the heating rates of 2, 5 and 10 °C/min.

3.1.5 Particle size distribution

Particle size distribution was determined using a Mastersizer 2000 (Malvern Instruments). Ilmenite was slurred in water and the mixture was subjected to agitation while measuring the particle size.

3.1.6 Scanning electron microscopy

Morphology analyses were conducted in a JEOL 840 SEM (scanning electron microscope). Samples were coated five times with gold. Coating was performed in a SEM auto-coating unit E2500 (Polaron Equipment Ltd) sputter coater.

3.1.7 Materials

Ilmenite sample was supplied by Kumba Iron Ore Limited, South Africa. It was obtained from Hillendale mine. The sample was used as received. For the effect of particle size the sample was milled in a laboratory ceramic ball mill and sieved afterwards.

Iron titanate ($FeTiO_3$) reactant as well as anatase powder (TiO_2) (analytical grade) were obtained from Sigma Aldrich. Sodium hydroxide, hydrochloric acid and sulphuric acid were of technical grade obtained from CC Imelmann (PTY) LTD.

3.2 Fusion Temperature

Fusion temperature was determined by the TGA method using water evolution as a measure of reaction progress. The sample was prepared by weighing proportional amounts of dried sodium hydroxide and ilmenite (or anatase) to obtain a mole ratio of 2:1 ($NaOH:FeTiO_4$). The mixture was ground in an agate mortar, in a nitrogen environment. A sample of approximately 11 mg was placed in a platinum 70 µl crucible with lid and subjected to a heating rate of 10 °C/min in an oxygen atmosphere.

3.3 Fusion Samples

Approximately 30.35 g of ilmenite, equivalent to 1/5 of mole, were used in each fusion experiment. The weighed sample was placed in a coffee grinder machine. To that a corresponding amount of sodium hydroxide was added (8, 16, 32 or 48 g). The mixture was then homogenised in the coffee grinder machine. After the required mixing time (≈ 5 min), the sample was transferred to a nickel crucible previously dried and weighed.

The crucible with the mixture was weighed again and placed in an oven previously set at the desired temperature. After the required fusion time, the crucible was removed, allowed to cool and weighed. The obtained cake, alkali fusion-decomposed ilmenite (AFDI), was allowed to cool. A sample of AFDI was collected for X-ray diffraction, FT-IR characterisation analysis and SEM for characterization.

3.4 Optimisation of Fusion Stage

The effect of temperature on the fusion process was tested between 300 and 950 °C (50 °C gradient). The fusions were conducted for one hour using two moles of sodium hydroxide per mole of ilmenite.

The effect of fusion time was studied by varying the fusion period from 30 min to 3 h. The fusions were conducted at 750 °C, using two moles of sodium hydroxide per mole of ilmenite. The optimum fusion time was determined as the one leading to the dissolution of the highest amount of titanium after sulfation step. The optimum time was used as the fusion time for the subsequent experiments.

The effect of mole ratio was investigated at ratios of 2:1, 4:1 and 6:1 ($NaOH:FeTiO_3$) at 750 °C. Non-stoichiometric conditions in terms of NaOH used per mole of $FeTiO_3$ were tested. A quarter, half and one mole of NaOH per mole of $FeTiO_3$ were used at 550 and 850 °C. The optimum mole ratio was determined as the one allowing to the dissolution of the highest amount of titanium in the solution. The optimum mole ratio was used in the subsequent experiments.

Two different particle sizes of ilmenite (corresponding to the extremes) were used in the fusion step, to assess the influence of particle size, namely $d_{50} \approx 6$ and $d_{50} \approx 139$ µm. The two particle sizes were used in the fusion reaction. The ideal particle size was determined as the one producing the maximum amount of titanium in the solution. The fusion reaction was conducted under the optimal conditions determined in previous steps.

3.5 Leaching

The AFDI, obtained in the fusion stage, was transferred to a beaker and approximately 150 mL of distilled water were added. The mixture was stirred in a Snijders hotplate magnetic stirrer 34532, using a 50 mm stirrer. The suspension was filtered by centrifugation. The process was repeated three times. A sample of the supernatant liquid was collected for elemental analysis. A sample of the residue was also collected for rational analysis. The collected samples were subjected to elemental analysis by ICP in solution. Essentially the solution was tested for losses in iron and titanium. The residue was subjected to XRD analysis for phase identification. For that the residue was dried overnight at 90 °C and da sample was then collected for XRD analysis. Elemental analyses for the residue were done by XRF. The aim was to identify impurities elements in the residue.

The effect of time was investigated over the range of 5 to 60 min of stirring at constant speed (mid-speed scale in the Snijders hotplate magnetic stirrer 34532). The efficiency of the process was tested by the amount of alkali leached in each experiment. The mixture was continually stirred and at indicated time a sample of the supernatant liquid was collected. The collected sample was filtered by centrifugation. The filtrated solution was titrated with standardized HCl solution for alkali content determination.

Three different amounts of water were used, namely 100, 150 and 200 mL, corresponding to solid:liquid ratios 0.2, 0.3 and 0.4 (solids in grams:water volume in mL). The most effective ratio was determined by the amount of alkali extracted.

AFDI obtained in the fusion stage was transferred to a beaker and the predefined amount of water was added. The mixture was stirred for the optimum time determined. After the required stirring time the slurry was filtered by centrifugation for 15 minutes. The filtered solution was titrated with standardized HCl solution, for alkali content determination.

The effect of temperature was tested at room temperature, 35, 40, 50 and 75 °C at 5 to 60 min of stirring time at constant speed. The slurry concentration was maintained at 0.4 (200 mL of distilled water).

For each experiment slurry was set at the predefined temperature and stirred in the conditions indicated in section 3.5. After a required stirring time a sample of the supernatant liquid was collected with a syringe and transferred into another beaker. This solution was titrated with standardized HCl solution, for alkali content determination.

3.6 Leaching Solution

The aim of leaching is to remove unreacted sodium hydroxide and to hydrolyse the ferrates and titanates of sodium eventually formed in the fusion stage. As a result, it enables the recovery of sodium hydroxide and reduces the acid consumption in further stages.

The leaching solution was placed in a beaker and titrated with standardised HCl solution using methyl orange as indicator. Alternatively, a pH meter was used to indicate the titration end-point. The results are presented in terms of percentage of NaOH present in the solution. The percentage was calculated on the bases of the initial amount of NaOH used in the fusion process according to the formula (Eq. 1)

$$\%\mathbf{NaOH} = \mathbf{100} \times \frac{\mathbf{m_{NaOH}}}{\mathbf{m^{a}_{NaOH}}} \qquad \text{(Eq. 1)}$$

Where $\mathrm{m}^{\mathrm{a}}_{\mathrm{NaOH}}$ is the weight of NaOH used in the fusion reaction in grams; m_{NaOH} is the weight of NaOH extracted by the leaching solution, determined according to the formula (Eq. 2)

$$\mathbf{m_{NaOH}} = \frac{\mathbf{V_{HCl}} \times \boldsymbol{C_{HCl}}}{\mathbf{25}} \qquad \text{(Eq. 2)}$$

Where V_{HCl} is the volume of HCl in mL; C_{HCl} concentration in mole/L.

3.7 Hydrolysis

The residual solid after leaching was placed in a beaker and titrated with standardised HCl solution up to pH 7. A pH meter was used to follow the titration. It is mainly ternary phases that are hydrolysed in this stage. The influential parameter here is the concentration of the acid.

The hydrolysis process is intended to remove the remaining sodium while avoiding the premature solubilisation of species of concern, especially titanium. The optimum hydrolysis pH was determined by measuring titanium losses by solubilisation. For this purpose, the hydrolysis pH was varied from 2 to 7 (at 0.5 intervals). Titanium and iron contents were assessed in the supernatant liquid by ICP-MS.

3.8 Sulfation Process

The acid-hydrolysed residue was washed three times with distilled water. A stoichiometric amount of concentrated H_2SO_4 was added to water-leached cake and stirred for 15 min. The resulting solution was clarified by centrifugation in order to remove the unreacted residue.

This residue was washed with water and the water added to the sulfate solution. The residue was dried in an oven at low temperature. The dry residue was transferred to a dried and previously weighed alumina crucible. The crucible was calcined at 900 °C overnight. The crucible was allowed to cool and weighed. The residue weight was determined as the difference between the weight of the empty crucible and the weight of the crucible with the calcined crucible (w_{residue}). The residue was expressed in terms of percentage of ilmenite feed as the unreacted ilmenite, as follows (Eq. 3)

$$\%\ \text{Residue} = \frac{w_{\text{residue}}}{w_{\text{FeTiO}_3}} \times 100 \qquad \text{(Eq. 3)}$$

Where $w_{residue}$ is the residue weighed in grams; w_{FeTiO3} is the weight of ilmenite sample used in the experiment.

The total sulfate solution obtained was weighed and subjected to chemical analysis for titanium and iron content. The elemental content was expressed in terms of percentage of ilmenite feed, according to the formulae (Eq. 4):

$$\%\ \text{Ti dissolved} = \frac{w_{\text{Ti}}}{w_{\text{Ti}}^{\text{FeTiO}_3}} \times 100 \qquad \text{and} \qquad \%\ \text{Fe dissolved} = \frac{w_{\text{Fe}}}{w_{\text{Fe}}^{\text{FeTiO}_3}} \times 100 \quad \text{(Eq. 4)}$$

Where w_{Ti} and w_{Fe} are the contents of titanium and iron in the sulfate solution in grams, respectively; $w_{\text{Ti}}^{\text{FeTiO}_3}$ and $w_{\text{Fe}}^{\text{FeTiO}_3}$ are the contents of titanium and iron in the ilmenite sample. Titanium and iron contents in the solution in grams were obtained by multiplying the titanium and iron concentrations determined by ICP elemental analysis with the total mass of sulfate solution obtained after sulfation process.

Titanium ($w_{\text{Ti}}^{\text{FeTiO}_3}$) and iron ($w_{\text{Fe}}^{\text{FeTiO}_3}$) contents in the ilmenite sample can be determined using the stoichiometry of the chemical formula. We considered in our calculation the elemental analysis results by XRF performed in this work (section 3.1.2), as well as the purity of the sample according to the following formula (Eq. 5)

$$w_{\text{element}}^{\text{FeTiO}_3} = \frac{w_{\text{FeTiO}_3} \times m \times C_{\text{EO}} \times A_E}{M_{\text{EO}}} \qquad \text{(Eq. 5)}$$

Where m is the moisture of the ilmenite sample; $C_{EO}$is the content of TiO_2 or Fe_2O_3 determined by XRF (section 3.1.2); A_E is the atomic weight of titanium or iron; M_{EO} is the molecular weight of TiO_2 or Fe_2O_3. For moisture determination a sample of ilmenite was weighed in a crucible previously dried and placed in a drying oven for one hour, at 110 °C. The crucible was then removed and allowed to cool in a desiccator. The cooled crucible was weighed and returned to the oven for another 15 minutes. The operation was repeated until a constant weight of the crucible was obtained. The moisture content was determined as the difference of initial weight of ilmenite and the constant weight of the dried ilmenite sample.

The sulfation process was optimised in terms of the quantity of sulphuric acid necessary for optimum dissolution in the reaction. For this purpose an excess of 5–15% above the stoichiometric amount of acid was added. The results were expressed in terms of the relative amounts of iron and titanium dissolved with each quantity of acid. Any increase in the concentration of iron or titanium would imply that an excess should added to the stoichiometric quantity of sulphuric acid required in reaction. The outline of the entire process is presented in Scheme 1.

Scheme 1: Outline of the alkali fusion process for titanyl sulfate

Process step	Notes
$FeTiO_4 + x\ NaOH$	
1 ↓ 550 °C – 950 °C	1. Fusion (Choose reaction conditions to maximise yield of sodium iron titanates)
$Na_2TiO_3 + NaFeTiO_4 + Na_{0.75}Fe_{0.75}Ti_{0.25}O_2$	
2 ↓ water leach	2. Cool down and mill. Remove sodium silicates, unreacted NaOH, and other sodium salts formed during fusion using a water leach.
$TiO_2.xH_2O + FeOOH.xH_2O$	
3 ↓ HCl to pH = 3.8	
4 ↓ leach	
$TiO_2.xH_2O + FeOOH.xH_2O$	3. Neutralise to hydrolyse sodium salts.
5 ↓ H_2SO_4 (stoichiometric)	
$TiOSO_4 + Fe_2(SO_4)_2$	4. Remove remnant sodium as NaCl using a water leach.
↓	
Sulphate Process	5. Formation of titanyl sulphate solution

4. Results and Discussions

4.1 Material Composition

Table 4 and Table 5 present the elemental analysis of the starting material. Table 6 shows the mineralogical results. The results were obtained by XRF for elemental composition and XRD for mineralogical analysis.

Table 4: Composition of ilmenite raw material (major elements)

Component	SiO_2	TiO_2	Al_2O_3	Fe_2O_3	MnO	MgO	CaO	Na_2O
Concentration	0.48%	47.3%	0.51%	51.6%	0.97%	0.70%	0.07%	0.42%
Component	K_2O	P_2O_5	Cr_2O_3	NiO	V_2O_5	ZrO_2	**LOI**	**Total**
Concentration	0.02%	0.01%	0.17%	0.03%	0.51%	0.38%	-2.90	100

The elemental analysis indicated titanium and iron as the main constituents. This ore contains chromium, phosphorus and vanadium, which are impurities harmful to the quality. Niobium must be reduced as well during processing. The level of alkaline earth elements, namely magnesium and calcium, is found to be above the recommended level (Aminesh *et al.*, 2005; Habashi, 1997; Hollitt *et al.*, 2002; Lahiri *et al.*, 2006; Nielsen and Chang, 1996).

According to results from Table 1 and Table 2, the ore can be considered sulfate grade ilmenite. It is not suitable for chlorination due its low TiO_2 content (Murphy and Frick, 2006).

Table 5: Composition of ilmenite raw material (minor elements)

Element	**As**	**Cu**	**Ga**	**Mo**	**Nb**	**Ni**	**Pb**	**Rb**
Conc., ppm	3	21	5	4	466	58	96	8
Element	**Sr**	**Th**	**U**	**W***	**Y**	**Zn**	**Zr**	**Cl***
Conc., ppm	2	87	15	149	90	286	3086	8
Element	**Co**	**Cr**	**F***	**S***	**Sc**	**V**		
Conc., ppm	190	1629	100	543	48	572		

* = Semi-quantitative analysis; Conc.= concentration; ppm = parts per million

Mineralogical analysis showed that the ilmenite sample has zircon and ferrous oxide (Fe_2O_3) as the main impurities. Traces of anatase and rutile are also present in the sample (Table 6).

Table 6: Phase composition of the ilmenite raw material

Phase	$FeTiO_3$	Fe_2O_3	$ZrSiO_4$	TiO_2 (rutile)	TiO_2 (anatase)
Observation	Major	Minor	Minor	Trace	Sub-trace

4.2 Thermogravimetric Analysis

The reaction of sodium hydroxide with ilmenite was followed by TGA/DTA thermal analysis. Figure 9 shows a TG/DTG curve recorded at a rate of 10 ^{o}C/min of sample prepared by mixing two moles of sodium hydroxide with one mole of ilmenite.

The TG curve (Figure 9) shows an intense mass loss beginning just above 350 °C and ending at 525 °C. The observed mass loss is 6.53%, which is approximately 84% of the total expected if mass loss was due to dehydration of NaOH alone. In reality the mass gain due to oxidation must also be accounted for. The alkali fusion reaction of ilmenite is characterised by the evolution of water according to the following reaction (1):

$$4FeTiO_3 + 12NaOH + O_2 \rightarrow 4NaFeO_2 + 4Na_2TiO_3 + 6H_2O \quad (1)$$

On the DTG curve a maximum is observed at 490 °C for ilmenite reactant ($FeTiO_3$ in Figure 9). For ilmenite ore this value is shifted to 530 °C (ore in Figure 9). The DTG curve was constructed by differentiating the TG signal and plotting the obtained DTG results against temperature.

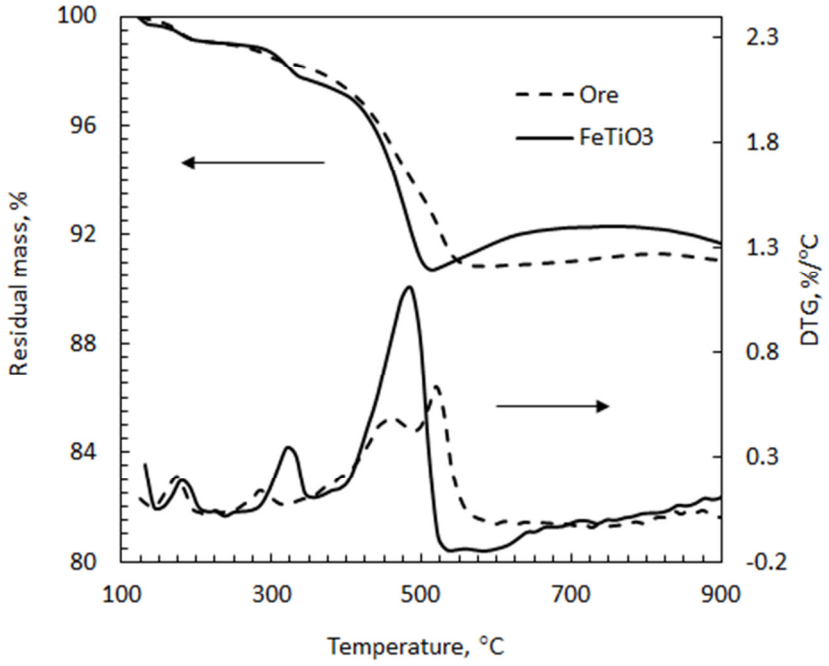

Figure 9:TG curves of the reaction of ilmenite ore and $FeTiO_3$ reactant (analytical grade) with two moles of NaOH (10 °C/min in oxygen)

With the ilmenite ore sample (Figure 9) the mass loss begins at comparatively lower temperatures, just above 200 to 560 °C. The stretching of the region corresponds to an overlapping of moisture release with water liberation from the reaction. The DTG curve shows a complex mechanism. This is an indication of two consecutive reactions with a large difference in the activation energy or in the frequency factor occurring (Wilburn, 2000). Two consecutive peaks, at 470 and 530 °C, are obtained. In this situation it is meaningless to determine the

activation energy values and the frequency factor, according to Wilburn (2000). Pure ilmenite (see Figure 9) shows a single peak in the DTG curve under similar conditions, at approximately 490 °C. This indicates that ilmenite itself reacts with NaOH in one single-step reaction with T_{max} ≈ 490 °C. This makes it possible to study the roasting reaction kinetically. The second reaction is believed to be that of other phases present as impurities in the ilmenite (see Table 4 and Table 5). The supplementary DTG peaks observed in the ilmenite ore curve were further investigated by heating mixtures of ilmenite ore and NaOH (2:1, NaOH:ilmenite mole ratio) and subjecting the product to XRD analysis for phases identification. Results are presented in Figure 10.

4.3 Fusion Results

4.3.1 Fusions at lower temperatures and extended periods

Experiments were performed at 250 and 500 °C. The identified phases in alkali fusion decomposed ilmenite (AFDI) in the XRD patterns are presented in Table 7.

Table 7: Identified phases in XRD patterns (Appendix A2–A6) of AFDI obtained after fusing for 336 h

Mol ratio (NaOH:$FeTiO_3$)	Temperature (°C)	Phases		
		$FeTiO_3$	Na_2TiO_3	Fe_2O_3
1:1	250	Major	-	-
2:1	250	Major	-	Minor
4:1	250	Major	-	-
6:1[8]	250	Major	-	-
4:1	500	Major	Major	Major[9]

In all samples sodium carbonate (Na_2CO_3) was present as the major phase. Sodium carbonate is a result of CO_2 absorption, by sodium hydroxide, from the atmosphere. Sodium silicate

[8] Amorphous
[9] As sodium iron silicon oxide, $Na_{0.925}(Fe_{0.925}Si_{0.075})O_2$

(Na_2SiO_3) and sodium iron silicate ($Na_{0,925}Fe_{0.925}Si_{0.075}O_2$) were observed at 500 °C, using four moles of sodium hydroxide per mole of ilmenite for 336 h.

The thermogravimetric results indicated that the reaction of ilmenite initiates just above 250 °C. The fusion experiments conducted at this temperature, using four different mole ratios (1:1, 2:1, 4:1 and 6:1, NaOH: $FeTiO_3$) for 336 h, did not produce noticeable changes (Appendix A2–A6, Table 1). At 500 °C, using four moles of NaOH, $FeTiO_3$ was still the dominant phase after 336 h of fusion. Na_2TiO_3 was the other major phase. $Na_{0.925}(Fe_{0.925}Si_{0.075})O_2$ was present as the concomitant iron phase (major). Silicon is incorporated, in a collateral reaction, in Fe^{3+} and Na^+ sites in $NaFeO_2$. The observed products are consistent with the following reaction (2):

$$4FeTiO_3 + 6Na_2O + O_2 \rightarrow 4Na_2TiO_3 + 4NaFeO_2 \quad (2)$$

4.3.2 Effect of fusion temperature

The effect of temperature was investigated using a 2:1 ($NaOH:FeTiO_3$) mole ratio. The temperature was varied from 300 to 950 °C, with a 50 °C gradient. The use of a 2:1 ($NaOH:FeTiO_3$) mole ratio is regarded as conducive to the formation of ternary phases and is economical in terms of NaOH consumption per mole of $FeTiO_3$. According to our results, Figure 10, no changes were observed at 300 °C. Ilmenite disappears from the products spectra only above 800 °C. Binary phases dominate below 600 °C, while ternary phases are observed above 650 °C. Figure 10 was plotted using the weight percent phase obtained as described in section 3.1.1. In order to minimize the number of phases presented in the graphic, for clarity, all the sodium titanate phases ($NaTiO_2$, $Na_8Ti_5O_{14}$ and Na_2TiO_3) were grouped as Na_2TiO_3. Sodium iron phases ($NaFeO_2.2H_2O$, $Fe_6(OH)_{12}CO_3.2H_2O$, and $NaFeO_2$) were grouped as $NaFeO_2$.

It is worth noting that the formation of ternary phases led to less NaOH being recovered. Figure 10 presents the identified phases in the XRD patterns (see Appendix A8–A19 and Table A 1). According to our results, no changes were observed at 300 °C. Ilmenite disappears from the products spectra only above 800 °C. Binary phases dominate below 600 °C, while ternary phases are observed above 650 °C.

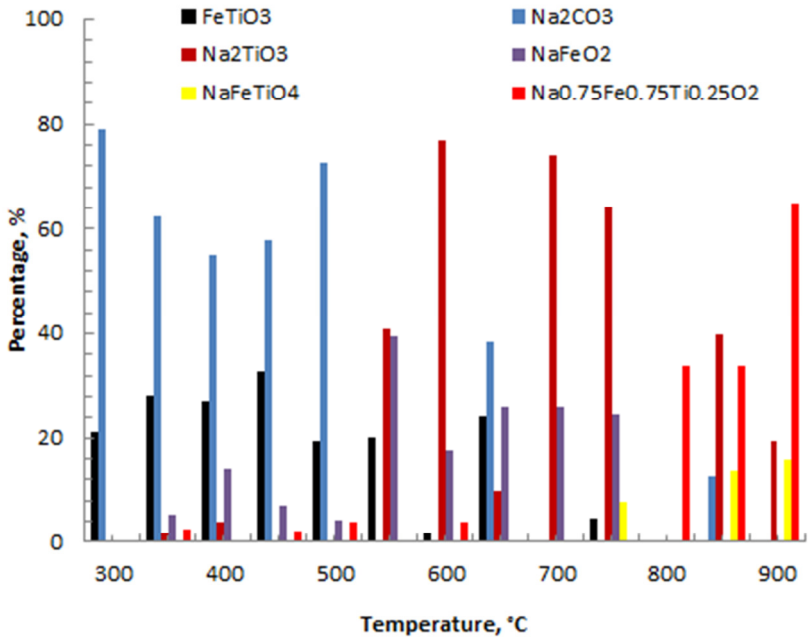

Figure 10: Effect of fusion temperature on the product spectra of the ilmenite alkali fusion reaction. Samples prepared with two mole NaOH per mole of ilmenite.

Five titanium-bearing phases were identified, namely $NaFeTiO_4$, $Na_8Ti_5O_{14}$, Na_2TiO_3, $Na_2Fe_2Ti_3O_{10}$ and $Na_{0.75}Fe_{0.75}Ti_{0.25}O_2$. No changes were detected at 300 °C. $Na_2Fe_2Ti_3O_{10}$ was observed only at 800 °C (Figure 11). Phases such as $Na_xFe_xTi_{2-x}O_4$, $Na_xFe_xTi_{8-x}O_{16}$, $Na_2Fe_2Ti_7O_{18}$, $NaFeTi_5O_{12}$, $Na_{2+x}Fe_xTi_{4-x}O_9$ and Na_4FeTiO_5 referred to in the literature were not observed in ourproducts (Bayer and Hoffman, 1965; Foley and Mackinnon, 1970; Li *et al.*, 1971; Reid and Sienko, 1967).

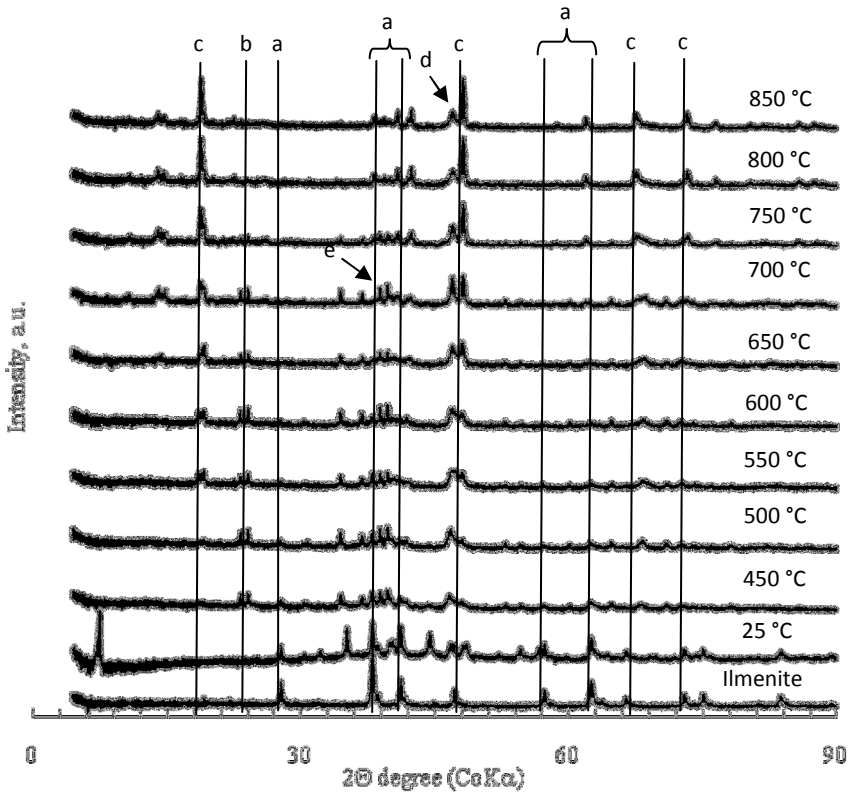

a = $FeTiO_4$; b = $NaFeO_2$; c = $Na_{0.75}Fe_{0.75}Ti_{0.25}O_2$; d = Na_2TiO_3; e = $NaFeTiO_4$

Figure 11: XRD difractograms of alkali fusion decomposed ilmenite. Samples of ilmenite:NaOH (2:1 mole ratio) were fused for 1 h at the indicated temperatures

Three temperature regions can be delimited in the reaction, according to the phases formed. From 350 to 550 °C, ilmenite is dominant, with $Na_{0.75}Fe_{0.75}Ti_{0.25}O_2$ as a minor phase. It is worth noting that Na_2CO_3 is also present as a major phase, indicating that the reaction was not completed under the conditions used. In two samples (at 350 and 400 °C) $NaTiO_2$ was detected. Its presence must be related to the non-availability of oxygen as oxidant, prompting to reduction of Ti^{4+} ions. $NaTiO_2$ is formed at the expense of Na_2TiO_3. Although single titanates, especially Na_2TiO_3, were not detected, the presence of $Na_{0.75}Fe_{0.75}Ti_{0.25}O_2$ and $NaFeO_2$ entails the formation of single titanates to accommodate the excess titanium. The Fe:Ti proportion in this phase is 3:1. The remaining Ti has to be accommodated in single titanates, mainly Na_2TiO_3. This is also supported by the findings of Foley and MacKinnon (1970). According to these

authors, when the Fe:Ti ratio is greater than 1:1 in the Na-Fe-Ti oxides, the surplus titania is accommodated as single titanates, mainly Na_2TiO_3. The presence of $NaFeO_2$ in the products is regarded as a collateral reaction of the Fe_2O_3 present in the sample as an impurity (see Table 6). The reaction (3) below the figure explains the observed transformations.

$$12FeTiO_3 + 14Na_2O + 3\ O_2 \rightarrow 16Na_{0.75}Fe_{0.75}Ti_{0.25}O_2 + 8Na_2TiO_3 \quad (3)$$

From 600 up to 800 °C a considerable proportion of $FeTiO_3$ was consumed. $Na_2Fe_2Ti_3O_{10}$, $NaFeTiO_4$, $Na_8Ti_5O_{14}$, Na_2TiO_3 and $Na_{0.75}Fe_{0.75}Ti_{0.25}O_2$ were detected in the products. $Na_8Ti_5O_{14}$, Na_2TiO_3 and $Na_{0.75}Fe_{0.75}Ti_{0.25}O_2$ were identified in the whole range of temperatures, while $NaFeTiO_4$ was identified at 750 and 800 °C. $Na_8Ti_5O_{14}$ tends to decrease with temperature, while Na_2TiO_3 and $Na_{0.75}Fe_{0.75}Ti_{0.25}O_2$ showed the opposite trend. This is in agreement with the findings of previous authors. $Na_8Ti_5O_{14}$ is involved in the Na_2TiO_3 formation reaction (Batygin, 1967; Belyaev *et al.*, 1970; Belyaev, 1976). The surplus iron was accommodated in $NaFeO_2$.

$NaFeO_2$ is present as a major phase in all samples. From these the following reaction was written (4):

$$16FeTiO_3 + 18Na_2O + 4O_2 \rightarrow 16Na_{0.75}Fe_{0.75}Ti_{0.25}O_2 + 2Na_2TiO_3 + 2Na_8Ti_5O_{14} + 4NaFeO_2 \quad (4)$$

From 850 to 950 °C ilmenite was completely consumed after the reaction time used. $NaFeTiO_4$, Na_2TiO_3 and $Na_{0.75}Fe_{0.75}Ti_{0.25}O_2$ are the only phases observed. $NaFeO_2$ is only observed at 850 °C, while $Na_8Ti_5O_{14}$ is observed at 950 °C. $NaFeTiO_4$ and Na_2TiO_3 tend to reduce as the temperature increases, while $Na_{0.75}Fe_{0.75}Ti_{0.25}O_2$ increases with temperature (see Figure 12). Na_2TiO_3 reduction is believed to be due to a further reaction (combination) with $NaFeO_2$ to form of $Na_{0.75}Fe_{0.75}Ti_{0.25}O_2$ or similar phases with high utilisation of alkali, according to reaction (5):

$$3NaFeO_2 + Na_2TiO_3 \rightarrow 4Na_{0.75}Fe_{0.75}Ti_{0.25}O_2 + Na_2O \quad (5)$$

$NaFeTiO_4$ and $Na_2Fe_2Ti_3O_{10}$ were sporadically observed. $NaFeTiO_4$ was present at 550 ^oC and at 750 ^oC and above (see Figure 12). This phase is consistent with a 1:1 $FeTiO_3$:NaOH mole ratio. $Na_2Fe_2Ti_3O_{10}$ was only observed at 800 ^oC (seeFigure 10). Figure 12was obtained using the weight percent phase calculations as described in section 3.1.1.

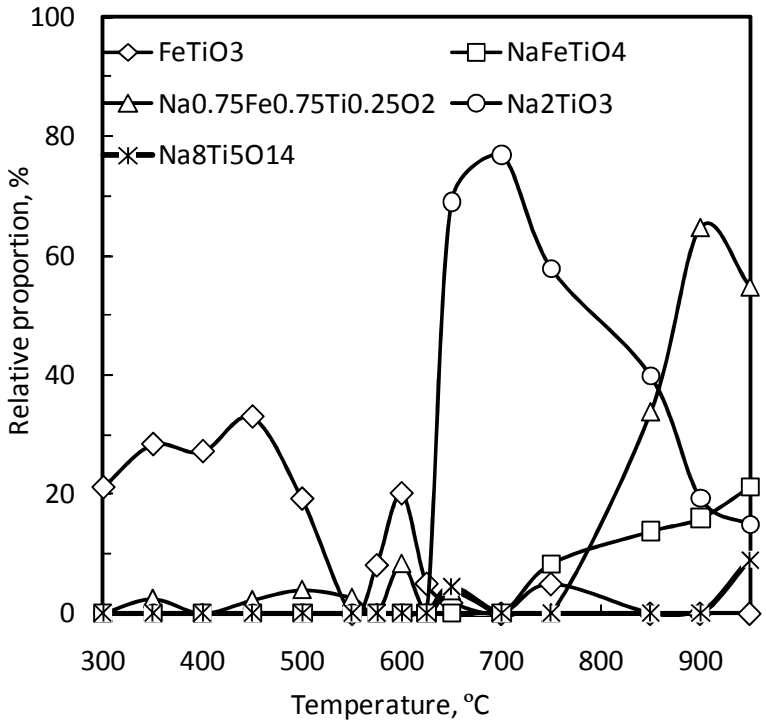

Figure 12: Phase correlation in the alkali fusion products, from the XRD semiquantitative weight percent. Samples were obtained by fusing the ore with NaOH (2:1 mole ratio) for 1 h

4.3.3 Effect of mole ratio and time

The effect of mole ratio was investigated at 750 ^oC using 2:1, 4:1 and 6:1 mole ratios ($NaOH:FeTiO_3$). The effect of time was tested at 30, 60 and 120 min of fusion. Table 8 shows the identified phases in the XRD analysis of alkali fusion decomposed ilmenite. The respective XRD diagrams are presented in Appendix A20–A28. Four titanium phases were identified in the

AFDI, namely $NaFeTiO_4$, $NaTiO_2$, $Na_8Ti_5O_{14}$ and Na_2TiO_3. Iron was chiefly accommodated in $NaFeO_2$.

Table 8: Identified phases by XRD in the AFDI diagrams obtained after roasting a mixture of ilmenite with sodium hydroxide for 1 h

Mole ratio, $NaOH:FeTiO_3$									
	2:1			**4:1**			**6:1**		
Time, min	30	60	120	30	60	120	30	60	120
$FeTiO_3$	minor	-	-	minor	-	-	minor	-	-
$NaFeTiO_4$	-	minor	major						
$NaTiO_2$	minor	minor	-	major	major	major	major	major	minor
$Na_8Ti_5O_{14}$	major	minor	-	minor	major	-	-	-	-
Na_2TiO_3	major	major	-	major	major	major	major	major	major
$Na_{0.75}Fe_{0.75}Ti_{0.25}O_2$	-	major	major	-	-	-	-	-	-
$NaFeO_2$	major	major	major	major	major	major	major	major	-
Na_2CO_3	trace	minor	-	major	trace	minor	major	major	-

Short periods of fusion produced mainly single titanates, irrespective of the mole ratio applied. At this temperature, fusions for a period of 30 and 60 min produced Na_2TiO_3 and $Na_8Ti_5O_{14}$. $Na_8Ti_5O_{14}$ was observed when two and four moles of NaOH were used, with a fusion period of up to 1 h. High mole ratios and extended periods of fusion did not favour $Na_8Ti_5O_{14}$. This was observed previously and was found to be consistent with the findings that this $Na_8Ti_5O_{14}$ is an intermediate in the roasting reaction (Batygin, 1967; Belyaev *et al.*, 1970; Belyaev, 1976).

At 2 h, at a mole ratio of 2:1 ($NaOH:FeTiO_3$), $NaFeTiO_4$ was the major phase. The existence of $NaFeO_2$ can be regarded as being a result of the reaction of Fe_2O_3 with NaOH, as was explained earlier. However, the relative amount in this case indicates that ilmenite was the source of iron. In fact, the major titanium phases are ternary ones.

4.3.4 Fusions under NaOH starved[10] conditions

Fusions under substoichiometric conditions were conducted in an effort to maximize the production of ternary phases. Those were considered as the most effective in recovering more titanium using the less amount of sodium hydroxide. Three mole ratios were analysed, namely 1:1, 1:2 and 1:4 ($NaOH:FeTiO_3$), at 550 and 850 ^oC fusion temperatures for 1 h. The identified phases in the XRD patterns are presented in Table. Under prevalent conditions, temperature is the determining factor. As is obvious from the results in Table, at 550 °C binary phases dominate (Na_2TiO_3 and $NaFeO_2$); while at 850 °C ternary phases dominate ($NaFeTiO_4$ and $Na_3Fe_3TiO_8$). At 550 ^oC, $FeTiO_3$ was the dominant phase irrespective of the mole ratio. At 850 ^oC $FeTiO_3$ was not observed in the products.

Table 9: Fusions of NaOH:Ilmenite ore under starving conditions for 1 h

	Temperature					
	550 °C			**850 °C**		
Mole ratio, $NaOH:FeTiO_3$	**1:4**	**1:2**	**1:1**	**1:4**	**1:2**	**1:1**
$FeTiO_3$	major	major	major	nd	nd	nd
$NaFeTiO_4$	nd	nd	nd	nd	minor	major
$NaTiO_2$	minor	nd	nd	nd	nd	nd
$Na_8Ti_5O_{14}$	minor	nd	nd	minor	nd	minor
Na_2TiO_3	minor	major	major	nd	nd	nd
$Na_3Fe_3TiO_8$	nd	nd	nd	major	major	major
$NaFeO_2$	major	major	major	nd	minor	minor

nd – non detected

At 550 ^{o} the principal titanium phase was Na_2TiO_3. $Na_8Ti_5O_{14}$ was present when a quarter of a mole of NaOH was used. Fe was accommodated chiefly in $NaFeO_2$. The phases obtained are improbable under the conditions used. Their formation indicates that the reaction did not proceed to its completion.

[10]Fusions using amounts of NaOH less than the stoichiometric amount

At 850 ^{o}C, $NaFeTiO_4$ and $Na_{0.75}Fe_{0.75}Ti_{0.25}O_2$ are the dominant phases. $Na_8Ti_5O_{14}$ and $NaFeO_2$ are present as minor phases. The former phases are non-equilibrium. The formation of $Na_8Ti_5O_{14}$ and $NaFeO_2$ has to be regarded as being kinetically driven. With longer fusion periods it is expected that $Na_8Ti_5O_{14}$ and $NaFeO_2$ will recombine and form ternary phases.

4.4 FT-IR Analysis

The fusion reaction was followed by infra-red spectroscopy. The spectra recorded at different fusion temperatures are presented in Figure 13. For AFDI samples obtained between 400 and 550 °C, a band at 3670–2350 cm^{-1} can be observed. This band can be attributed to different modes of O-H vibration in water (Ryskin, 1974). The presence of O-H bands indicates that NaOH did not react completely. These bands result from NaOH and from water absorbed by NaOH.

An overview of the region between 1800 and 400 cm^{-1} indicates the existence of two distinct regions: the first from 400–900 cm^{-1} and the second between 1300 and 1600 cm^{-1}, according to the disposition of the absorption bands in the spectra. Vibrations of ions in the crystal lattice are observed in the region of 1000–400 cm^{-1}, according to Sertkol *et al.* (2009).

In the first region (900–400 cm^{-1}), taking the ilmenite spectrum as the starting material, significant changes can be observed after NaOH addition with new bands at 630 and 900 cm^{-1}. The band at 900 cm^{-1} disappears above 550 ^{o}C, while the one at 630 cm^{-1} broadens with temperature.

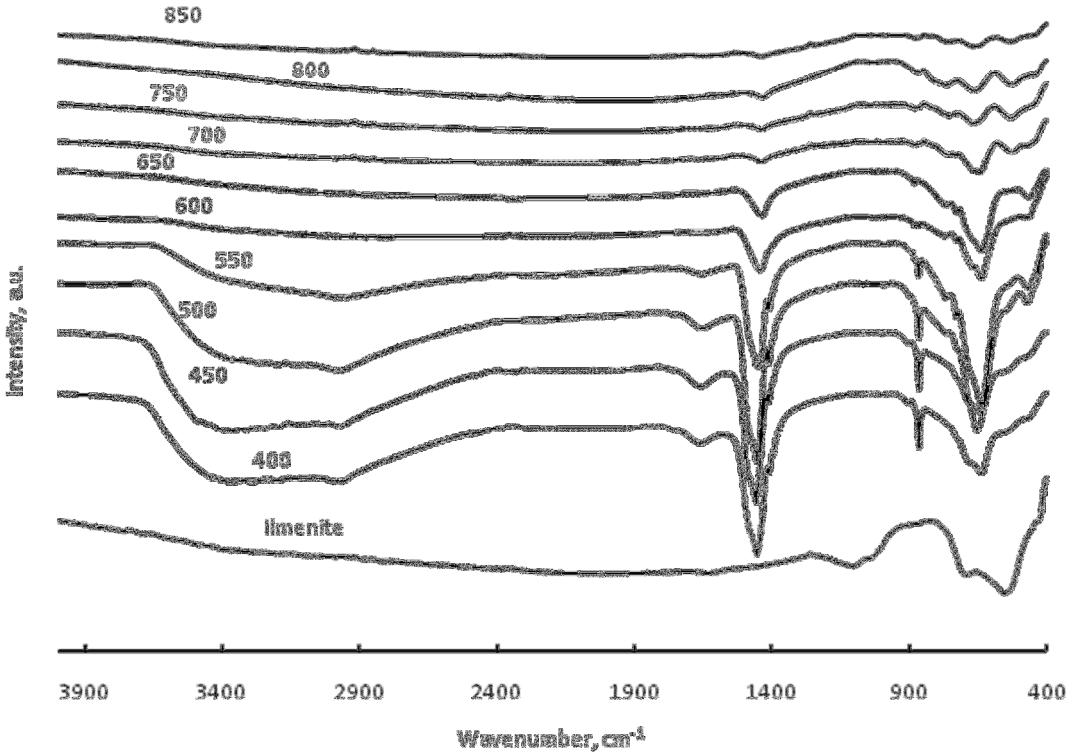

Figure 13:FT-IR spectra of alkali fusion decomposed ilmenite. Samples were obtained by fusing NaOH:$FeTiO_3$ mixtures (2:1 mole ratio) for 1 h at the indicated temperatures

In the 1600–1300 cm^{-1} region, AFDI at lower temperatures presents an absorption band from 1530–1340 cm^{-1}, with peaks at 1453, 1408 and a shoulder at 1484 cm^{-1}. This band weakens as the fusion temperature increases (see Figure 12).

The aim of the FT-IR analyses was to identify active groups at different fusion temperatures to elucidate the reaction mechanism. We looked into the evidence of formation of different groups. Under adequate conditions, temperature and mole ratios, the reaction of ilmenite (FeTiO3) with NaOH produces titanates and iron titanates. Ilmenite mineral ore, however, contains other chemical species present as impurities (see Table 4, Table 5 and Table 6).

Theexistence of such impurities, the mole ratio applied and the processing temperature can lead to different products, as can be seen in our results (see Table 7, Figure 10, and Table 8).

Iron silicates can be identified by a band in the region 930–1020 cm^{-1} (Jambor and Dutrizac, 1998). This band is observed in all AFDI samples. The band reduces intensity above 500 ^{o}C. It is an indication that iron silicates are part of the mechanism in earlier stages of the reactions. Above this temperature iron silicates apparently decompose. The XRD results show the existence of a sodium iron silicate ($Na_{0,925}Fe_{0.925}Si_{0.075}O_2$) phase at 500 ^{o}C (Appendix A-6; see Figure 14). This is important since it reduces sodium consumption, contributing to the economy of the process.

The presence of titanosilicates can be unequivocally established by the presence of bands at 960 and 1125 cm^{-1}, according to Ratnasamy *et al.* (2004). The peaks at around 1060 and 970 cm^{-1} are due to Si-O-Si asymmetric stretching in silicates (Muroya, 1999; Vicente-Rodríguez *et al.*, 1996).

Three groups of titanium structures are observed, according to our results: the TiO_4 tetrahedra, TiO_6 octahedra and TiO_5 groups. A band observed in all samples between 650 and 750 cm^{-1} is assigned to TiO_4 tetrahedra, while bands below or near 500 cm^{-1} are due to TiO_6 octahedra (Tarte *et al.*, 1979); these are also present in all samples. The TiO_5 group is present at 450, 500, 550, 600, 650, 700 and 850 ^{o}C (Figure 14 and Table 10). A band at 725 cm^{-1} is observed and is assigned to the TiO_5 group (Peng and Liu, 1995). The TiO_4 group is present in $M^{II}TiO_4$ compounds, the TiO_6 octahedra in sodium titanates and the TiO_5 group is present in Ti-O_x fresnoite-like ($Ba_2TiOSi_2O_7$) compounds (Gabelica-Robert and Tarte, 1981; Peng and Liu, 1995). Sodium iron titanates of the family $Na_xFe_xTi_{2-x}O_4$ are reported to have TiO_6 octahedra (Kuhn *et al.*, 1996). The ilmenite structure also possesses such groups. Pure TiO_2 presents an intense band between 900-450 cm^{-1} with a peak at 550 cm^{-1}.

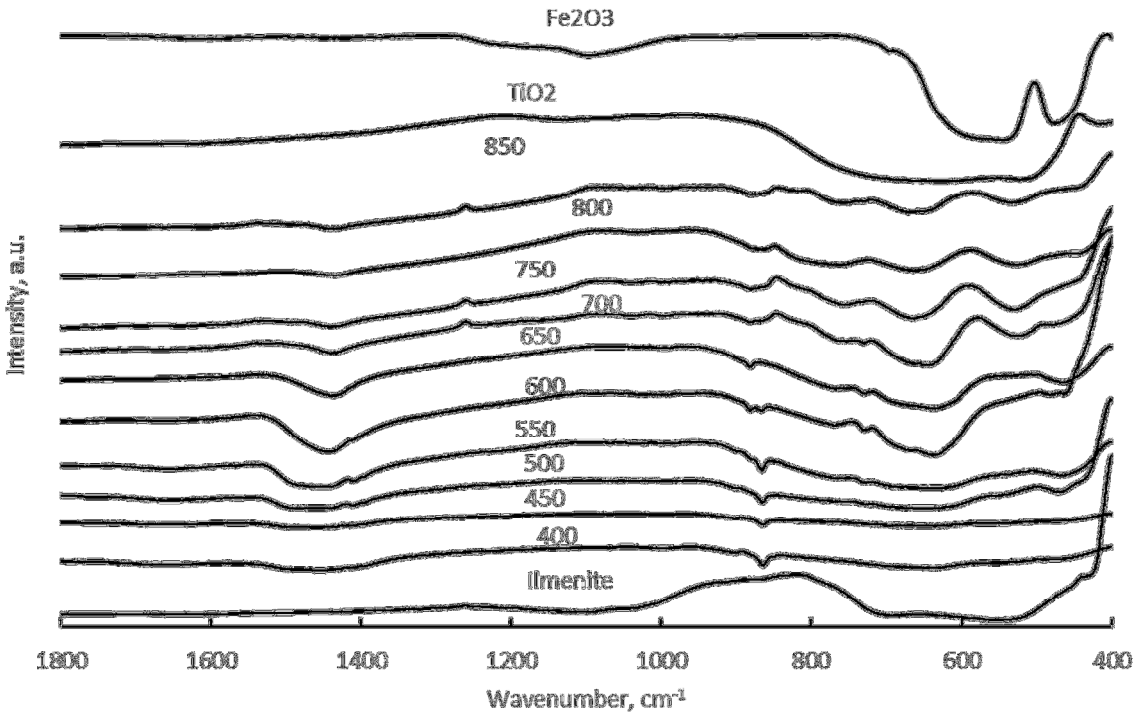

Figure 14: FT-IR spectra of the fusion-processed NaOH:$FeTiO_4$ mixtures (2:1 mole ratio), mid infra-red range. Samples were fused for 1 h at the indicated temperatures

Iron, as expected, is present in all samples. All samples exhibit maximum absorption in the region of 650–550 cm^{-1}. FeO_4 tetrahedra absorb in this region (Sertkol *et al.*, 2009; Tarte *et al.*, 1979). This is also observed in Fe_2O_3 spectrum, an intense absorption band is observed between 700-500 cm^{-1}. FeO_4 also absorbs in the region of 780 to 750 cm^{-1} (Licht *et al.*, 2005; Xu *et al.*, 2007). All samples present absorption bands in this region.The FT-IR assignments are summarised in Table 10.

Table 10: Assignments of FT-IR bands in ilmenite and fused products

Sample	Band position (cm^{-1})	Assignment	References
Below 600 °C	2400 and 3800	O – H stretching vibration in M – OH groups	Nagarajan and Rajendran, 2009 Ryskin, 1974
All	1600	Absorbed water	
All	1080	Si – O stretching in SiO_4 tetrahedral groups	Farmer, 1974; Méndez-Vivar *et al.*, 2001; Ratnasamy *et al.*, 2004
700 °C	1130	Ti – O in TiO_4 groups and MO – OM in terminal groups	Ratnasamy *et al.*, 2004
Below 800 °C	861	Ti – O stretching in TiO_6 Si – O symmetric vibration	Gabelica-Robert and Tarte, 1981
All	550–650	FeO_4 tetrahedral groups	Tarte *et al.*, 1979
450–700 °C	500	Ti – O stretching in TiO_6	Tarte *et al.*, 1979

4.5 Scanning Electron Microscopy

The ilmenite alkali fusion reaction was also studied by scanning electron microscopy (SEM). A panoramic view of the ilmenite ore SEM micrographs shows a random morphology of crystals (Figure 15(a)). In a closer look, the ilmenite crystals present lamellar aggregates (Figure 15(b)).

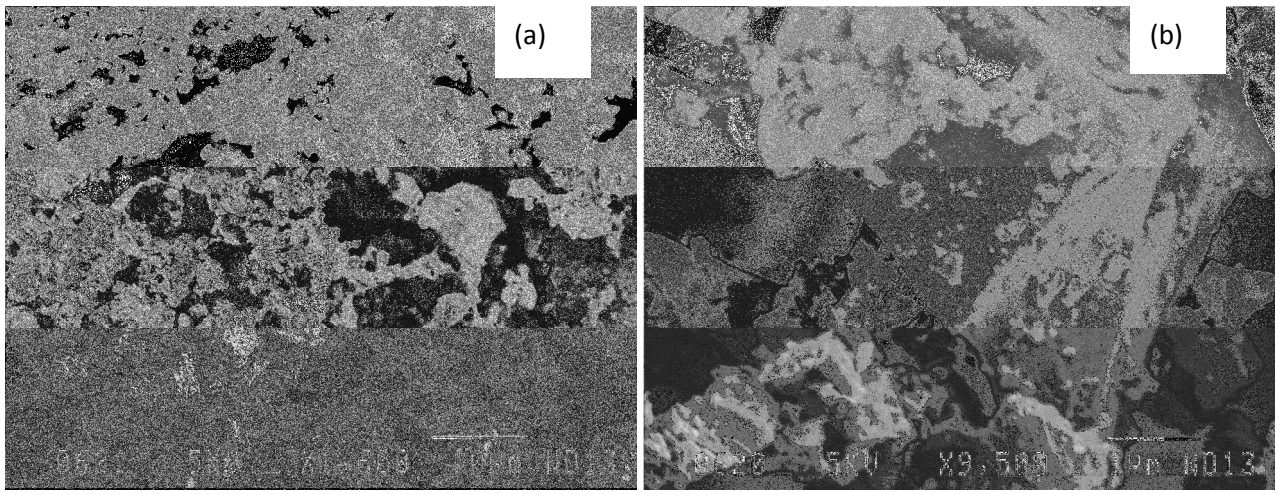

Figure 15: Microphotography of ilmenite ore material used in this study. (a) Lower magnification; (b) higher magnification

Variation in the crystal morphology during the reaction was identified by SEM. Figure 16shows ilmenite crystals (Figure 16(a)) collapsing to form a wafer-like morphology at 700 ^{o}C (Figure 16 (b)). As the fusion temperature increases, the wafer morphology is abandoned to assume a more disordered structure, a cotton seed-like morphology (Figure 16(c)), at 750 ^{o}C. A further increase in the fusion temperature, to 850 ^{o}C, resulted in the AFDI reacquiring the wafer-like morphology (Figure 16 (d)). This indicates the formation of ternary compounds by inclusion of sodium ions into the ilmenite crystal lattice.

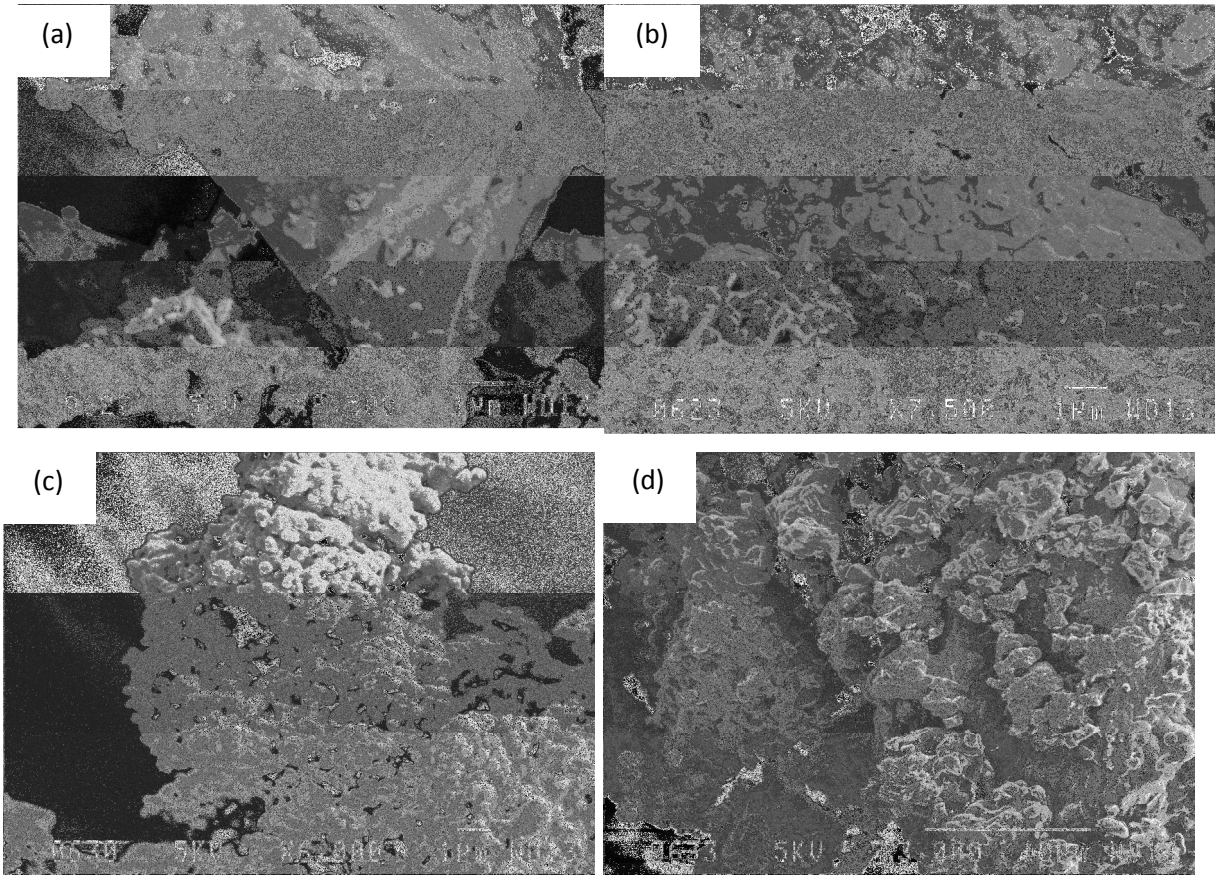

Figure 16: Microstructure evolution induced by the ilmenite alkali fusion reaction. (a) Ilmenite raw material; (b) NaOH:$FeTiO_3$ fused at 700 ^oC for 1 h; (c) NaOH:$FeTiO_3$ fused at 750 ^oC for 1 h; (d) NaOH:$FeTiO_3$ fused at 850 ^oC for 1 h

This reversibility of the crystal morphology was not observed in the colour of the crystals (Figure 17). The colour changes from black (ilmenite) to a maroon (850 ^oC). Intermediate AFDI samples present as green (500 ^oC) to a mixture of brown and green (650 ^oC).

Ferrous ion (Fe^{2+}) salts are green, while ferric ions (Fe^{3+}) are brown (or red). AFDI samples below 550 ^oC present a green colour, suggesting the predominance of iron in the ferrous oxidation state. This indicates that iron oxidises after being released from the ilmenite structure. In preliminary stages of the reaction, iron is released from the ilmenite structure. The

oxidation proceeds as the ilmenite structure is destroyed. Thus oxygen is the oxidant. Above 600 ^{o}C, iron oxidation to the ferric state is significant. The colour changes to red (brown).

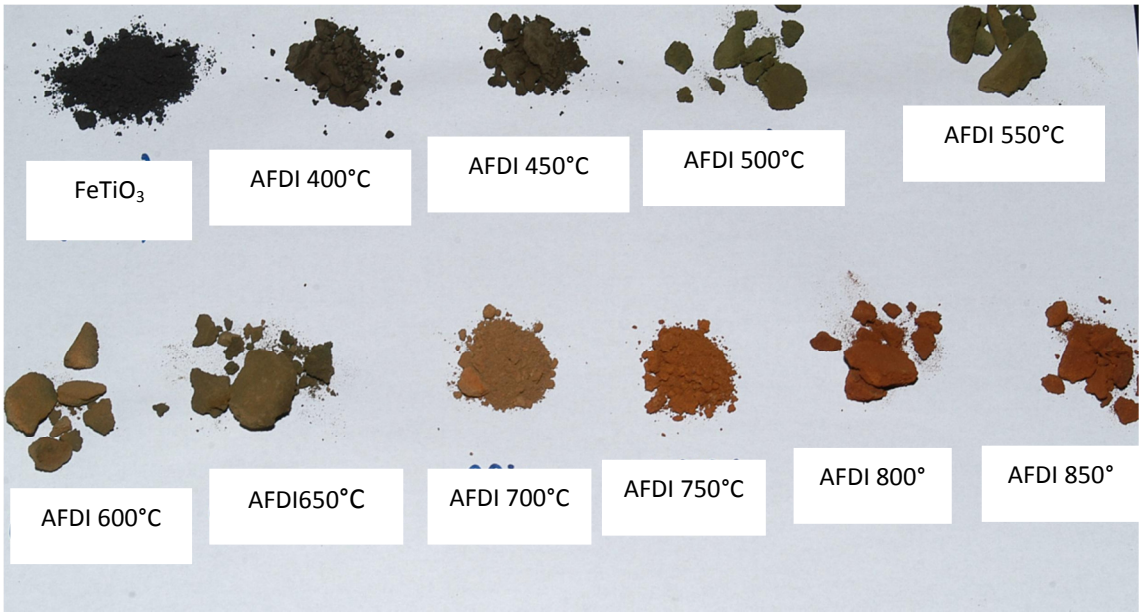

Figure 17: Colour evolution in ilmenite:NaOH mixtures (2:1 mole ratio) after fusion for 1 h at the indicated temperatures

4.6 Ilmenite Alkali Fusion Reaction

Five titanium-bearing phases were identified in our fusion products, namely $NaFeTiO_4$, $Na_8Ti_5O_{14}$, Na_2TiO_3, $Na_2Fe_2Ti_3O_{10}$ and $Na_{0.75}Fe_{0.75}Ti_{0.25}O_2$. The product spectrum is dependent on the mole ratio, temperature and time. Foley and Mackinnon (1970) also observed the dependency on the mole ratio.

At higher mole ratios, i.e. NaOH:$FeTiO_3$ equal to 4 or greater, alkali titanates and alkali ferrates are obtained. In this case the ilmenite structure is destroyed. Ti–O–Fe bonds are broken, forming Na–O–Fe and Na–O–Ti bonds. Ternary phases are not prevalent under these conditions. The reaction in this case is consistent with reaction equation (2) given in Section 4.3.1.

The results obtained show the presence of $Na_8Ti_5O_{14}$ as well. This can be explained by the observation made by Batygin (1967) on heating Na_2TiO_3, which can be assumed to be the following reaction (6):

$$5Na_2TiO_3 \rightarrow Na_8Ti_5O_{14} + Na_2O \quad (6)$$

$Na_8Ti_5O_{14}$ forms whenever there are insufficient sodium ions in the melt for the reaction to proceed. It is present when two or four moles of NaOH are used per mole of $FeTiO_3$. Its prevalence, however, reduces during prolonged fusion periods, as can be seen at 2 h (Table 8 and Figure 12).

Lower mole ratios combined with lower fusion temperatures or short periods of fusion produce similar results. This can be explained using melt viscosity and diffusion on the surface of the ilmenite crystals. As NaOH melts, it soaks the surface of the ilmenite crystals, dissolving them. The dissolved crystals are in an environment with a high concentration of sodium ions. This leads to a reaction in “artificial” mole ratio conditions. At lower fusion temperatures the melt viscosity is higher, which does allow the ions high mobility. The same results are observed when the fusion is conducted over short periods.

Mole ratios lower than 4:1 ($NaOH:FeTiO_3$), allied with high temperatures (above 550 ^oC) and fusion periods above 30 min, are conducive to the formation of ternary phases. It is worth noting that binary phases are also present. They accommodate the excess of either titanium (as titanates) or iron (as ferrates) upon the formation of the ternary phase (Foley and Mackinnon, 1970).

Alkali fusion of ilmenite is, however, better represented as sum of reactions (1) to (5). Depending on the parameters applied to the reaction, any of the products can be obtained.

Therefore the "net equation" will include all the observed phases in the product spectrum, and the proportions of each phase will be determined by the following parameters: temperature, time and mole ratio of the reactants. The following equation represents the net reaction (7).

$$28FeTiO_3 + 22Na_2O + 7O_2 \rightarrow 16Na_{0.75}Fe_{0.75}Ti_{0.25}O_2 + 3NaFeTiO_4 + 4Na_2Fe_2Ti_3O_{10} + 4Na_2TiO_3 + 2Na_8Ti_5O_{14} + 10NaFeO_2 \quad (7)$$

In fusions with 2:1 mole ratios ($NaOH:FeTiO_3$) at temperatures above 700 ^oC, $Na_{0.75}Fe_{0.75}Ti_{0.25}O_2$ is the dominant phase. This was also found by Foley and Mackinnon (1970) who indicated $Na_{0.75}Fe_{0.75}Ti_{0.25}O_2$ as the dominant phase when the ratio Na:Ti is equal to or above to 1:1. Simple titanates are also favoured under these conditions, due to the surplus titanium from $Na_{0.75}Fe_{0.75}Ti_{0.25}O_2$ (67% according to reacted Fe).

Other phases might be present, as indicated by other authors (Bayer and Hoffman, 1965; Foley and MacKinnon, 1970; Li *et al.*, 1971; Reid and Sienko, 1967), but they are beyond the detection limit of the method or else did not crystallise perfectly.

Based on our results, it is proposed that the reaction path proceeds according to the following mechanism:

- Initially, sodium ions, from NaOH melt, break the ilmenite lattice, producing titanates (Na_2TiO_3 mainly) and ferrates (mainly $NaFeO_2$).
- As the reaction proceeds and the concentration of Na^+ ions in the melt reduces, Na_2TiO_3 polymerises, favouring the reaction of Na^+ ions (reaction 2).
- Because Na^+ is proportionally insufficient to compensate for the demand for Ti^{4+} and Fe^{3+} ions in the event of the ilmenite lattice breaking, Na^+ ions are incorporated into the ilmenite lattice, resulting in the partial substitution of Ti^{4+} and Fe^{3+} ions in the lattice.

The SEM images indicate the regeneration of ilmenite crystal morphology as the reaction proceeds (Figure 16(a–d)), suggesting the incorporation of Na ions into the ilmenite lattice.

Silica impurities are trapped by sodium ions, forming sodium silicates. Titanium silicates are not formed, which could reduce the titanium yield. This was indicated by infra-red analyses.

4.7 Kinetics of the Ilmenite Alkali Fusion Reaction

4.7.1 Theoretical Background

Kinetic analyses provide information on the parameters of a chemical process. These parameters include the temperature (T) and the degree of conversion (α), essentially. The idea is to associate these reaction parameters with the rate equation ($f(\alpha)$), the pre-exponential factor (A) and the activation energy (E). This can be accomplished by thermal analysis. ICTAC[11] committee recommends the recommends a multiple heating rate program for computation of reliable kinetic parameters (Brown *et al.*, 2000; Vyazovkin *et al.*, 2011). The degree of conversion is obtain by the following equation

$$\boldsymbol{\alpha = \frac{w_0 - w}{w_0 - w_f}} \qquad \text{(Eq. 6)}$$

Where w_0 is the initial weight percent, w the actual weight and w_f the residual weight percent. The rate equation, in general, is a function of temperature and the degree of conversion according to the relation (Eq. 7)

$$\boldsymbol{\frac{d\alpha}{dt} = k(T)f(\alpha)} \qquad \text{(Eq. 7)}$$

Where K is the rate constant of the reaction. The rate constant gives the dependency of the process on the temperature. The influence of temperature on the constant rate is given by Arrhenius equation (Eq. 8)

[11] International Confederation for Thermal Analysis and Calorimetry

$$k(T) = A \exp\left(-\frac{E}{RT}\right) \quad \text{(Eq. 8)}$$

Where *A* is the pre-exponential factor, *E* is the activation energy and *R* is the universal gas constant. *A* and *E* are termed Arrhenius or kinetic parameters.

Combining Eq. 7 and Eq. 8 we obtain

$$\frac{d\alpha}{dt} = A \exp\left(-\frac{E}{RT}\right) f(\alpha) \quad \text{(Eq. 9)}$$

Eq. 9 is the basis of differential kinetic programs. In this form can be used to obtain all the kinetic parameters using any temperature program, isothermal or non-isothermal. A non-isothermal program will require a substitution of the actual temperature of the sample (Vyazovkin *et al*., 2011). This can be achieved by introducing the heating rate (β) in Eq. 9

$$\beta \frac{d\alpha}{dT} = A \exp\left(-\frac{E}{RT}\right) f(\alpha) \quad \text{(Eq. 10)}$$

The introduction of β in Eq. 10 implies that the sample has to follow exactly the heating program ideally. That means sample temperature as to be always equal to reference temperature. In most experimental cases there is a deviation from the reference temperature. This reduces the applicability of Eq. 10 (Vyazovkin *et al*., 2011; Lick *et al.,* 2012). Integration of Eq. 10 gives

$$g(\alpha) = \int \frac{d\alpha}{f(\alpha)} = \frac{A}{\beta} \int \exp\left(-\frac{E}{RT}\right) dT = \left(\frac{AE}{R\beta}\right) \int \exp \frac{(-x)dx}{x^2} = \left(\frac{AE}{R\beta}\right) p(x) \quad \text{(Eq. 11)}$$

g(α) is the integral form of the rate equation; *p(x)* is the temperature integral for *x* = E/RT. Eq. 11 contains the term β, as was indicated it reduces its applicability.

Isoconversional principle states that the reaction rate at constant degree of conversion is only function of temperature (Vyazovkin *et al*., 2011). These methods allow the determination of the activation energy without the assumption of a specific reaction rate model. The application of this method requires a series of curves recorded at different heating rates. There are a number of mathematical expressions used which differ on the approximations made on the temperature integral. The most common is the Kissinger-Akahira-Sonose equation (Vyazovkin *et al*., 2011)

$$\ln\left(\frac{\beta}{T_p^2}\right) = \ln\left(\frac{AR}{E\, g(\alpha)}\right) - \frac{E}{RT} \qquad \text{(Eq. 12)}$$

where T_p is maximum in the DTA or DTG curves. Plotting $\ln(\beta/T^2)$ versus 1/T the activation energy can be obtained from the slope of the curve. The isoconversional method is unable to calculate the pre-exponential factor and to determine the kinetic model of the rate reaction model (Vyazovkin, 2008).

The model-fitting or the Coats-Redfern allows the determination of the kinetic triplet, activation energy, pre-exponential factor and the kinetic model. In this approach the difference between measured and calculated data on the reaction rate is minimized. This minimization can be achieved by linear methods. According to ICTAC recommendation this procedure is reliable when multiple sets of data are fitted to the models (Vyazovkin *et al.*, 2011).

The mathematical expression used for model fitting can be derived from Eq. 12. Rearranging this equation (Eq. 12) it gives (Eq. 13) (Khawam and Flanagan, 2005; Lick *et al.,* 2012; Manikandan *et al*., 2011).

$$\ln\frac{g(\alpha)}{T^2} = \ln\left(\frac{AR}{\beta E}\left[1 - \left(\frac{2RT}{E}\right)\right]\right) - \frac{E}{RT} \qquad \text{(Eq. 13)}$$

Plotting ln[g(α)/T^2] versus 1/T using the correct $g(\alpha)$ function gives a straight line which slope gives E/R. The pre-exponential factor can be calculated from the obtained activation energy.

The most probable mechanism was further confirmed by using the master plot method. This method is more accurate and less influenced by experimental conditions (Criado, 1978; Criado *et al*., 1989; Jin *et al*., 2009). The master plot curve can be obtained by plotting the conversion degree α against z(α). The former can be calculated for a chosen pair of rate function by (Eq. 14)

$$z(\alpha) = f(\alpha) \times g(\alpha) \qquad \text{(Eq. 14)}$$

The most probable mechanism is the one best fitting the experimental results.

4.7.2 Kinetic Analysis of Alkali Fusion Reaction

To study the kinetic of the ilmenite alkali fusion reaction, we conducted TGA experiments using three different heating rates, namely 2, 5 and 10 ^{o}C/min. In order to avoid concurrent reactions from ilmenite ore impurities, analytical grade $FeTiO_3$ from Sigma Aldrich was used. Ilmenite was mixed with powdered NaOH in an agate mortar. The mixed sample was weighed and subjected to thermogravimetric analysis at. The TGA and DTG curves are presented in Figure 18.

No changes were observed bellow 100 °C in all heating rates. A smooth change in the shape of the TG curves with an increase in the heating rate is observed. Although the initial temperature of mass loss is clearly observable at 2 ^{o}C/min, at 10 ^{o}C/min that point is difficult to determine. Above 400 °C the TGA signal, in Figure, shows a mass gain in the reaction. The DTA curves, as well as the DTG curves (in Figure 18), indicate an increase in T_{max} with heating rate (Table 11).

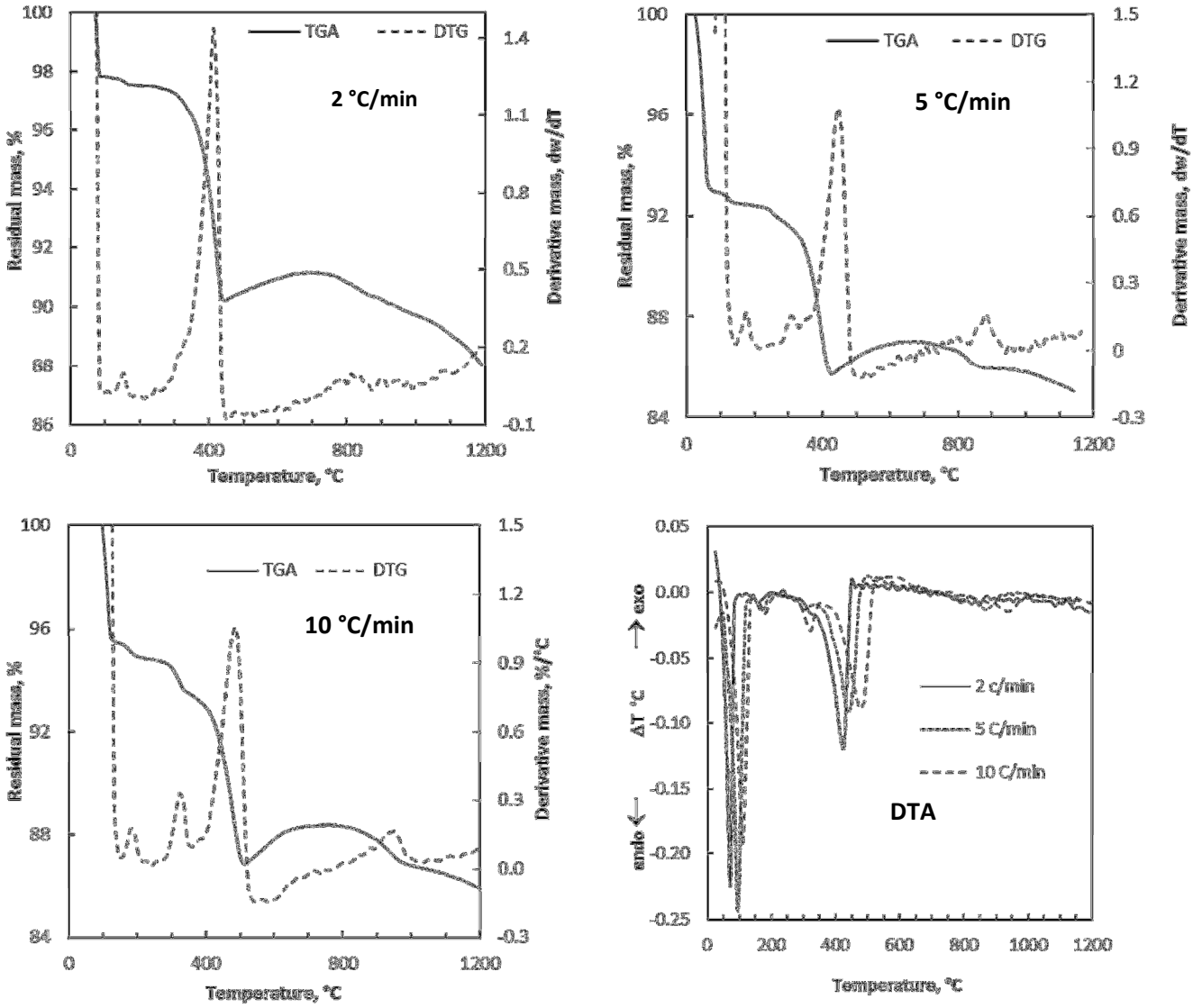

Figure 18: TGA, DTG and DTA curves of the ilmenite alkali fusion reaction at three different heating rates, 2, 5 and 10 °C/min

Table 11: Characteristics of TGA and DTA results of the ilmenite alkali fusion reaction

Heating rate (°C/min)	T_i (°C)	T_f (°C)	T_{max} (°C)	Mass loss (%)
2	155	449	425.5	7.449
5	143	424	448.2	3.948
10	193	512	488.6	8.001

T_i= initial temperature; T_f= final temperature; T_{max} = temperature at the maximum reaction rate

It was expected that mass loss would diminish with increasing heating rate. The highest mass loss was recorded at 10 °C/min. This is certainly due to the overlapping of moisture release and water released due to the reaction itself. DTG and DTA curves at the former heating rate (10 °C/min) show the appearance of a new maximum at 323 °C, see Figure 19. Apparently there is another endothermic reaction taking place at this temperature.

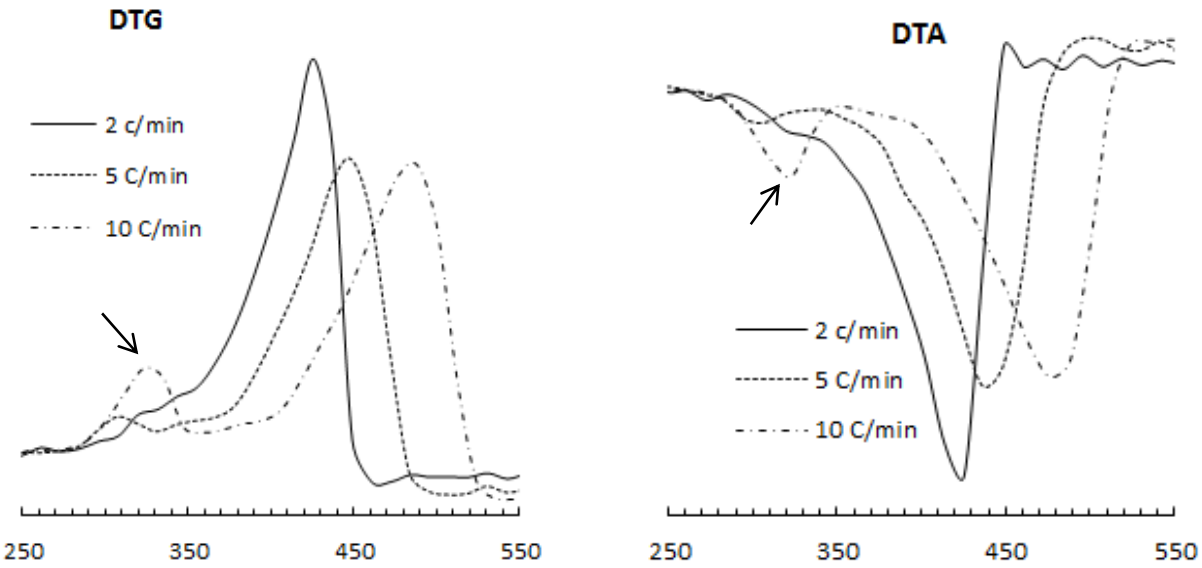

Figure 19: Section of the DTG and DTA signal displaying the new maximum

Based on Figure 19 and Figure 20 it is clear that there are at least two different reactions occurring. This makes it very difficult to fit kinetic models to the data, especially considering the fact that reaction occurring below 350 °C is accentuated as the temperature scan rate is increased. The simplistic models listed in Table 12 are unable to account for such effects.

For simpler kinetic behaviours the Dollimore procedure could be used to estimate the most probable mechanism. See Table for common models. Unfortunately that was not possible for the present data set (Chowlu *et al.*, 2009; Dollimore*et al.*, 1996; Jin *et al.*, 2009).

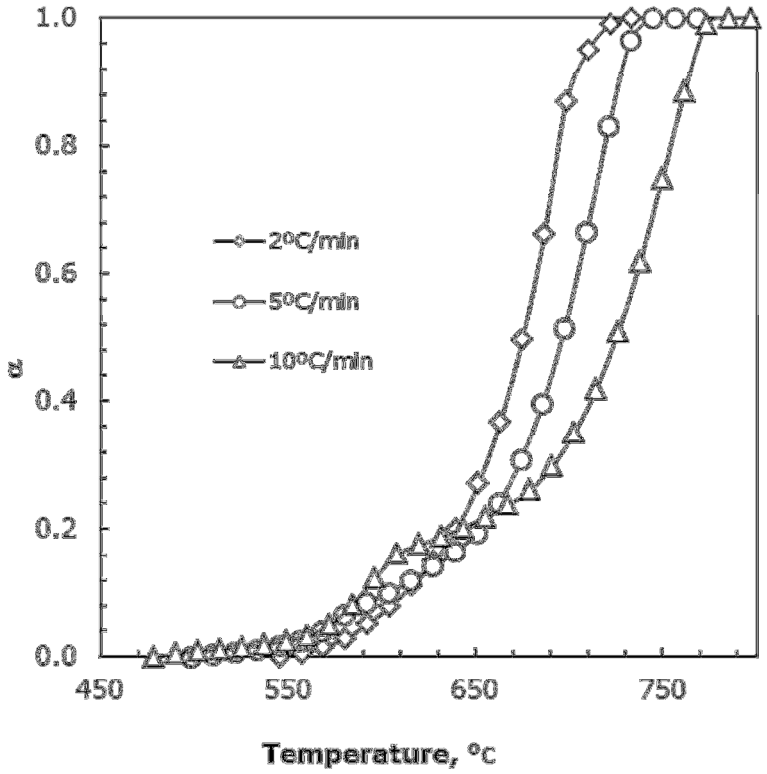

Figure 20: Conversion (α) as function of temperature in the alkali fusion reaction of ilmenite

However, it is clear that the reaction occurring at the higher temperature is the dominant one. Figure 20 shows that it accounts for more than 75% of the conversion. The activation energy for this reaction step can be estimated using the Kissinger method (Khawam and Flanagan, 2006). The basic assumption here is that this step can be described by n^{th} order reaction. In that case the activation energy is given by the slope of the plot of $\ln(\beta/T_p^2)$ versus $1/T_p$.

$$\ln\frac{\beta}{T_p^2} = \ln\left(\frac{AR\left(n(1-\alpha)_p^{n-1}\right)}{E_a}\right) - \frac{E_a}{RT_p} \qquad \text{(Eq. 15)}$$

Where T_p is the temperature of the maximum rate of conversion. Figure 21 shows the results of such an analysis. It is clear that the dada points do not fall on straight line. The implication is that the kinetics of the alkali fusion reaction cannot be modelled in such simple terms.

Table 12: Selected mathematical functions of the reaction mechanisms tested with produced data

Model	**Differential form** $f(\alpha)=\frac{1}{k}\frac{d\alpha}{dt}$	**Integral form** g(α)
Geometrical contraction models		
Contracting area (R2)	$2(1-\alpha)^{1/2}$	$[-(1-\alpha)^{1/2}]$
Contracting volume (R3)	$3(1-\alpha)^{2/3}$	$[-(1-\alpha)^{1/3}]$
Diffusion models		
1D Diffusion (D1)	$1/2\alpha$	α^2
2D Diffusion (D2)	$[-\ln(1-\alpha)]^{-1}$	$[(1-\alpha)\ln(1-\alpha)]+\alpha$
3D Diffusion – Jander Eq. (D3)	$3(1-\alpha)^{2/3}/2(1-(1-\alpha)^{1/3})$	$[1-(1-\alpha)^{1/3}]^2$
Ginstling-Brounshtein (D4)	$(3/2((1-\alpha)^{-1/3}-1)$	$1-(2\alpha/3)-(1-\alpha)^{2/3}$

Geometric models take into account systematic variations in the total area of the reaction interface. These variations are due to continuous change in geometry resulting from the advance of the reaction. Diffusion models consider that the rate determining step is the mass transport through product layer (Harrison, 1969).

The Jander equation and the Ginstling-Brounshtein equation are used in the case of advancing reaction interface. The Jander equation presents a rough approximation and should be used only for small extents of conversion ($\alpha = 0.15$). The Jander equation considers the convergence of the diffusion paths as the centre of the sphere is approached (Harrison, 1969).

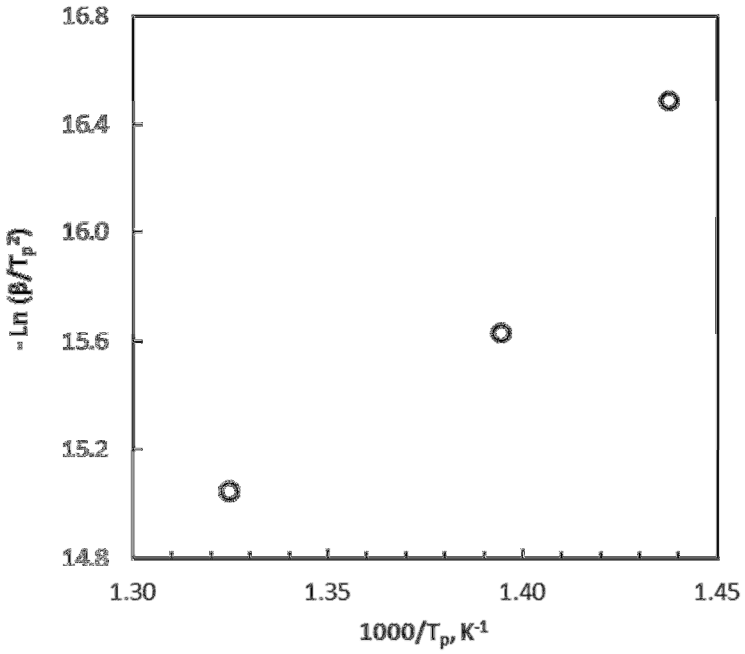

Figure 21: Kissinger plot for the dominant alkali fusion reaction

4.8 Optimisation of the Fusion Process

4.8.1 Effect of particle size

The effect of particle size was tested using an extreme particle size difference, $d_{50} \approx 6$ and 139 µm. Fusions were conducted at 550 to 900 ^{o}C (in 50 ^{o}C increments) for 1 h at a 2:1 mole ratio ($FeTiO_3$:NaOH). The results are presented in Figure 22 (a–c).

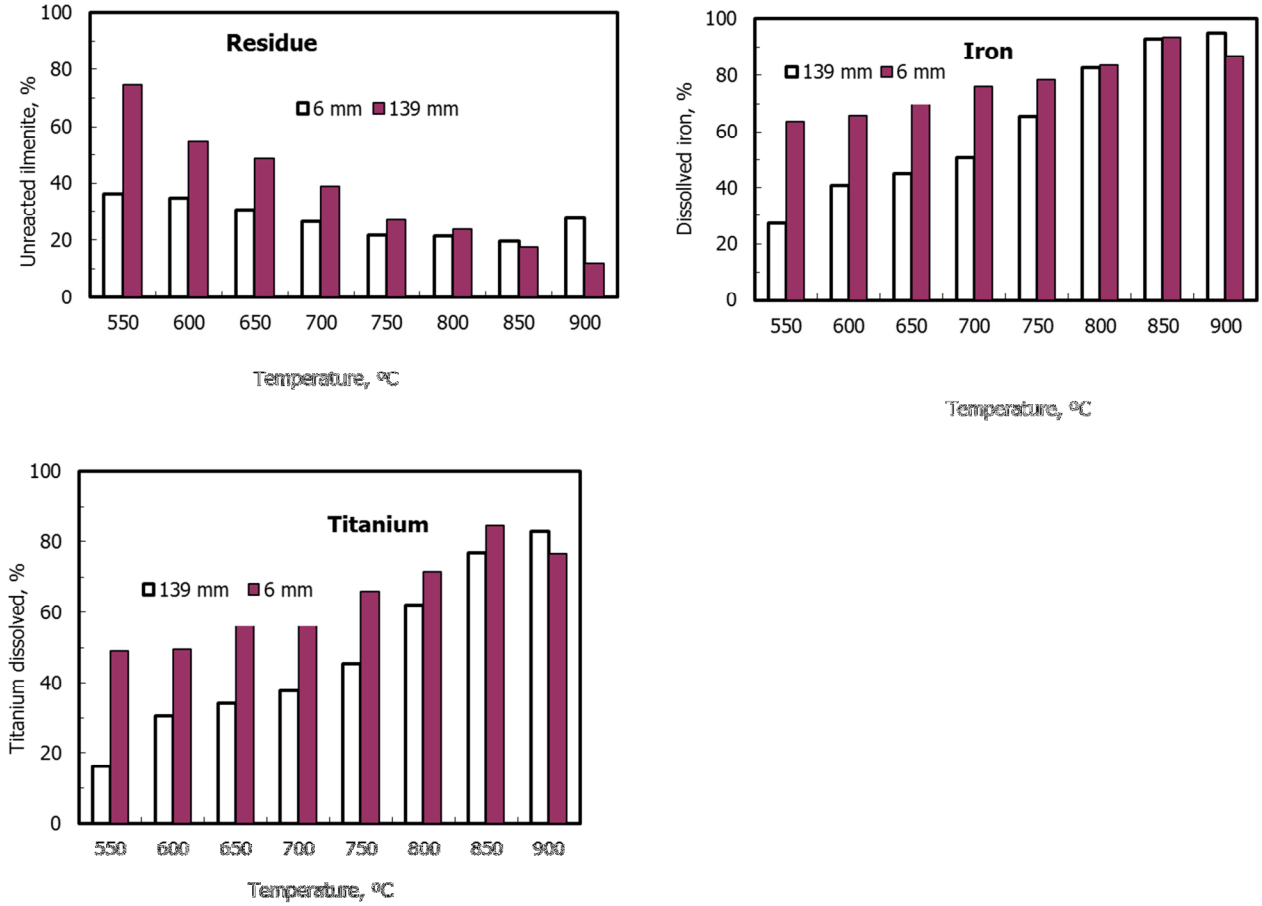

Figure 22: Effect of particle size. (a) Residue; (b) iron; (c) titanium[12]

At lower temperatures the coarser ilmenite produces, comparatively, high amounts of residue. At high temperatures this difference disappears. Such behaviour reinforces the finding of a diffusion-controlled reaction mechanism.

The comparatively higher amount of residue observed at 850 and 900 ^{o}C with finer ilmenite must be considered to be a result of agglomeration, which prevented part of the ilmenite from reacting. Higher temperatures lead to internal structure porosity breackdown (Johansson, 2007). Leion *et al*. (2008) reported the oxidation of ilmenite to Fe_2TiO_5 + TiO_2, around this temperature.

[12] mm stands for µm

4.8.2 Effect of mole ratio

Figure 23 indicates a steady increase in the amount of dissolved iron from 1:1 up to 2:1 ($NaOH:FeTiO_3$). High alkali recoveries are achieved when high quantities of NaOH per mole of ilmenite are used. Binary phases are predominant which are promptly hydrolysed in water, as shown in Figure 12. Around 96% are recovered when six moles of NaOH are used per mole of $FeTiO_3$. A temperature of 850 ^{o}C was used in an attempt to produce ternary phases, sodium iron titanates, especially when fusing below a 2:1 mole ratio (Lasheen, 2008). This was also confirmed in this work (Figure 12).

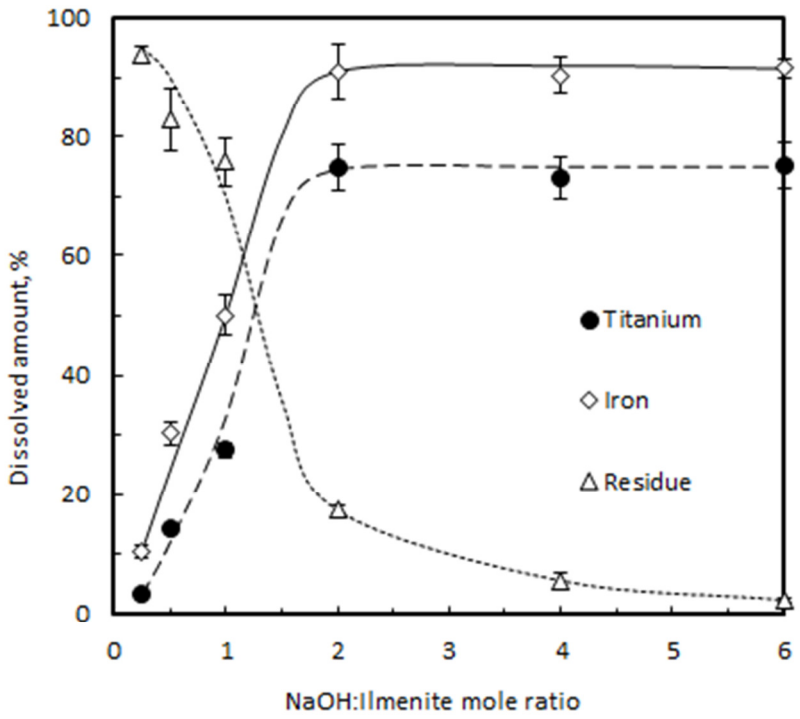

Figure 23: Effect of mole ratio on fusions conducted at 850 ^{o}C for 1 h

4.8.3 Effect of time

The effect of time in the fusion process was studied at 750 °C. Fusions were conducted 30, 60, 90, 120, 150 and 180 min, using two moles of NaOH per mole of $FeTiO_3$. The results are presented in Figure 24.

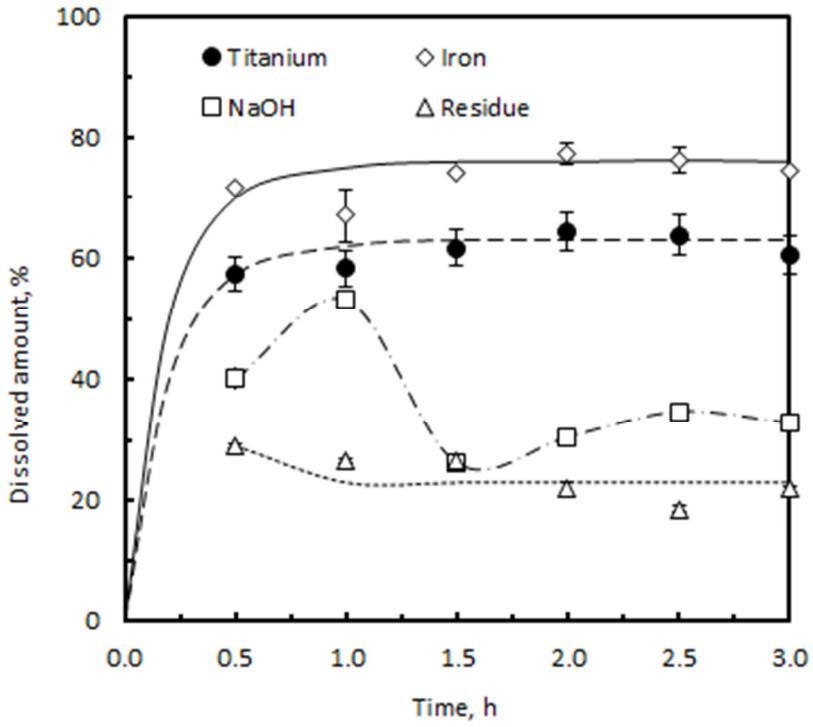

Figure 24: Effect of fusion time on the ilmenite alkali reaction (2:1 NaOH:$FeTiO_3$ mole ratio, 750 °C)

A plateau is observed after 1 h of fusion, meaning that extended periods of fusion do not increase the amount of species dissolved. In other words, under prevailing conditions the reaction between NaOH and $FeTiO_3$ is completed after 1 h. The alkali recovery reduces with time due to the formation of less hydrolysable species, supposedly ternary phases. The XRD results showed an increase in $NaFeTiO_4$ content with time of fusion (see Figure 24).

4.8.4 Effect of temperature

The effect of temperature was investigated using two moles of NaOH per mole of $FeTiO_3$ for 1 h of fusion in the 300 to 950 ^{o}C temperature range, gradient 50 ^{o}C. The results are presented in Figure 25.

Our results indicate a steady increase in the yields between 400 and 900 ^{o}C. A maximum is achieved closer to the 900 ^{o}C point, with 95% for iron and 81% for titanium. Above the 900 ^{o}C point, the solubilised amount of titanium and iron decreased.

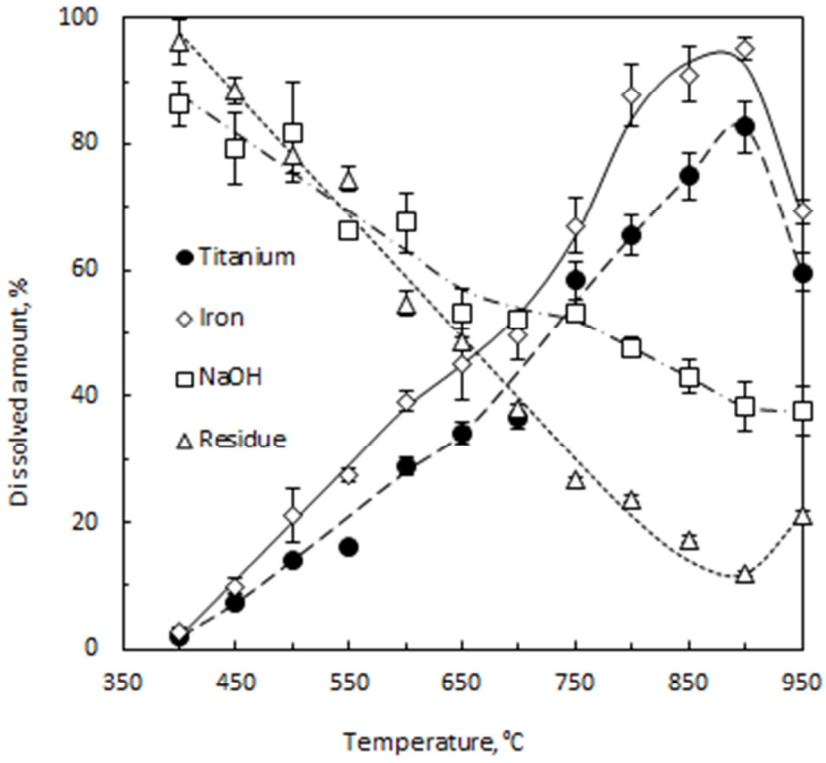

Figure 25: Effect of fusion temperature on titania recovery

The residue curve decreases steadily up to 900 ^{o}C where it reaches its minimum, 19%. This is in accordance with the iron and titanium solubilisation curve. Meanwhile the alkali recovery curve

shows a reduction in recoverable alkali. This is an indication of the formation of species that are not easily hydrolysable at high temperature. Higher levels of ternary phases were observed at this temperature from the XRD results, with $Na_{0.75}Fe_{0.75}Ti_{0.25}O_2$ being the main phase, as indicated in Figure 12.

4.9 Reagent Consumption

The efficiency of the process was investigated by comparing the titania yield against the amount of sodium hydroxide consumed (mass per mass basis), using six mole ratios (1:4, 1:2, 1:1, 2:1, 4:1 and 6:1 NaOH:$FeTiO_3$) for 1 h of fusion. The results are presented in Figure 26. The highest efficiency was attained using two moles of sodium hydroxide at 850 ^{o}C. Approximately 0.41 units are liberated per unit mass of NaOH. The theoretical maximum for this point is 0.53.

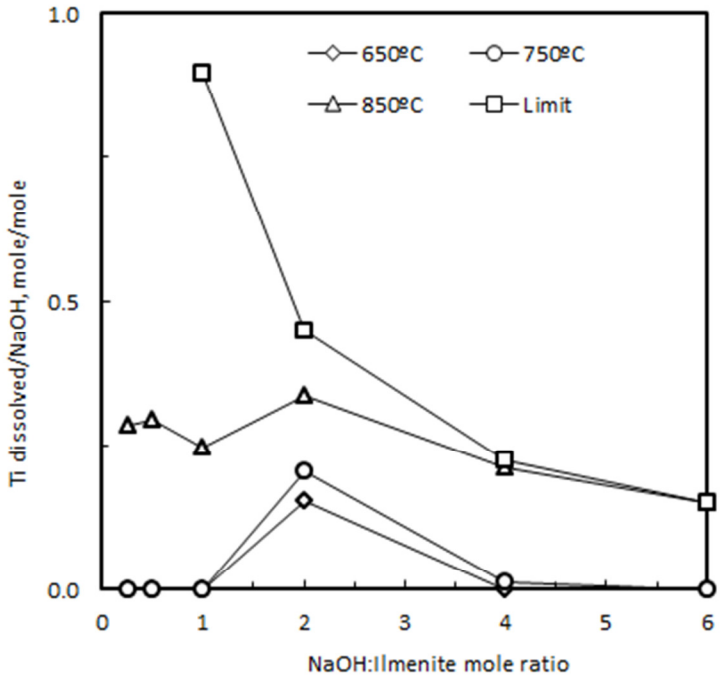

Figure 26: Efficiency of the fusion process

4.10 Optimisation of the Leaching Process

4.10.1 Effect of solid:liquid ratio

The effect of the solid:liquid (S:L) ratio was investigated at room temperature, using AFDI prepared by fusing two moles of NaOH per mole of $FeTiO_3$ at 750 ^{o}C for 1 h. Three ratios were tested, namely 0.20, 0.26 and 0.39, corresponding respectively to 200, 150 and 100 mL of distilled water per 30.35 g of ilmenite ore and a corresponding mass of NaOH. The results obtained are presented in Figure 27. Results are presented in terms of alkali recovered and determined by titration with HCl. This is the alkali that can be recycled.

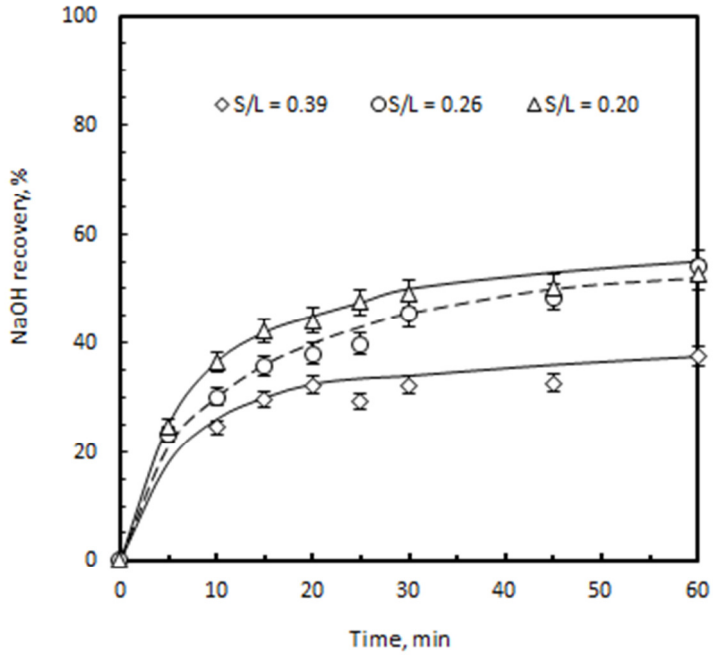

Figure 27: Effect of solid:liquid ratio on the leaching process at room temperature. Samples of AFDI were prepared by fusing two moles of NaOH with one mole of $FeTiO_3$ for 1 h at 750 ^{o}C

Our results indicate that S:L = 0.20 presents optimal extraction conditions. A maximum of 54% was obtained after 1 h of leaching, with 50% extracted after 30 min. In the first 5 min, no difference in terms of the amount of alkali extracted was observed.

4.10.2 Effect of time and temperature

The effect of time and temperature on the leaching process was investigated at intervals of 10 to 60 min at room temperature, 35, 40, 50 and 75 ^{o}C, using AFDI obtained by fusing a mixture of two moles of NaOH per mole of $FeTiO_3$ for 1 h at 750 ^{o}C. The solid:liquid ratio (S:L ≈ 0.26) was kept constant. The results are presented in Figure 28.

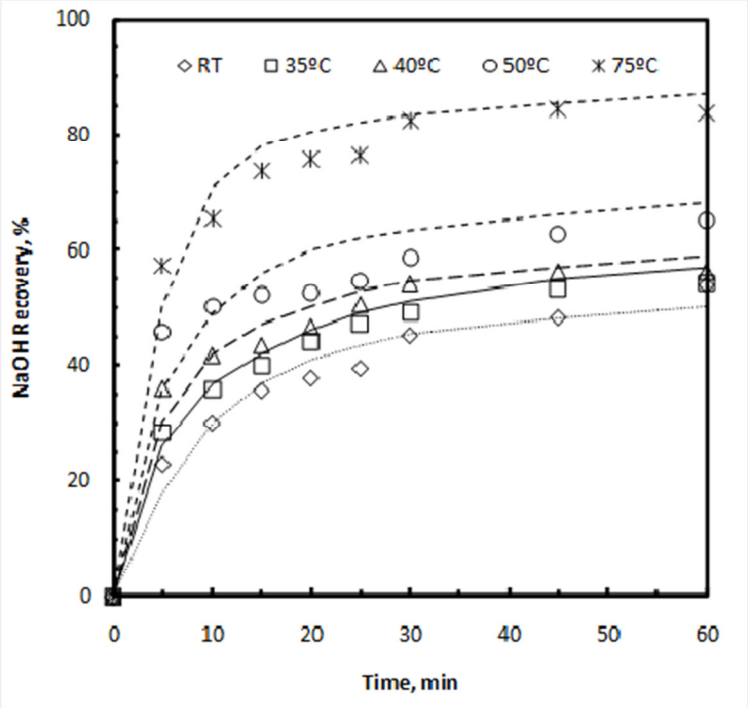

Figure 28: Effect of time and temperature on the leaching process. Samples of AFDI were prepared by fusing two moles of NaOH with one mole of $FeTiO_3$ for 1 h at 750^{o}C

In general, alkali recovery increases sharply up to 15 min. Above 15 min the rate of extraction does not increase. Approximately 75% of the total NaOH was extracted after 15 min of leaching at 75 ^{o}C, while at room temperature only 40% had been extracted after the same leaching time. The existence of phases that hydrolyse only at high temperatures is the rational explanation for the significant difference.

4.10.3 Batch leaching

The significance of repeated leaching was tested by repeating the leaching process three times, 5, 10 and 15 min for each leaching. The results are presented in Figure 29.

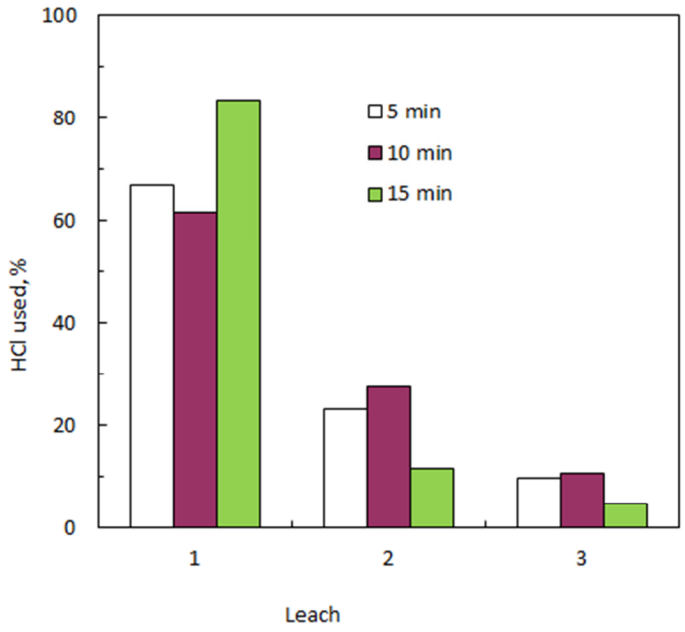

Figure 29: Effect of repeated leaching at indicated leaching times (batch leaching)

According to our results, a single leach can remove up to 83% (15 min leaching) of the total of recoverable alkali. Leaching tests were conducted at room temperature.

4.10.4 Kinetics of the leaching process

During leaching alkali fusion products are hydrolysed and sodium hydroxide used in the fusion process is recovered. The reactions occurring during hydrolysis can be summarised as follows, according to the net equation (7) presented before:

$$Na_2TiO_3 + 2H_2O \rightarrow 2NaOH + TiO(OH)_2$$

$$Na_8Ti_5O_{14} + 9H_2O \rightarrow 8NaOH + 5TiO(OH)_2$$

$$NaFeO_2 + H_2O \rightarrow NaOH + FeOOH$$

For practical purposes it was assumed that only one of the above reactions is occurring, the reaction of $NaFeO_2$ was considered as the most probable to occur under the considered fusion conditions. Ternary phases are stable to aqueous hydrolysis. These phases hydrolyse under acidic conditions, as was reported by Foley and MacKinnon (1970).

The experimental data were fitted to leaching models in order to determine the rate-controlling step and kinetic parameters. According to Demirkiran (2008), these processes are controlled either by diffusion through the fluid film, diffusion through the product layer, or by the chemical reaction at the surface. The mathematical expressions of such models are (Eq. 16):

$$1 - (1 - \alpha)^{\frac{1}{3}} = \frac{K_C MC}{\rho a r_0} t = k_r t \qquad \text{(Eq. 16)}$$

for the surface chemical reaction and (Eq. 17):

$$1 - \frac{2}{3}\alpha - (1 - \alpha)^{\frac{2}{3}} = \frac{2MDC}{\rho a r_0} t = k_d t \qquad \text{(Eq. 17)}$$

for the diffusion-controlled reaction.

where α is the reacted fraction, M is the molecular mass of the solid, C is the concentration of the leachant in the solution, ρ is the density of the solid, a is the stoichiometric coefficient of the leaching reaction, r_0 is the initial radius of the solid particle, D is the diffusion coefficient in the product layer, t is time, and K_r and K_d are the rate constants for the reaction.

In some cases the leaching process can be controlled by a mixed mechanism. In this case the two mathematical expressions are combined, resulting in the following equation (18) (Dehgan *et al*., 2009):

$$\left[1-(1-\alpha)^{\frac{1}{3}}\right]+B\left[1-\frac{2}{3}\alpha-(1-\alpha)^{\frac{2}{3}}\right]=kt \qquad \text{(Eq. 18)}$$

Where$B=K_r/K_d$ and K are the rate constants of the mixed mechanism.

Dickinson and Heal (1999) suggested a new equation for a shrinking core mechanism during leaching (Eq. 19). Dehghan *et al.* (2009) used the same model for experimental data of sphalerite leaching with HCl-$FeCl_3$.

$$\frac{1}{3}\ln(1-\alpha)+\left[(1-\alpha)^{-\frac{1}{3}}-1\right]=kt \qquad \text{(Eq. 19)}$$

Our experimental data, however, did not fit any of the above proposed models. Figure 30 shows the degree of conversion versus time obtained from our experimental data.

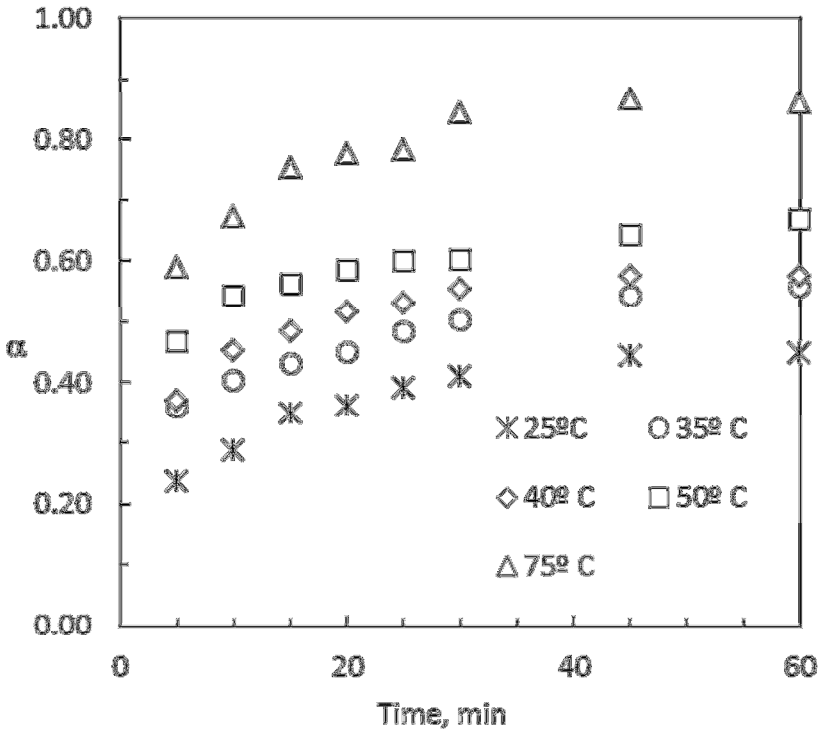

Figure 30: Plot of leaching kinetics

4.11 Optimal Hydrolysis pH

The optimal hydrolysis pH was determined by varying the final pH from 2 to 7 (0.5 intervals) and determining the relative amount of iron and titanium in the solution. The results are presented in Figure 31.

According to our results, the pH value is not significant above 3. Less than 1% of titanium and iron is dissolved above that point, for both titanium and iron. Based on that, a pH of 7 is recommended since it will require less acid consumption for hydrolysis.

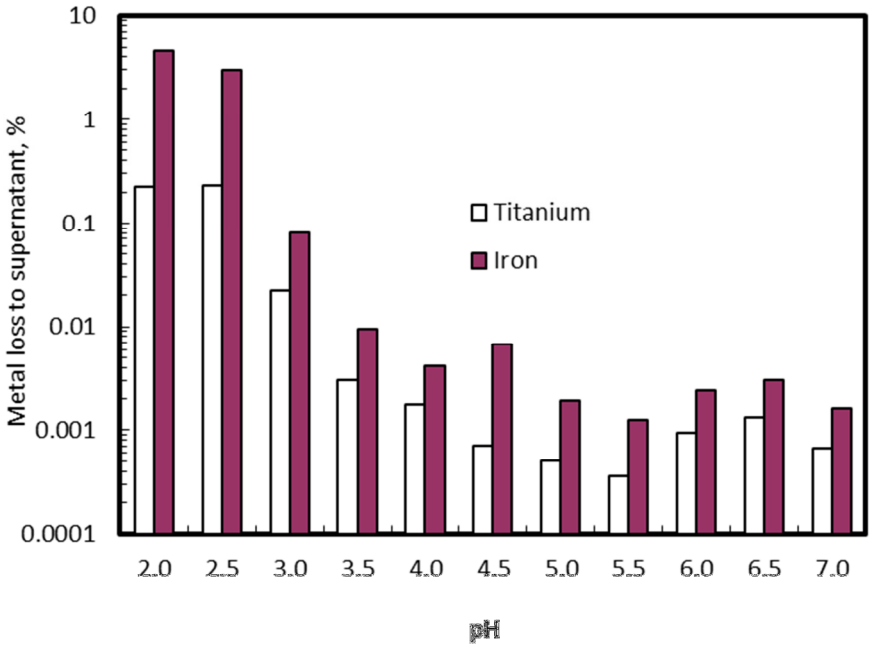

Figure 31: Determination of the optimal hydrolysis pH

4.12 Sulfation Process

The sulfation process was optimised by determining the most effective amount of sulphuric acid used in the process. The stoichiometric amount and an excess of 5–15% was used (excess of H_2SO_4 over the stoichiometric amount required for the reaction to form iron(III) sulfate and titanium(IV) sulfate). The results are presented in Figure 32. The AFDI used was obtained by fusing NaOH:ilmenite mixtures (2:1 mole ratio) at 750 ^{o}C for 1 h.

The results obtained indicate that the sulfation process was not affected by any excess above the stoichiometric amount of sulphuric acid required for the reaction. The relative quantities of iron and titanium did not vary with the addition of any excess of the acid.

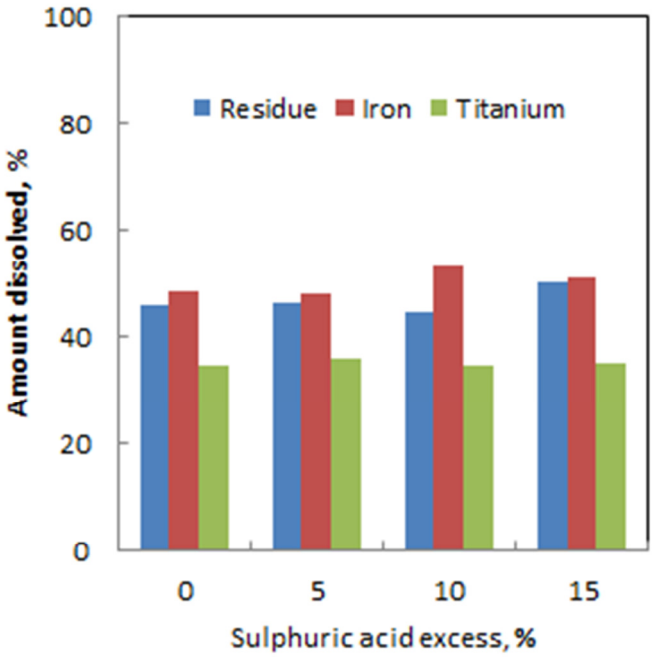

Figure 32: Optimisation of the sulfation process

4.13 Trials with Anatase

There are important world reserves of titanium in the form of anatase, but this mineral is not yet being commercially exploited. Existing commercial routes are incapable of processing such ores (de Matos *et al.*, 2002; Nielsen and Chang, 1996; Paixão and de Mendonça, 1979). In order to assess the applicability of the alkali fusion procedure to such ores, an anatase sample was used to obtain the optimal parameters.

Stoichiometric amounts of anatase reactant were mixed with sodium hydroxide (2:1 NaOH:TiO_2 mole ratio) and subjected to TGA analysis. The aim was to determine the fusion temperature.

The thermogravimetric results (Figure 33) indicated a mass loss from 220 to 850 ^{o}C. The DTG curve indicates two broad peaks, at approximately 670 and 870 ^{o}C. The total mass loss was 20.85%, which corresponds to approximately 97% of the expected total mass loss, calculated from the perspective of the NaOH mass loss. The SDTA curve (from the simultaneous TGA-DTA thermal analyser) shows a peak at 756 ^{o}C.

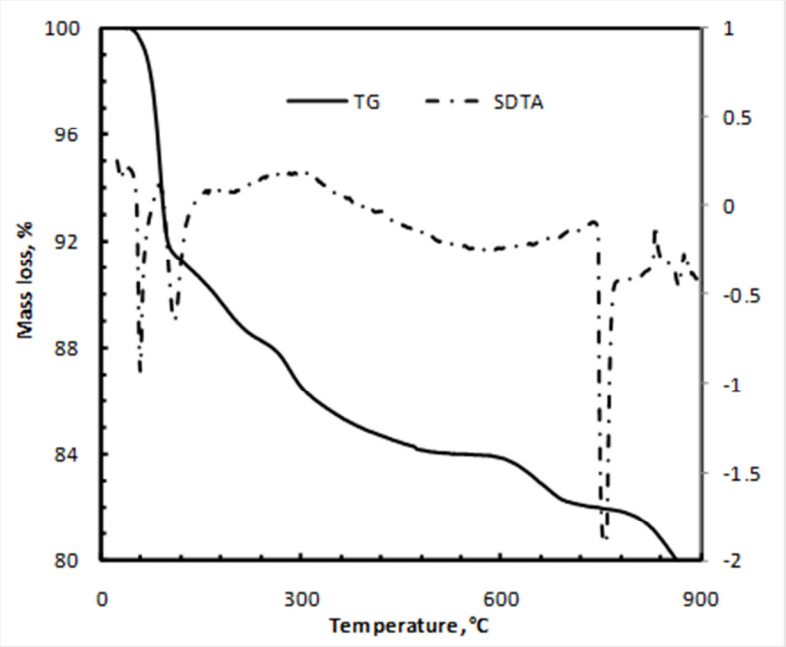

Figure 33: TGA and DTA curves of the alkali fusion reaction

Using the TGA findings, mixtures of NaOH and TiO_2 (anatase, 2:1 mole ratio) were fused at 500, 600, 700 and 800 ^{o}C. The fused samples were subjected to XRD analysis (Figure 34). The XRD patterns revealed the presence of Na_2TiO_3, $Na_{16}Ti_{10}O_{28}$, $Na_8Ti_5O_{14}$ and $Na_2Ti_6O_{13}$ (Figure 34). The polymeric phases are dominant at lower temperatures. The reaction appears to follow the path below:

$$24Na_2O + 30TiO_2 \rightarrow 6Na_8Ti_5O_{14} \rightarrow 3Na_{16}Ti_{10}O_{28} + 6Na_2O \rightarrow$$

$$30Na_2TiO_3 \rightarrow 5Na_2Ti_6O_{13} + 25Na_2O \quad (14)$$

From the economic point of view, phases with the lowest Na:Ti ratio are advantageous. They require less NaOH to combine with Ti in the ore. The most efficient here is $Na_2Ti_6O_{13}$, with a 1:3 atom ratio. It requires 10 moles of NaOH to combine 30 moles of TiO_2, according to equation 14. This phase was obtained above 700 ^oC, according to the XRD results in Figure 34.

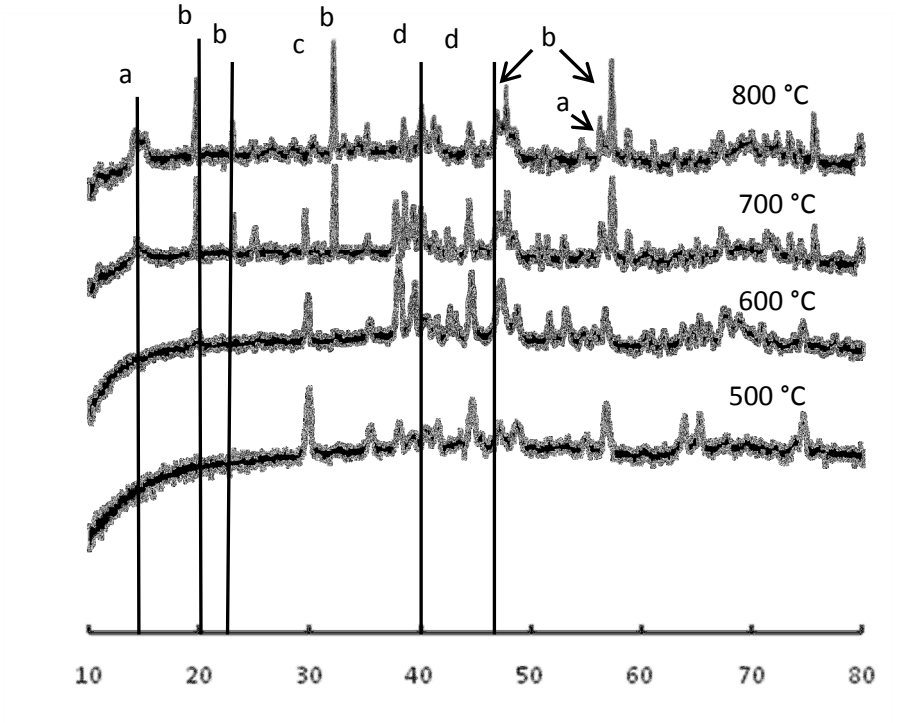

a = $Na_2Ti_6O_3$; b = Na_2TiO_3; c = $Na_8Ti_5O_{14}$; d = $Na_{16}Ti_{10}O_{28}$

Figure 34: XRD patterns of alkali fused anatase (2:1 NaOH:TiO_2 mole ratio)

Optimisation of the processing was conducted by analysing the effect of time and temperature on the process. The effect of time was investigated using a sample fused at 800 ^oC. The results indicated that a maximum recovery can be attained at 120 min. Over 99% of the titania was recovered after this time. Fifty-four percent of the total NaOH used was recovered after this time. The residue reaches its minimum at this point (Figure 34).

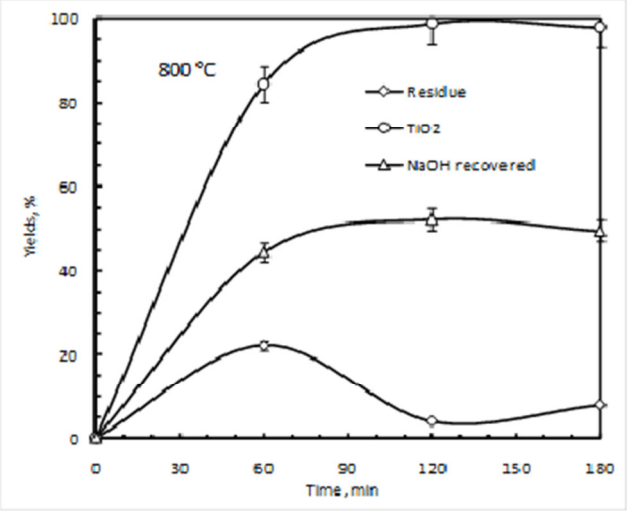

Figure 35: Effect of time on the recovery of titania from anatase ores using the proposed process

The effect of temperature was investigated between 500 and 800 ^{o}C. The results, presented in Figure 36, indicated that at 800 ^{o}C, 84% of the total titania can be recovered from the ore, as well as 45% of the NaOH used.

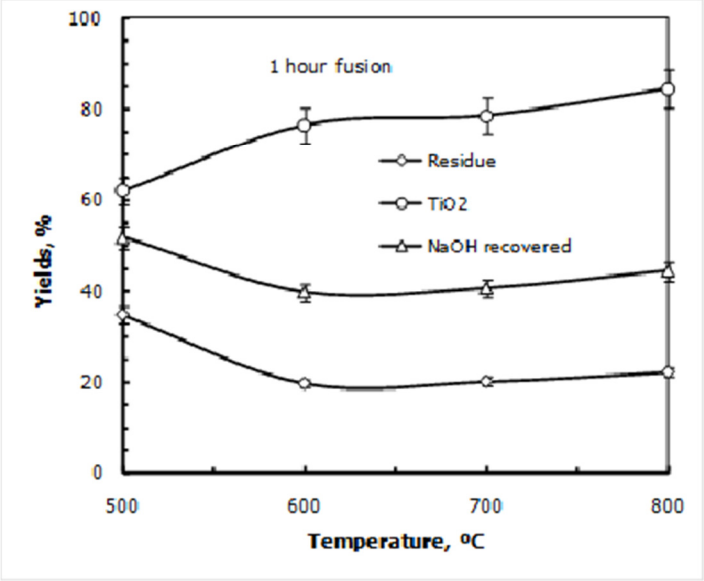

Figure 36: Effect of temperature on the titania recovery from anatase ores using the proposed process

4.14 Summary of the Discussions

In the present work we propose a method of extracting of titanium from titanoferrous minerals. In titanoferrous minerals we include anatase, pseudorutile, altered ilmenite, leucoxene, ulvospinel, pseudobrookite, titanomagnetite and titanohematite, as per Table 1, as well as ilmenite. According to this method titanoferrous mineral is roasted preferable with sodium hydroxide. The fused product is subsequently leached with water, hydrolysed with dilute mineral acid and the residue dissolved in sulphuric acid as indicated in section 2.7.3 of this work.

The proposed process was studied in terms optimum conditions of fusion temperature, mole ratio and time of fusion (duration of the fusion reaction). For the leaching process the slurry density (solid:liquid ratio), temperature of leaching and time were the optimized parameters. For the acid hydrolysis the concentration of the mineral acid was the optimized parameter. The main findings are:

A. Fusion Reaction

- The optimum conditions for the alkali fusion reaction were found to be
  - Temperature – 900 °C
  - Fusion time – 1 h
  - Mole ratio – 2:1 (NaOH:titanoferrous mineral)
  - Particle size – bellow 139 µm

- The overall fusion reaction was found to be

$$28FeTiO_3 + 22Na_2O + 7O_2 \rightarrow 16Na_{0.75}Fe_{0.75}Ti_{0.25}O_2 + 3NaFeTiO_4 + 4Na_2Fe_2Ti_3O_{10} + 4Na_2TiO_3 + 2Na_8Ti_5O_{14} + 10NaFeO_2$$

- The mechanism was predicted to proceed in the following path
    - Initially Na_2TiO_3 and $NaFeO_2$ are produced as result of the high localized concentration of Na^+ in the melt;
    - As the reaction proceeds and the concentration of Na^+ ions in the melt reduces, Na_2TiO_3 polymerises, producing $Na_8Ti_5O_{14}$.
    - Because Na^+ is proportionally insufficient to compensate the demand by Ti^{4+} and Fe^{3+} ions in the event of the ilmenite lattice breaking, Na^+ ions are incorporated into the ilmenite lattice, resulting in the partial substitution of Ti^{4+} and Fe^{3+} ions in the lattice.

Fusion data fitted both contracting area mechanism as well as diffusion. The multiple mechanism of the reaction was proved by the dependence of the activation energy on the heating rate.

B. Leaching

Optimum leaching conditions were found to be

- Temperature – 75 °C
- Slurry density (solid:liquid ratio) – 0.20 g/mL
- Time – 15 min

It was also found that the leaching process obeys the shrinking core mechanism.

C. Hydrolysis

The pH of 7 was found to be the optimum final pH in hydrolysis.

4.15 References

Aminesh, J., Antony, M.P., and Dattatray, T.V., **2007**. US Patent Application No. 20070110647.

Batygin, V.G., **1967**. Formation and some properties of sodium titanates. *Russian Journal of Inorganic Chemistry*, 12(6): 762–767.

Bayer, Von G., Hoffman, W., **1965.** Über Verbindungen vom Na_xTiO_2 – Typ. *Zeitschrift für Kristallographie*, 121: 9–13.

Belyaev, E.K., **1976**. The formation of sodium metatinate in sodium carbonate – Titanium dioxide mixtures. *Russian Journal of Inorganic Chemistry*, 21(6): 830–833.

Belyaev, E.K., Panasenko, N.M., and Linnik, E.V., **1970**. Formation of tetrasodium trititanate in mixtures of sodium carbonate and titanium dioxide. *Russian Journal of Inorganic Chemistry*, **15**(3): 336–338.

Brown, M.E., *et al*., **2000**. Computacional aspects of kinetic analysis. Part I: The ICTAC kinetics project-data, methods and results. *Thermochimica Acta*, 355:125-143.

Chowlu, A.C.K., Reddy, P.K., and Ghoshal, A.K., **2009**. Pyrolytic decomposition and model-free kinetics analysis of mixture of polypropylene (PP) and low density polyethylene (LDPE). *Thermochimica Acta*, 484(1–2): 41–47.

Criado, J.M., **1978**. Kinetic analysis of DTG data from master curves. *Thermochimica Acta*, 24:186-189.

Criado, J.M., Málek, J., and Ortega, A., **1989**. Aplicability of the master plots in kinetic analysis of non-isothermal data. *Thermochimica Acta*, 147:377-385.

De Matos, J. M. J., de Freitas, L. R., and Horta, R. de M., **2002**. Process for the production of titanium concentrate from anatase ores with high utilisation of the iron contents of the ore. US Patent 6 346 223.

Dehghan, R., Noaparast, M., and Kolahdoozan, M., **2009**. Leaching and kinetic modelling of low-grade calcareous spharelite in acidic ferric chloride solution. *Hydrometallurgy*, 96(4): 275–282.

Dellimore, D., Tong, P., and Alexander, K.S., **1996**. The kinetic interpretation of the decomposition of calcium carbonate by use of relationships other than the Arrhenius equation. *Thermochimica Acta*, 282/283: 13–27.

Demirkiran, N., **2008.** Dissolution kinetics of ulexite in ammonium nitrate solutions. *Hydrometallurgy*, 95(3–4): 198–202.

Dickinson, F.C., and Heal, G.R., **1999**. Solid-liquid diffusion controlled rate equations. *Thermochimica Acta*, 340–341: 89–103.

Farmer, V.C., **1974**. The infrared spectra minerals, V.C. Farmer Edition. Mineralogical Society Monograph, 4. Mineralogical Society, London.

Foley, E., and MacKinnon, K.P., **1970.** Alkaline roasting of ilmenite. *Journal of Solid State Chemistry*, 1: 566–575.

Gabelica-Robert, M., and Tarte, P., **1981**. Vibrational spectrum of fresnoite ($Ba_2TiOSi_2O_7$) and isostructural compounds. *Physics and Chemistry of Minerals*, 7: 26–30.

Habashi, F. (Ed.), **1997.** Titanium. In: *Handbook of Extractive Metallurgy, Vol. II*. Weinheim, Germany: Wiley-VCH, pp 1129–1180

Harrison, L.G., **1969**. The Theory of Solid Phase Kinetics. In: Bamford, C.H., and Tipper, C.F.H., *Comprehensive Chemical Kinetics*, 2nd edition, vol. 2, Elsevier Publishing Company, pp. 377-458.

Hollitt, M.J., McClelland, R.A., and Tuffley, J.R., **2002**. Upgrading titaniferous materials. US Patent Application No. 20020104406.

Jambor, J.L., Dutrizac, J.E., **1998**. Occurrence and constitution of natural and synthetic ferrihydrite, a widespread iron oxyhydroxide. *Chemical Reviews*, 98 (7): 2549–2585.

Jin, D., Yu, X., Yue, L., and Wang, L., **2009**. Decomposition kinetics study of AlOOH-coated calcium carbonate. *Materials Chemistry and Physics*, 115(1): 418–422.

Johansson, M., **2007**. Screening of oxygen-carrier particles based on iron-, manganese-, copper- and nickel oxides for use in chemical-looping technologies. PhD. Thesis Chalmers University of Technology, Goteborg –Sweeden.

Khawam, A., and Flanagan, D.R., **2005**. Role of isoconversional methods on varying activation energies of solid state kinetics. II. Non-isothermal kinetic studies. *Thermochimica Acta*, 436: 101–112.

Kuhn, A., García-Alvarado, F., Morán, E., Alario-Franco, M.A., and Amador, U., **1996**. Structural effects of sodium extraction on $Na_xFe_xTi_{2-x}O_4$ single crystals. *Solid State Ionics*, 86–88: 811–818.

Lahiri, A., Kumari, E. J., and Jha, A., **2006**. Kinetic studies on the soda-ash roasting of titanoferous ores for the extraction of TiO_2. *Proceedings of theSohn International Symposium. Advanced Processing of Metals and Materials. Vol. 1: Thermo and Physicochemical Principles: Non-Ferrous High-Temperature Processing*, pp 115–123.

Lasheen, T.A., **2008**. Soda ash roasting of titania slag product from Rosetta ilmenite. *Hydrometallurgy*, 93:124-128.

Leion, H., Lyngfelt, A., Johansson, M., Jerndal, E., and Mattisson, T., **2008**. The use of ilmenite as an oxygen carier in chemical-looping combustion. *Chemical Engineering Research and Design*, 86:1017-1026.

Li, C., Reid, A.F., and Saunders, S., **1971**. Nonstoichiometric alkali ferrites and aluminates in the systems $NaFeO_2 – TiO_2$, $KFeO_2 – TiO_2$, $KAlO_2 – TiO_2$, $KAlO_2 – SiO_2$.*Journal of Solid State Chemistry*, 3: 614–620.

Licht, S., Yang, L., and Wang, B., **2005**. Synthesis and analysis of Ag_2FeO_4Fe(VI) ferrate super-iron cathodes. *Electrochemistry Communications*, 7: 931–936.

Lick, I.D., Villalba, M.L., and Gavernet, L., **2012**. Synthesis of diketopiperazine: A kinetic study by means of thermoanalytical methods. *Thermochimica Acta*, 527:143-174.

Maitra, S., Chakrabarty, N., and Pramanik, J., **2008**. Decomposition kinetics of alkaline earth carbonates by integral approximation method. *Cerâmica*, 54: 268–272.

Manikandan, G., Jayabharathi, J., Rajarajan, G., and Thanikachalam, V., **2011**. Kinetics and vaporization of anil in nitrogen atmosphere – non-isothermal condition. *Journal of King Saud University – Science*, doi: 10.1016/j.jksus.2011.04.002 (in press).

Méndez-Vivar, J., Mendoza-Serna, R., and Valdez-Castro, L., **2001**. Control of the polymerization process of multicomponent (Si, Ti, Zr) sols using chelating agents. *Journal of Non-Crystalline Solids*, 288:200-209.

Muroya, M-A., **1999**. Correlation between the formation of silica skeleton structure and Fourier transform reflection infrared absorption spectroscopy spectra. *Colloids and Surfaces A: Physicochemical and Engineering Aspects*, 157: 147–155.

Nagarajan, S., and Rajendra, N., **2009**. Surface characterization and electrochemical behaviour of porous titanium dioxide coated 316L stainless steel for orthopaedic applications. *Applied Surface Science*, 255:3927-3932.

Nielsen, R., and Chang, T.W. **1996**. In: Elvers, B., Hawkins, S. and Schultz, G. (Eds), *Ullman's Encyclopaedia of Industrial Chemistry,* 5th edition, Vol. A28, Weinheim, Germany, Wiley VCH, pp 543–567 and 95–122.

Noisong, P., Danvirutai, C., Srithanratana, T., and Boonchom, B., **2008**. Synthesis, characterization and non-isothermal decomposition kinetics of manganese hypophosphite monohydrate. *Solid State Sciences*, 10: 1598–1604.

Paixão, J. M. J., and de Mendonça, P. A. F., **1979**. Process for concentration of titanium containing anatase ore. US Patent 4 176 159.

Peng, G.-W., and Liu, H.-S., **1995**. FT-IR and XRD characterization of phase transformation of heat-treated synthetic natisite ($Na_2TiOSiO_4$) powder. *Materials Chemistry and Physics*, 42: 264–275.

Ratnasamy, P., Srinivas, D., and Knözinger, H., **2004**. Active sites and reactive intermediates in titanium silicate molecular sieves. *Advances in Catalysis*, 48:1-169.

Reid, A.F., and Sienko, M.J., **1967**. Some characteristics of sodium titanium bronze and related compounds. *Inorganic Chemistry*, 6(2): 321–324.

Ryskin, Ya.I, **1974**. The Infrared Spectra of Minerals. Mineralogical Society Monograph 4. Farmer, V.C., edition. Adlard and Son Ltd., London.

Roth, R.S., Negas, T., and Cook, L.P. (Eds), **1981**. *Phase Diagrams for Ceramists*, Columbus, US: American Ceramic Society, Figs. 5123, 5124 and 5338.

Sbirrazzuoli, N., Vicent, L., and Vyazovkin, S., **2000**. Comparison of several computational procedures for evaluating the kinetics of thermally stimulated condensed phase reactions. *Chemometrics and Intelligent Laboratory Systems*, 54:53-60.

Sertkol, M., Köseoğlu, Y., Baykal, A., Kavas, H., and Basaran, A.C., **2009**. Synthesis and magnetic characterisation of $Zn_{0,6}Ni_{0,4}Fe_2O_4$ nanoparticles Via a polyethylene glycol-assisted hydrothermal route. *Journal of Magnetism and Magnetic Materials*, 321: 157–162.

Tarte, P., Cahay, R., and Garcia, A., **1979**. Infrared Spectrum and structural role of titanium in synthetic Ti-garnets. *Physics and Chemistry of Minerals*, 4: 55–63.

Vicente-Rodríguez, M.A., Suarez, M., Banãres-Munõz, M.A., Lopez-Gonzalez, J. de D.,**1996**. Comparative FT-IR study of removal of octahedral of cations and structural modifications during acid treatment of several silicates. *Spectrochimica Acta A*, 52: 1685–1694.

Vyazovkin, S., Burnham, A.K., Criado, J.M., Pérez-Maqueda, L.A., Popescu, C., and Sbirrazzuoli, N., **2011**. ICTAC kinetics committee recomendations for performing kinetic computations on termal analysis data. *Thermochimica Acta*, 520:1-19.

Wilburn, F.W., **2000**. Kinetics of overlapping reactions.*Thermochimica Acta*, 354: 99–105.

Xu, Z., Wang, J., Shao, H., Tang, Z., and Zhang, J., **2007**. Preliminary investigation on the physicochemical properties of calcium ferrate (VI). *Electrochemistry Communications*, 9: 371–377.

Zhang, J-Q., Hong-xu, G., Li-Hong, S., Rong-Zu, H., Feng-qi, Z., and Bo-Zhou, W., **2009**. Non-isothermal thermal decomposition reaction kinetics of 2-nitroimino-5-nitro-hexahydro-1,3,5-triazine. *Journal of Hazardous Materials*, 163(1–3): 205–208.

Zhang, M., Salje, E.K.H., Ewing, R.C., Farnan, I., Ríos, S., Schlüter, J., and Leggo, P., **2000**. Alpha-decay damage and recrystallization in zircon: Evidence for an intermediate state from infrared spectroscopy. *Journal of Physics: Condensed Matter*, 12: 5189–5199.

5 Conclusions

Titania is an important white pigment and opacifier for various applications. It is obtained from rutile, ilmenite and from synthetic sources, such as synthetic rutile and titanium slag. However, there are several other titanium minerals, as well as some ilmenite ores, which cannot be exploited due to the lack of appropriate technology. Such minerals include anatase, perovskite, sphene, titanomagnetites and low-grade ilmenites with a higher content of quality-degrading impurities.

Existing technologies face numerous challenges related to their (i) inability to treat most of the existing ores, (ii) higher energy consumption, (iii) high waste generation, and (iv) generation of greenhouse gases. Another important factor in the titania industry is the decrease in availability of reachable reserves and reserves free of radioactive impurities. Therefore, new processes for titania processing have to be found.

The aim of this work was to develop a new route for upgrading titania raw materials into pigment. The route proposed here entails: the use of sodium hydroxide to reduce iron content, and to immobilise or extract radioactive impurities; wet treatment to hydrolyse titanium oxide and iron oxide; and sulfation to extract titanium. This process is able to treat a broad range of ores.

There are three critical stages in the process:

1. **Fusion** – sodium hydroxide reacts with ilmenite.
2. **Leaching** – water is used to leach out impurities and recover sodium hydroxide.
3. **Sulfation** – titanium and iron are solubilised.

Further, the sulfate solution is hydrolysed to copperas and titania, via the normal sulfate process. Alternatively, hydrolysed AFDI can be introduced into the chloride process as titanium

feedstock after calcination. Each of these steps was separately studied and the following conclusions were drawn.

5.1 Fusion Step

Economic conditions necessitate the use of smaller amounts of the alkali while releasing the highest quantity of titanium. This is consistent with the formation of ternary phases ($Na_2O.Fe_2O_3.TiO_2$). The mole ratio of 2:1 (NaOH:ilmenite) was found to be the most effective in producing ternary phases. Using this mole ratio, 0.41 mass units were released per unit mass of sodium hydroxide, fusing at 900^{o}C, for 1 h. The theoretical limit is 0.53 units for this mole ratio.

When the aforementioned conditions (2:1 mole ratio, 900 ^{o}C, 1 h) were used for fusion, $Na_{0.75}Fe_{0.75}Ti_{0.25}O_2$, $NaFeTiO_4$ and $Na_2Fe_2Ti_3O_{10}$ were the ternary phases identified in the fused products. Binary phases were also present; they accommodate the surplus titanium or iron whenever the atom ratio of Fe:Ti is different from 1:1. Na_2TiO_3, $Na_8Ti_5O_{14}$ and $NaFeO_2$ were identified in the product spectrum.

Fusion mole ratios higher than 2:1 (NaOH:ilmenite) produced essentially binary phases. Na_2TiO_3 and $NaFeO_2$ are binary phases the observed. $NaTiO_2$ was observed in the products when fusions were conducted for 1 h or less of fusion time. The formation of $NaTiO_2$ results from the non-availability of oxygen to act as oxidant in the iron oxidation reaction. With short periods of fusion (less than 1 h) binary phases were also dominant. This was also observed when fusions were conducted below 600 ^{o}C.

When mole ratios below 2:1 (NaOH:ilmenite) were used at 850 ^{o}C for 1 h in fusion, $Na_2Fe_2Ti_3O_{10}$ and $NaFeTiO_4$ were the sole ternary phases in the product spectrum. Fusions conducted below 850 ^{o}C under these conditions produced binary phases as well as unreacted ilmenite. Although the reaction was completed after 1 h at 850 ^{o}C in these non-stoichiometric conditions, only ≈ 30% of the total titanium was recovered using a 1:1 mole ratio.

The maximum yield (81% of total titanium) was achieved at 900 ^{o}C, using a 2:1 (NaOH:ilmenite) mole ratio, for 1 h of fusion time. Increasing the fusion time did not result in significant changes in the titanium yield. The fusion reaction appeared to be independent of the ilmenite particle size above 750 ^{o}C.

When anatase reactant was used to resemble an anatase ore, four phases were obtained, namely $Na_2Ti_6O_3$, Na_2TiO_3, $Na_8Ti_5O_{14}$ and $Na_{16}Ti_{10}O_{28}$. The highest recoveries of titanium were obtained after fusing at 800 ^{o}C for 2 h, and with a 1:1 (NaOH:TiO_2) mole ratio. Approximately 100% of titanium was recovered under these conditions.

5.2 Leaching Step

It was found that the leaching step was dependent on time, solid:liquid ratio and temperature. The optimum conditions for solid:liquid ratio, time and temperature were found to be 0.20, and 15 min at 75 ^{o}C respectively.

5.3 Other Steps

Other optimised steps were acidic hydrolysis and sulfation. Acidic hydrolysis was controlled by the relative amount of iron and titanium in solution. It was found that less than 1% was dissolved between 3 and 7 in pH units. Higher pH values are recommended since less acid will be used.

Any excess of sulphuric acid in the sulfation step proved to be unnecessary. No significant changes were observed in the amount of dissolved iron and titanium. Therefore the stoichiometric amount can be used in the sulfation process.

5.4 Recommendations

Our work was aimed to develop a route which will broaden the spectrum of titanium minerals that could be used in the sulfate process. The main problems of the process are (i) the high amount of non-saleable by-product iron sulfate; (ii) the inability of the process to deal with radioactive impurities.

Although we might claim success in broadening the spectrum of titanium minerals that can be used in titania production via sulfate route, we are aware that we were unable to tackle the issue of high amounts of iron sulfate. Our process also produces amounts of this by-product. There is therefore a challenge of transforming the iron sulfate by-product in a more useful product. This can be attained by encountering new uses or else to transform it in new chemicals that can find a wider market.

The second problem, of the radioactive impurities, although we might have been successful on targeting we were unable to certify the existence of phases containing these impurities. The idea was to produce phases that would make possible the separation of radionuclides from the product and from the waste stream.

Appendix A: X-ray diffraction diagrams

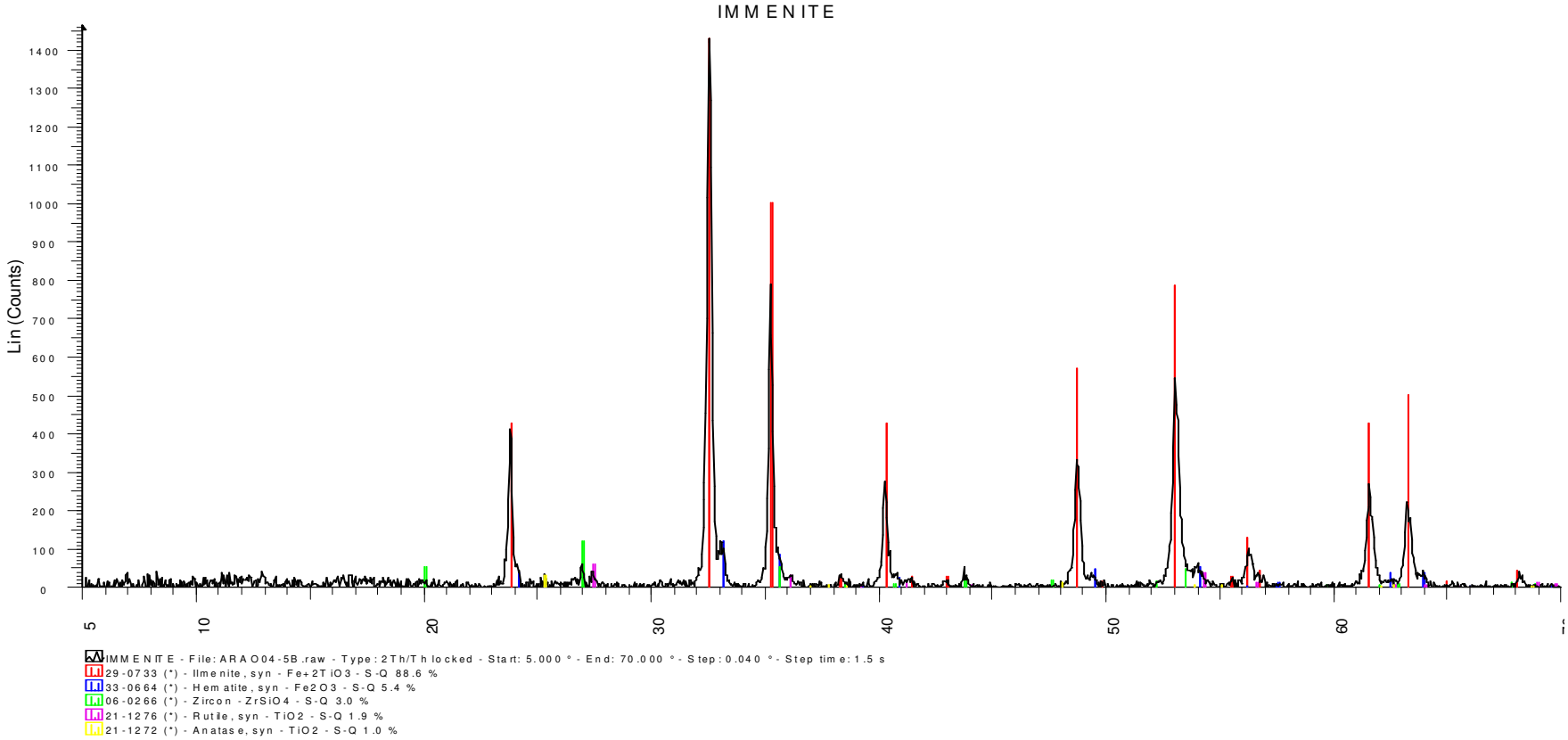

Appendix A- 1:XRD diagram of ilmenite raw material

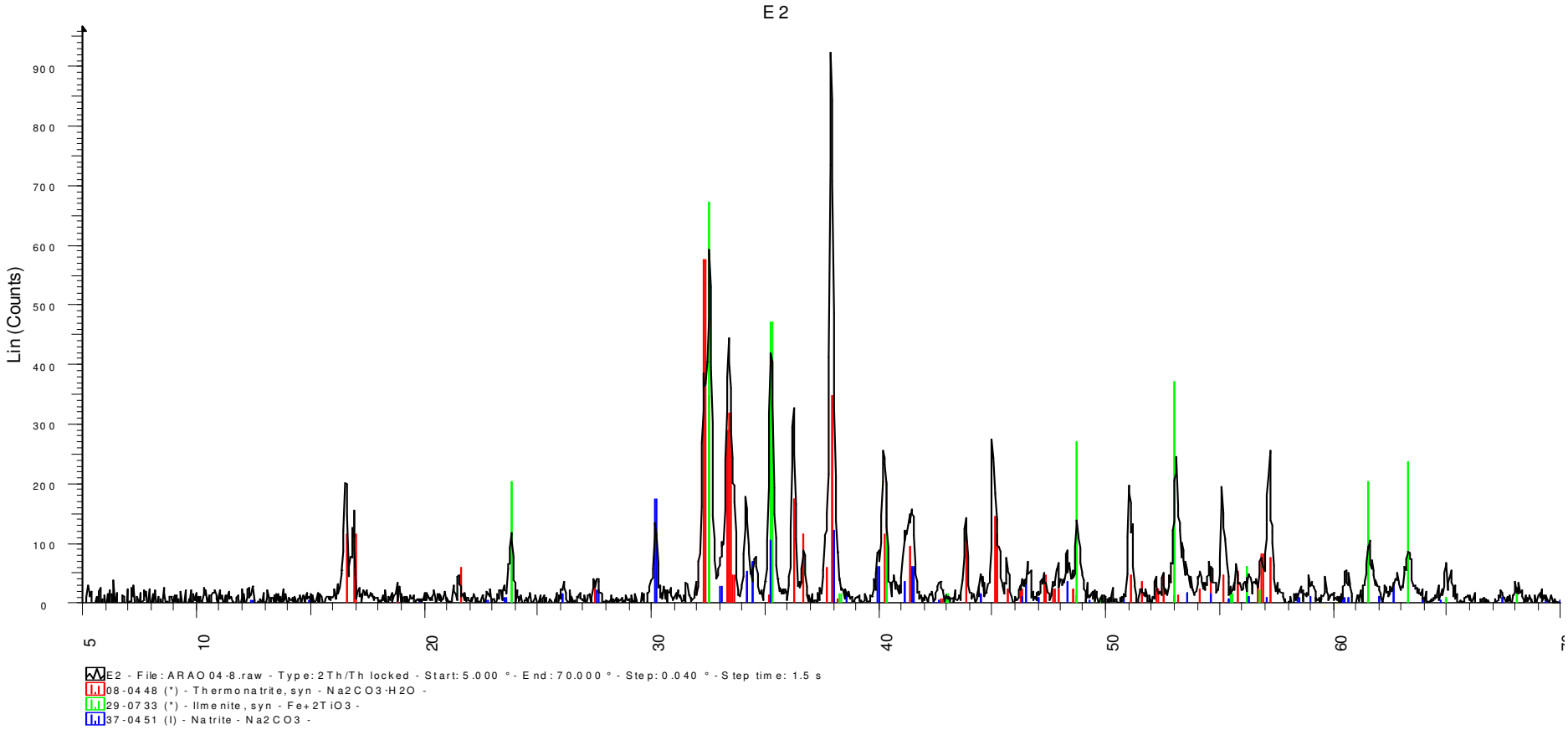

Appendix A- 2:XRD diagram of Alkali fused ilmenite. One mole of ilmenite was fused with one mol of sodium hydroxide at 250 °C for 336 hours, with intermediate milling every 24 hours

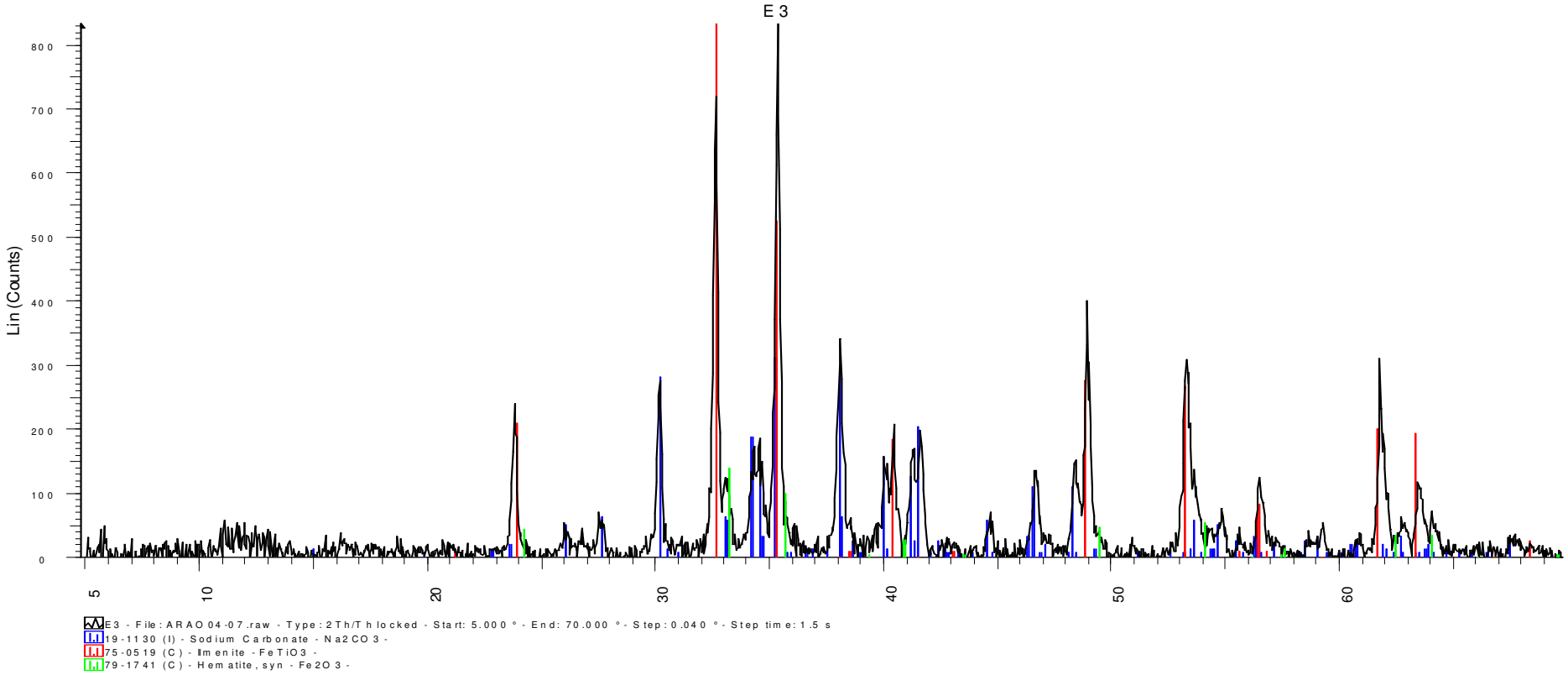

Appendix A- 3: XRD diagram of Alkali fused ilmenite. One mole of ilmenite was fused with two mole of sodium hydroxide at 250 °C for 336 hours, with intermediate milling every 24 hours

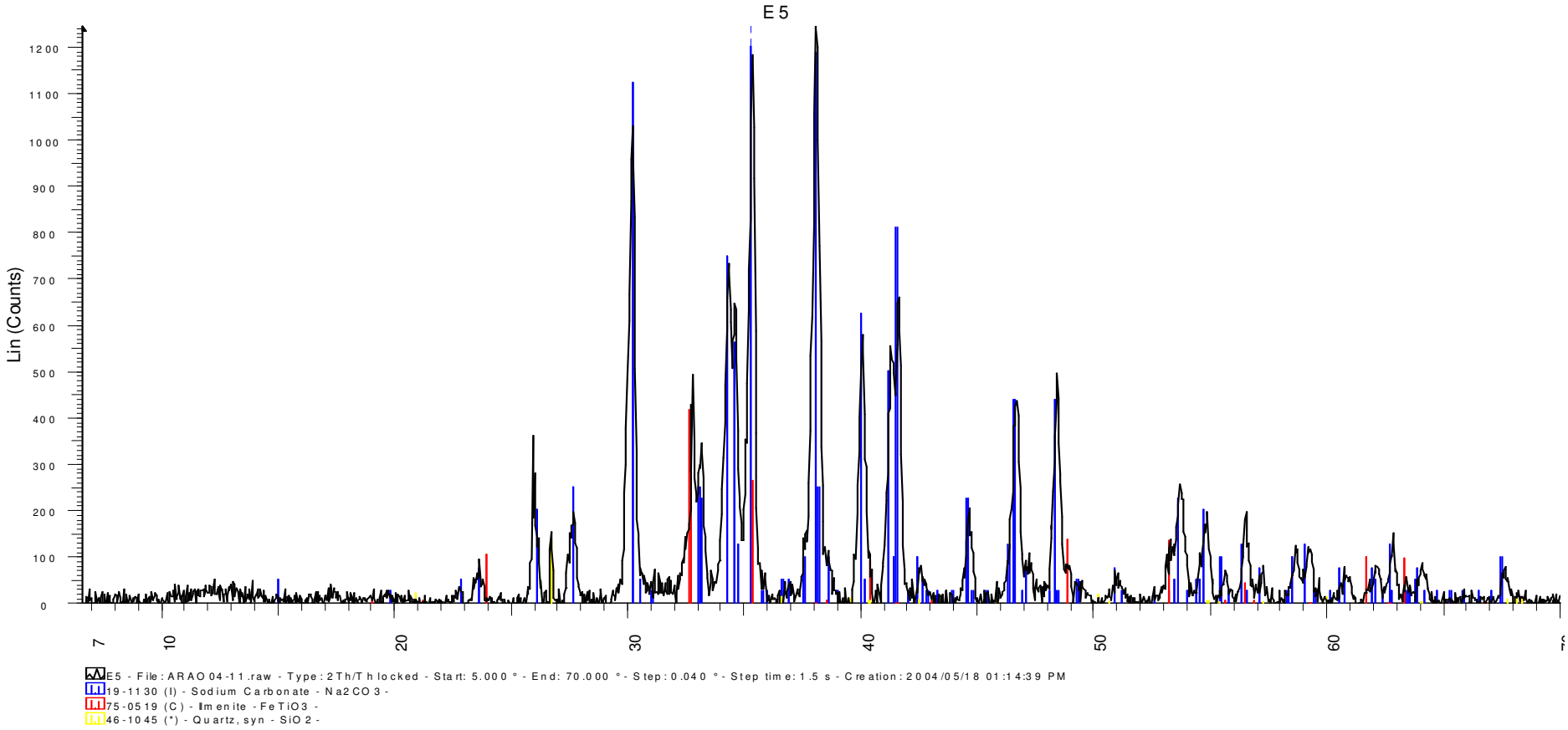

Appendix A- 4:XRD diagram of Alkali fused ilmenite. One mole of ilmenite was fused with four mole of sodium hydroxide at 250 °C for 336 hours, with intermediate milling every 24 hours

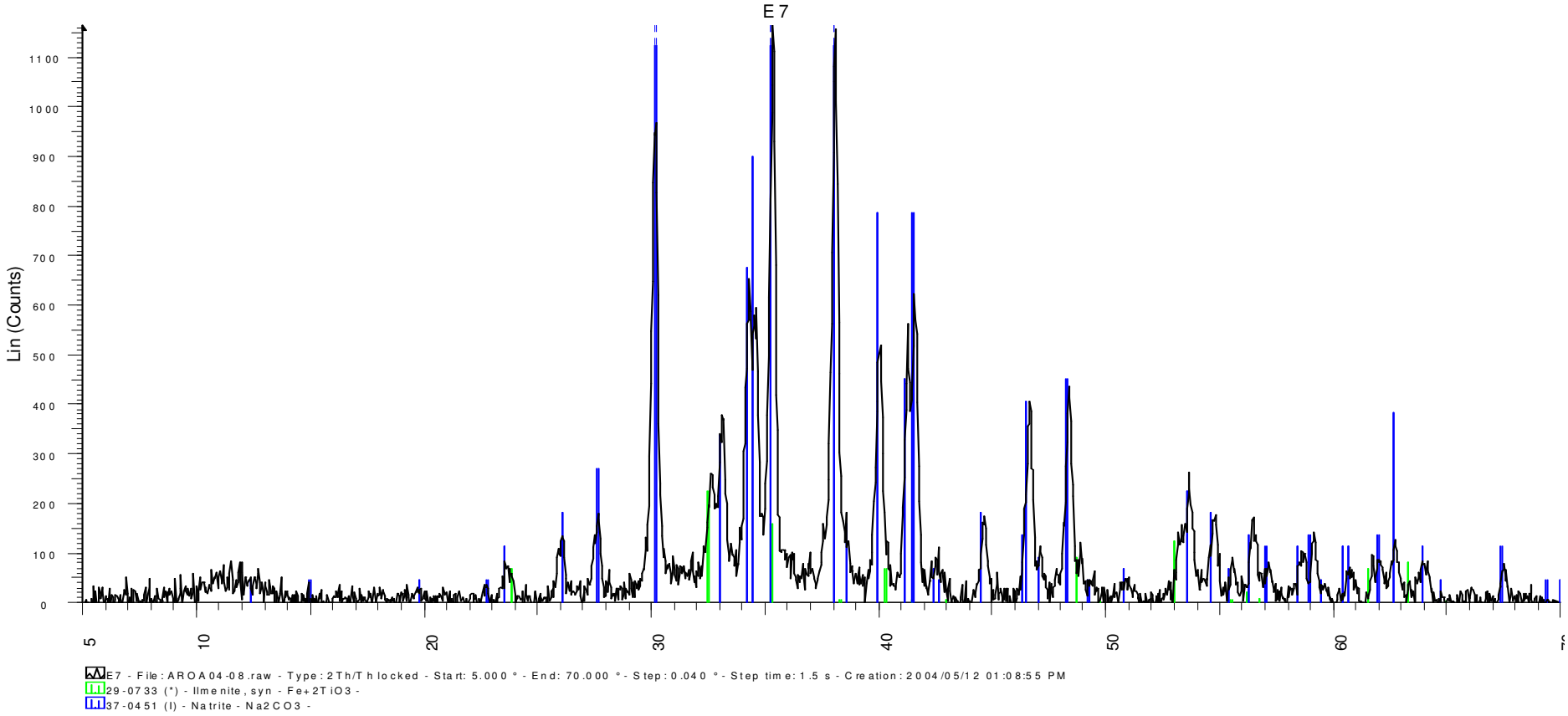

Appendix A- 5:XRD diagram of Alkali fused ilmenite. One mole of ilmenite was fused with six mole of sodium hydroxide at 250 °C for 336 hours, with intermediate milling every 24 hours

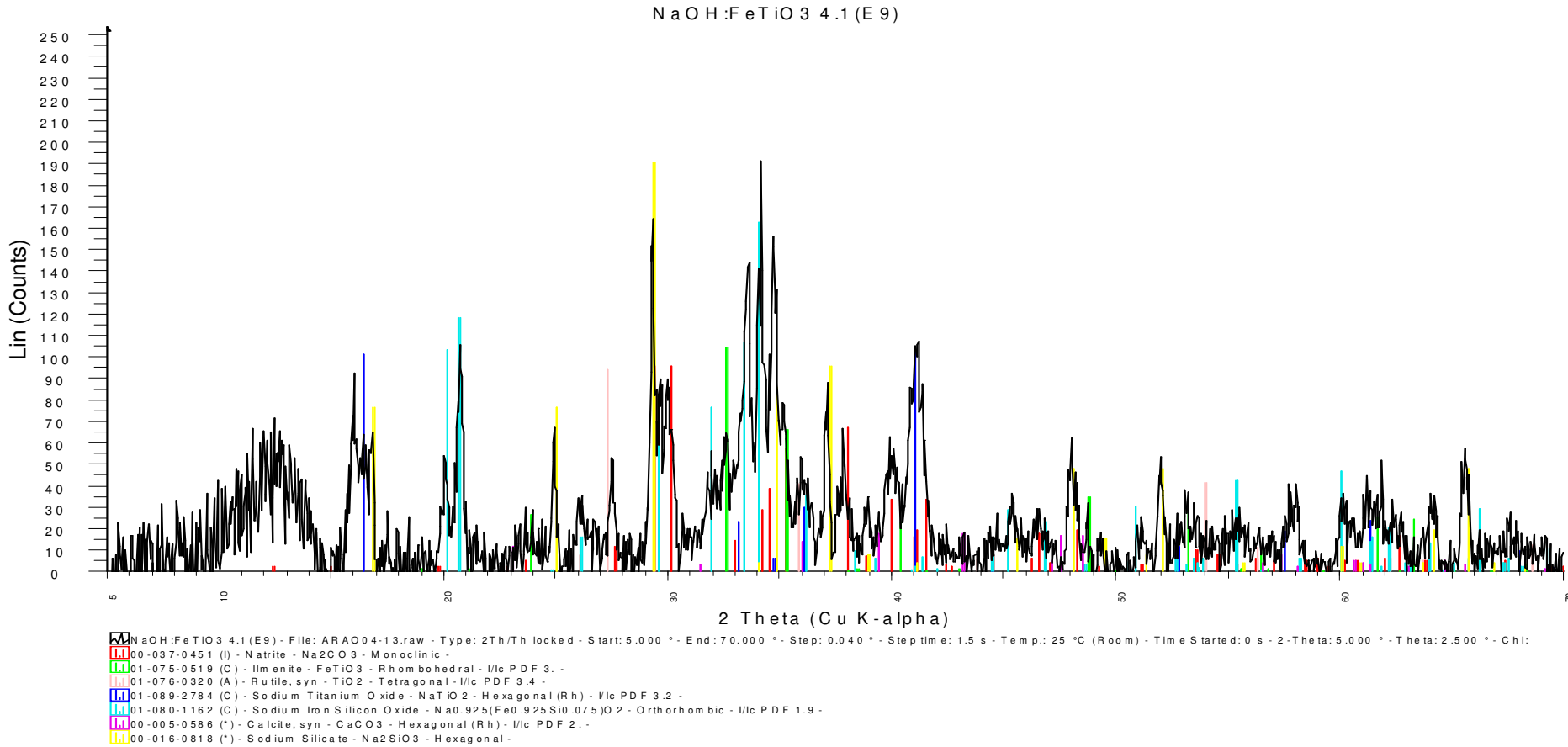

Appendix A- 6:XRD diagram of Alkali fused ilmenite. One mole of ilmenite was fused with four mole of sodium hydroxide at 500 °C for 336 hours, with intermediate milling every 24 hours

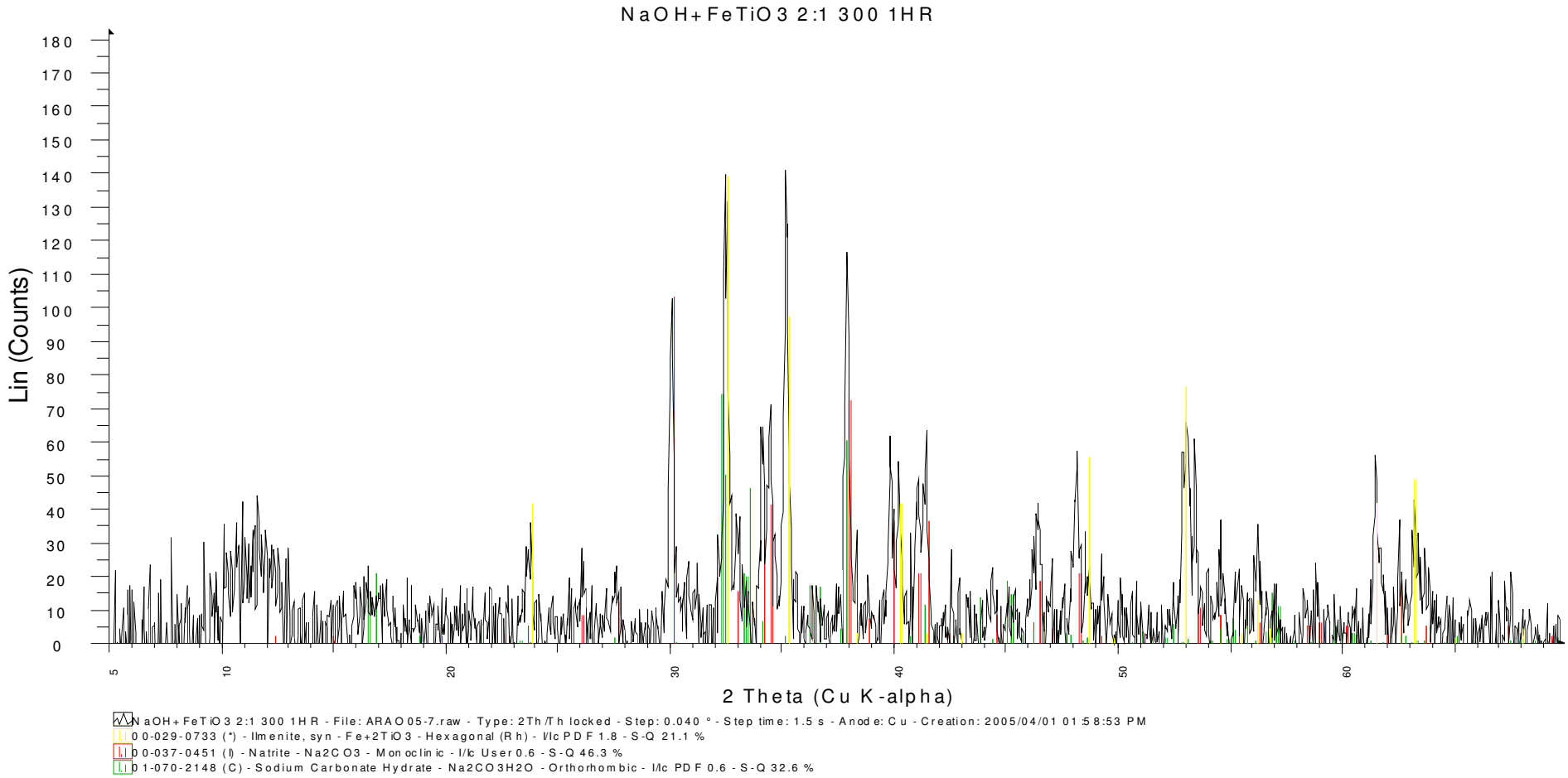

Appendix A- 7:XRD diagram of Alkali fused ilmenite. One mole of ilmenite was fused with two mol of sodium hydroxide at 300 °C for one hour

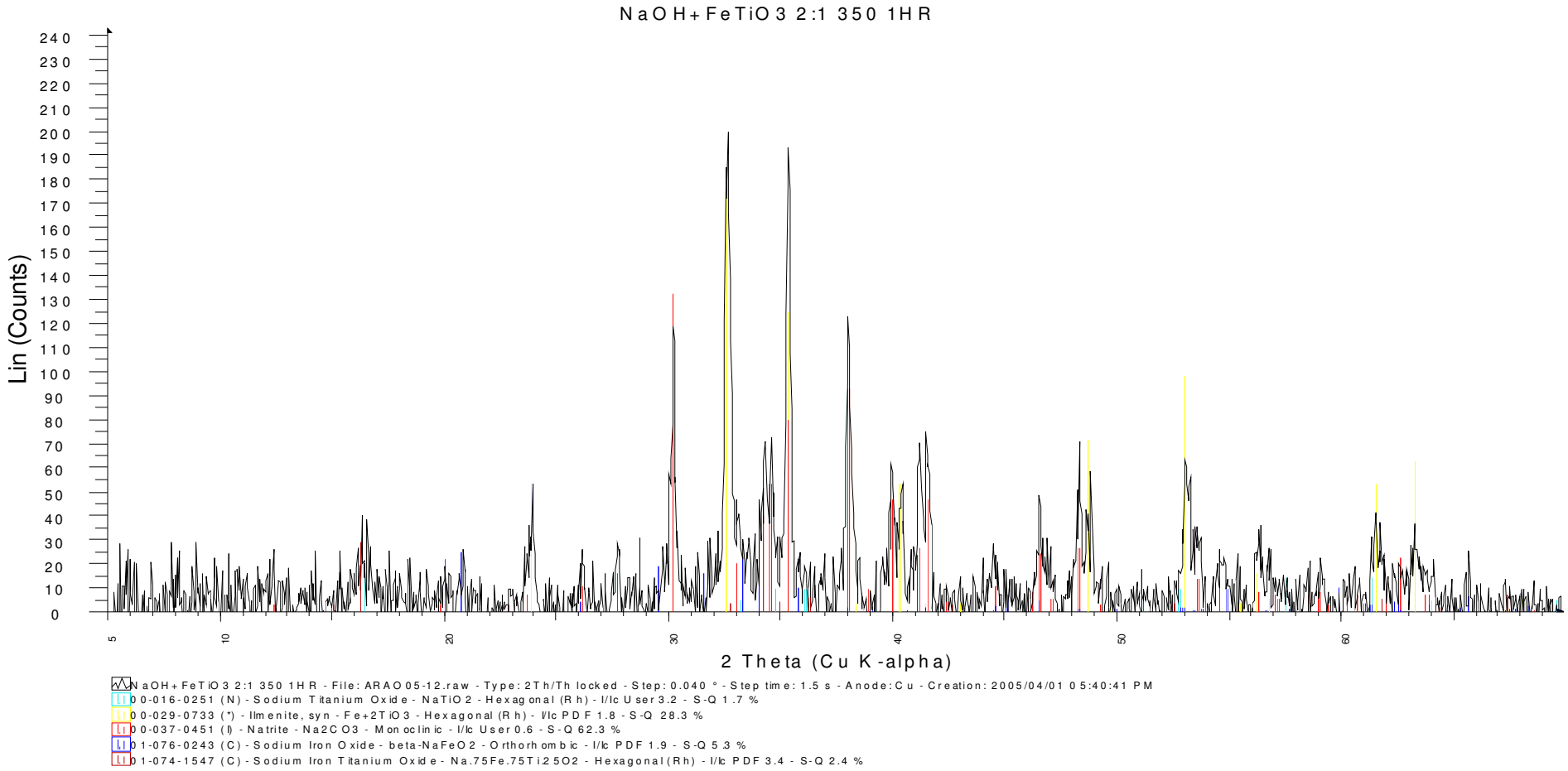

Appendix A- 8: XRD diagram of Alkali fused ilmenite. One mole of ilmenite was fused with two mole of sodium hydroxide at 350 °C for one hour

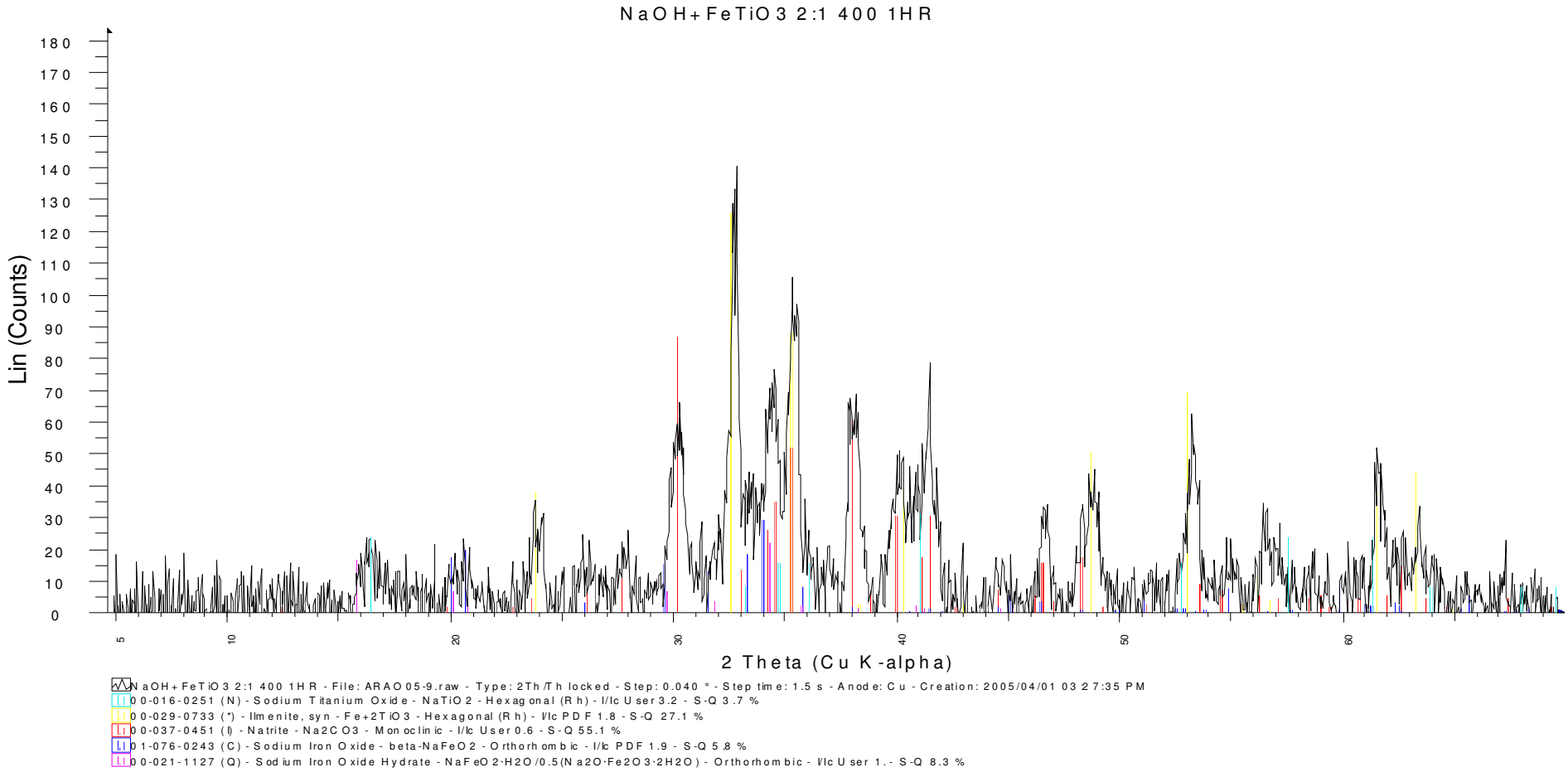

Appendix A- 9:XRD diagram of Alkali fused ilmenite. One mole of ilmenite was fused with two mole of sodium hydroxide at 400 °C for one hour

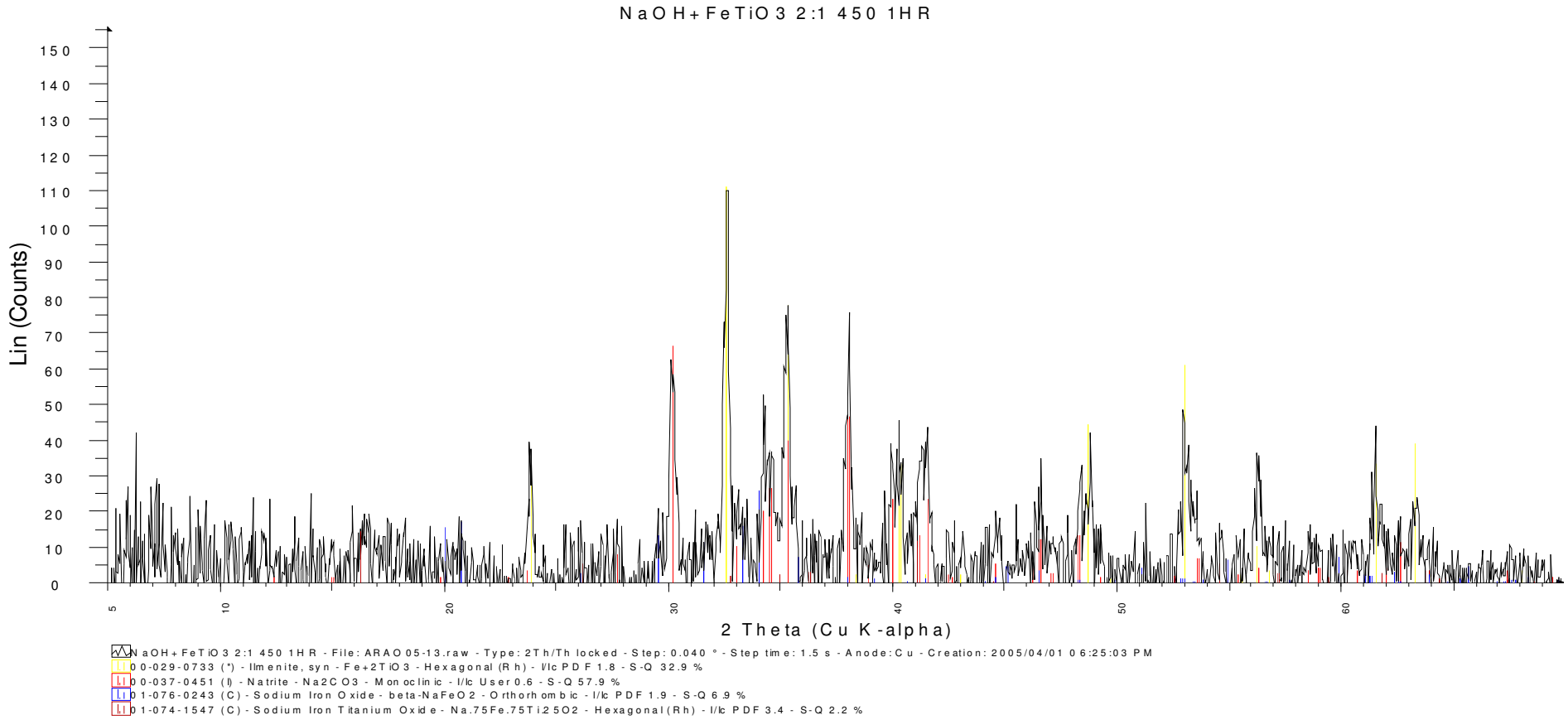

Appendix A- 10:XRD diagram of Alkali fused ilmenite. One mole of ilmenite was fused with two mole of sodium hydroxide at 450 °C for one hour

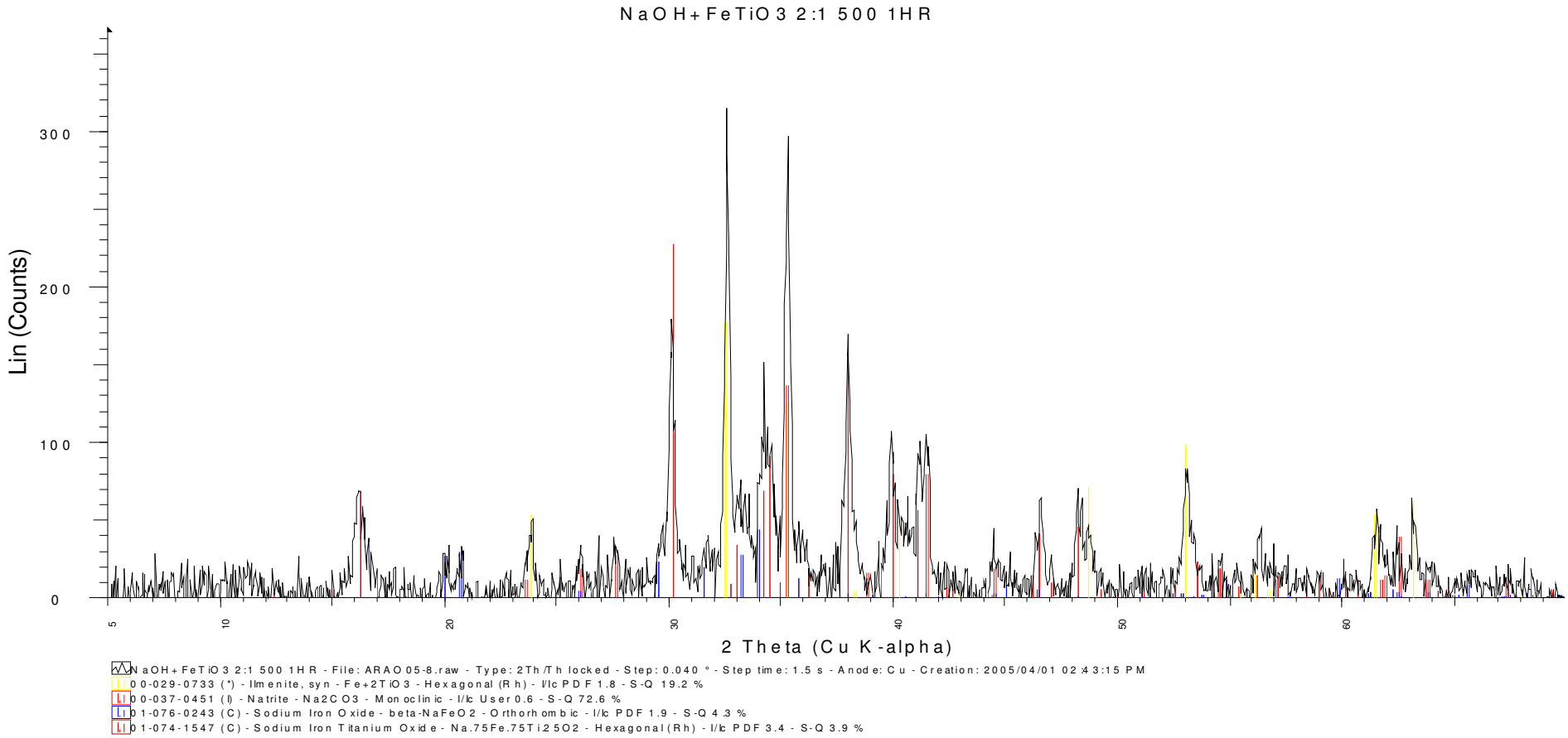

Appendix A- 11:XRD diagram of Alkali fused ilmenite. One mole of ilmenite was fused with two mole of sodium hydroxide at 500 °C for one hour

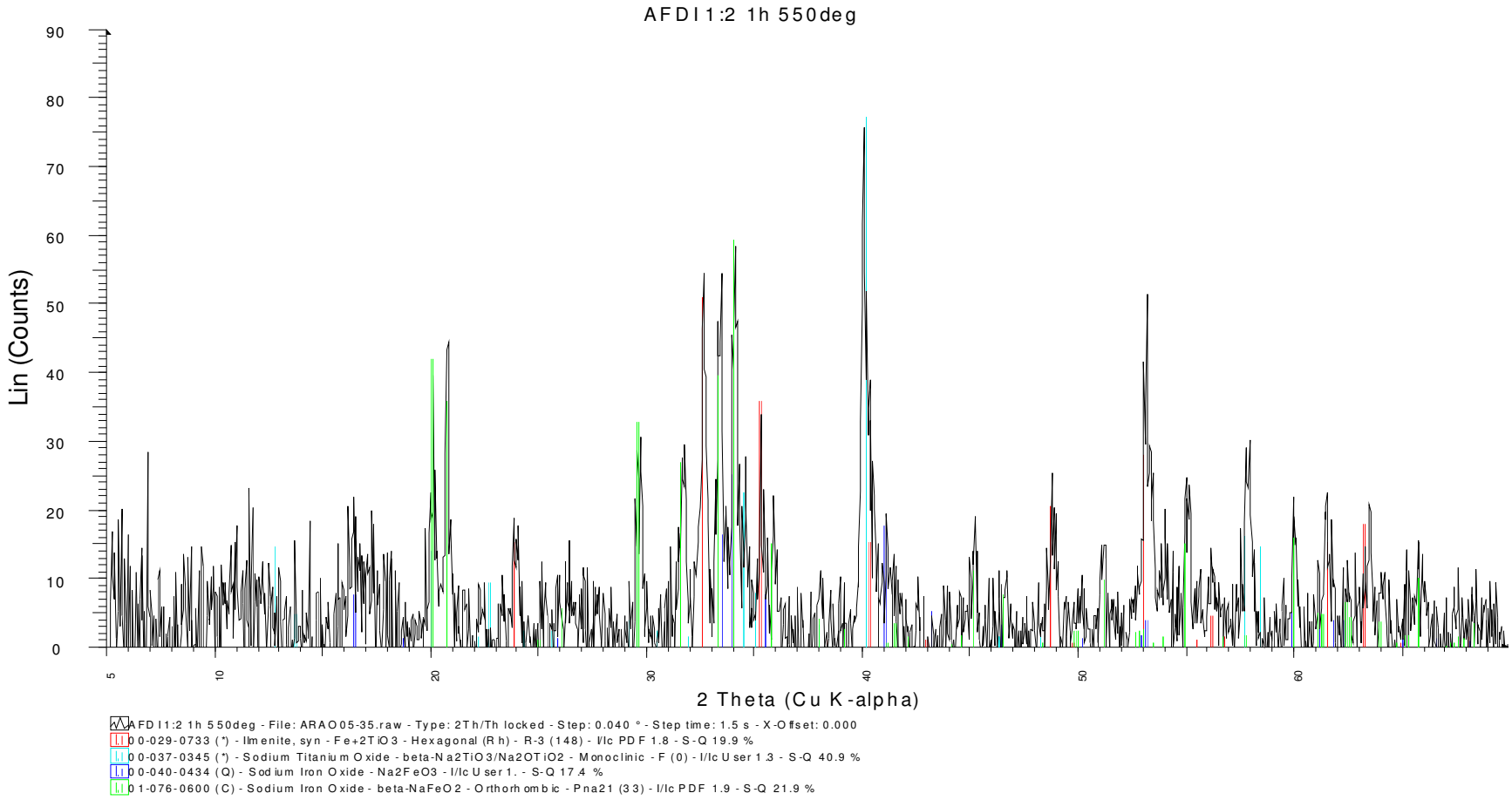

Appendix A- 12:XRD diagram of Alkali fused ilmenite. One mole of ilmenite was fused with two mole of sodium hydroxide at 550 °C for one hour

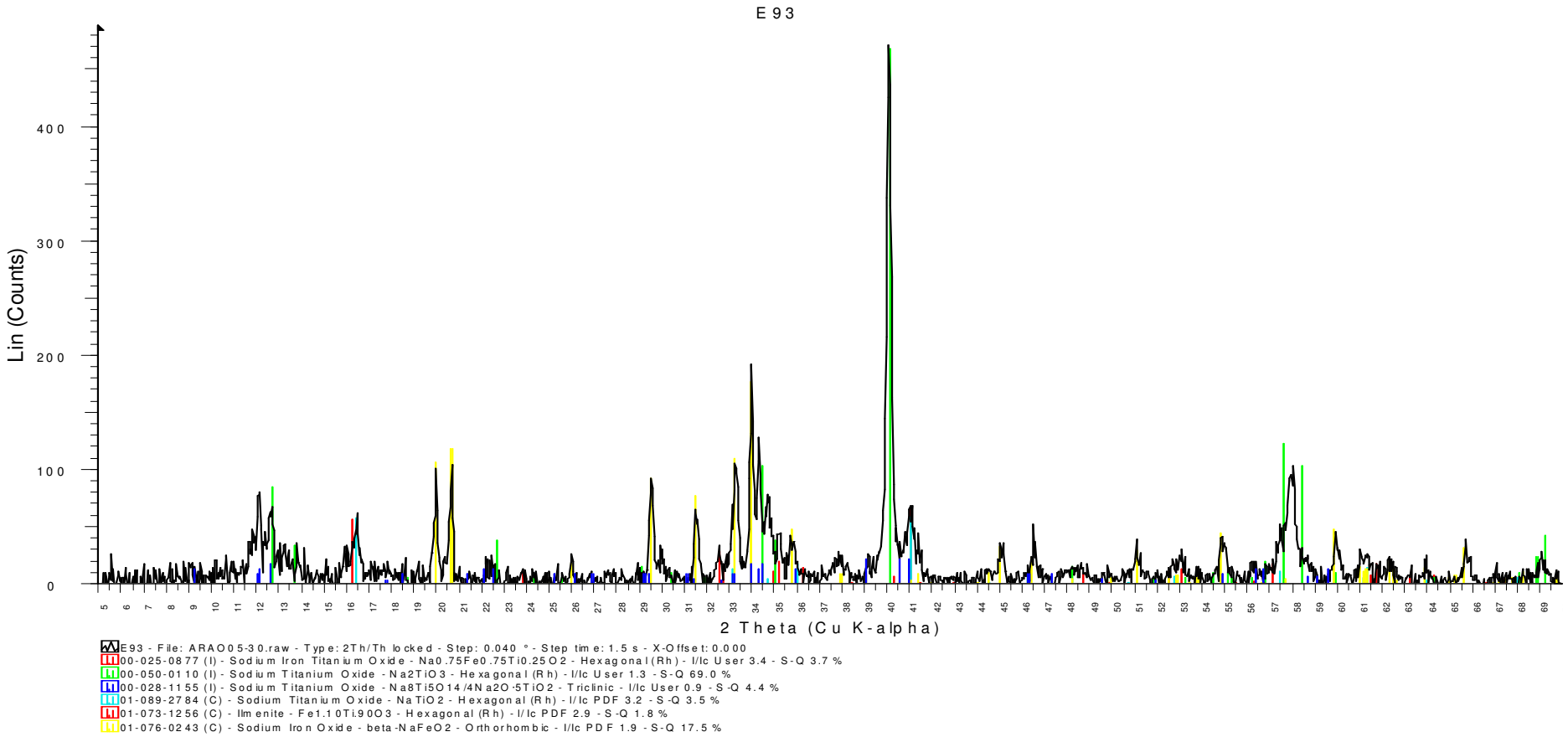

Appendix A- 13:XRD diagram of Alkali fused ilmenite. One mole of ilmenite was fused with two mole of sodium hydroxide at 600 °C for one hour

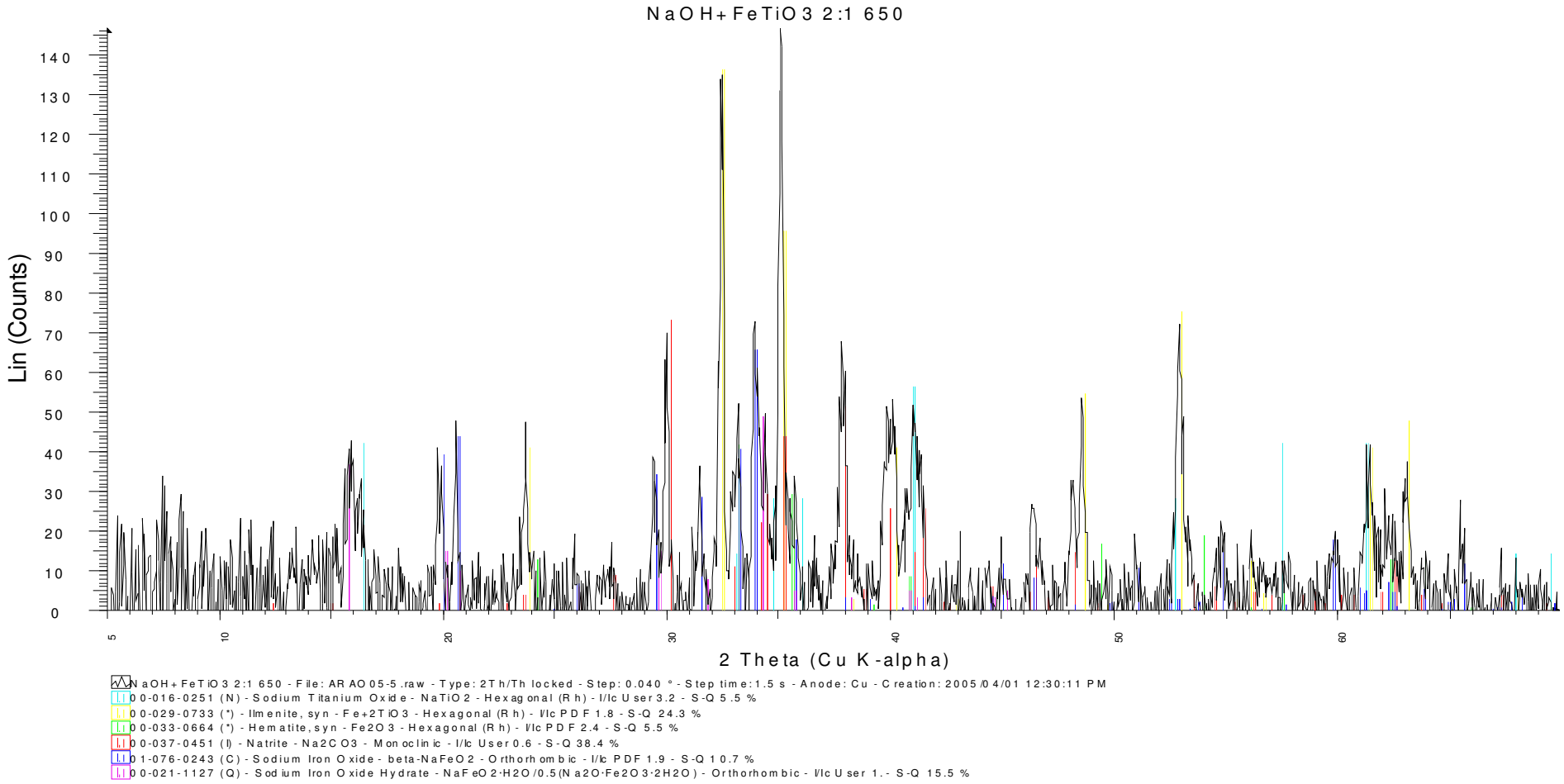

Appendix A- 14:XRD diagram of Alkali fused ilmenite. One mole of ilmenite was fused with two mole of sodium hydroxide at 650 °C for one hour

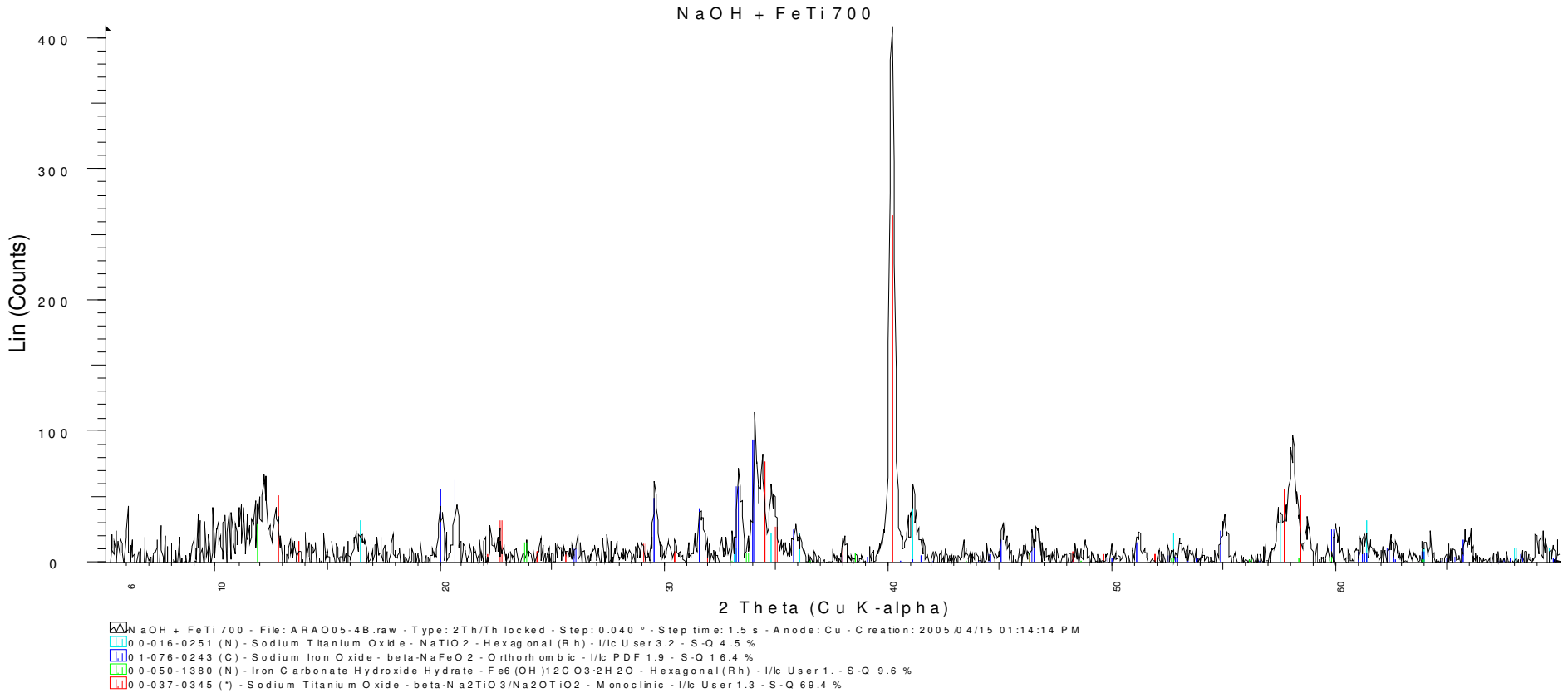

Appendix A- 15: XRD diagram of Alkali fused ilmenite. One mole of ilmenite was fused with two mole of sodium hydroxide at 700 °C for one hour

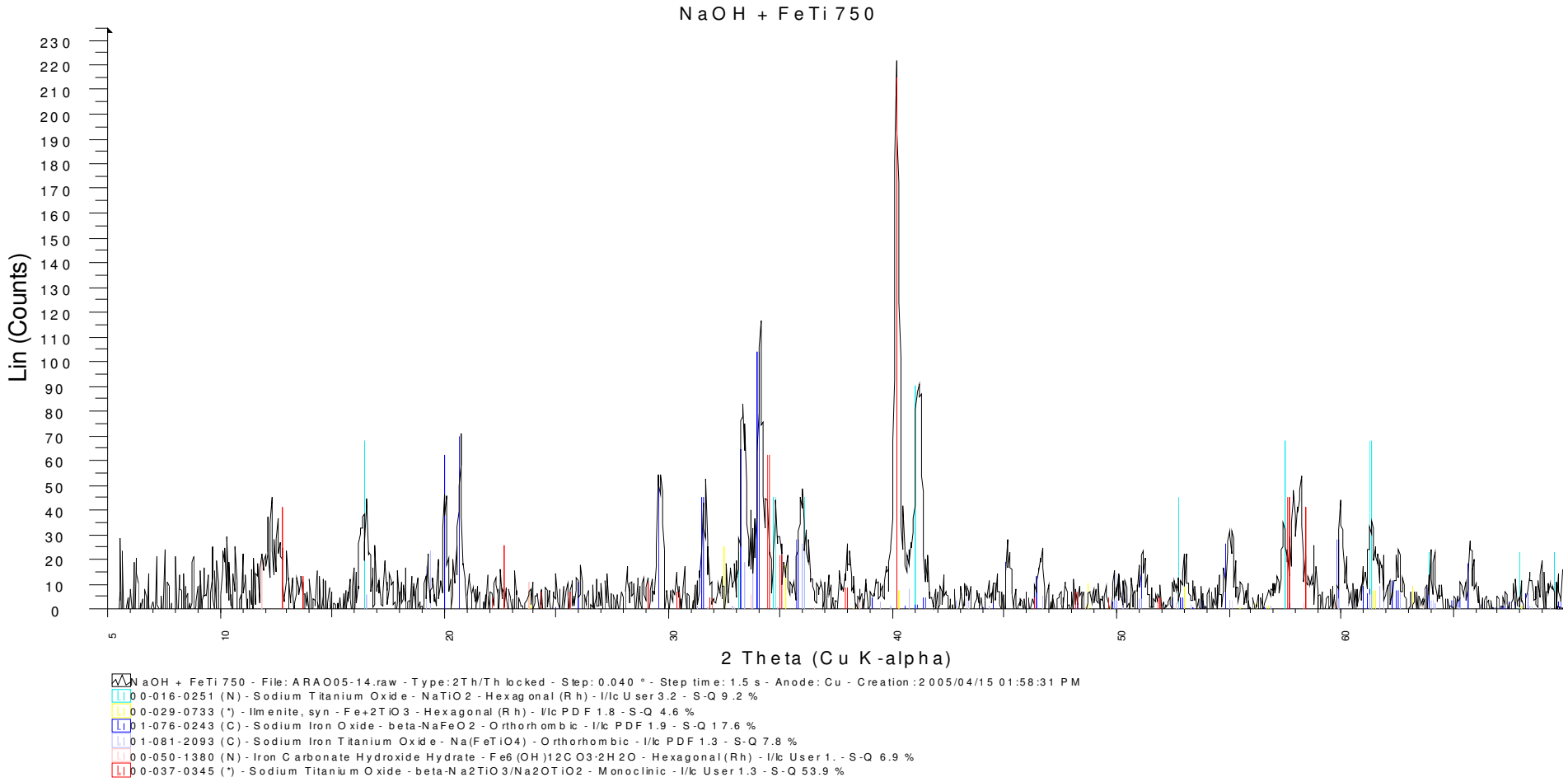

Appendix A- 16:XRD diagram of Alkali fused ilmenite. One mole of ilmenite was fused with two mole of sodium hydroxide at 750 °C for one hour

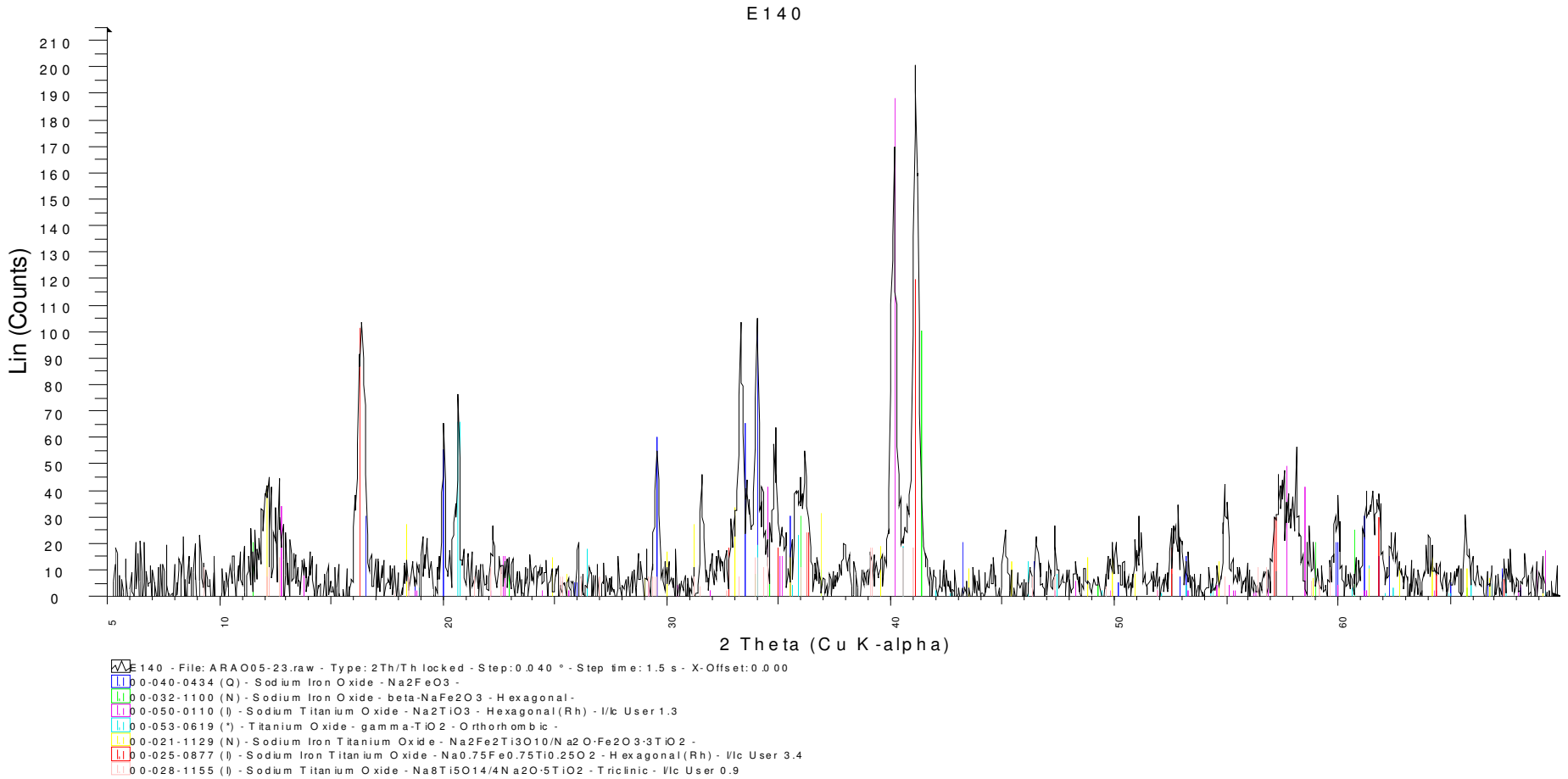

Appendix A- 17: XRD diagram of Alkali fused ilmenite. One mole of ilmenite was fused with two mole of sodium hydroxide at 800 °C for one hour

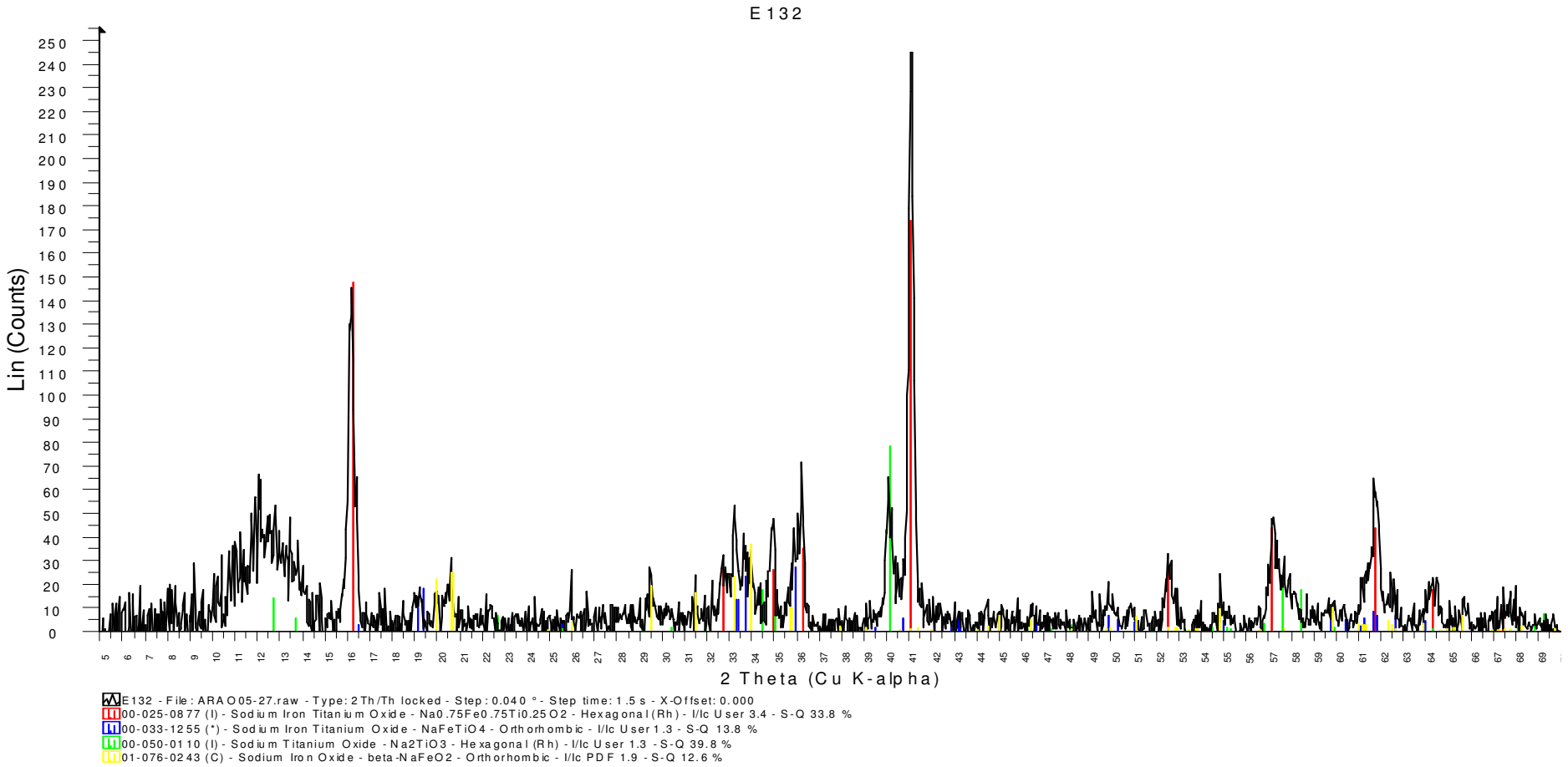

Appendix A- 18: XRD diagram of Alkali fused ilmenite. One mole of ilmenite was fused with two mole of sodium hydroxide at 850 °C for one hour

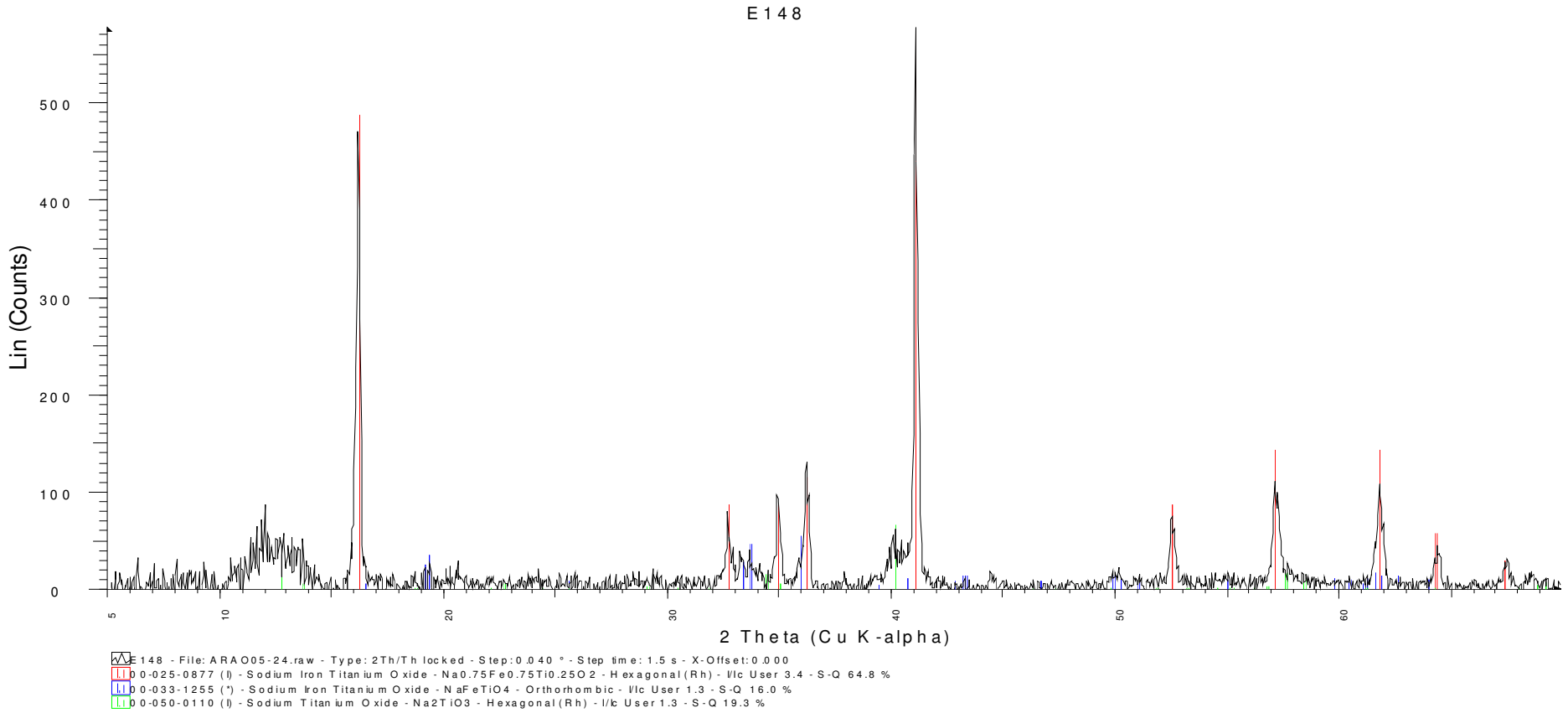

Appendix A- 19: XRD diagram of Alkali fused ilmenite. One mole of ilmenite was fused with two mole of sodium hydroxide at 900 °C for one hour

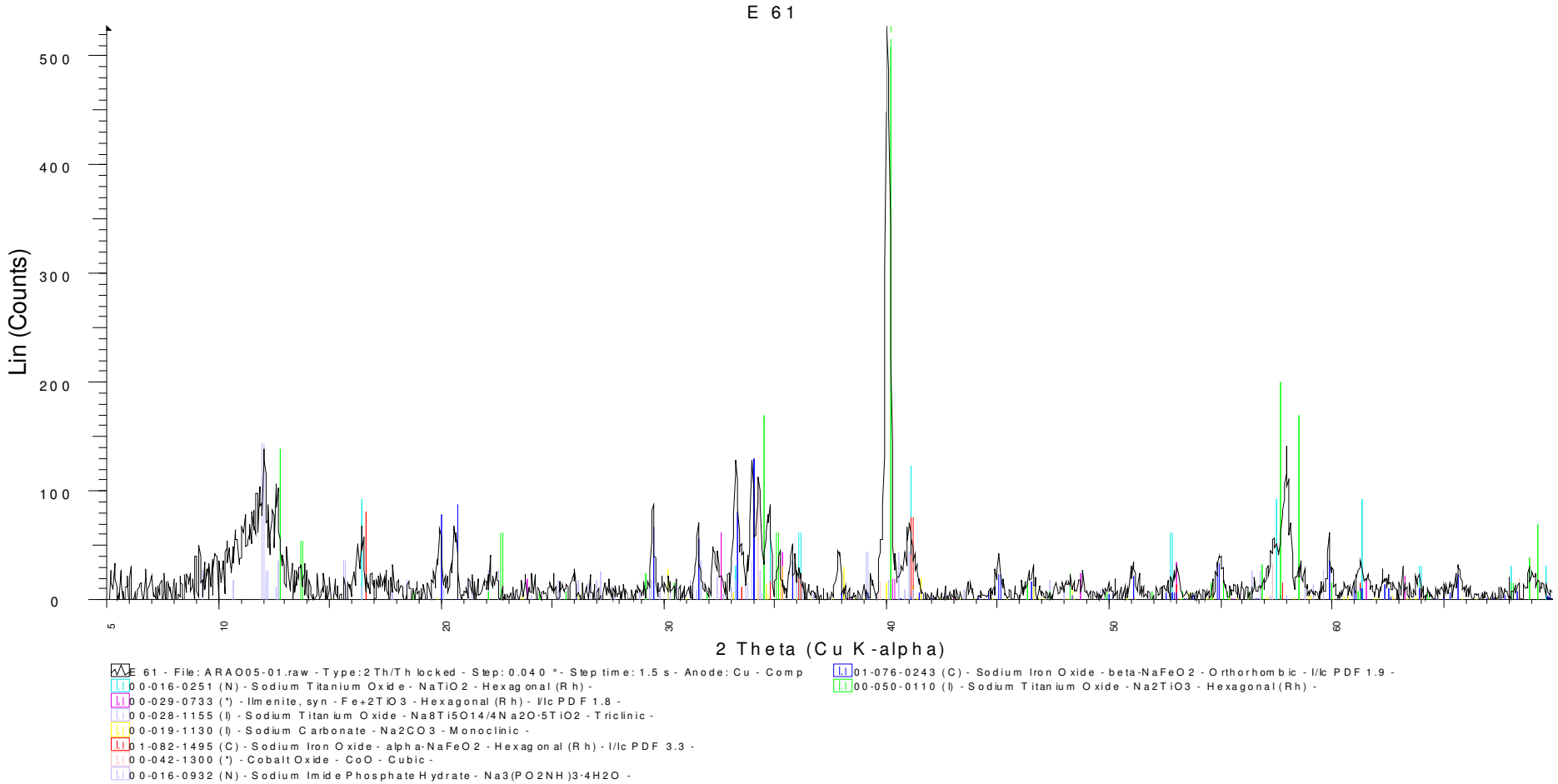

Appendix A- 20:XRD diagram of Alkali fused ilmenite. One mole of ilmenite was fused with two mole of sodium hydroxide at 750 °C for thirty minutes

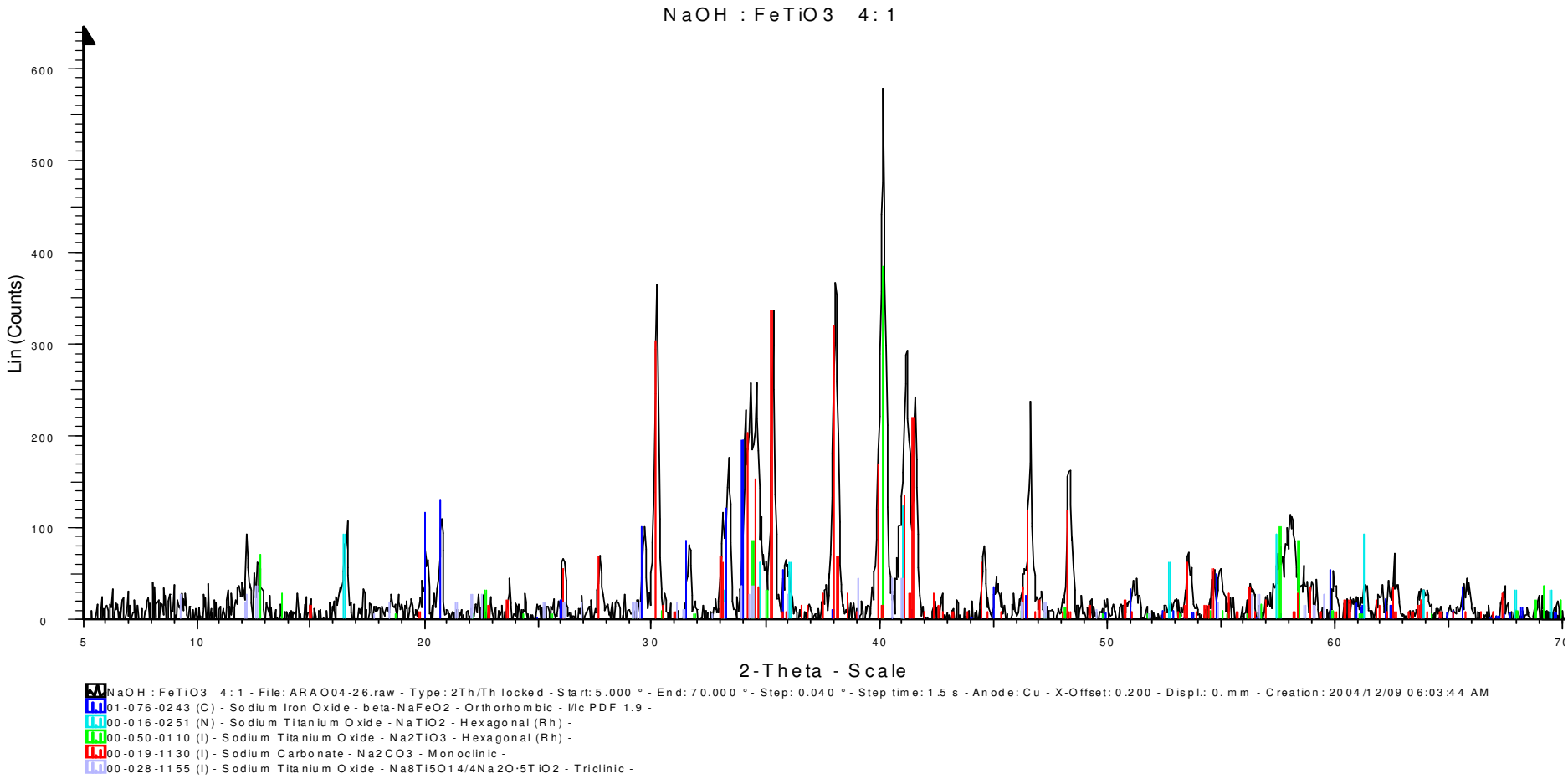

Appendix A- 21:XRD diagram of Alkali fused ilmenite. One mole of ilmenite was fused with four mole of sodium hydroxide at 750 °C for thirty minutes

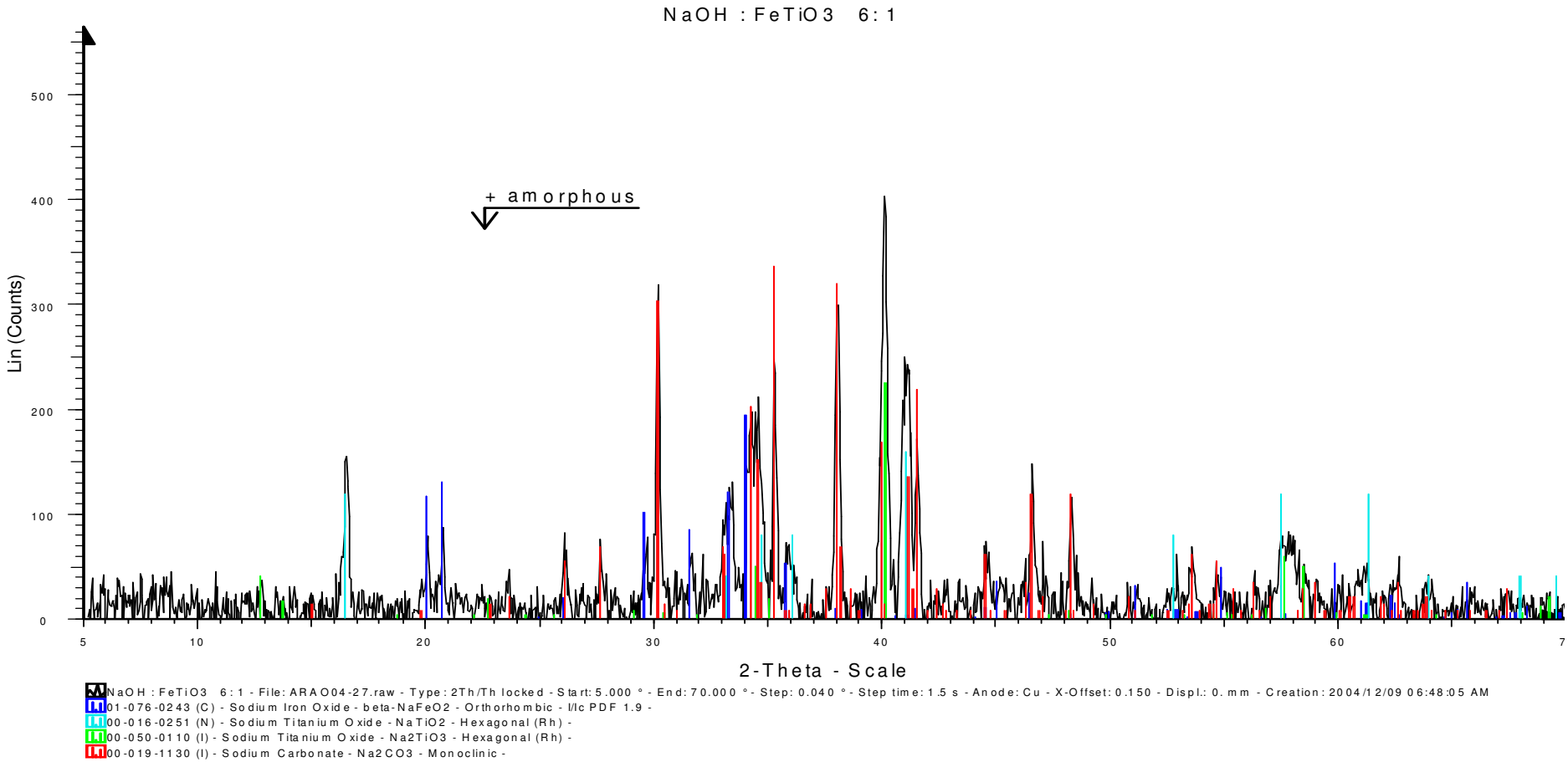

Appendix A- 22: XRD diagram of Alkali fused ilmenite. One mole of ilmenite was fused with six mole of sodium hydroxide at 750 °C for thirty minutes

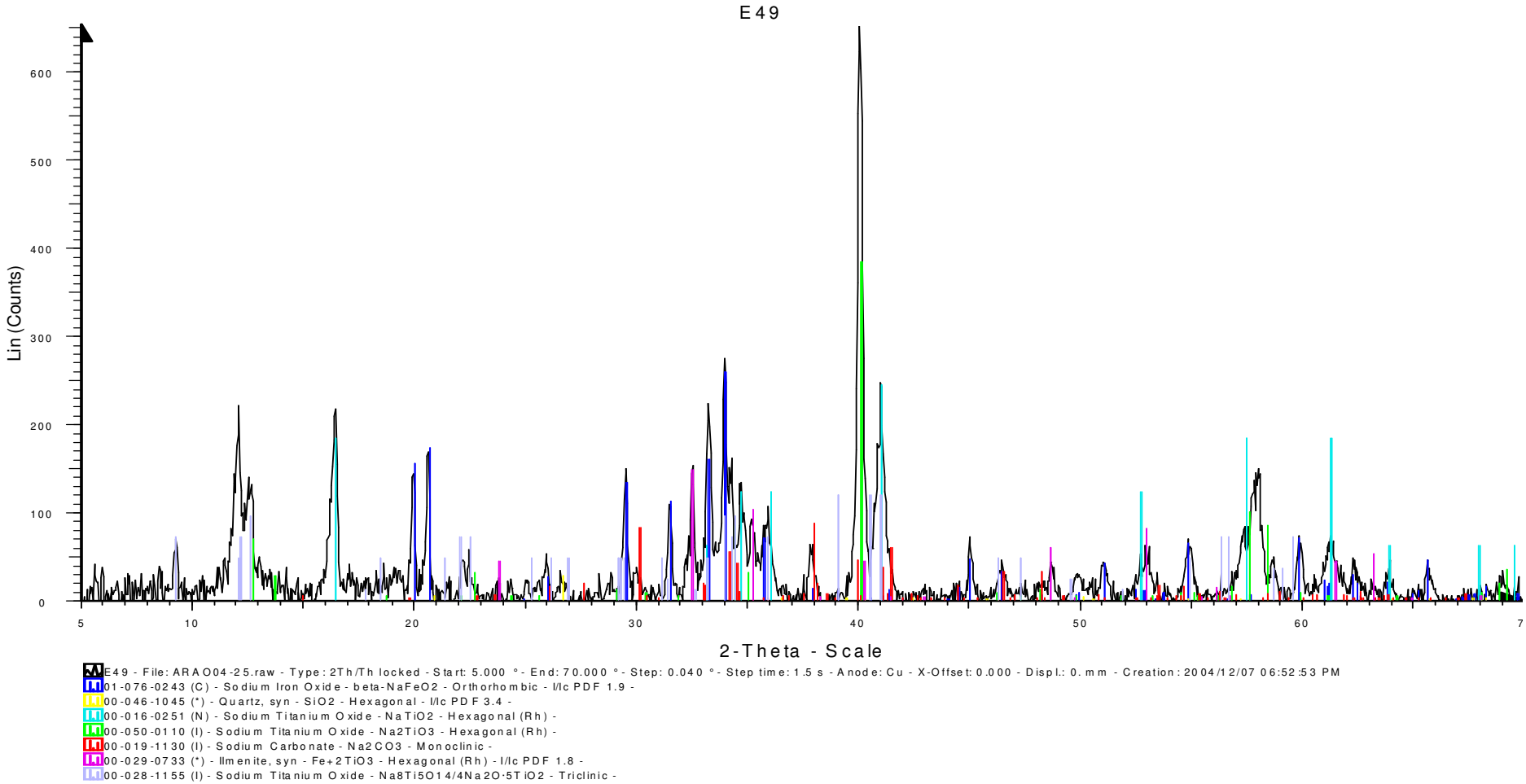

Appendix A- 23: XRD diagram of Alkali fused ilmenite. One mole of ilmenite was fused with two mole of sodium hydroxide at 750 °C for an hour

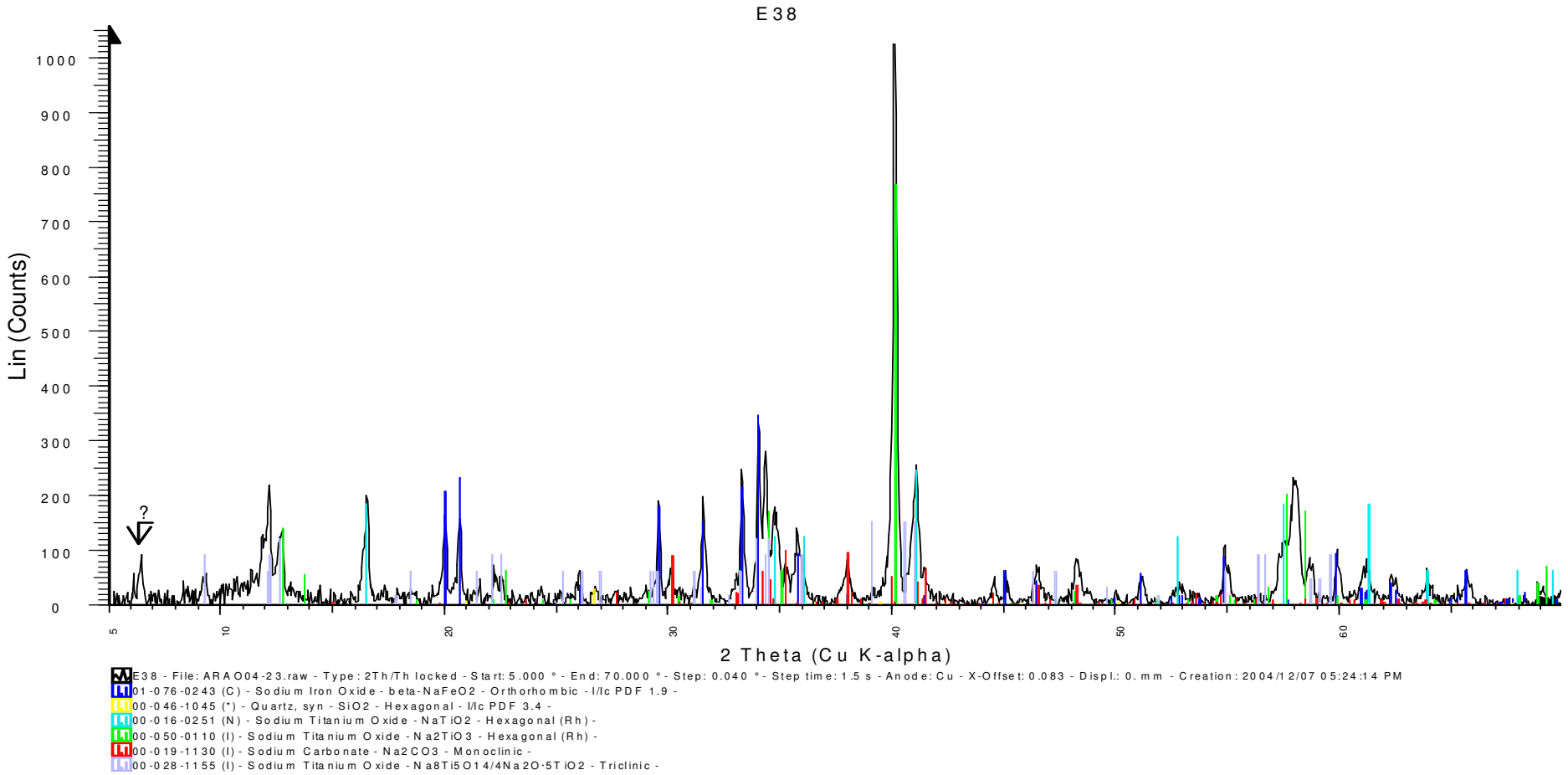

Appendix A- 24:XRD diagram of Alkali fused ilmenite. One mole of ilmenite was fused with four mole of sodium hydroxide at 750 °C for an hour

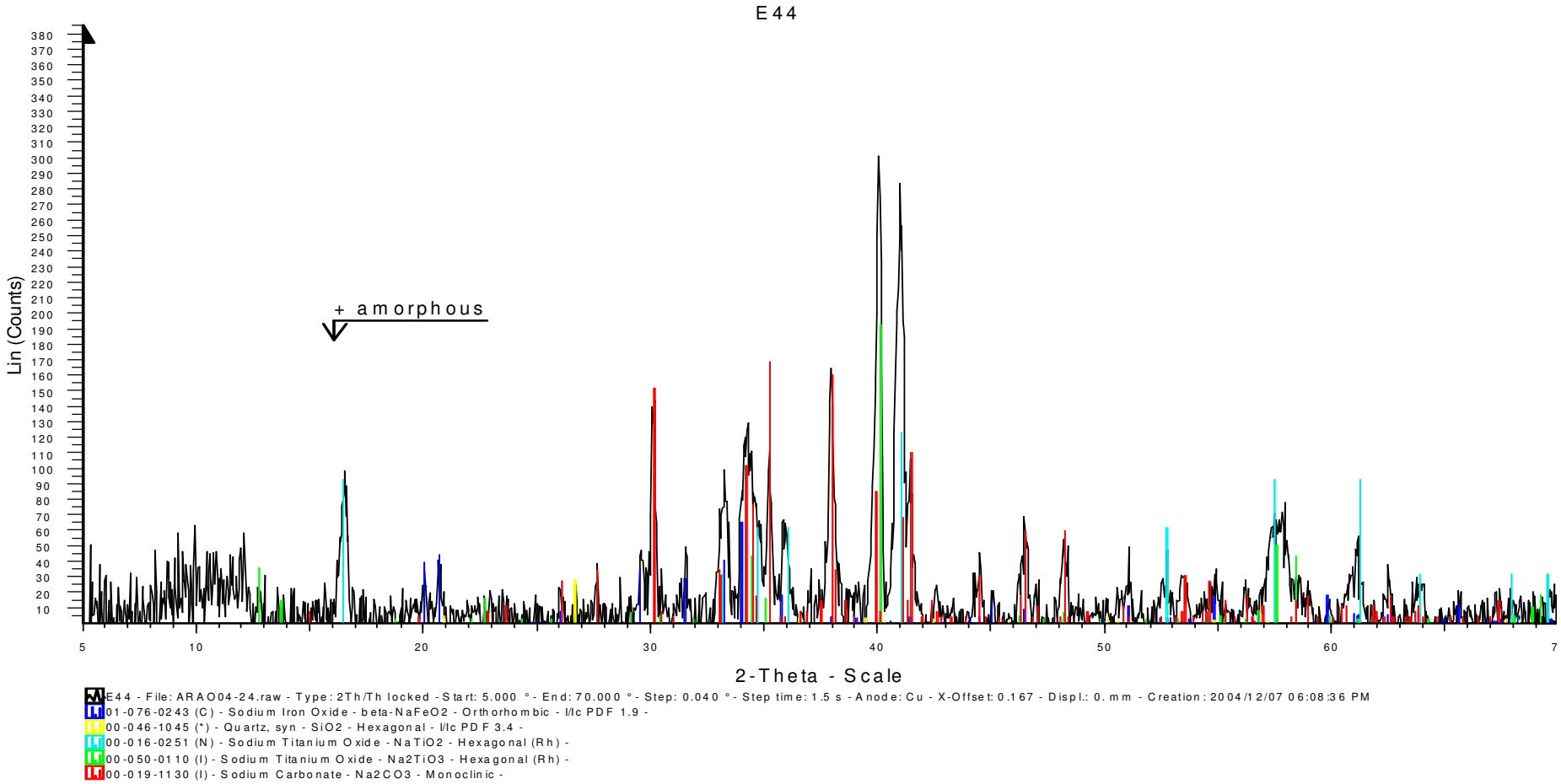

Appendix A- 25: XRD diagram of Alkali fused ilmenite. One mole of ilmenite was fused with six mole of sodium hydroxide at 750 °C for an hour

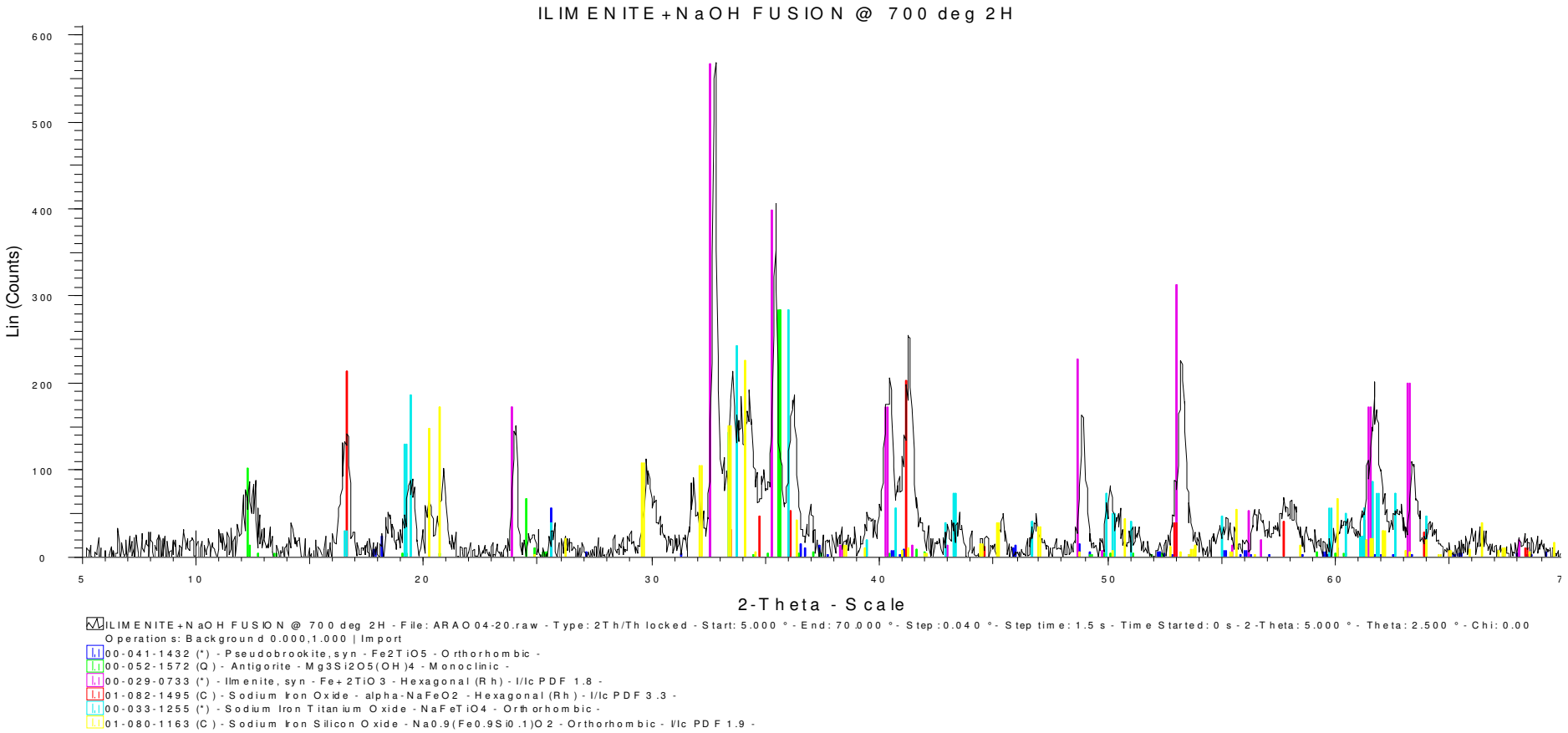

Appendix A- 26: XRD diagram of Alkali fused ilmenite. One mole of ilmenite was fused with two mole of sodium hydroxide at 750 °C for two hours

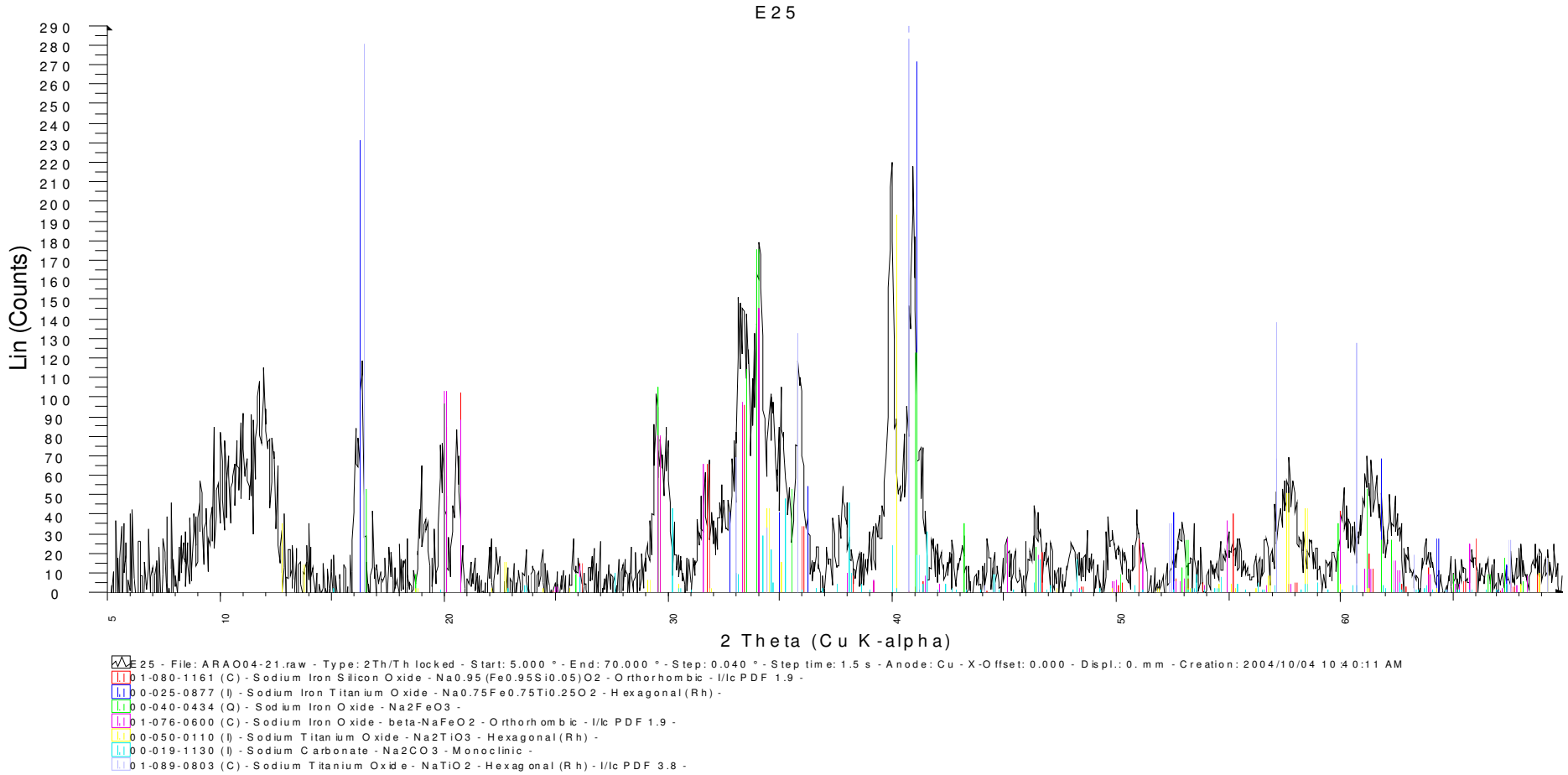

Appendix A- 27: XRD diagram of Alkali fused ilmenite. One mole of ilmenite was fused with four mole of sodium hydroxide at 750 °C for two hours

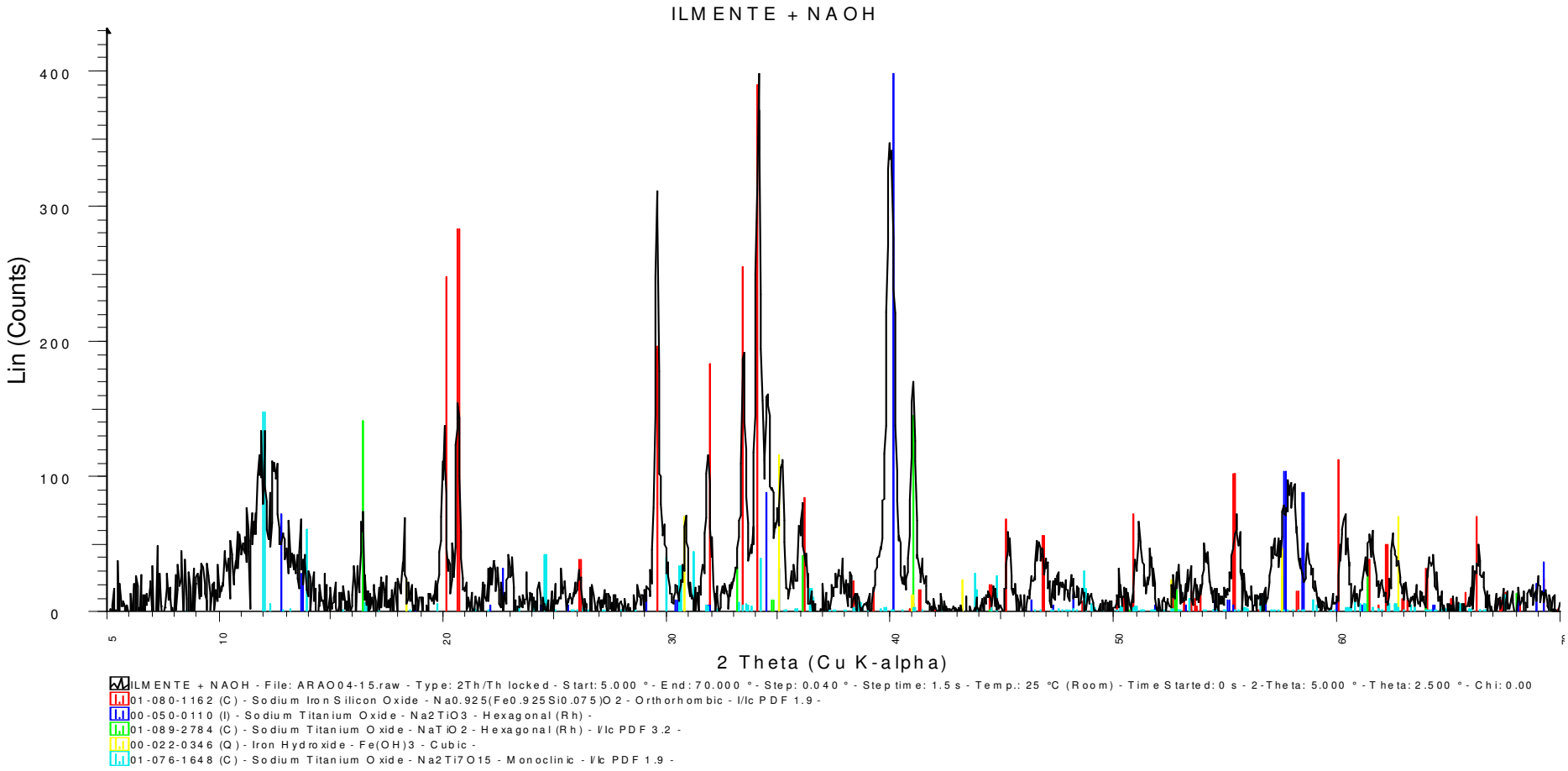

Appendix A- 28: XRD diagram of Alkali fused ilmenite. One mole of ilmenite was fused with six mole of sodium hydroxide at 750 °C for two hours

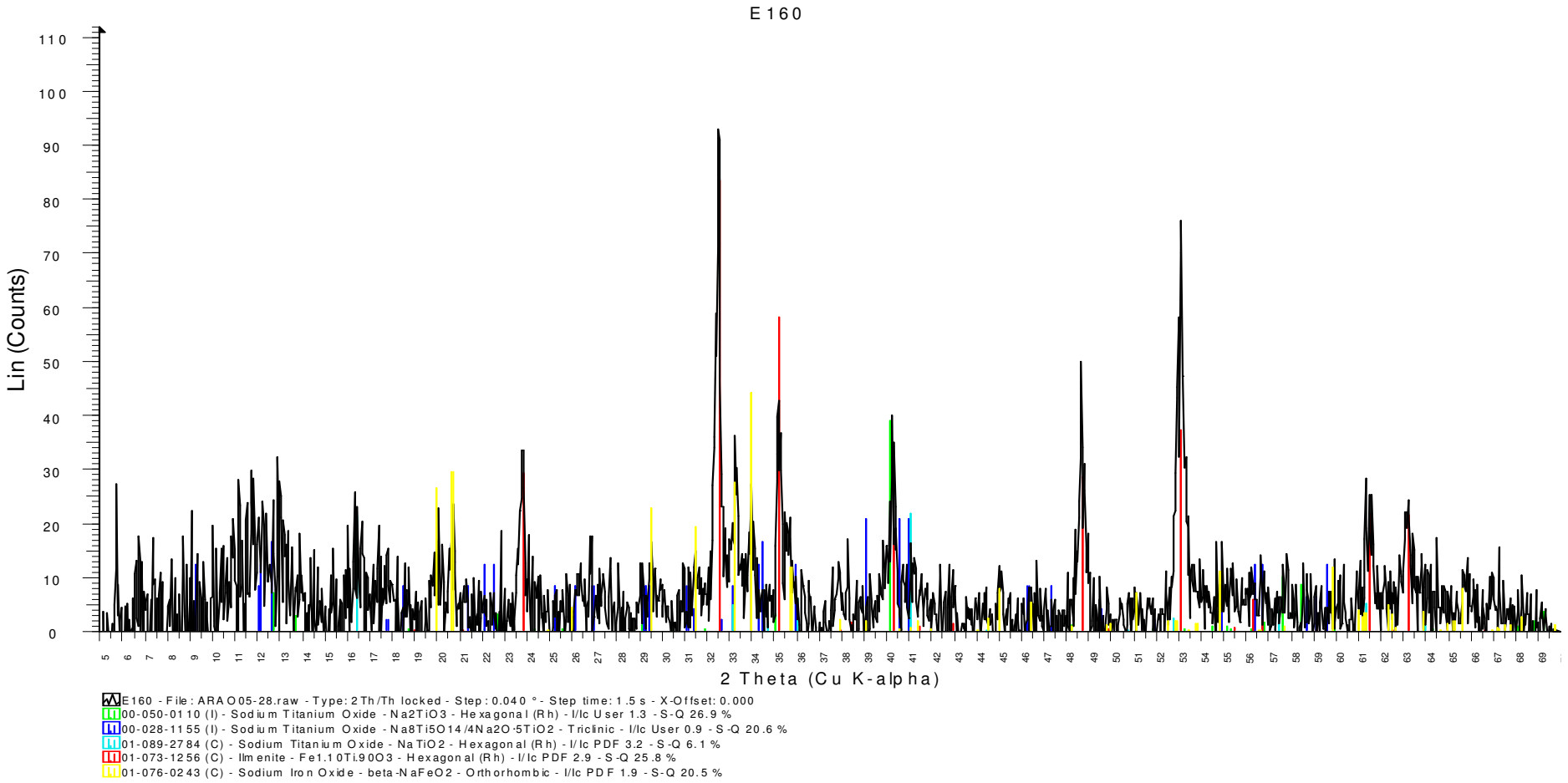

Appendix A- 29: XRD diagram of Alkali fused ilmenite. Four mole of ilmenite was fused with one mole of sodium hydroxide at 550 °C for two hours

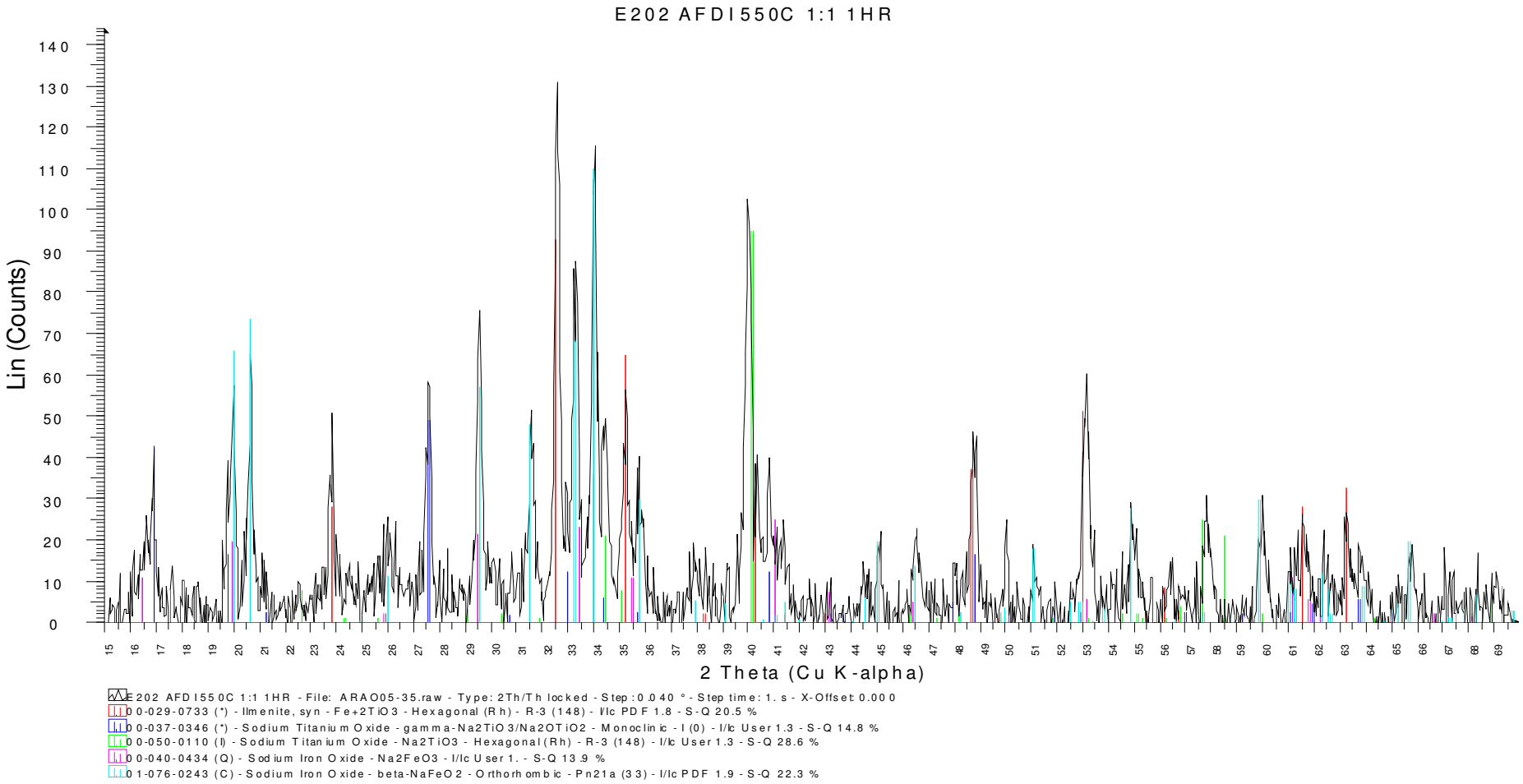

Appendix A- 30: XRD diagram of Alkali fused ilmenite. One mole of ilmenite was fused with one mole of sodium hydroxide at 550 °C for two hours

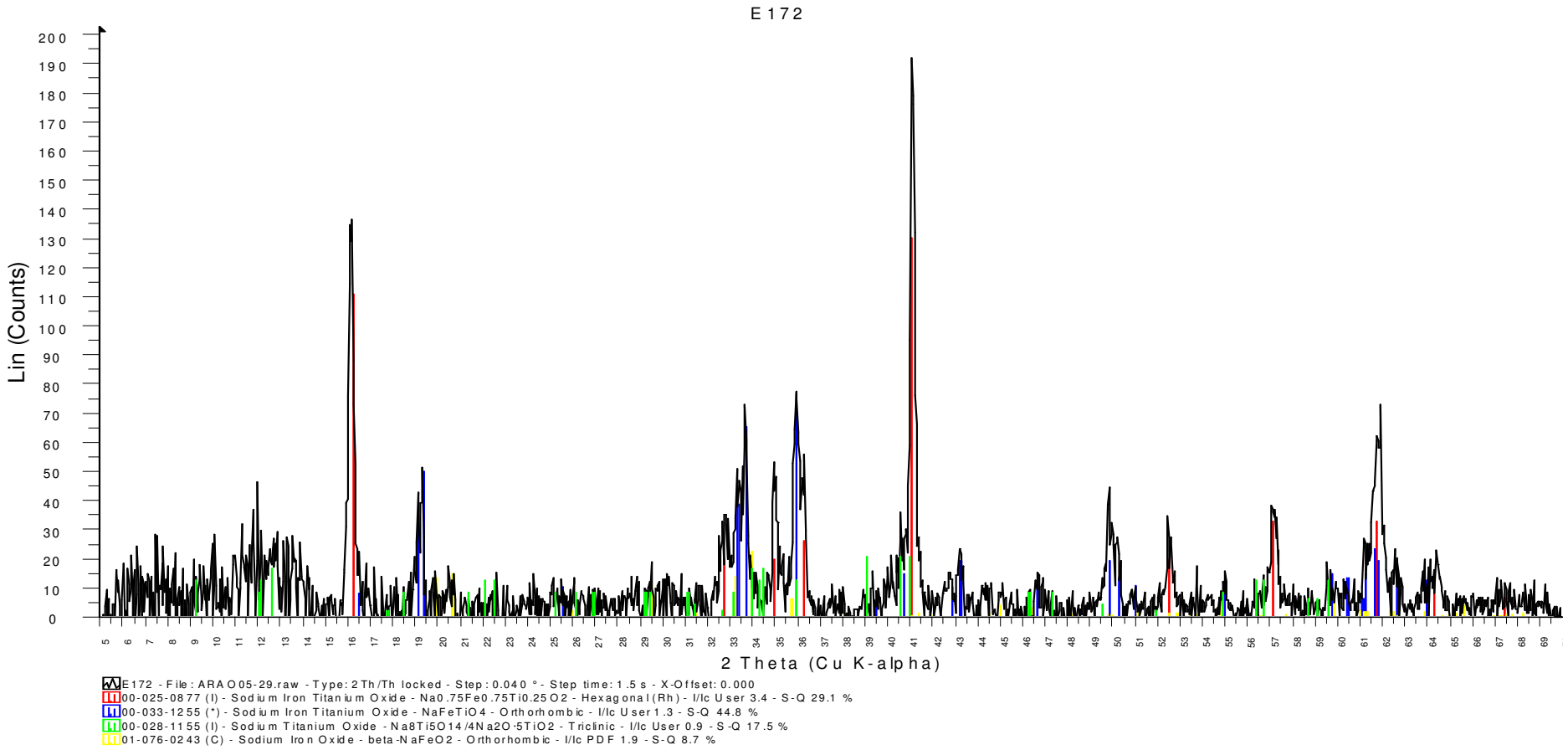

Appendix A- 31: XRD diagram of Alkali fused ilmenite. One mole of ilmenite was fused with one mole of sodium hydroxide at 850 °C for two hours

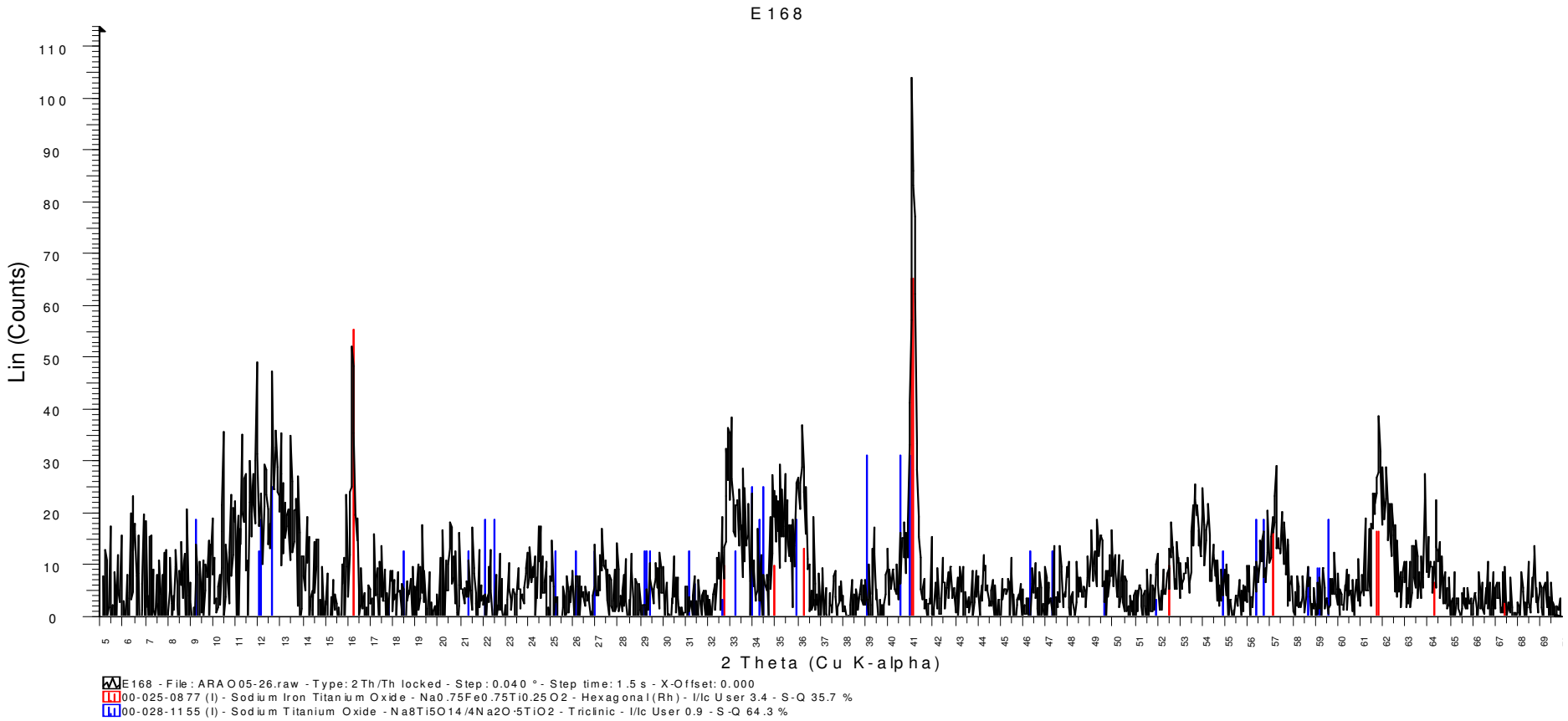

Appendix A- 32: XRD diagram of Alkali fused ilmenite. Four mole of ilmenite were fused with one mole of sodium hydroxide at 850 °C for two hours

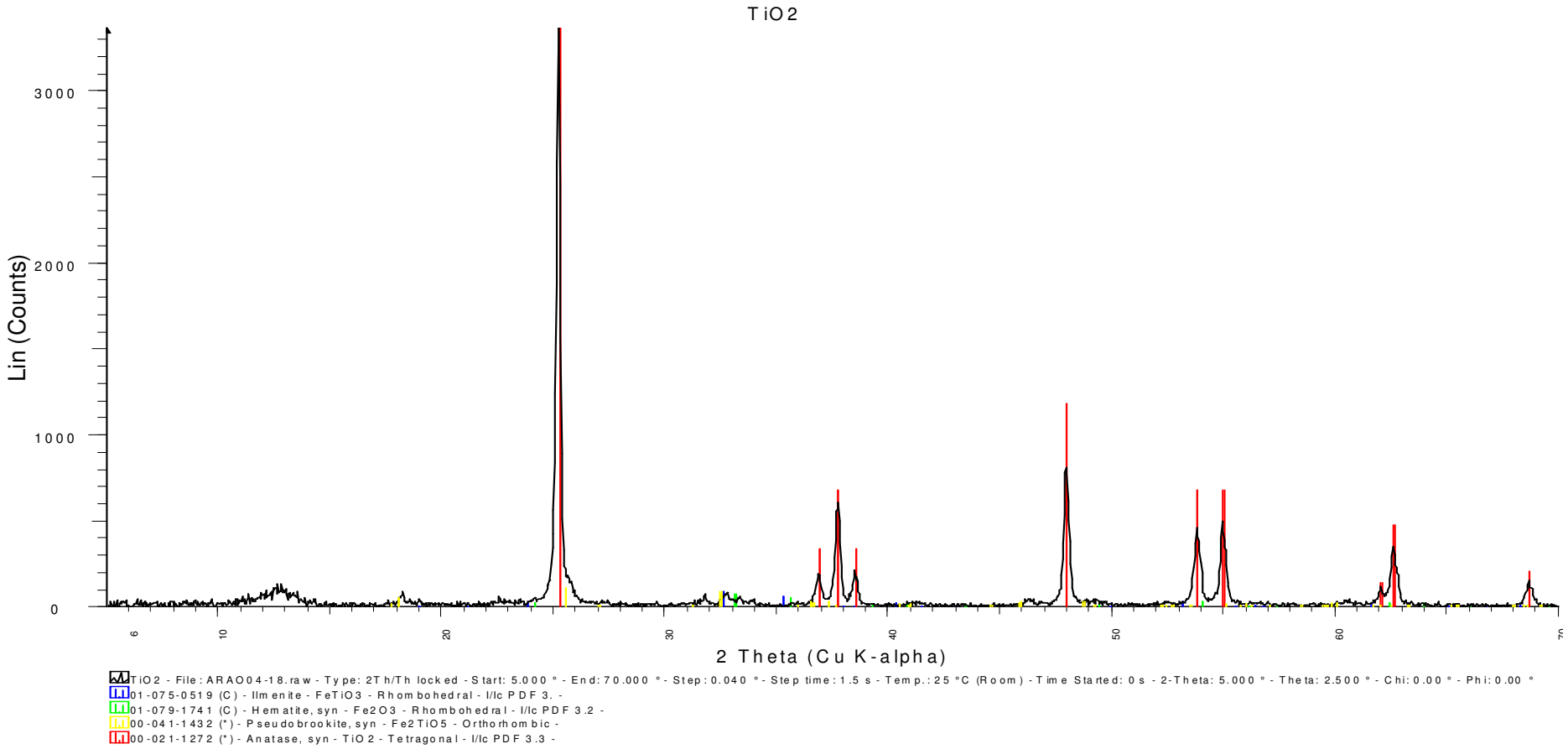

Appendix A- 33: XRD diagram of titania produced in the new method (not purified)

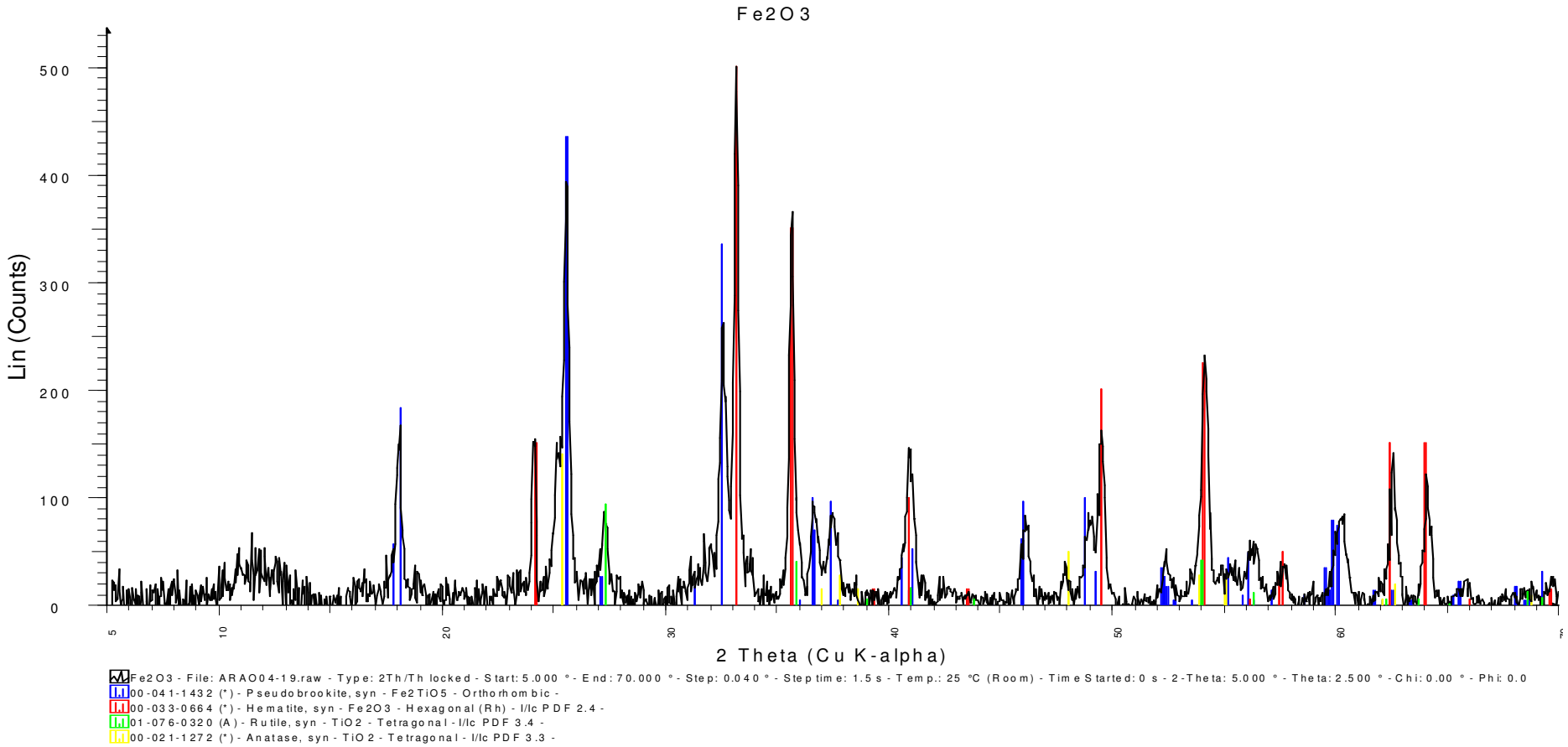

Appendix A- 34: XRD diagram of the by-product produced in the new method

Table A 1: Identified phases by XRD in the AFDI diagrams obtained after roasting a mixture of a mole of ilmenite with two moles of sodium hydroxide for 1 h

Phases	Temperature, °C													
	300	350	400	450	500	550	600	650	700	750	800	850	900	950
$FeTiO_3$	major	major	major	major	major	minor	trace	trace	trace	trace	trace	-	-	-
$Na_2Fe_2Ti_3O_{10}$	-	-	-	-	-	-	-	-	-	-	minor	-	-	-
$NaFeTiO_4$	-	-	-	-	-	minor	-	-	-	minor	minor	major	minor	minor
$NaTiO_2$	-	trace	trace	-	-	-	-	-	trace	minor	-	-	-	-
$Na_8Ti_5O_{14}$	-	-	-	-	-	-	trace	trace	minor	minor	minor	-	-	minor
Na_2TiO_3	-	trace	trace	trace	-	-	major	major	trace	major	major	major	minor	minor
$Na_{0.75}Fe_{0.75}Ti_{0.25}O_2$	-	trace	trace	trace	trace	trace	trace	trace	trace	minor	major	major	major	major
$NaFeO_2$	-	minor	minor	minor	minor	minor	major	major	major	major	major	major	-	-
Na_2CO_3	major	major	major	major	major	major	minor	minor	-	-	-	-	-	-

Appendix B: Particle size analysis

MASTERSIZER 2000

Result Analysis Report

Sample Name: Sand 5/3035F+UtraSound
SOP Name:
Measured: Wednesday, March 15, 2006 10:39:29 AM
Sample Source & type: Works
Measured by: ms
Analysed: Wednesday, March 15, 2006 10:39:30 AM
Sample bulk lot ref:
Result Source: Measurement

Particle Name: Quartz
Accessory Name: Hydro 2000MU (A)
Analysis model: General purpose
Sensitivity: Enhanced
Particle RI: 1.544
Absorption: 0.1
Size range: 0.100 to 1000.000 um
Obscuration: 11.55 %
Dispersant Name: Water
Dispersant RI: 1.330
Weighted Residual: 0.300 %
Result Emulation: Off

Concentration: 0.0050 %Vol
Span : 8.031
Uniformity: 5.13
Result units: Volume
Specific Surface Area: 4.15 m²/g
Surface Weighted Mean D[3,2]: 1.447 um
Vol. Weighted Mean D[4,3]: 34.912 um

d(0.1): 0.448 um d(0.5): 6.363 um d(0.9): 51.547 um

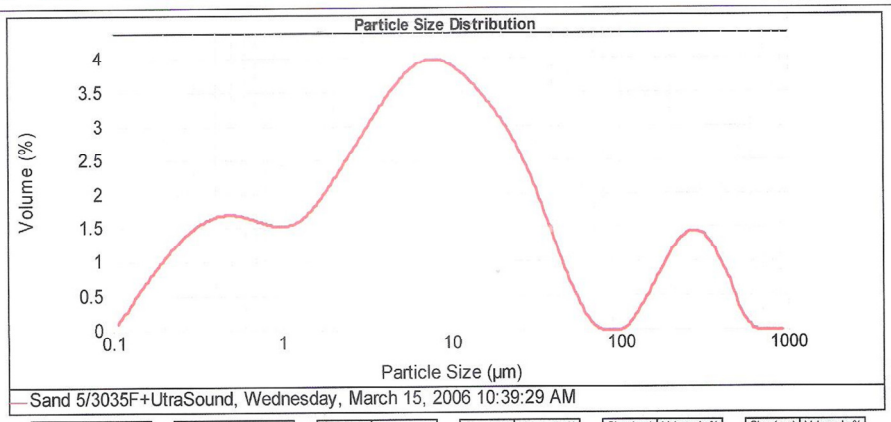

Size (µm)	Volume In %
0.100	0.04
0.110	0.13
0.120	0.21
0.132	0.31
0.145	0.39
0.158	0.47
0.174	0.55
0.191	0.62
0.209	0.69
0.229	0.76
0.251	0.82
0.275	0.87
0.302	0.92
0.331	0.95
0.363	0.98
0.398	1.00
0.437	1.01
0.479	

Size (µm)	Volume In %
0.479	1.02
0.525	1.01
0.575	1.00
0.631	0.98
0.692	0.96
0.759	0.94
0.832	0.92
0.912	0.91
1.000	0.91
1.096	0.93
1.202	0.96
1.318	1.00
1.445	1.06
1.585	1.14
1.738	1.22
1.905	1.31
2.089	1.40
2.291	

Size (µm)	Volume In %
2.291	1.49
2.512	1.59
2.754	1.69
3.020	1.78
3.311	1.86
3.631	1.97
3.981	2.05
4.365	2.14
4.786	2.21
5.248	2.27
5.754	2.33
6.310	2.36
6.918	2.39
7.586	2.39
8.318	2.39
9.120	2.36
10.000	2.33
10.965	

Size (µm)	Volume In %
10.965	2.28
12.023	2.23
13.183	2.16
14.454	2.10
15.849	2.03
17.378	1.95
19.055	1.86
20.893	1.77
22.909	1.66
25.119	1.54
27.542	1.40
30.200	1.25
33.113	1.10
36.308	0.93
39.811	0.77
43.652	0.60
47.863	0.45
52.481	

Size (µm)	Volume In %
52.481	0.31
57.544	0.19
63.096	0.09
69.183	0.02
75.858	0.00
83.176	0.00
91.201	0.00
100.000	0.00
109.648	0.05
120.226	0.13
131.826	0.23
144.544	0.33
158.489	0.44
173.780	0.56
190.546	0.66
208.930	0.76
229.087	0.83
251.189	

Size (µm)	Volume In %
251.189	0.86
275.423	0.87
301.995	0.83
331.131	0.77
363.078	0.66
398.107	0.54
436.516	0.42
478.630	0.23
524.807	0.12
575.440	0.03
630.957	0.00
691.831	0.00
758.578	0.00
831.764	0.00
912.011	0.00
1000.000	

Operator notes:

Malvern Instruments Ltd.
Malvern, UK
Tel := +[44] (0) 1684-892456 Fax +[44] (0) 1684-892789

Mastersizer 2000 E Ver. 5.21
Serial Number : MAL101026

File name: Ilmenite Rou 1
Record Number: 7
08 May 2009 9:58:35 AM

MASTERSIZER 2000

Result Analysis Report

Sample Name: Sand 5/3035F+UtraSound
SOP Name:
Measured: Monday, January 30, 2006 2:49:38 PM
Sample Source & type: Works
Measured by: ms
Analysed: Monday, January 30, 2006 2:49:39 PM
Sample bulk lot ref:
Result Source: Measurement

Particle Name: Quartz
Accessory Name: Hydro 2000MU (A)
Analysis model: General purpose
Sensitivity: Enhanced
Particle RI: 1.544
Absorption: 0.1
Size range: 0.100 to 1000.000 um
Obscuration: 12.12 %
Dispersant Name: Water
Dispersant RI: 1.330
Weighted Residual: 0.421 %
Result Emulation: Off

Concentration: 0.1518 %Vol
Span : 1.007
Uniformity: 0.325
Result units: Volume
Specific Surface Area: 0.0701 m²/g
Surface Weighted Mean D[3,2]: 85.642 um
Vol. Weighted Mean D[4,3]: 145.083 um

d(0.1): 82.627 um d(0.5): 138.746 um d(0.9): 222.281 um

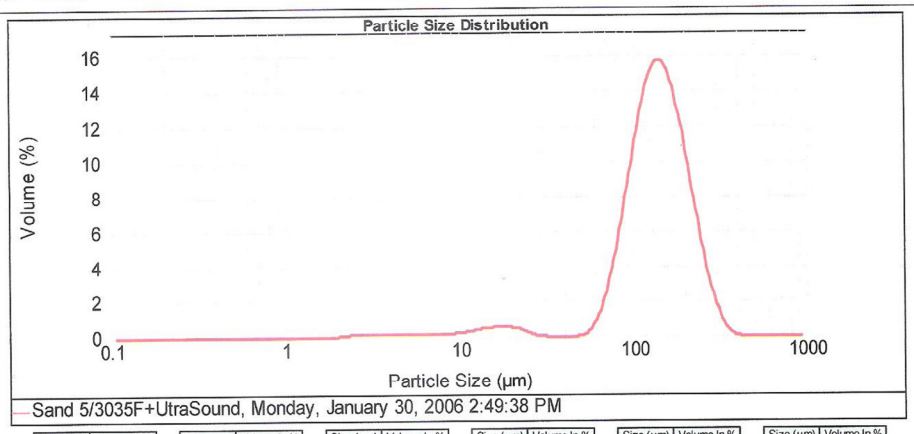

Size (µm)	Volume In %
0.100	0.00
0.110	0.00
0.120	0.00
0.132	0.00
0.145	0.00
0.158	0.00
0.174	0.00
0.191	0.00
0.209	0.00
0.229	0.00
0.251	0.00
0.275	0.00
0.302	0.00
0.331	0.00
0.363	0.00
0.398	0.00
0.437	0.00
0.479	0.00

Size (µm)	Volume In %
0.479	0.00
0.525	0.00
0.575	0.00
0.631	0.00
0.692	0.00
0.759	0.00
0.832	0.00
0.912	0.00
1.000	0.00
1.096	0.00
1.202	0.00
1.318	0.00
1.445	0.00
1.585	0.00
1.738	0.00
1.905	0.00
2.089	0.00
2.291	0.02

Size (µm)	Volume In %
2.291	0.06
2.512	0.07
2.754	0.08
3.020	0.09
3.311	0.09
3.631	0.09
3.981	0.09
4.365	0.08
4.786	0.08
5.248	0.07
5.754	0.06
6.310	0.06
6.918	0.05
7.586	0.05
8.318	0.06
9.120	0.08
10.000	0.11
10.965	0.14

Size (µm)	Volume In %
10.965	0.18
12.023	0.23
13.183	0.27
14.454	0.31
15.849	0.33
17.378	0.33
19.055	0.31
20.893	0.27
22.909	0.18
25.119	0.08
27.542	0.01
30.200	0.00
33.113	0.00
36.308	0.00
39.811	0.00
43.652	0.00
47.863	0.00
52.481	0.00

Size (µm)	Volume In %
52.481	0.12
57.544	0.43
63.096	1.02
69.183	1.86
75.858	2.96
83.176	4.30
91.201	5.71
100.000	7.09
109.648	8.29
120.226	9.11
131.826	9.50
144.544	9.36
158.489	8.75
173.780	7.71
190.546	6.41
208.930	5.00
229.087	3.62
251.189	

Size (µm)	Volume In %
251.189	2.41
275.423	1.44
301.995	0.73
331.131	0.29
363.078	0.03
398.107	0.00
436.516	0.00
478.630	0.00
524.807	0.00
575.440	0.00
630.957	0.00
691.831	0.00
758.578	0.00
831.764	0.00
912.011	0.00
1000.000	

Operator notes:

Malvern Instruments Ltd.
Malvern, UK
Tel := +[44] (0) 1684-892456 Fax +[44] (0) 1684-892789

Mastersizer 2000 E Ver. 5.21
Serial Number : MAL101026

File name: Ilmenite Rou 1
Record Number: 5
08 May 2009 9:56:40 AM

MASTERSIZER 2000

Result Analysis Report

Sample Name: Sand 5/3035F+UtraSound
Sample Source & type: Works
Sample bulk lot ref:

SOP Name:
Measured by: ms
Result Source: Measurement

Measured: Monday, January 30, 2006 2:49:05 PM
Analysed: Monday, January 30, 2006 2:49:07 PM

Particle Name: Quartz
Particle RI: 1.544
Dispersant Name: Water

Accessory Name: Hydro 2000MU (A)
Absorption: 0.1
Dispersant RI: 1.330

Analysis model: General purpose
Size range: 0.100 to 1000.000 um
Weighted Residual: 0.418 %

Sensitivity: Enhanced
Obscuration: 11.94 %
Result Emulation: Off

Concentration: 0.1498 %Vol
Specific Surface Area: 0.0699 m²/g

Span : 1.004
Surface Weighted Mean D[3,2]: 85.848 um

Uniformity: 0.324
Vol. Weighted Mean D[4,3]: 145.056 um

Result units: Volume

d(0.1): 82.756 um d(0.5): 138.722 um d(0.9): 222.069 um

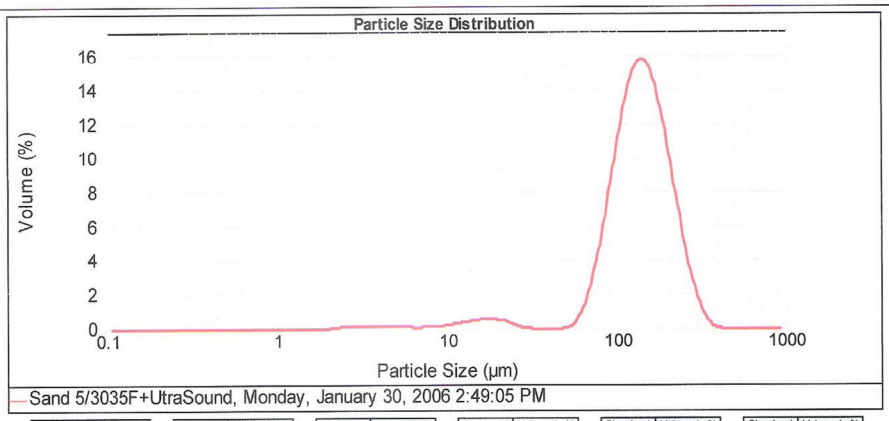

Size (µm)	Volume In %
0.100	0.00
0.110	0.00
0.120	0.00
0.132	0.00
0.145	0.00
0.158	0.00
0.174	0.00
0.191	0.00
0.209	0.00
0.229	0.00
0.251	0.00
0.275	0.00
0.302	0.00
0.331	0.00
0.363	0.00
0.398	0.00
0.437	0.00
0.479	0.00

Size (µm)	Volume In %
0.479	0.00
0.525	0.00
0.575	0.00
0.631	0.00
0.692	0.00
0.759	0.00
0.832	0.00
0.912	0.00
1.000	0.00
1.096	0.00
1.202	0.00
1.318	0.00
1.445	0.00
1.585	0.00
1.738	0.00
1.905	0.00
2.089	0.00
2.291	0.02

Size (µm)	Volume In %
2.291	0.06
2.512	0.07
2.754	0.08
3.020	0.09
3.311	0.09
3.631	0.09
3.981	0.09
4.365	0.08
4.786	0.08
5.248	0.07
5.754	0.06
6.310	0.05
6.918	0.05
7.586	0.05
8.318	0.06
9.120	0.08
10.000	0.10
10.965	0.14

Size (µm)	Volume In %
10.965	0.18
12.023	0.22
13.183	0.27
14.454	0.30
15.849	0.33
17.378	0.33
19.055	0.33
20.893	0.31
22.909	0.27
25.119	0.18
27.542	0.08
30.200	0.01
33.113	0.00
36.308	0.00
39.811	0.00
43.652	0.00
47.863	0.00
52.481	0.00

Size (µm)	Volume In %
52.481	0.11
57.544	0.43
63.096	1.02
69.183	1.86
75.858	2.96
83.176	4.31
91.201	5.72
100.000	7.10
109.648	8.30
120.226	9.13
131.826	9.52
144.544	9.38
158.489	8.76
173.780	7.72
190.546	6.41
208.930	5.00
229.087	3.61
251.189	

Size (µm)	Volume In %
251.189	2.40
275.423	1.43
301.995	0.72
331.131	0.28
363.078	0.03
398.107	0.00
436.516	0.00
478.630	0.00
524.807	0.00
575.440	0.00
630.957	0.00
691.831	0.00
758.578	0.00
831.764	0.00
912.011	0.00
1000.000	

Operator notes:

Malvern Instruments Ltd.
Malvern, UK
Tel := +[44] (0) 1684-892456 Fax +[44] (0) 1684-892789

Mastersizer 2000 E Ver. 5.21
Serial Number : MAL101026

File name: Ilmenite Rou 1
Record Number: 4
08 May 2009 9:56:20 AM

MASTERSIZER 2000

Result Analysis Report

Sample Name: Sand 5/3035F+UtraSound
SOP Name:
Measured: Monday, January 30, 2006 2:47:28 PM
Sample Source & type: Works
Measured by: ms
Analysed: Monday, January 30, 2006 2:47:30 PM
Sample bulk lot ref:
Result Source: Measurement

Particle Name: Quartz
Accessory Name: Hydro 2000MU (A)
Analysis model: General purpose
Sensitivity: Enhanced
Particle RI: 1.544
Absorption: 0.1
Size range: 0.100 to 1000.000 um
Obscuration: 11.75 %
Dispersant Name: Water
Dispersant RI: 1.330
Weighted Residual: 0.439 %
Result Emulation: Off

Concentration: 0.1506 %Vol
Span : 0.999
Uniformity: 0.321
Result units: Volume
Specific Surface Area: 0.0684 m²/g
Surface Weighted Mean D[3,2]: 87.743 um
Vol. Weighted Mean D[4,3]: 145.368 um

d(0.1): 83.370 um d(0.5): 138.828 um d(0.9): 222.000 um

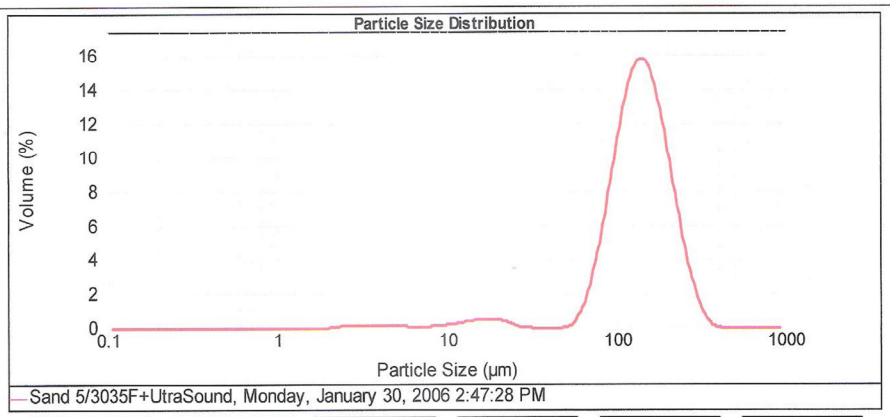

Size (µm)	Volume In %	Size (µm)	Volume In %	Size (µm)	Volume In %	Size (µm)	Volume In %	Size (µm)	Volume In %	Size (µm)	Volume In %
0.100	0.00	0.479	0.00	2.291	0.06	10.965	0.16	52.481	0.11	251.189	2.39
0.110	0.00	0.525	0.00	2.512	0.07	12.023	0.20	57.544	0.43	275.423	1.42
0.120	0.00	0.575	0.00	2.754	0.08	13.183	0.25	63.096	1.02	301.995	0.72
0.132	0.00	0.631	0.00	3.020	0.08	14.454	0.28	69.183	1.87	331.131	0.26
0.145	0.00	0.692	0.00	3.311	0.09	15.849	0.31	75.858	2.97	363.078	0.03
0.158	0.00	0.759	0.00	3.631	0.09	17.378	0.31	83.176	4.33	398.107	0.00
0.174	0.00	0.832	0.00	3.981	0.08	19.055	0.29	91.201	5.75	436.516	0.00
0.191	0.00	0.912	0.00	4.365	0.07	20.893	0.25	100.000	7.14	478.630	0.00
0.209	0.00	1.000	0.00	4.786	0.07	22.909	0.16	109.648	8.35	524.807	0.00
0.229	0.00	1.096	0.00	5.248	0.06	25.119	0.06	120.226	9.18	575.440	0.00
0.251	0.00	1.202	0.00	5.754	0.05	27.542	0.01	131.826	9.56	630.957	0.00
0.275	0.00	1.318	0.00	6.310	0.04	30.200	0.00	144.544	9.41	691.831	0.00
0.302	0.00	1.445	0.00	6.918	0.04	33.113	0.00	158.489	8.78	758.578	0.00
0.331	0.00	1.585	0.00	7.586	0.05	36.308	0.00	173.780	7.73	831.764	0.00
0.363	0.00	1.738	0.00	8.318	0.07	39.811	0.00	190.546	6.42	912.011	0.00
0.398	0.00	1.905	0.00	9.120	0.09	43.652	0.00	208.930	5.00	1000.000	
0.437	0.00	2.089	0.00	10.000	0.12	47.863	0.00	229.087	3.61		
0.479		2.291	0.02	10.965		52.481		251.189			

Operator notes:

Malvern Instruments Ltd.
Malvern, UK
Tel := +(44) (0) 1684-892456 Fax +(44) (0) 1684-892789

Mastersizer 2000 E Ver. 5.21
Serial Number : MAL101026

File name: Ilmenite Rou 1
Record Number: 3
08 May 2009 9:55:56 AM

MASTERSIZER 2000

Result Analysis Report

Sample Name: Sand 5/3035F+UtraSound
SOP Name:
Measured: Monday, January 30, 2006 2:46:56 PM
Sample Source & type: Works
Measured by: ms
Analysed: Monday, January 30, 2006 2:46:57 PM
Sample bulk lot ref:
Result Source: Measurement

Particle Name: Quartz
Accessory Name: Hydro 2000MU (A)
Analysis model: General purpose
Sensitivity: Enhanced
Particle RI: 1.544
Absorption: 0.1
Size range: 0.100 to 1000.000 um
Obscuration: 11.72 %
Dispersant Name: Water
Dispersant RI: 1.330
Weighted Residual: 0.472 %
Result Emulation: Off

Concentration: 0.1926 %Vol
Span : 0.985
Uniformity: 0.313
Result units: Volume
Specific Surface Area: 0.0545 m²/g
Surface Weighted Mean D[3,2]: 110.081 um
Vol. Weighted Mean D[4,3]: 147.072 um

d(0.1): 85.269 um d(0.5): 139.871 um d(0.9): 223.044 um

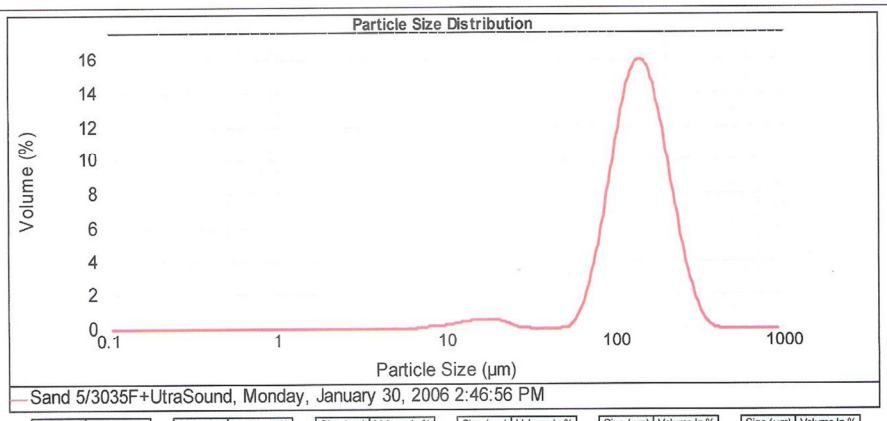

Size (µm)	Volume In %
0.100	0.00
0.110	0.00
0.120	0.00
0.132	0.00
0.145	0.00
0.158	0.00
0.174	0.00
0.191	0.00
0.209	0.00
0.229	0.00
0.251	0.00
0.275	0.00
0.302	0.00
0.331	0.00
0.363	0.00
0.398	0.00
0.437	0.00
0.479	0.00

Size (µm)	Volume In %
0.479	0.00
0.525	0.00
0.575	0.00
0.631	0.00
0.692	0.00
0.759	0.00
0.832	0.00
0.912	0.00
1.000	0.00
1.096	0.00
1.202	0.00
1.318	0.00
1.445	0.00
1.585	0.00
1.738	0.00
1.906	0.00
2.089	0.00
2.291	0.00

Size (µm)	Volume In %
2.291	0.00
2.512	0.00
2.754	0.00
3.020	0.00
3.311	0.00
3.631	0.00
3.981	0.00
4.365	0.00
4.786	0.00
5.248	0.00
5.754	0.00
6.310	0.00
6.918	0.01
7.586	0.06
8.318	0.07
9.120	0.09
10.000	0.13
10.965	

Size (µm)	Volume In %
10.965	0.17
12.023	0.21
13.183	0.26
14.454	0.29
15.849	0.31
17.378	0.31
19.055	0.29
20.893	0.24
22.909	0.15
25.119	0.05
27.542	0.00
30.200	0.00
33.113	0.00
36.308	0.00
39.811	0.00
43.652	0.00
47.863	0.00
52.481	

Size (µm)	Volume In %
52.481	0.10
57.544	0.41
63.096	1.00
69.183	1.85
75.858	2.95
83.176	4.31
91.201	5.75
100.000	7.16
109.648	8.38
120.226	9.24
131.826	9.64
144.544	9.51
158.489	8.90
173.780	7.85
190.546	6.52
208.930	5.09
229.087	3.69
251.189	

Size (µm)	Volume In %
251.189	2.45
275.423	1.47
301.995	0.75
331.131	0.29
363.078	0.03
398.107	0.00
436.516	0.00
478.630	0.00
524.807	0.00
575.440	0.00
630.957	0.00
691.831	0.00
758.578	0.00
831.764	0.00
912.011	0.00
1000.000	

Operator notes:

Malvern Instruments Ltd.
Malvern, UK
Tel := +1441 (0) 1684-892456 Fax +1441 (0) 1684-892789

Mastersizer 2000 E Ver. 5.21
Serial Number : MAL101026

File name: Ilmenite Rou 1
Record Number: 2
08 May 2009 9:55:00 AM